Probing(breaking!) old rules in Nuclear Structure: Studies with Radioactive Ion Beams

Andrei Andreyev
University of York, UK
Japan Atomic Energy Agency (JAEA), Tokai, Japan

(Some of the) Topics to cover:

- Introduction – frontiers of nuclear landscape and nuclear structure ($E(2^+)$, S_{2n} systematics, radii)
- Experimental techniques for RIB production (ISOL, in-flight)
- Laser spectroscopy (radii, moments, pure isotopic/isomeric beams)
- Shape coexistence in the lead read region
- Ca chain in "all details": $E(2^+_1)$, radii, masses
- Superallowed alpha decays
- Coulex of post-accelerated RIBs (e.g. octupole shapes)
- Superheavy Elements

UNIVERSITY of York

NUSYS, Lanzhou, 12th -18th August 2019

Four Frontiers for Modern Nuclear Spectroscopy

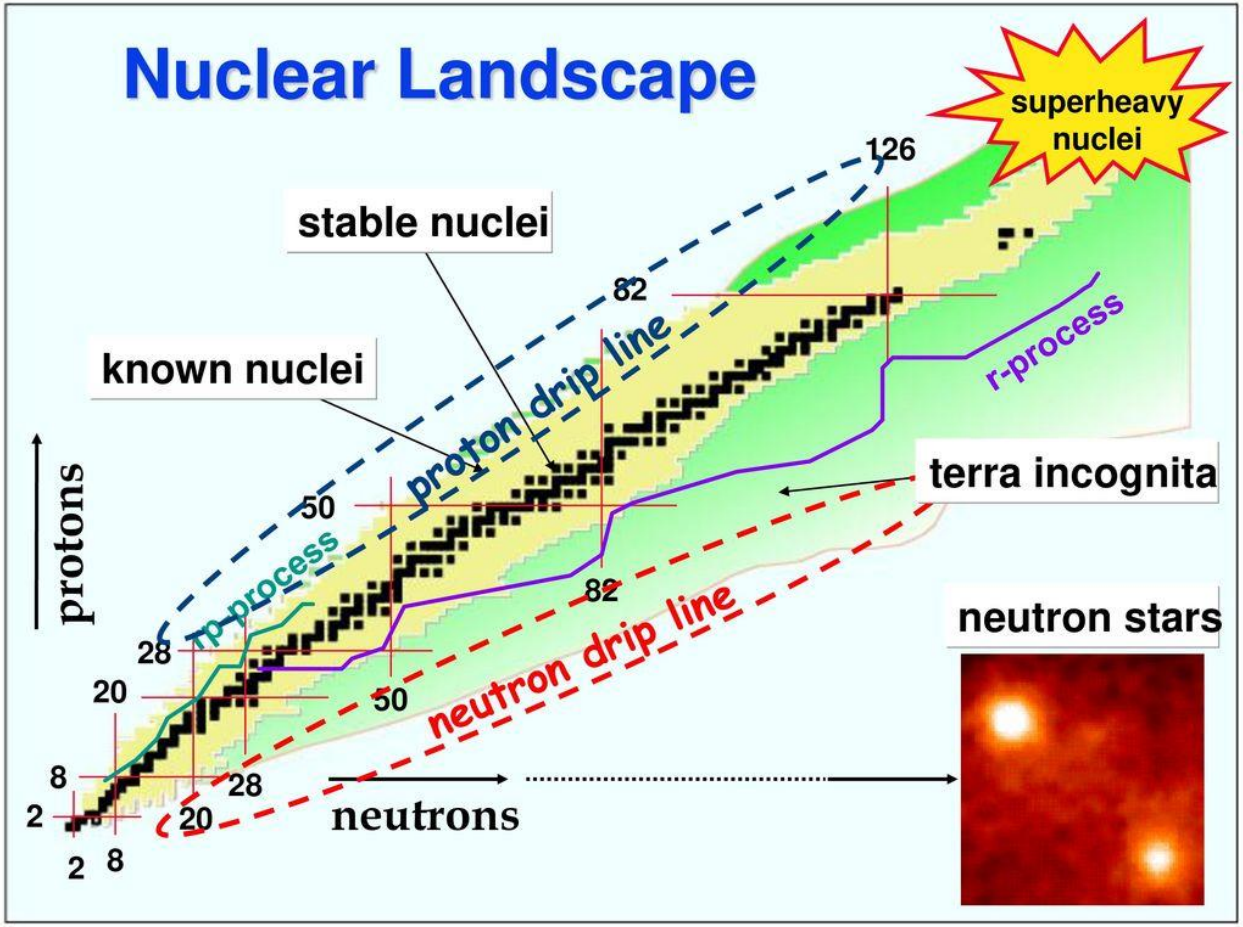

- **Black: 283 stable isotopes**
- **Yellow: ~3500 known isotopes (mostly man-made)**
- **Green: ~7000 isotopes can theoretically exist (we concentrate on 'key' ones!)**

- **Proton-rich nuclei**: "small" N/Z ratio, e.g. N/Z=0.33 for ^{8}C(Z=6,N=2) Recall, stable ^{12}C (Z=N=6) has N/Z=1
- **Neutron-rich nuclei:** "large" N/Z ratio, e.g. N/Z=2.66 for ^{22}C (Z=6,N=16)
- **Super-heavy elements,** the heaviest known ^{294}Og(Z=118,N=176)
- **The Evolution of Nuclear structure between these boundaries (isospin-dependence of nuclear properties)**

Quiz: Characterize the nature of these 3 nuclei (e.g. rotational, vibrational, spherical?). Explain your reasoning.

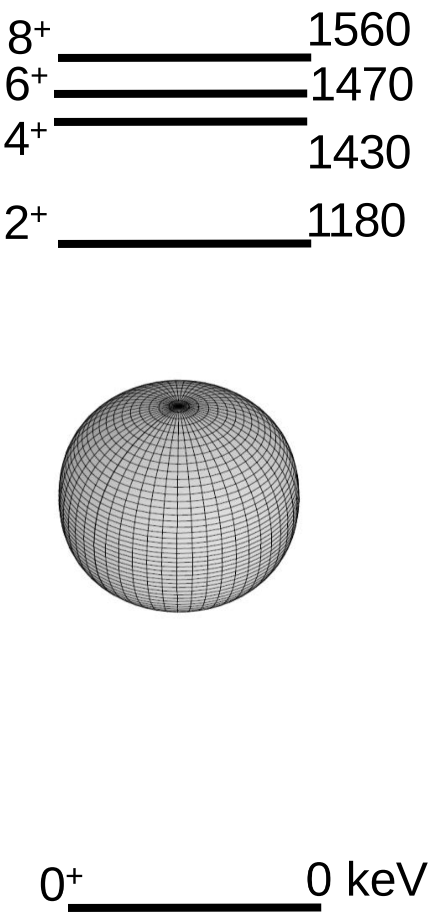

^{210}Po (Z=84, N=126)

Spherical, near-doubly-magic

High $E(2^+_1)$

Ratio $E(4^+_1)/E(2^+_1)$=1.2

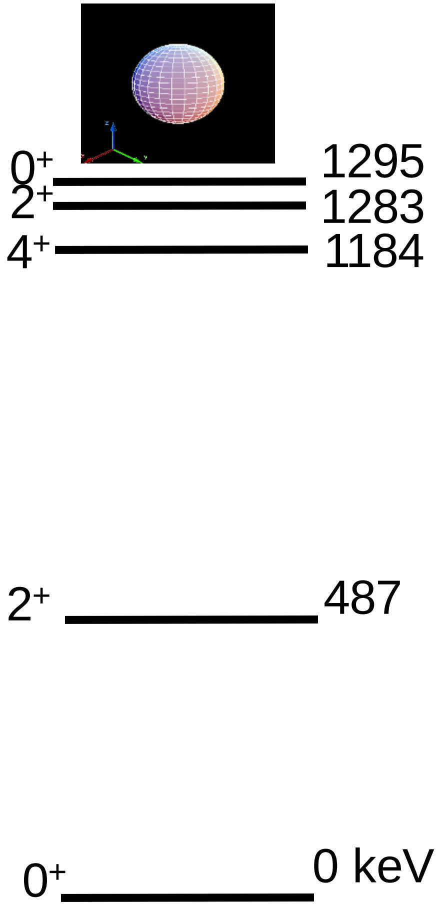

^{118}Cd (Z=48, N=70)

Vibrational pattern 1ph/2ph

Relatively high $E(2^+_1)$

Ratio $E(4^+_1)/E(2^+_1)$=2.4

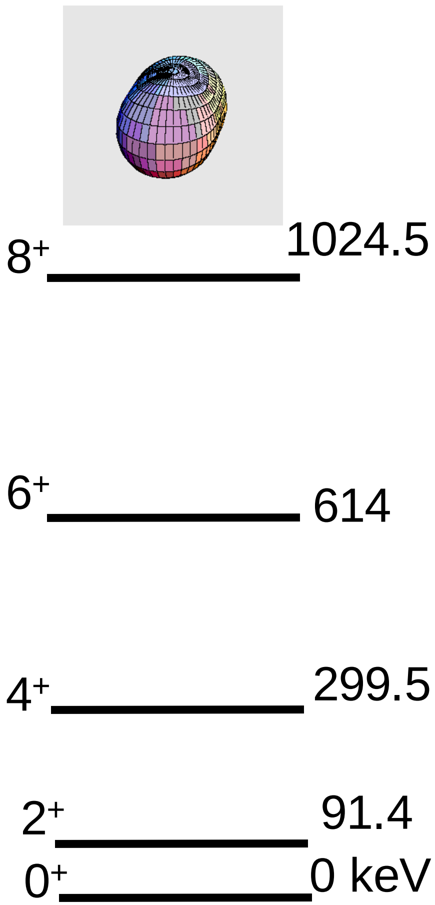

^{164}Er (Z=68, N=96)

Well-deformed rotor

Low $E(2^+_1)$

Ratio $E(4^+_1)/E(2^+_1)$=3.28

One of the key questions:
Probing Old/New Magic Numbers at the Limits

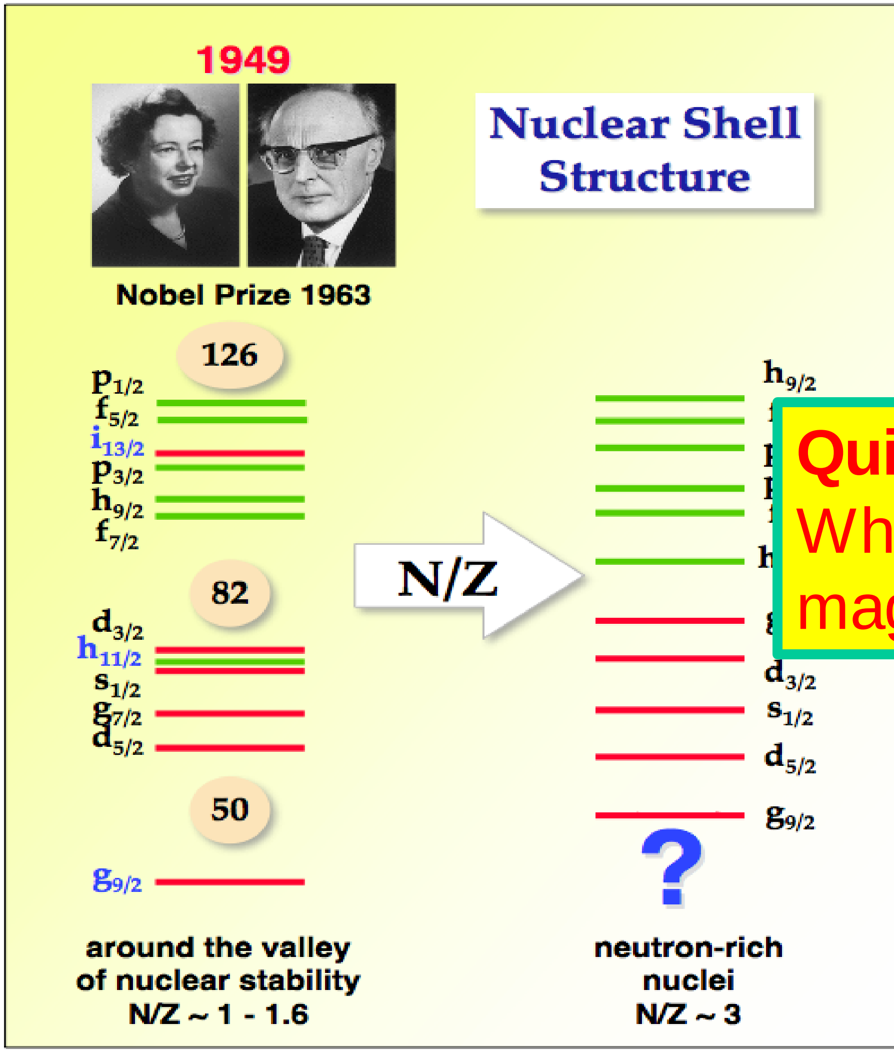

Quiz:
What are experimental evidences of a magic number (or of deformation)?

- Mean-field near stability
- Strong spin-orbital coupling
- Magic numbers N,Z=2,8,20,28,50,82,126…?

- $E(2^+_1)$ energies, ratio $4^+/2^+$
- Kinks in masses, Q_α, S_{2n}-values
- Kinks in radii
- Magnetic/quadrupole moments
- B(E2) values

….

S_{2n}-values as the indicators of magic numbers

$$S_{2n}(Z,N) = BE(Z,N+2) - BE(Z,N)$$

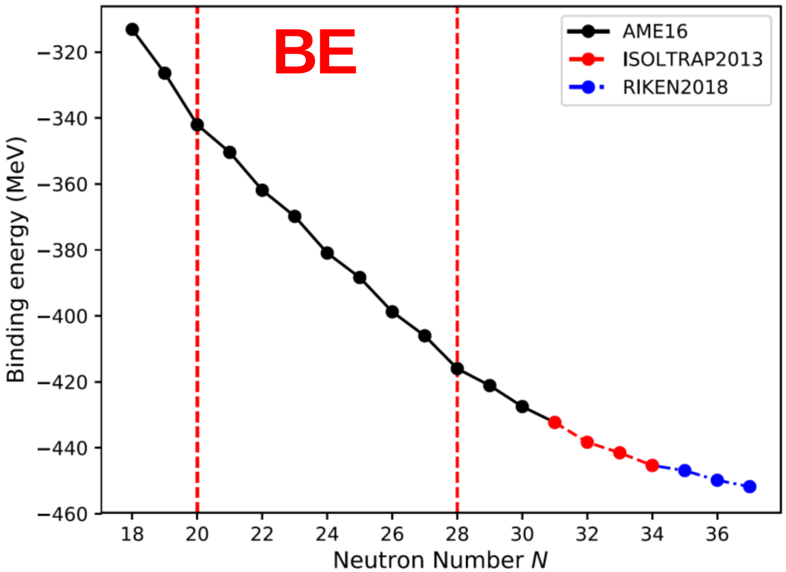

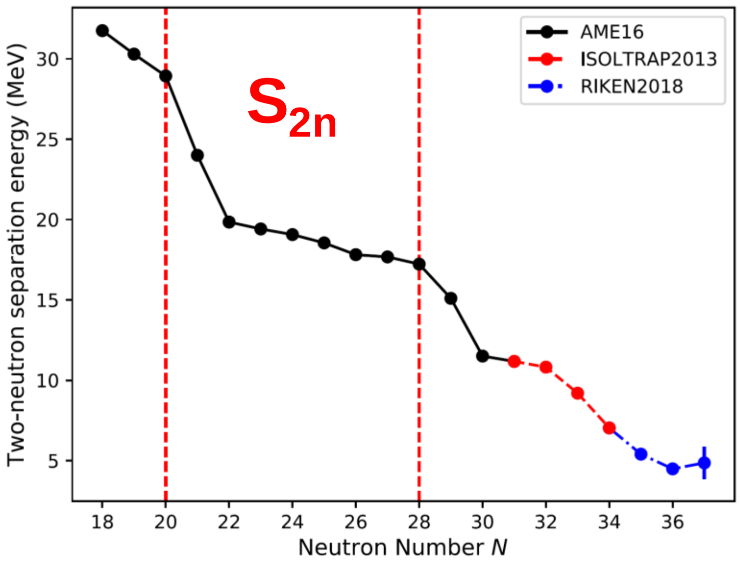

Ca isotopes

- **Note the Y-scale!**
- BE's: large values, look smooth, difficult to see any effects at N=20,28
- **S_{2n}'s: much smaller values, irregularities are seen much easier at N=20,28!**
- Possibly, N=32? (We will come back to this later on)

S_{2n}-values as the indicators deformation!

$S_{2n}(Z,N) = BE(Z,N+2) - BE(Z,N)$

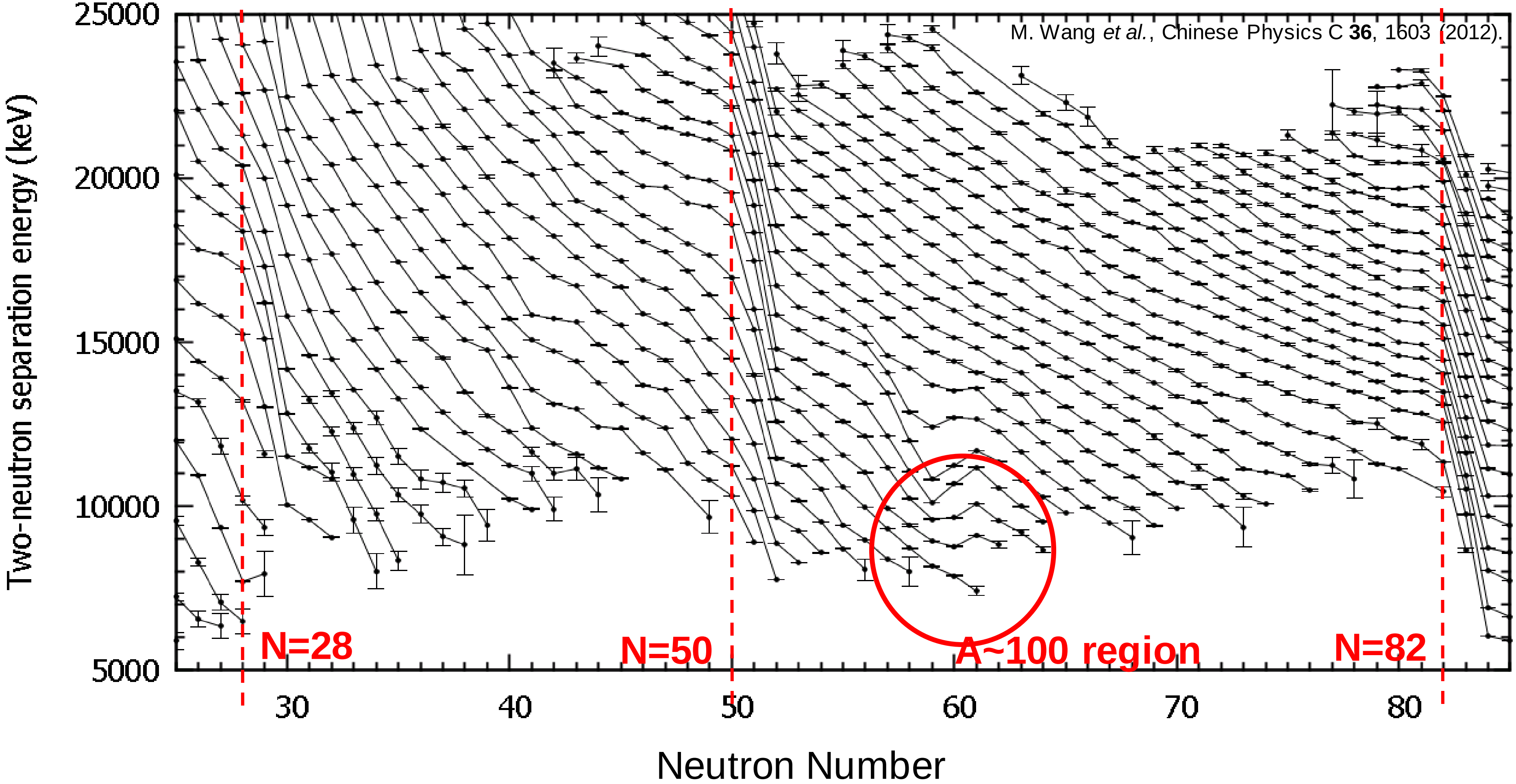

- A kink at magic numbers N=28,50,82
- Also a non-smooth trend at N=60 and A~100 (evidence for onset of deformation)
- However, difficult to measure masses for very exotic nuclei (with sufficient precision)

Power of Complementarity of Different Approaches/Observables
S_{2n}, Radii and $E(2^+_1)$ as evidence of onset of deformation around N=60

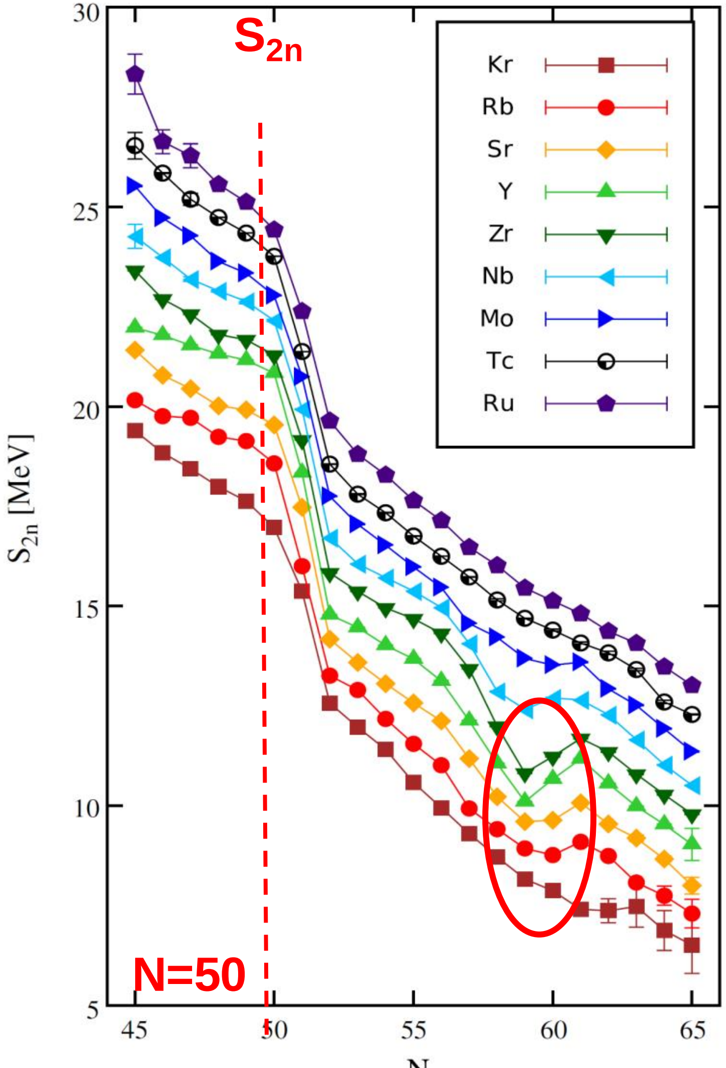

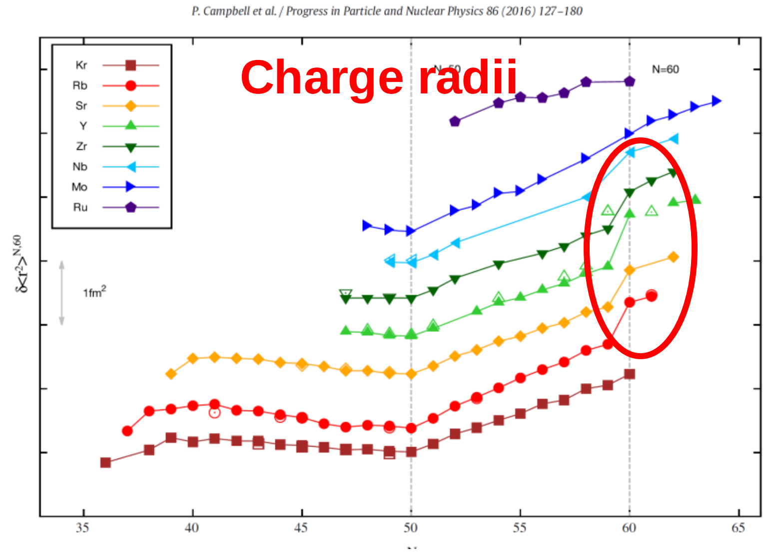

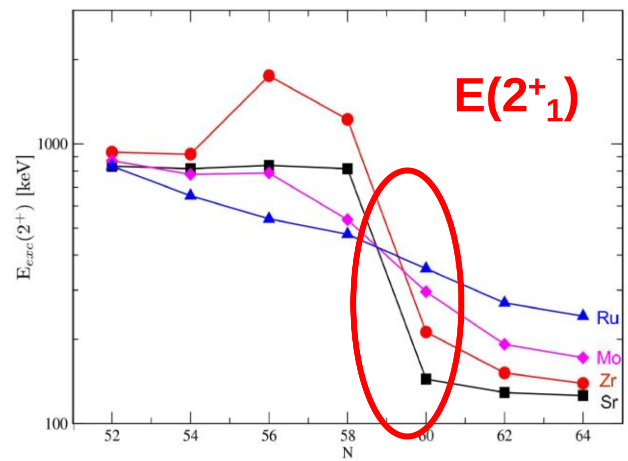

All three observables clearly confirm an onset of deformation at N=60

Introduction to Evolution of Collectivity: Systematics of $E(2^+_1)$ energies

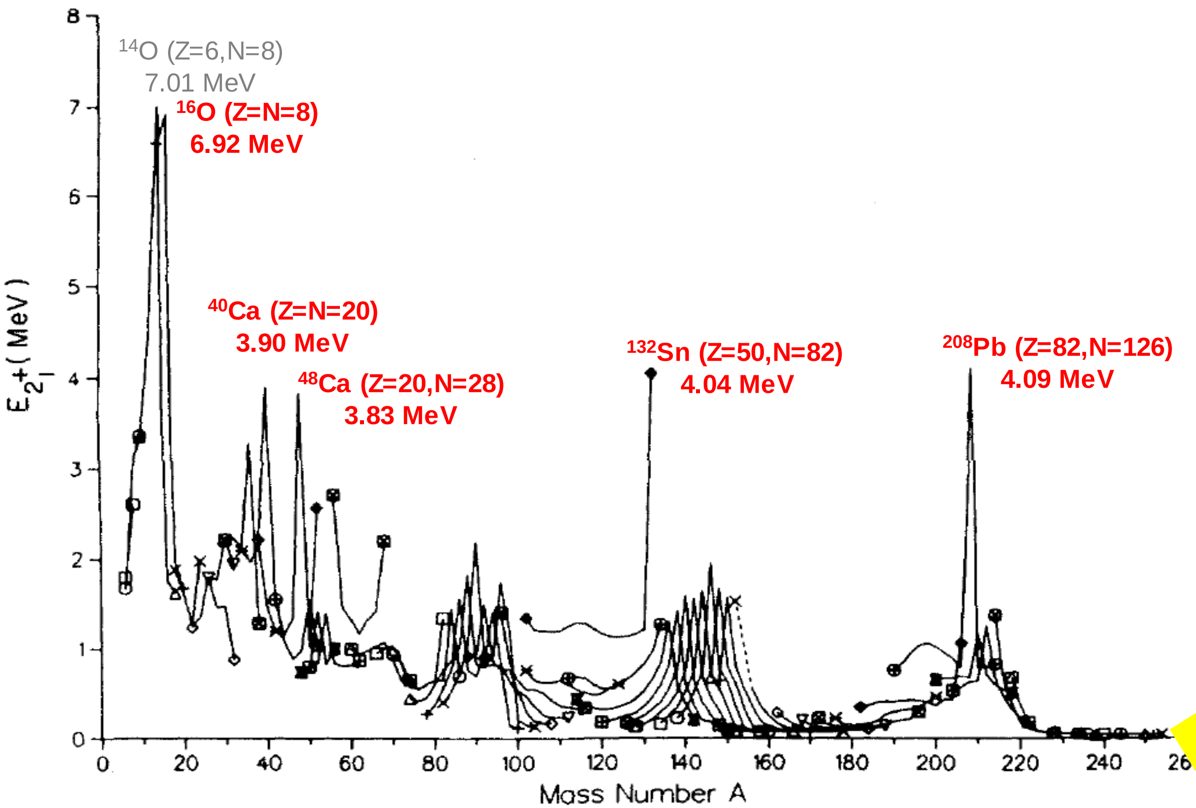

Fig. 2.12. $E_{2_1^+}$ values for all even–even nuclei (Raman, 1987).

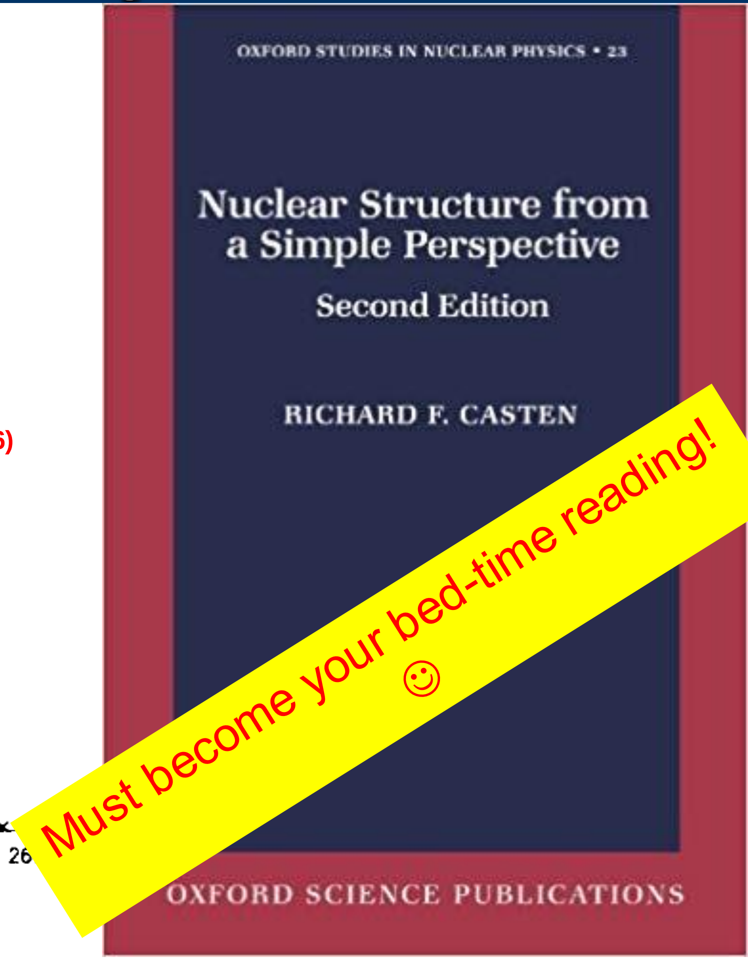

Systematics of $E(2^+_1)$ energies: Except for very high values for doubly-magic nuclei, not simple to see systematic features if plotted against mass number A=>plot as a function on N and Z


Phys. Scr. 91 (2016) 033004 (24pp) doi:10.1088/0031-8949/91/3/033004

Invited Comment **Highly-recommended to read!**

The evolution of collectivity in nuclei and the proton–neutron interaction

R F Casten[1,3] and R B Cakirli[2]

Introduction to Evolution of Collectivity: Systematics of E(2$^+_1$) energies

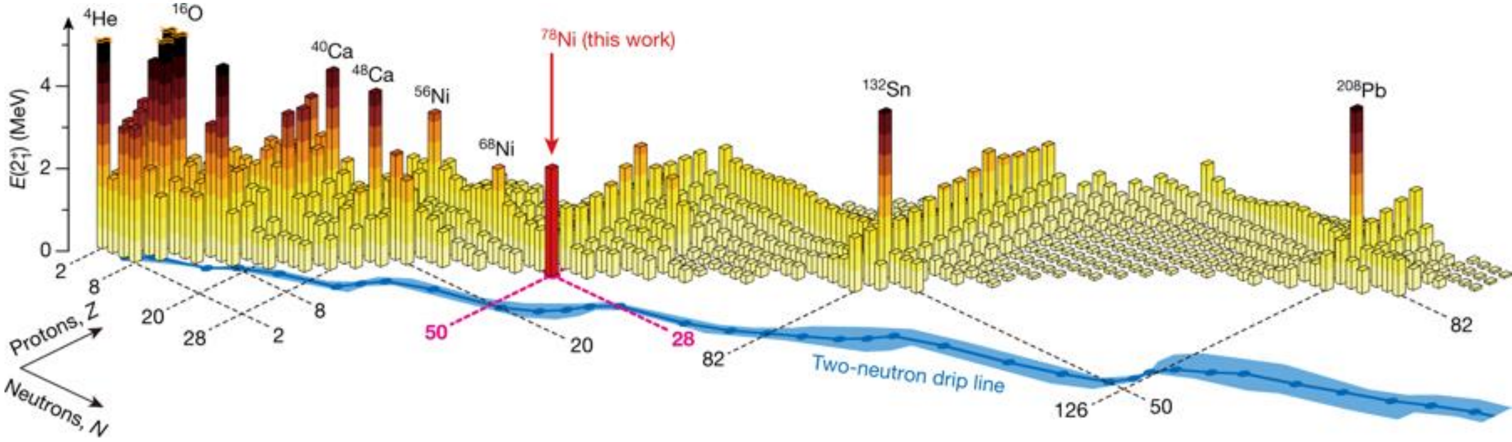

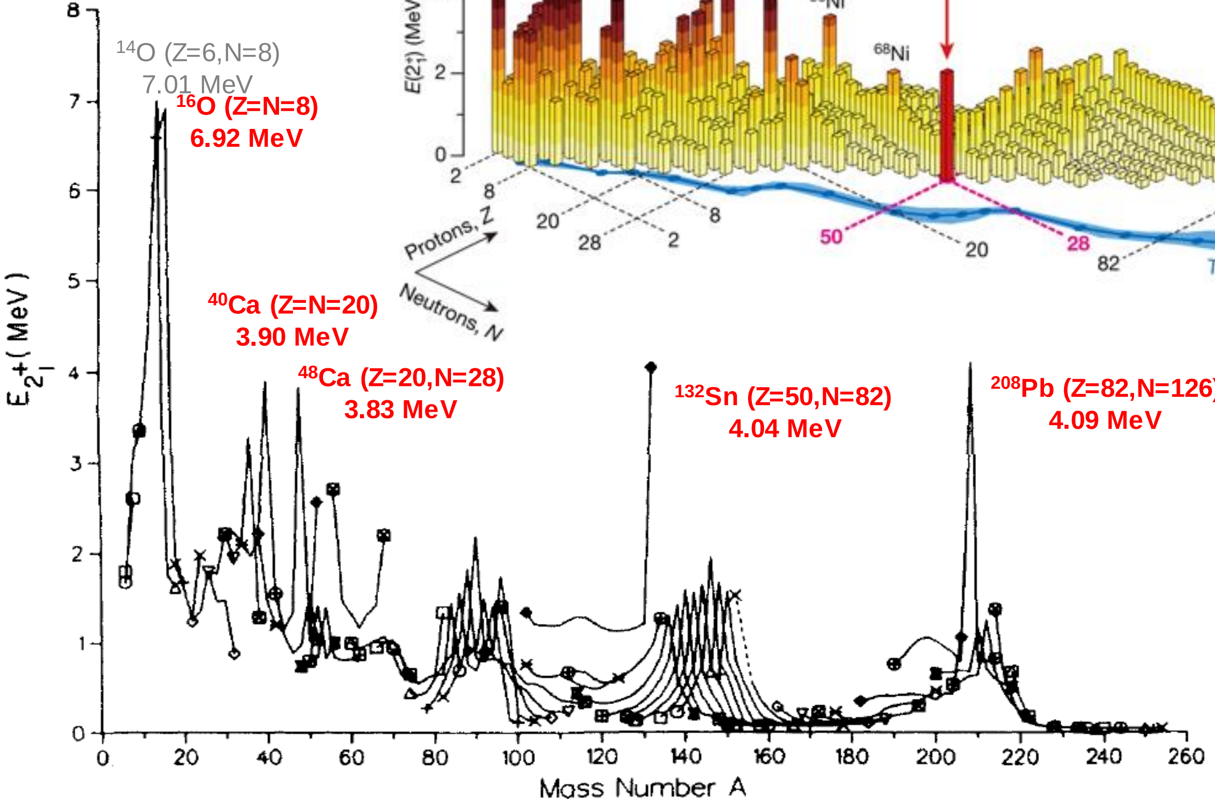

Fig. 2.12. $E_{2^+_1}$ values for all even–even nuclei (Raman, 1987).

Systematics of E(2$^+_1$) energies: Except for very high values for doubly-magic nuclei, not simple to see systematic features if plotted against mass number A=> plot as a function on N and Z

Introduction to Evolution of Collectivity: Systematics of $E(2^+_1)$ energies

R F Casten and R B Cakirli 2016 *Phys. Scr.* **91** 033004

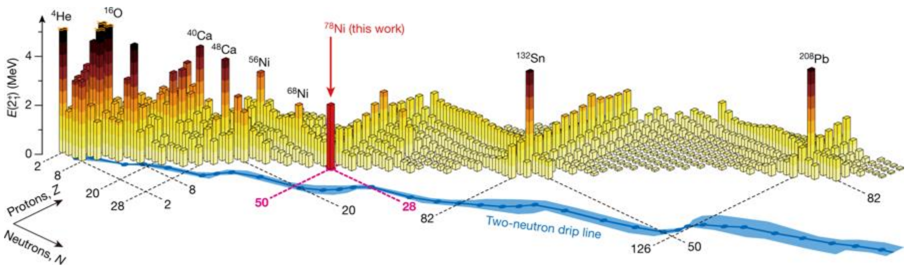

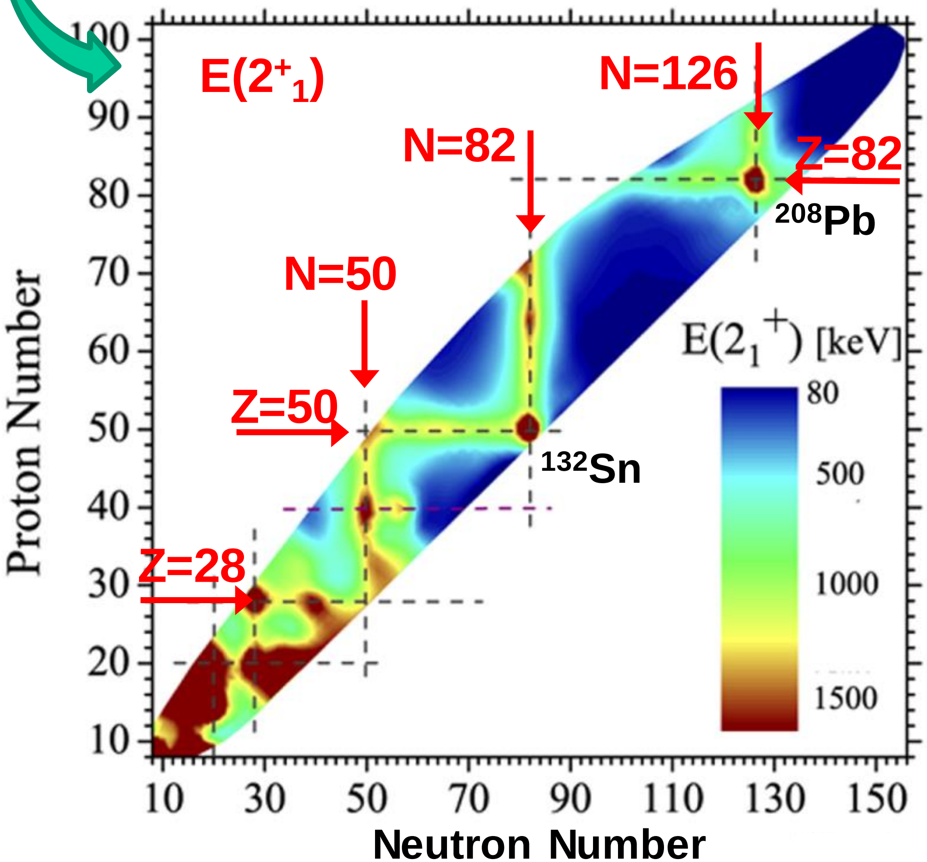

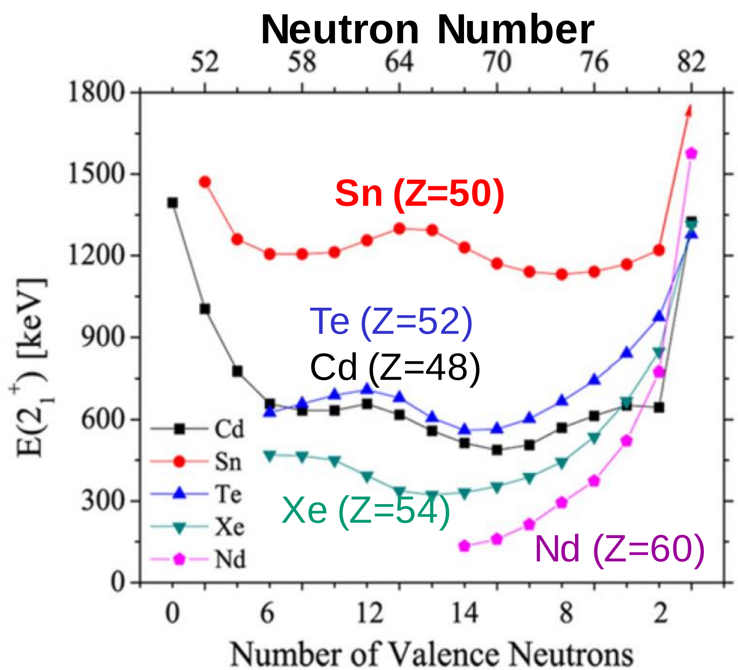

Figure 3. $E(2^+_1)$ energies for nuclei in the Sn region within the $N = 50$–82 shell showing the lower values (greater collectivity) for a given neutron number the greater is the number of valence protons.

NB: High $E(2^+_1)$ values at doubly and singly-magic nuclei (however, the argument is not fully valid for light nuclei)

Disappearance of N=20 and N=28 in the Mg-Ca region?

R F Casten and R B Cakirli 2016 *Phys. Scr.* **91** 033004
^{54}Ca: D. Steppenbeck et al., Nature 502, 207 (2013)
^{40}Mg: H. Crawford et al., Phys. Rev. Letts, 122, 052501 (2019)

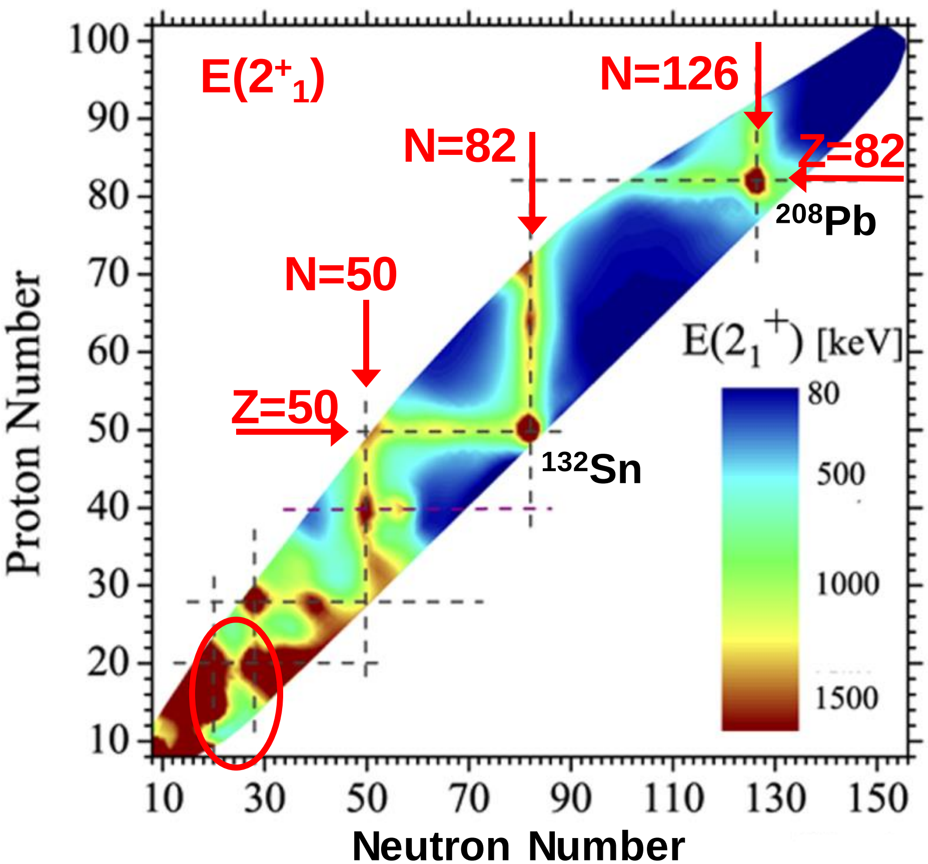

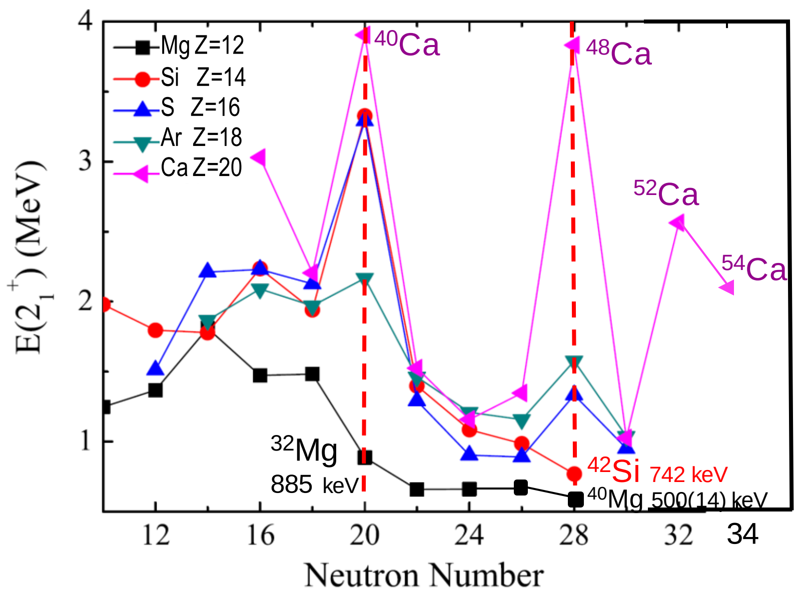

Figure 6. 2_1^+ energies in the Mg–Ca region showing the breakdown of $N = 20$, 28 as magic numbers for certain elements: Mg at $N = 20$ and for Si (and partially for S and Ar) at $N = 28$ [1].

- N=20 is good for ^{40}Ca(Z=20), but absent for ^{32}Mg(Z=12)
- N=28 is good for ^{48}Ca(Z=20), absent for Z=12,14,16,18
- However, what happens for ^{52}Ca (N=32)– again a high value, followed by a smaller value in ^{54}Ca (N=34): evidence for a new magic number at N=32? (We will look in all this via other observables, e.g. charge radii and masses)

Introduction to Evolution of Collectivity: Systematics of $E(2^+_1)$ energies and the $4^+_1/2^+_1$ ratios

R F Casten and R B Cakirli 2016 *Phys. Scr.* **91** 033004

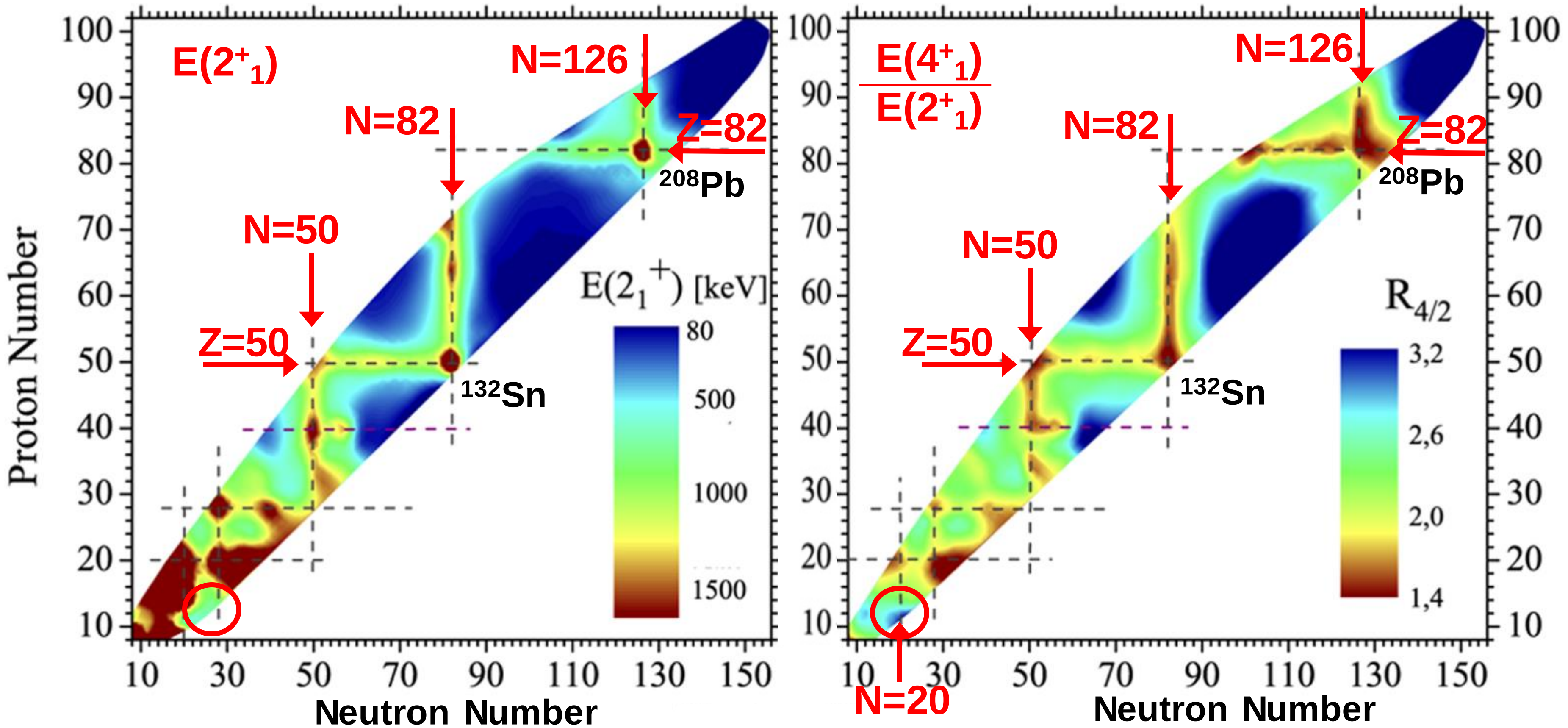

- Disappearance of N=20 magic number around ^{32}Mg (Z=12, N=20), also seen in $E(2^+_1)$ value

Figure 1. $E(2^+_1)$ (left) and $R_{4/2}$ (right) for the entire nuclear chart. The color coding varies from brown for nuclei near closed shells (large $E(2^+_1)$ and small $R_{4/2}$) to dark blue for well-deformed nuclei (small $E(2^+_1)$) and $R_{4/2}$ near the rotor value of 3.33. Note that the boundaries of these colored contours become blurred in light nuclei as new research in nuclei far from stability reveals the breakdown of the traditional magic numbers. Here and in many figures below, the data on level energies and $B(E2)$ values are taken from reference [1].

Why Some Magic Numbers change at the Limits?

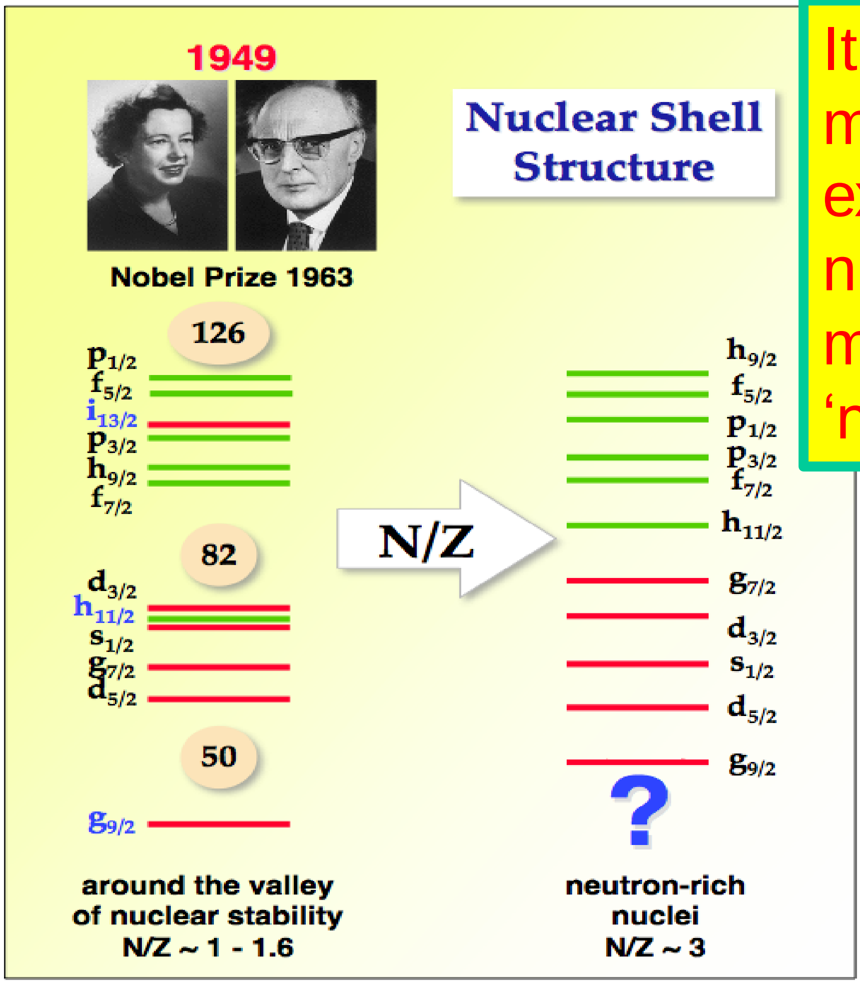

It is expected that the nuclear structure might change far from stability, for example for extremely neutron-rich nuclei. e.g. classical magic numbers may disappear (or weaken), while ‘new’ magic numbers appear.

Quiz: What could be the reasons for such changes (e.g. why N=20,28 might weaken or disappear at all in some nuclei)?

- Mean-field near stability
- Strong spin-orbital coupling
- Magic numbers N,Z=2,8,20,28,50,82,126…?

Mean-field change?
Weak spin-orbital coupling?
Diffuse surface?
Tensor interaction?

Possible Effects at the Drip Lines?

R F Casten and R B Cakirli 2016 *Phys. Scr.* **91** 033004

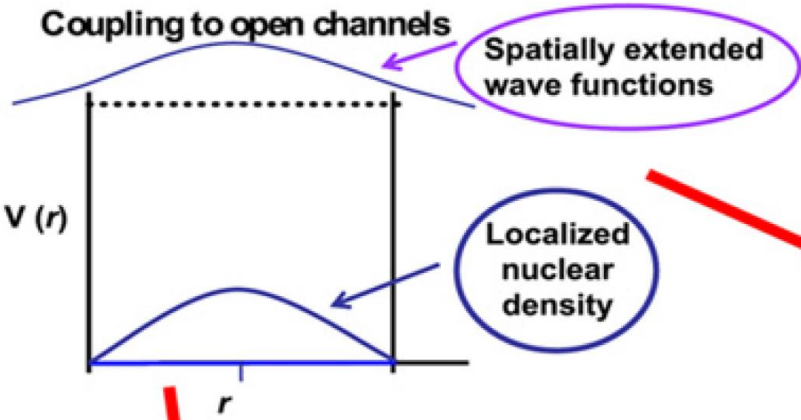

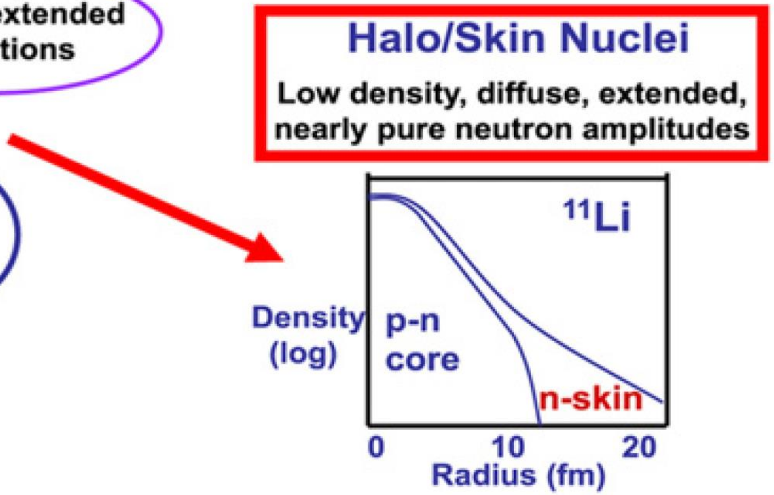

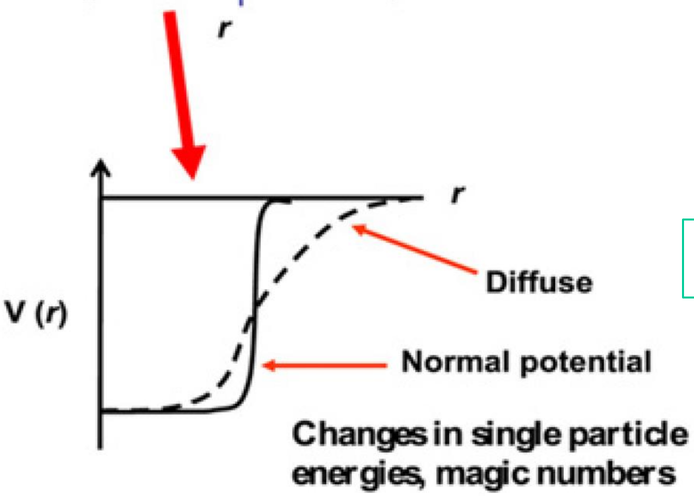

Weak binding

Quiz: What are the possible effects of the diffuseness of the potential? (a hint: what happens to LS-coupling?)

(Homework!) Cartoon of some new features in exotic nuclei with proton/neutron ratios far from those near stability and with one kind of particle filling to the top of the independent particle model potential. The **weak binding leads to diffuse nuclear surfaces** that can change the potential itself, and therefore shell structure. An excess of one kind of **weakly bound particle can also lead to halo structure** extending to very large radii. In heavier nuclei, **neutron skins may develop**. The figure also indicates the importance, near the drip lines, of taking into account coupling to the continuum. In addition to these effects, residual interactions, such as the pairing and proton–neutron interactions can have a major effect on structure, magic gaps, and collectivity.

Change of the neutron central potential?

Proton-rich ^{100}Sn (N=Z=50) vs Neutron-rich ^{100}Zr (Z=30, N=70)

J. Dobaczewski et al, PRL72 (1994)

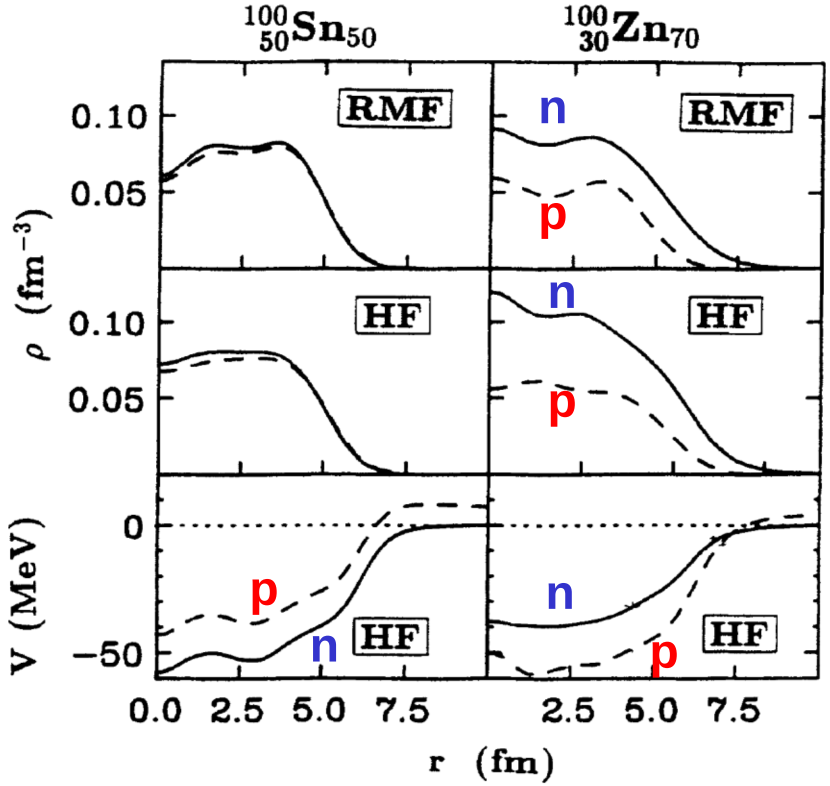

FIG. 1. Top: Single-particle nucleonic densities of the NL1 RMF model for the $A = 100$ drip-line nuclei, ^{100}Sn and ^{100}Zn (neutrons: solid line, protons: dashed line). Middle (bottom): corresponding single-particle densities (central potentials) of the SkP HF approach.

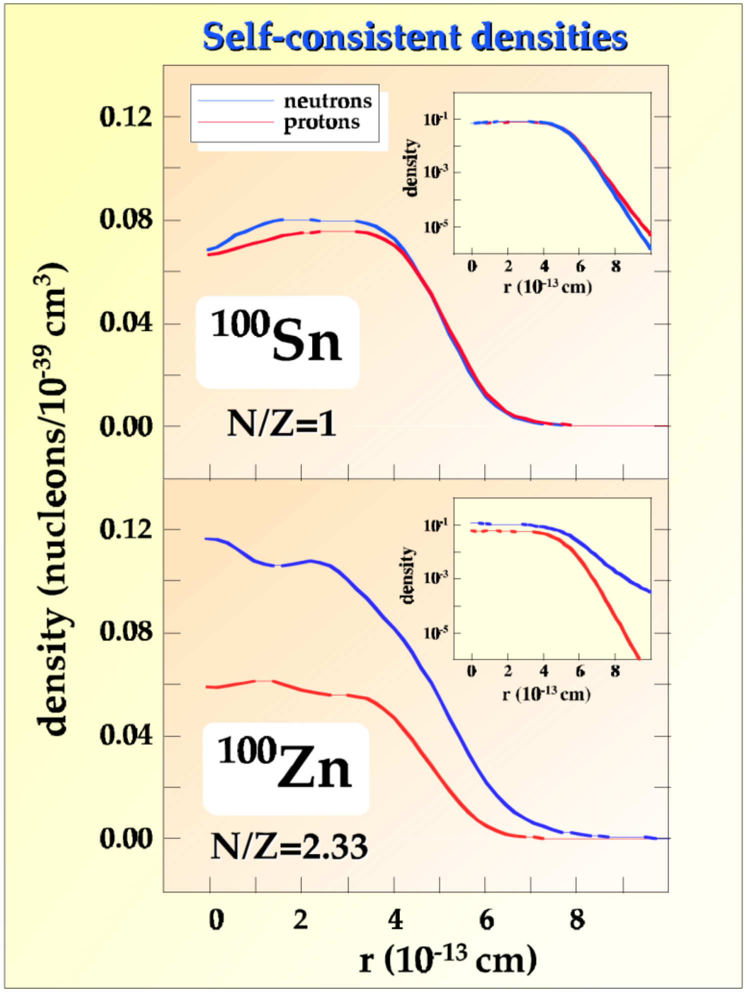

- Nearly identical densities/potentials for protons and neutrons in ^{100}Sn (N=Z=50), (Coulomb needs to be accounted for protons, of course)
- Shallower neutron potential in neutron-rich ^{100}Zn (cf to ^{100}Sn!)
- Development of halo-like tail for neutrons in ^{100}Zn (see insets in log-scale on the RHS)

Neutron Skins/Halos?

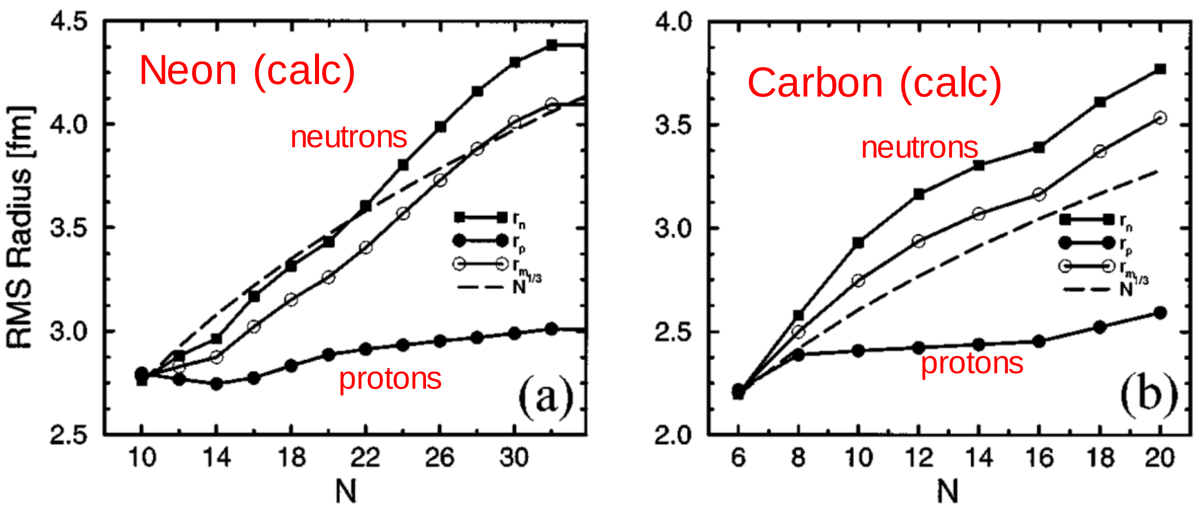

FIG. 1. Calculated rms radii for Ne (a) and C (b) isotopes as function of neutron number.

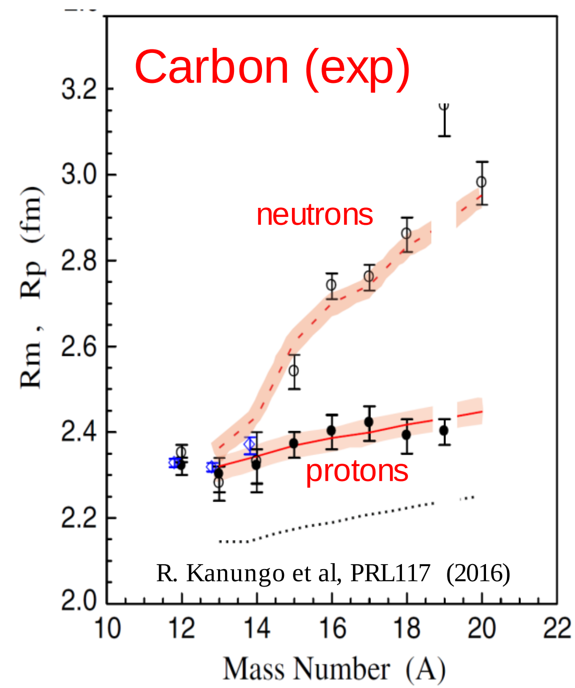

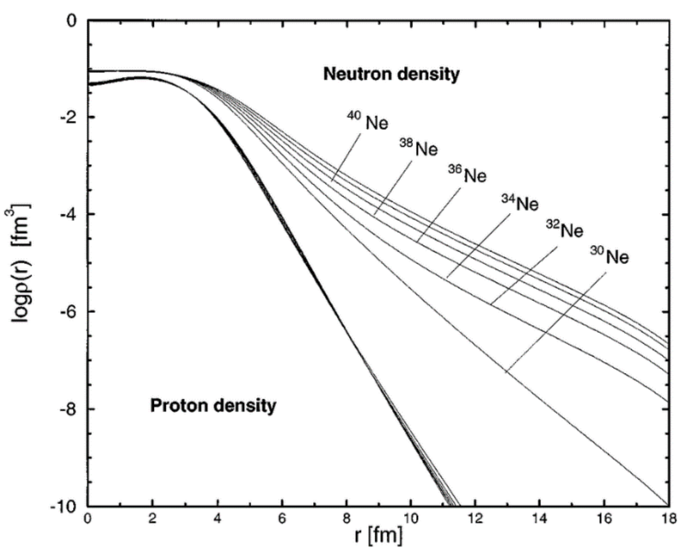

W. Pöschl et al, PRL79 (1997)

- Note the **constancy of proton radius/density**
- **Gradually increasing neutron tail** (halo) for more neutron-rich isotopes

We will discuss charge radii measurements later on (can also discuss matter radii measurements, if time allows)

Topic I: Radii, Shapes and Shape Coexistence

Or is $R=r_oA^{1/3}$?

(as it is said in all textbooks)

RIBs: Breaking Old Rules in Nuclear Physics: is $R=r_oA^{1/3}$?

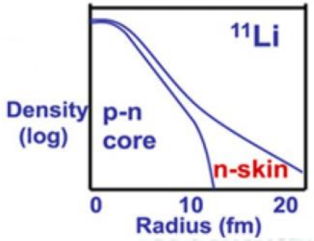

^{11}Li (halo nucleus)

^{48}Ca

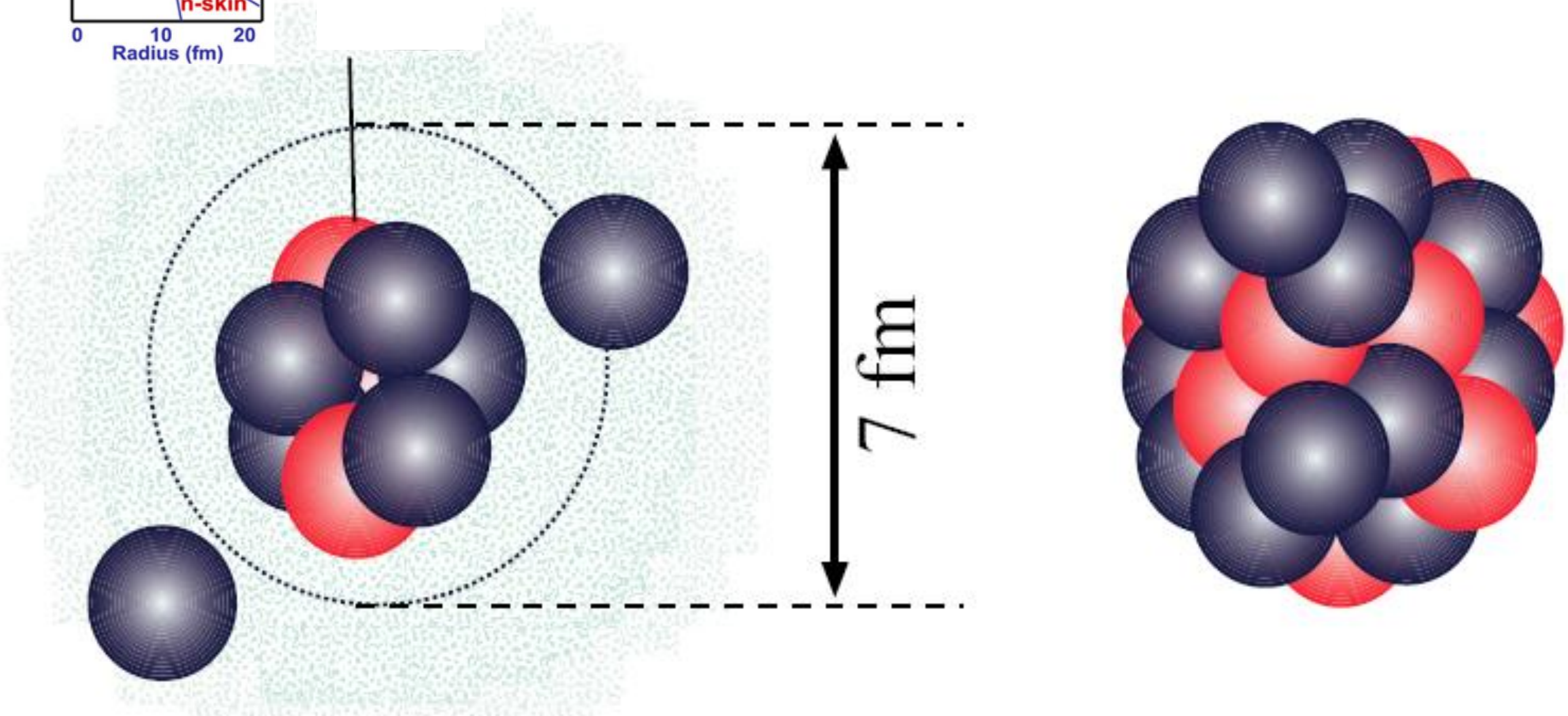

If $R=r_oA^{1/3}$ then $D(^{48}Ca)/D(^{11}Li)=2*(48/11)^{1/3}\sim3.2$

Quiz: How can one measure the radius (matter or charge) of a nucleus? (How was it done in the past, how we can do it now?)

Traditional Techniques to Measure Charge Radii/Densities of Nuclei

1915-1990

ROBERT HOFSTADTER

The electron-scattering method and its application to the structure of nuclei and nucleons

Nobel Lecture, December 11, 1961

https://www.nobelprize.org/uploads/2018/06/hofstadter-lecture.pdf
Review of Modern Physics, 28,1956

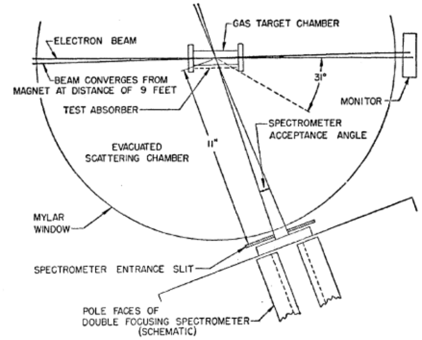

FIG. 17. Schematic diagram of scattering geometry employed with the gas target chamber.

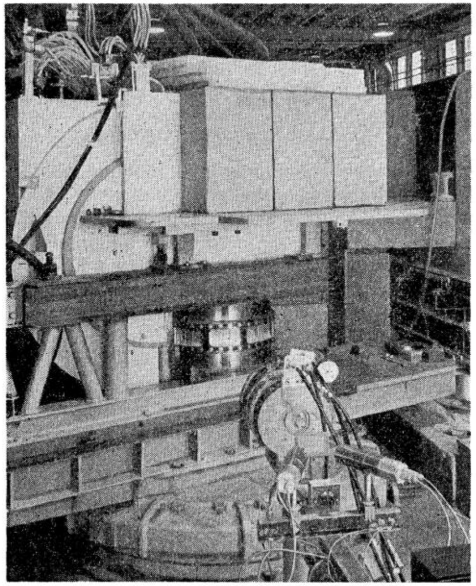

FIG. 15. The semicircular 190-Mev spectrometer, to the left, is shown on the gun mount. The upper platform carries the lead and paraffin shielding that encloses the Čerenkov counter. The brass scattering chamber is shown below with the thin window encircling it. Ion chamber monitors appear in the foreground.

Electron Angular Distribution

also as a function of e^- energy

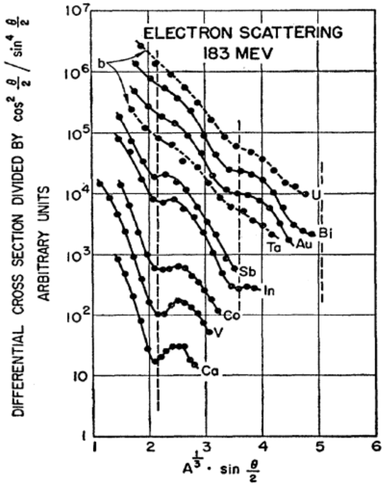

Charge Distribution

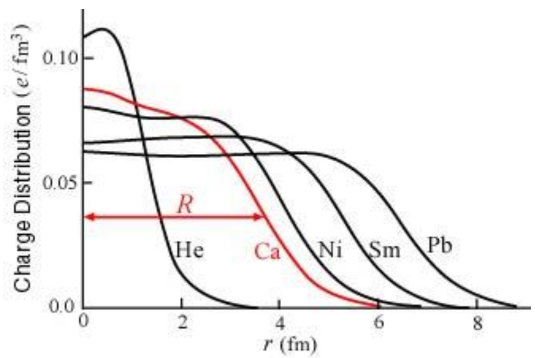

$$\rho(r) = \frac{\rho_0}{1 + e^{(r-R)/a}},$$

r = distance from the center

Charge Radius R

$R = r_o A^{1/3}$

- **Measurements of Muonic X rays** – also charge distributions
- **Optical Isotope Shift (IS) measurements** for stable isotopes – provide radius

- Electron scattering/Muonic X rays **provided absolute charge radii/densities for all stable isotopes**, but both methods require **large amount of material** (often ~ many milligrams)

- **Modern experiments with RIBs allow the use of Isotope Shifts measurements for short-lived nuclides, up to ~ a few ms (depends on intensity), up to 0.01 pps!**
- **Also, the electron scattering on RIBs in colliding geometry started (SCRIT@RIKEN)**

RIBs: Breaking Old Rules in Nuclear Physics: is $R=r_oA^{1/3}$?

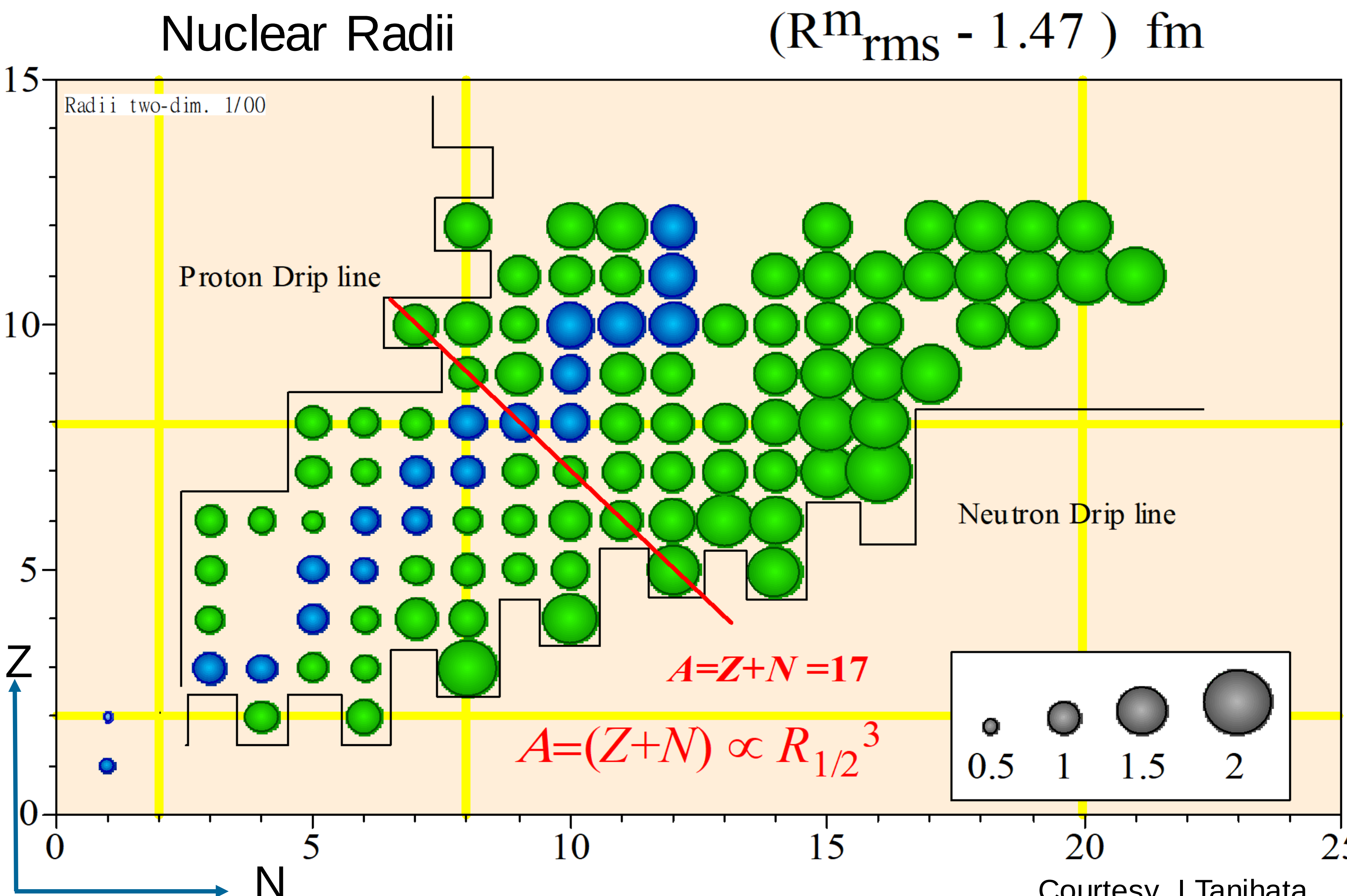

Courtesy I.Tanihata

Shapes and Deformations of Atomic Nuclei

Moller Chart of Nuclides 2000
Ground state β_2 deformation
http://ie.lbl.gov/systematics

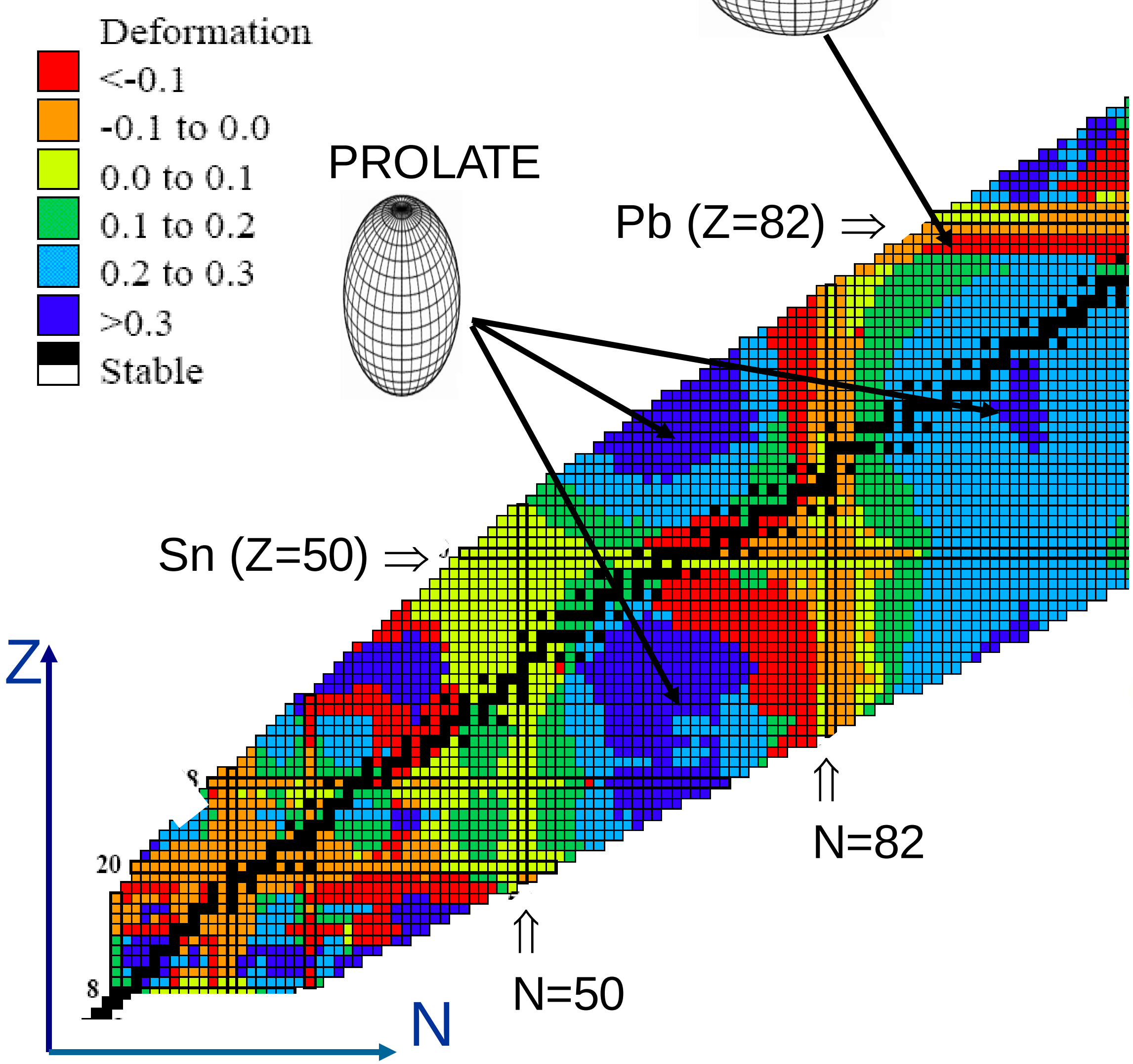

Superdeformation
Hyperdeformation

Jacobi shapes

Triaxial shapes
3-dimensional rotation

Higher-order shapes
(with high-rank symmetrie)
tetrahedral, octahedral

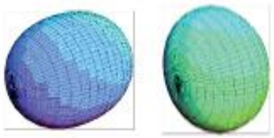

Shape coexistence

dynamic deformation
vibrations etc.

Pear-Shaped Nuclei?

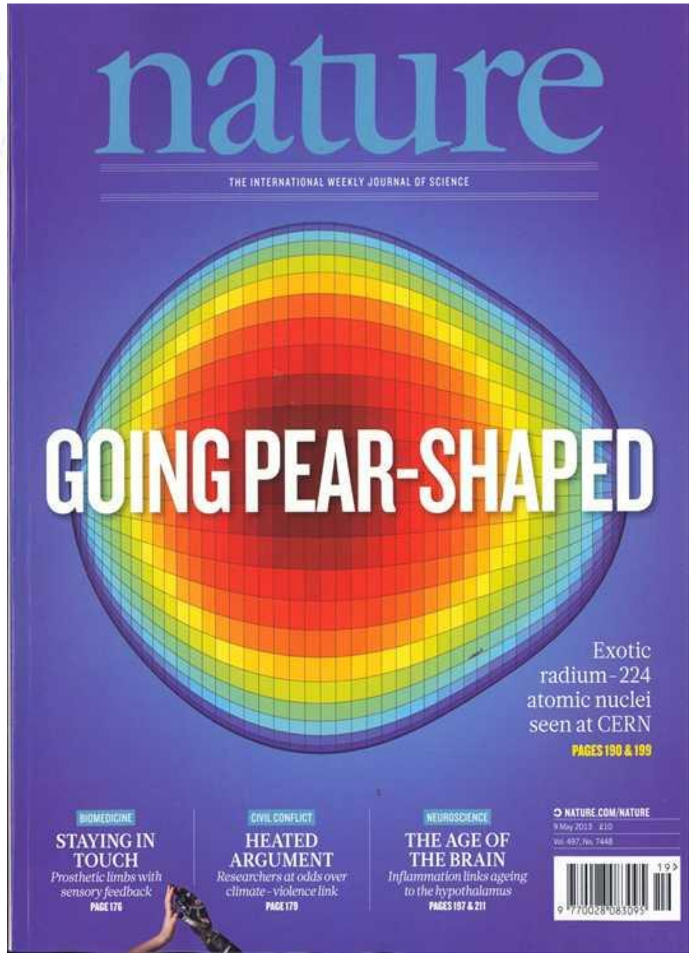

Studies of pear-shaped nuclei using accelerated radioactive beams
L. P. Gaffney et al. Nature 497, 199 (09 May 2013)

Shape Coexistence in Nuclei
(a brief introduction)

Spherical Doubly-Magic ^{16}O (Z=N=8)

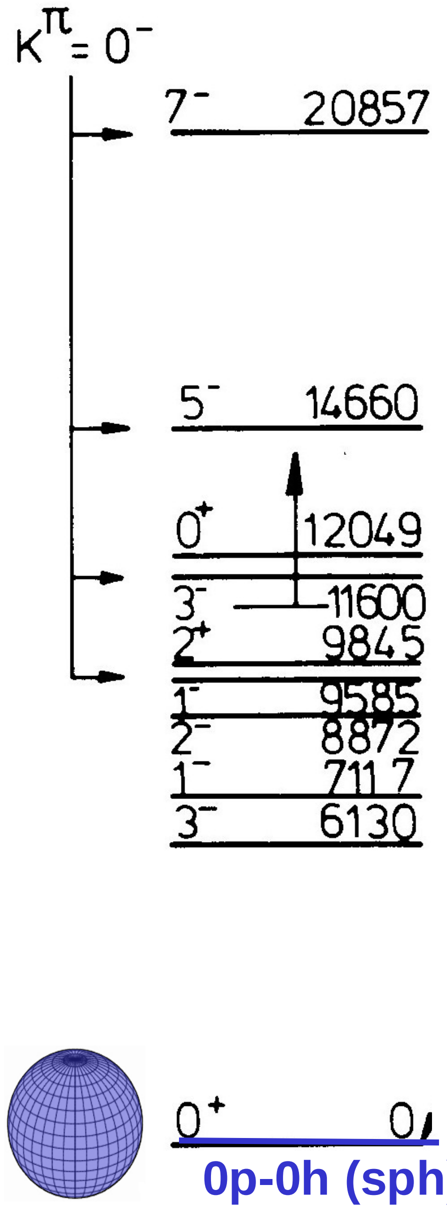

0p-0h (sph)

H. Morinaga, Phys. Lett., 101, 254(1956)

Ground State 0p-0h Spherical configuration

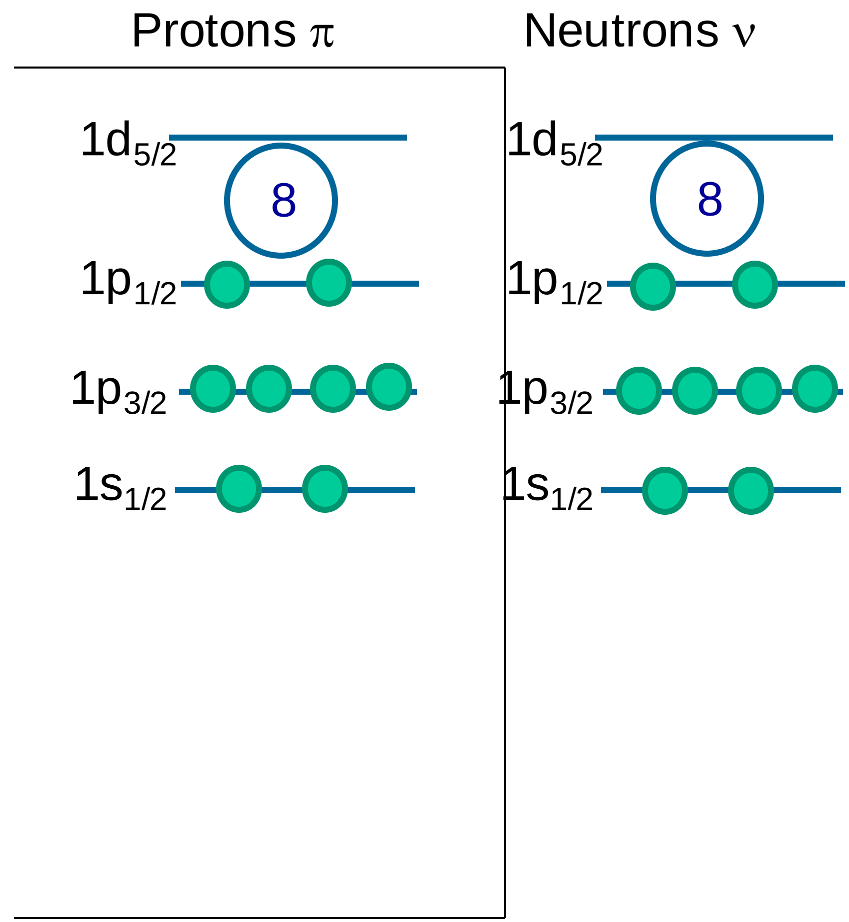

Rotational Band in Doubly-Magic ^{16}O?

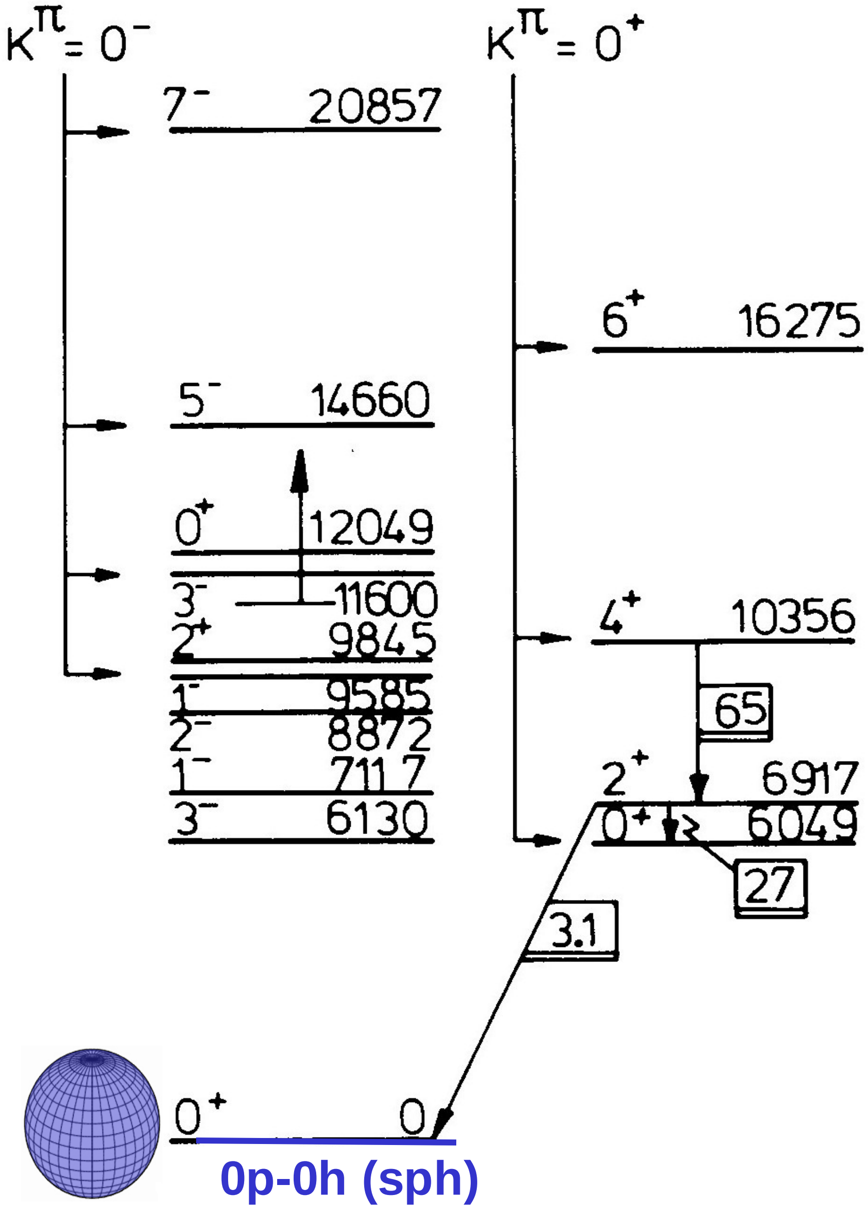

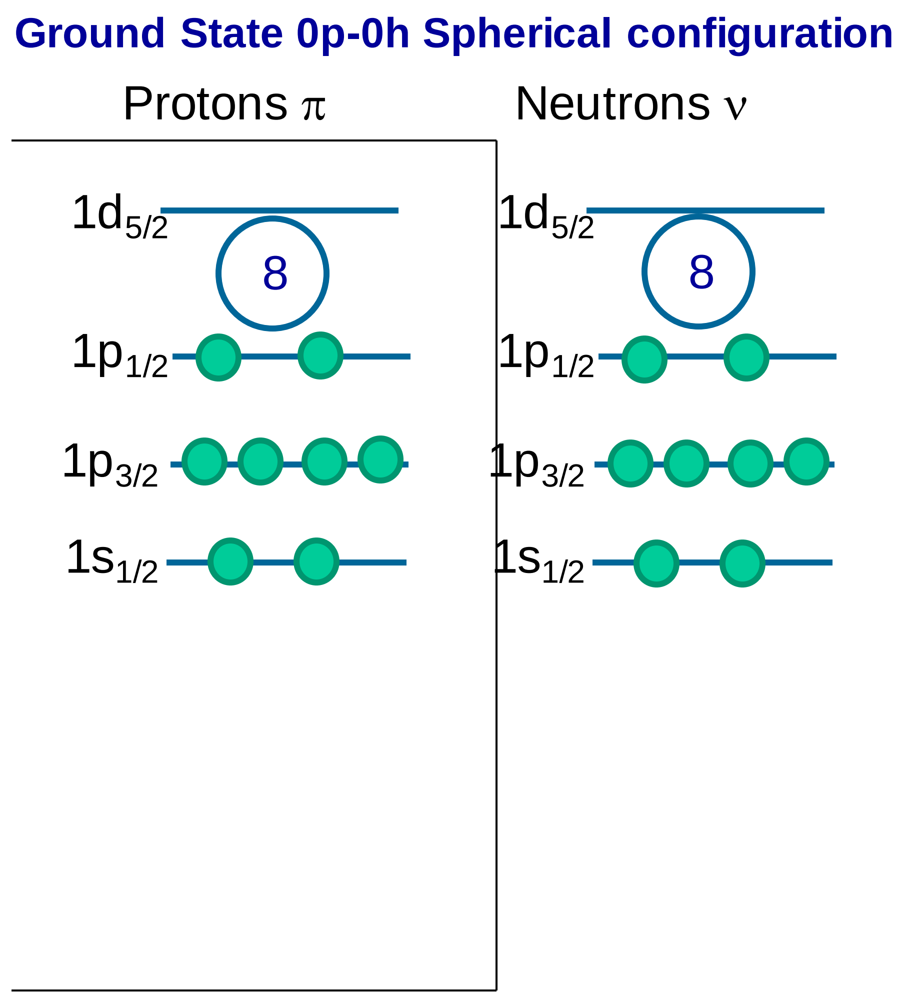

H. Morinaga, Phys. Lett., 101, 254(1956)

Shape Coexistence in Doubly-Magic ^{16}O (Z=N=8)
(intruder states)

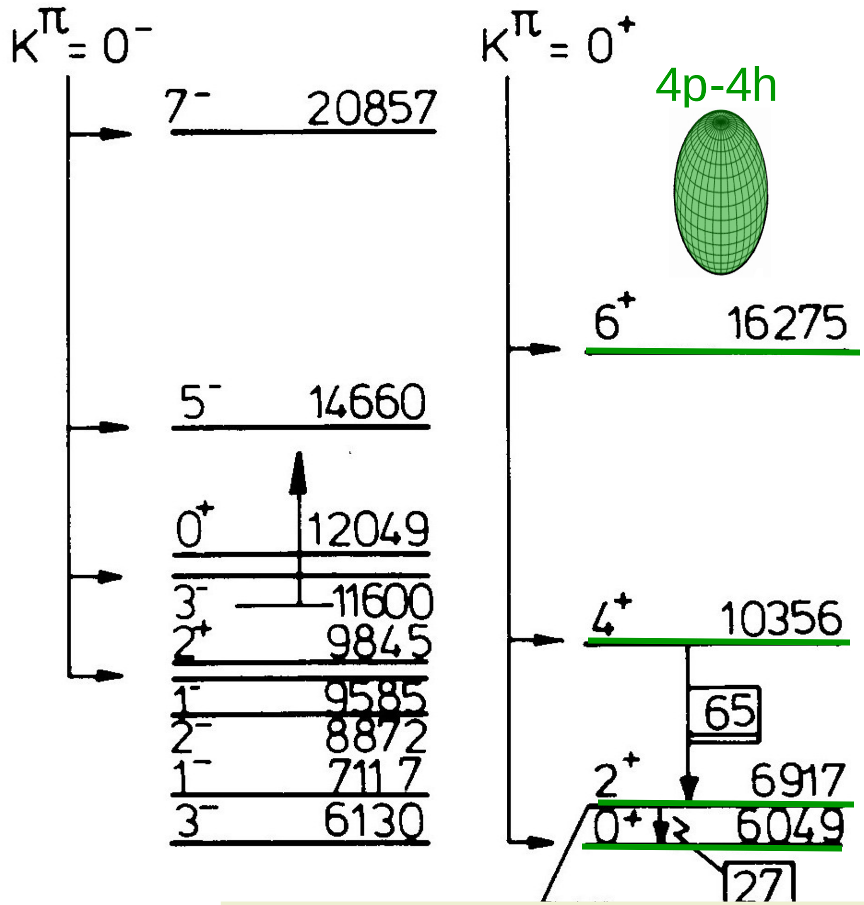

0⁺ Ground State 0p-0h Spherical configuration

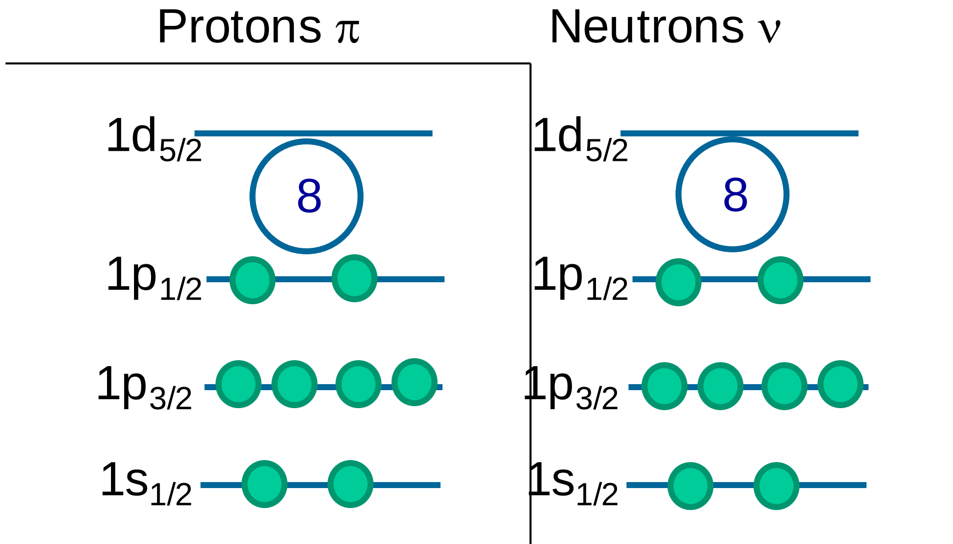

0⁺ Excited State 4p-4h Deformed configuration

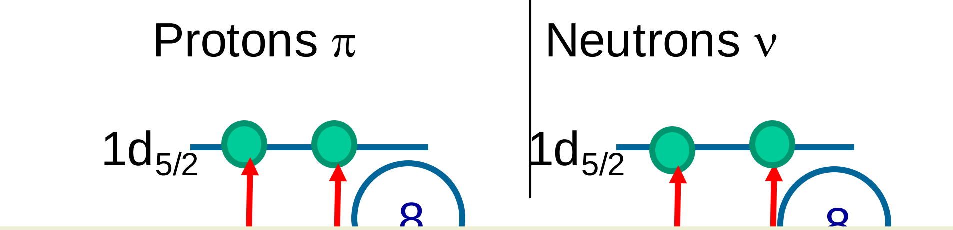

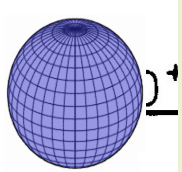

Shape Coexistence: coexistence of two or more configurations in the same atomic nucleus (so, the same N and Z)

H. Morinaga, Phys.

3 coexisting shapes in Doubly-Magic ^{40}Ca (Z=N=20)

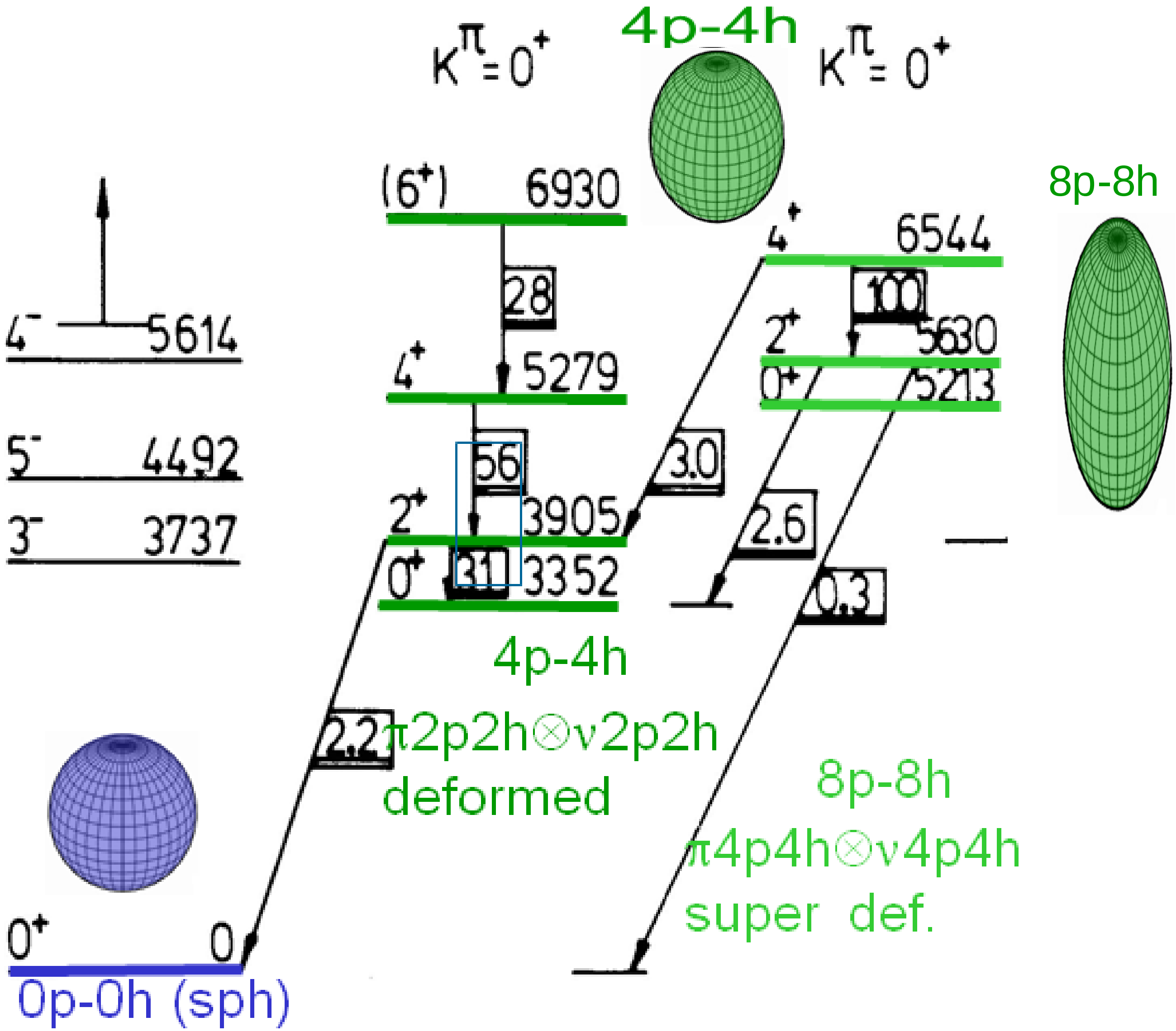

Shape coexistence around closed proton and/or neutron shells (and subshells)

- spherical and deformed structures co-exist in the nucleus at low energy
- its study can contribute in finding a unified description for atomic nuclei
- supplies information about the mixing between these configurations

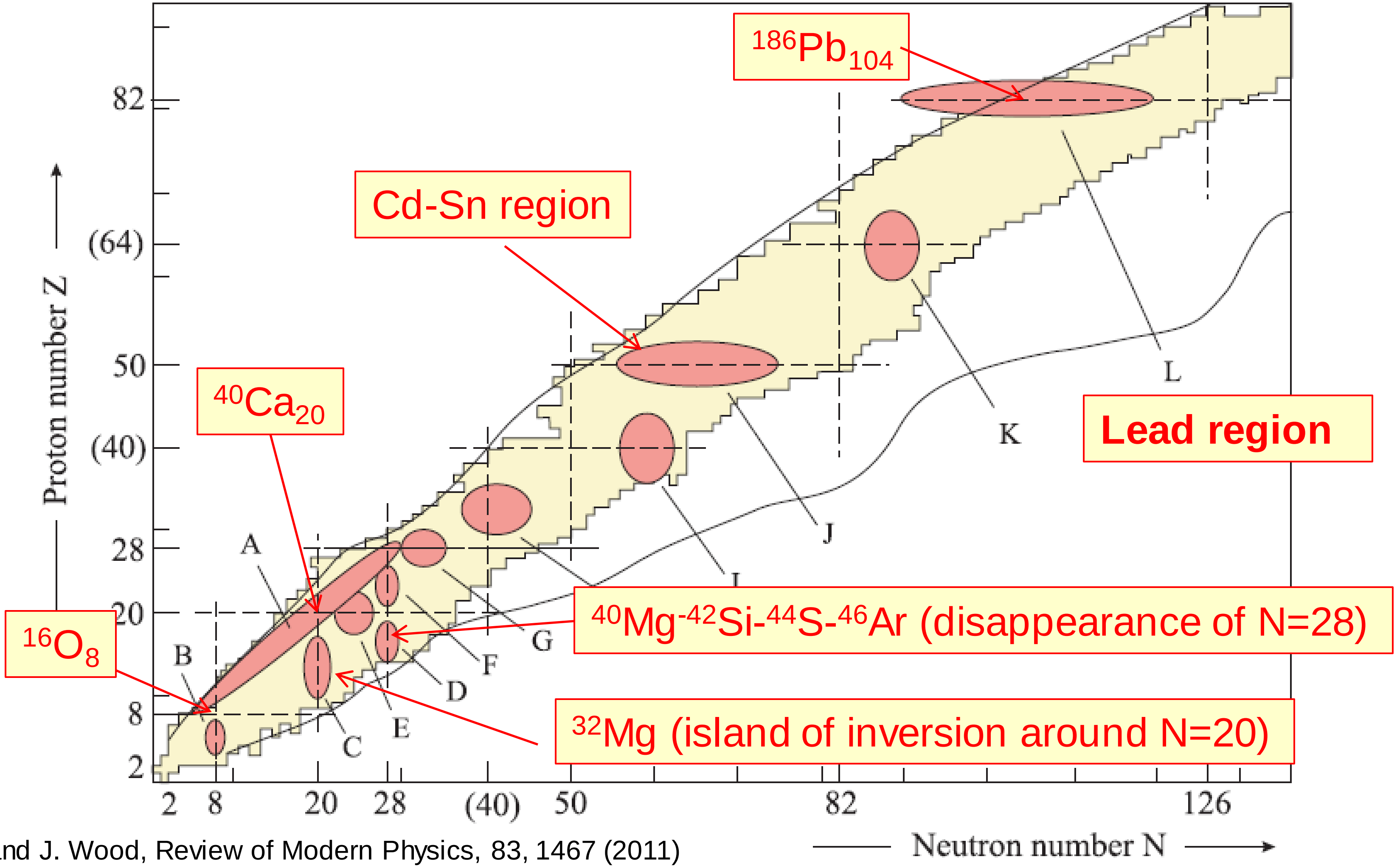

K. Heyde and J. Wood, Review of Modern Physics, 83, 1467 (2011)

Experimental Probes

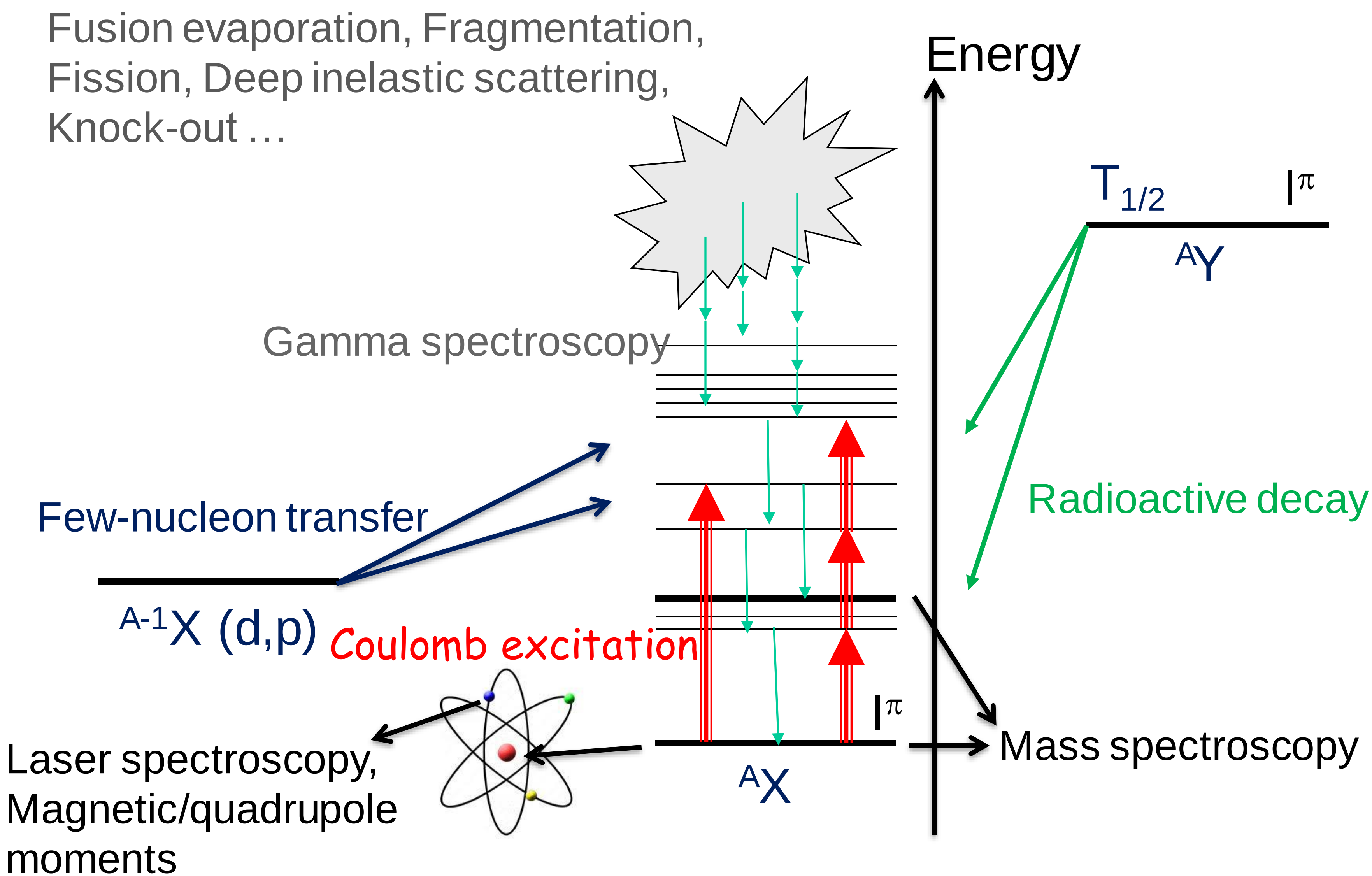

Case 1: Laser-assisted Nuclear Spectroscopy Studies in the Lead (Z=82) Region at ISOLDE-CERN

(nice physics with modern experimental techniques)

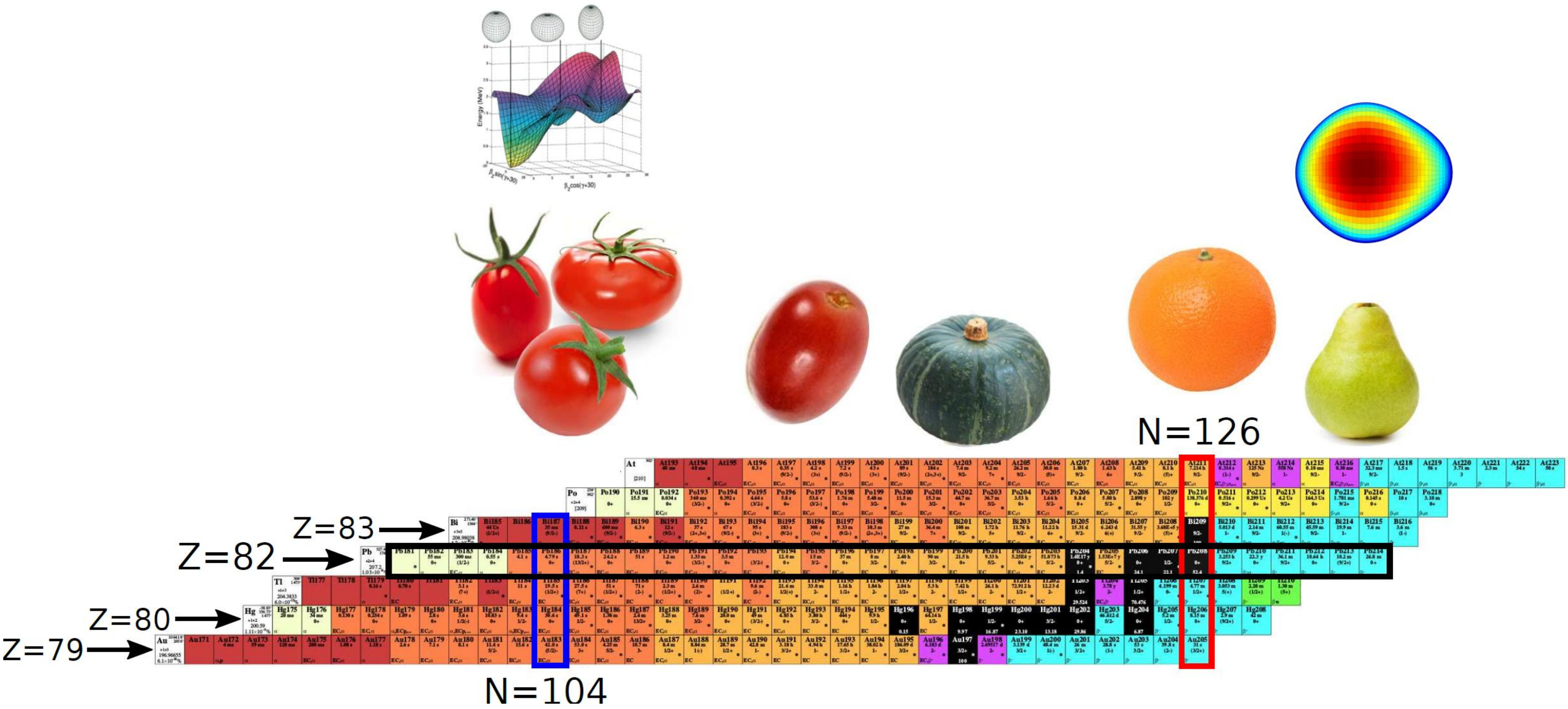

- Shape coexistence around N~104 (coexistence of several shapes)
- Sphericity around N=126, kink in radii, high-spin isomers
- Octupole effects around N~132, inverse odd-even radii staggering

Progress in Particle and Nuclear Physics 86 (2016) 127–180

Contents lists available at ScienceDirect

Progress in Particle and Nuclear Physics

journal homepage: www.elsevier.com/locate/ppnp

Review

Laser spectroscopy for nuclear structure physics

P. Campbell [a], I.D. Moore [b,*], M.R. Pearson [c]

[a] School of Physics and Astronomy, University of Manchester, Oxford Road, Ma

[b] Department of Physics, University of Jyväskylä, Survontie 9, Jyväskylä, FI-40

[c] TRIUMF, 4004 Westbrook Mall, Vancouver BC, V6T 2A3, Canada

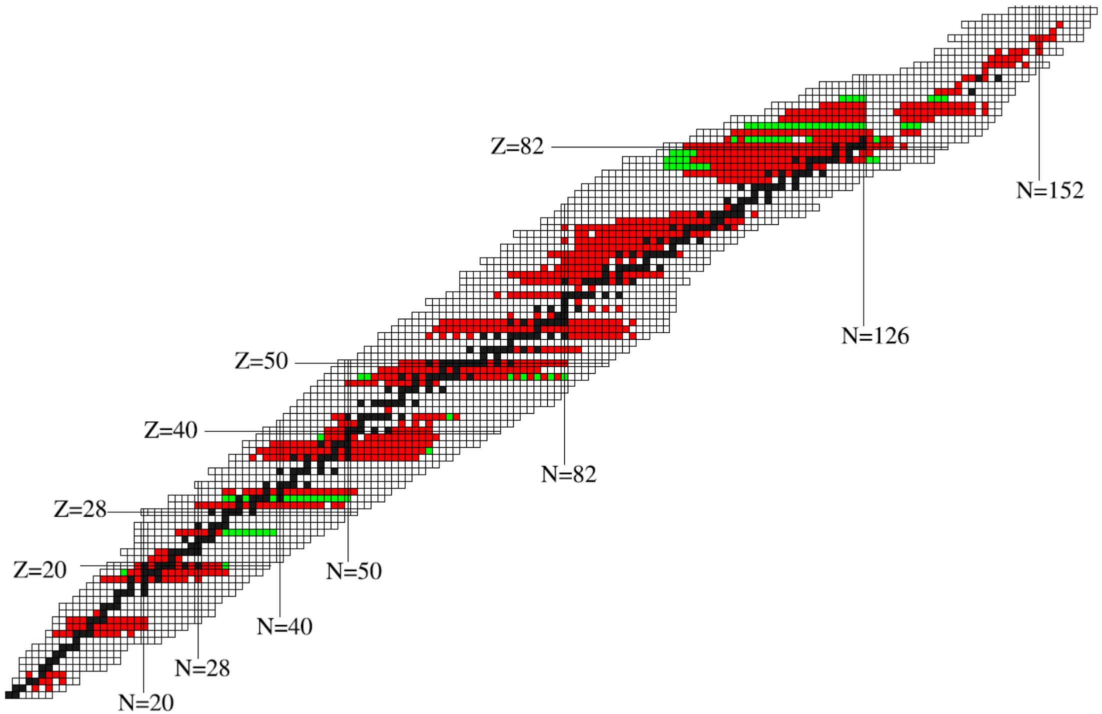

The chart of the nuclides according to optical spectroscopy. Black squares indicate the stable or very long-lived nuclei, red squares indicate optical measurements of radioactive isotopes/isomers. Isotopes coloured green are measurements for which data as of July 2015 are currently unpublished.

Pre-2003: Charge Radii in the Lead Region

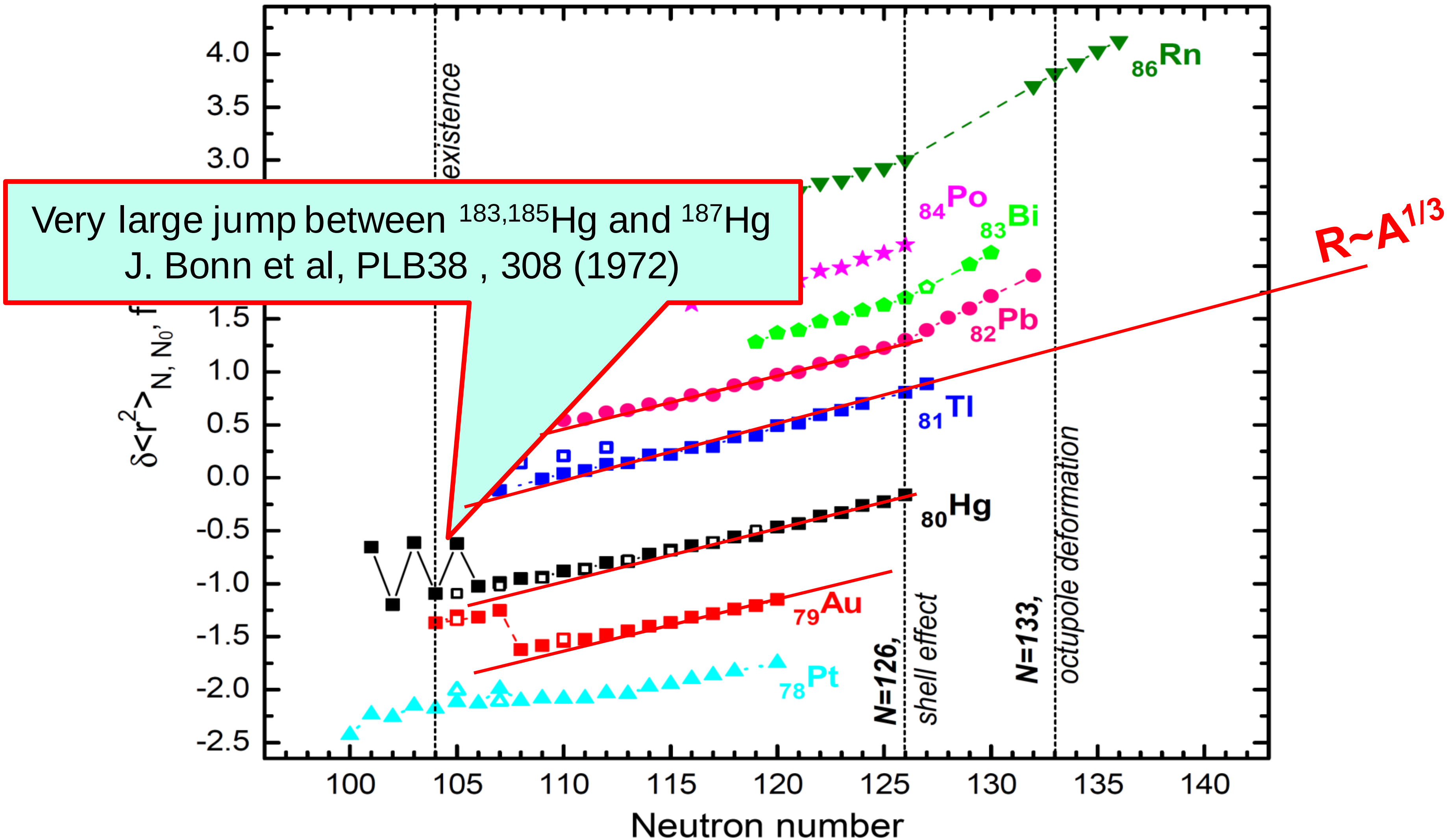

- Shape coexistence around N~104
- Sphericity around N=126, kink in radii, high-spin isomers
- Octupole effects around N~132, inverse odd-even radii staggering

Thick Targets ISOL Method: RIBs Production Reactions at ISOLDE (CERN) induced by p(1 GeV) on a thick Uranium Target

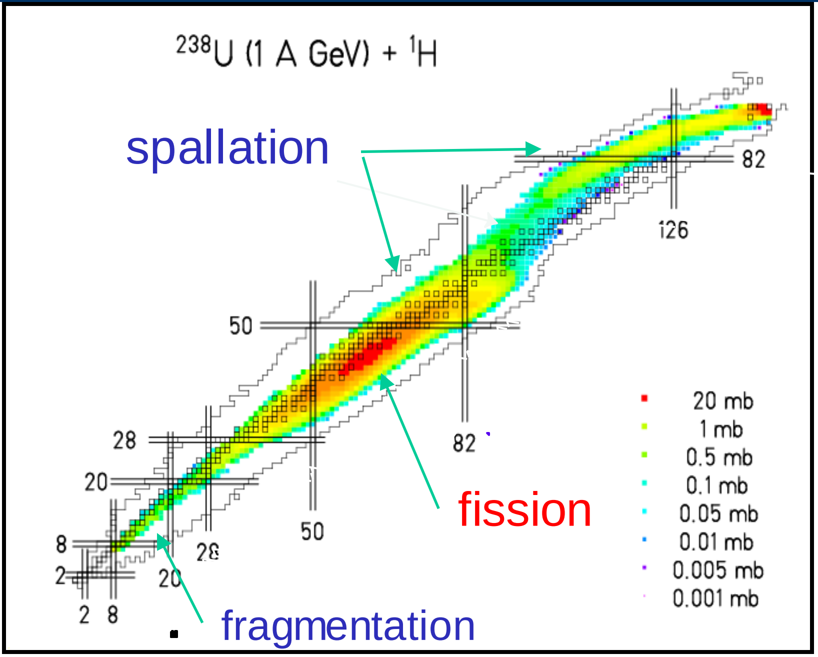

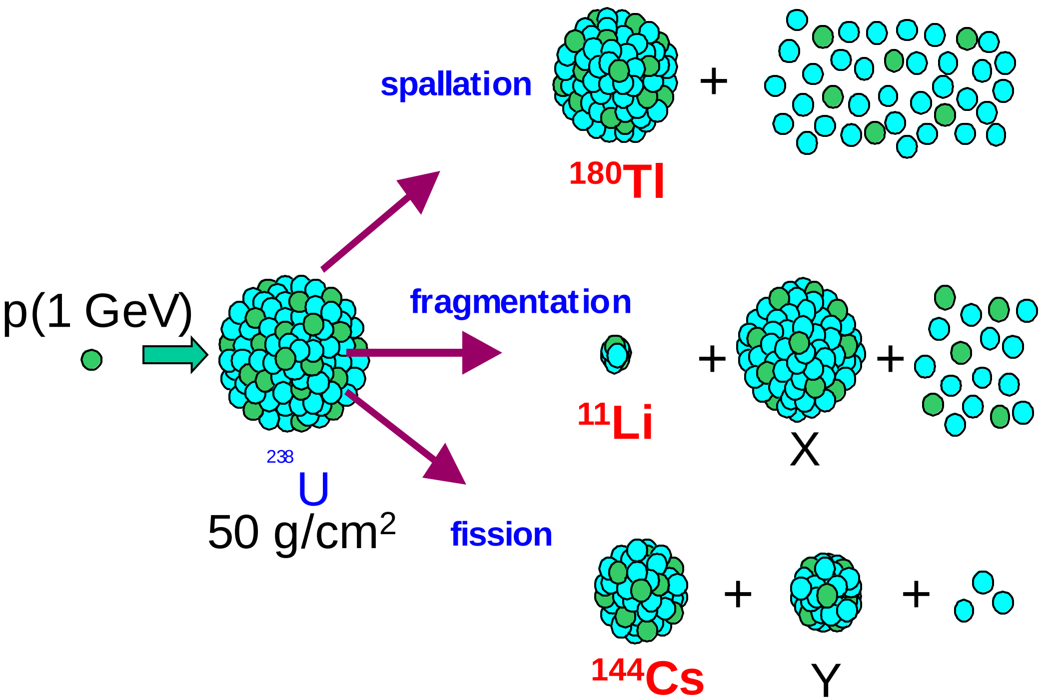

- One can use different (lighter) targets, e.g La,W to produce lighter elements
- **Chemically-selective** - not all elements can be extracted (e.g. refractory elements are difficult)
- Half-life limitations (>10-20 ms, often >100 ms), limited by diffusion through thick target
- **Hundreds of isotopes produced simultaneously, need a separator!**

Similar method is used at TRIUMF (Vancouver, Canada), they use 500 MeV protons

In-flight RIBs Production at GSI facility induced by ^{238}U beam (1 AGeV) on a 'thin' H target (similar methods at RIBF@RIKEN and FRIB@NSCL but lower energies)

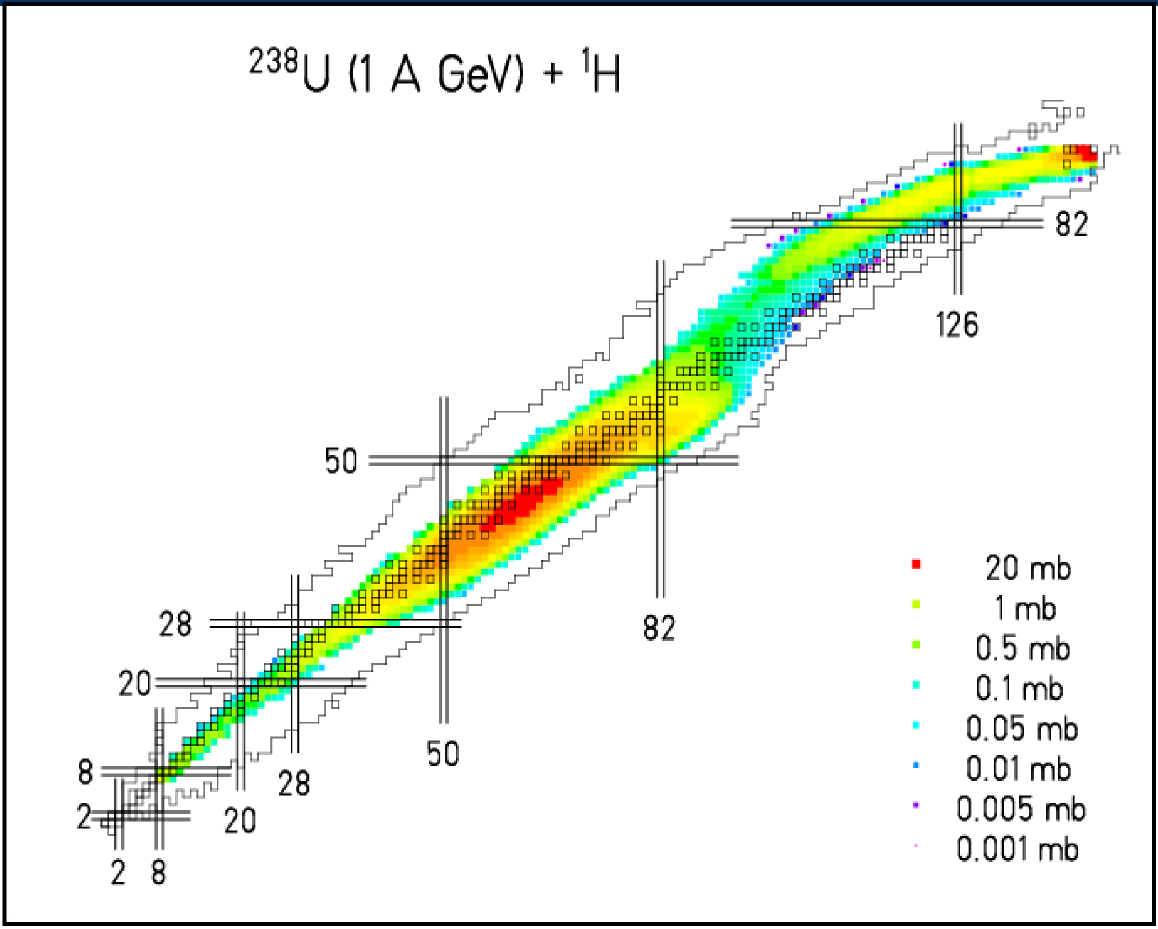

- Physics-wise: similar production mechanism as at ISOLDE and TRIUMF
- But very different experimental techniques, e.g. in-flight separators
- Relativistic RIBs energies (shortest half-lives from ~100 ns possible)
- Chemically independent (all isotopes/elements can be studied)

ISOLDE Facility (CERN, Geneva)
(example of a surface-ionization ion source)

Quiz: What are typical ionization energies of an **atom?** (e.g. H atom)
How are they compared to e.g. typical proton/neutron separation energies?

ISOLDE Target Unit

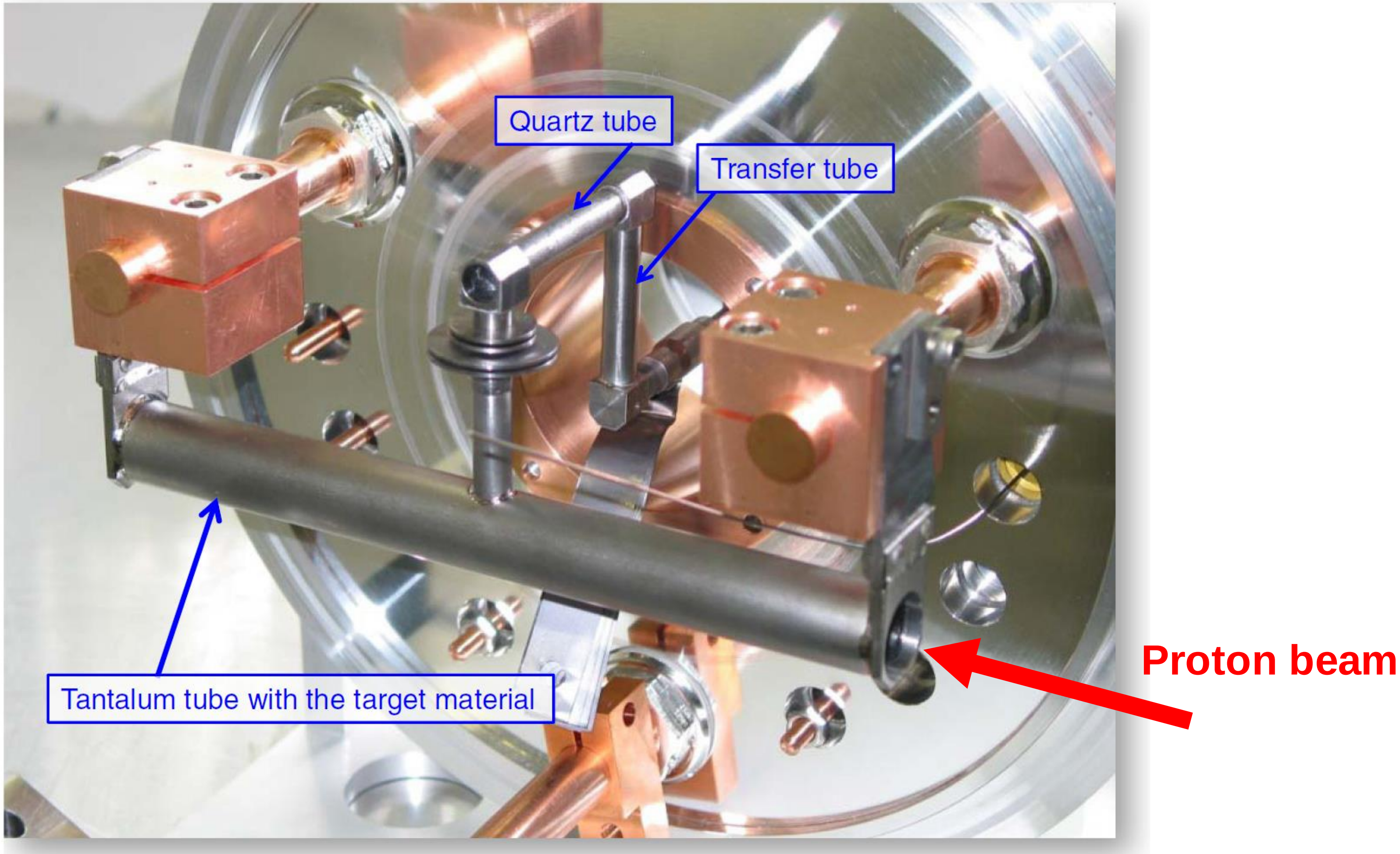

Figure 16. A photo of the ISOLDE target unit. The tantalum target container is ohmically heated. The radioactive atoms are transported to the ion source via the transfer tube. Part of the tube contains a quartz container that absorbs the rubidium atoms. This configuration was used to produce zinc beams using laser resonant ionization. Adapted from [48].

Keywords for Modern Nuclear Spectroscopy:

Selectivity (laser spectroscopy!)
Sensitivity

Selective Resonance Laser Spectroscopy of an Atom

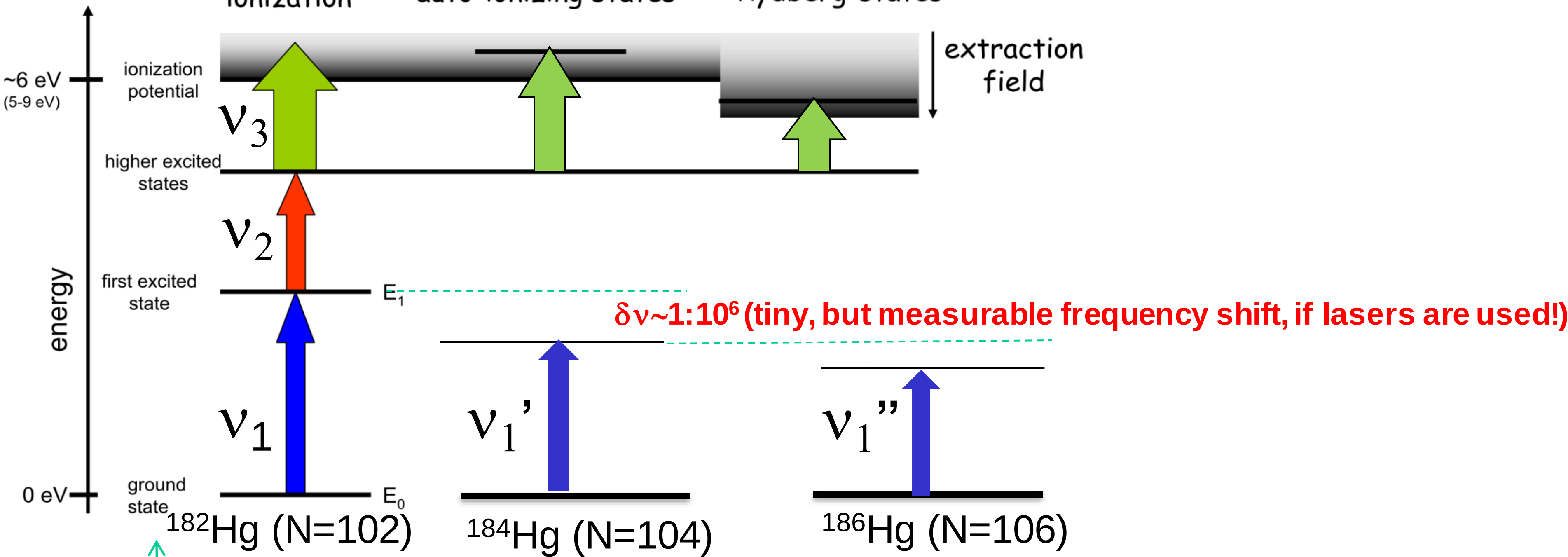

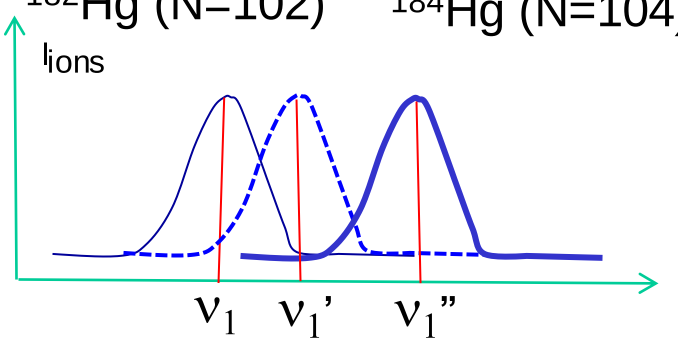

- Ionization Frequency shift $\delta\nu=\nu_1-\nu_1'$: Isotope Shift (IS) or HFS

IS/HFS proportional to the charge radius

$$\delta v^{A,A`} = M_i \frac{A' - A}{AA'} + F_i\, \delta\langle r^2\rangle^{A,A`}$$

Mass shift — Field shift

Schemes of Atomic Resonance Ionization used with Cu-Vapor Laser

Available lasers: visible light, 2-3 eV energy: Multi-step Ionisation!

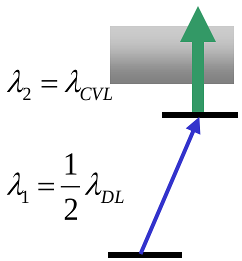

Al (5.99 eV)
Ca (6.11 eV)
Ga (6.00 eV)
In (5.79 eV)
Tl (6.11 eV)

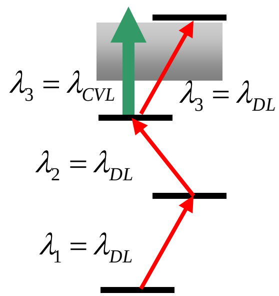

Li (5.39 eV)
Na (5.14 eV)
Sr (5.69 eV)
Ce (5.54 eV)
Nd (5.52 eV)
Sm (5.64 eV)
Eu (5.67 eV)
Gd (6.15 eV)
Tb (5.86 eV)
Ho (6.02 eV)
Tm (6.18 eV)
Yb (6.25 eV)
Lu (5.43 eV)
Actinides… (at Mainz)

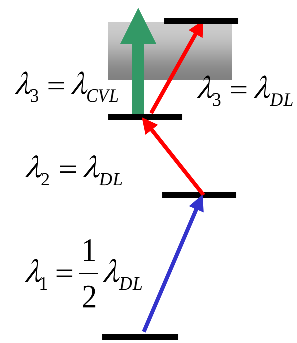

Mg (7.65 eV)
Mn (7.43 eV)
Co (7.86 eV)
Ni (7.64 eV)
Cu (7.73 eV)
Y (6.22 eV)
Ag (7.58 eV)
Tc (7.28 eV)
Sn (7.34 eV)
Pb (7.42 eV)
Bi (7.29 eV)

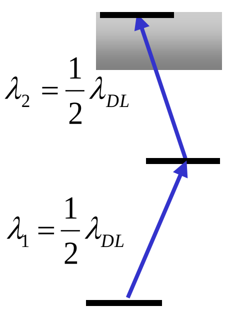

Cu (7.73 eV)

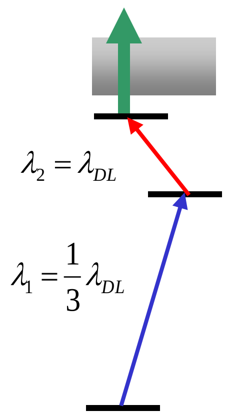

Be (9.32 eV)
Zn (9.39 eV)
Cd (8.99 eV)

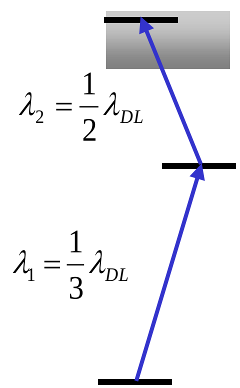

Be (9.32 eV)

Resonance Laser Spectroscopy of an odd-A nucleus

- A **single peak** in 'optical/frequency' spectra for **even-even nuclei**
- More complex in odd-A (odd-odd-A) cases, need to consider Hyperfine Splitting (HFS), due to coupling of nuclear I and electron spin J, giving a **total atomic spin F=I+J**
- This often results in **many peaks** in the frequency spectrum

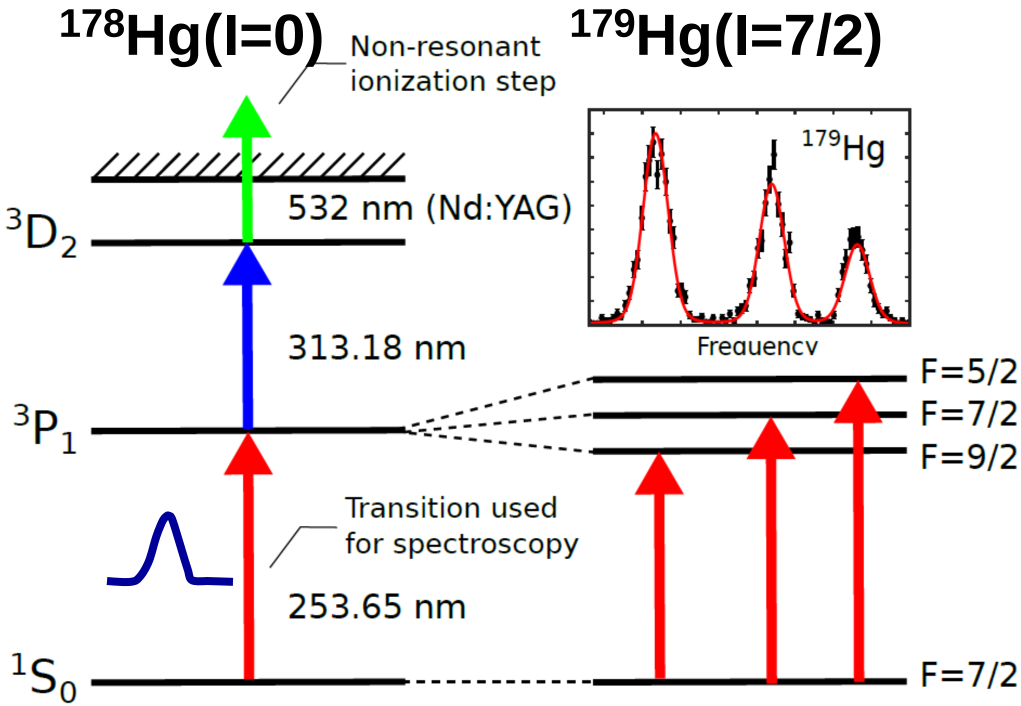

$$\boldsymbol{F}_{atom} = \boldsymbol{I}_{nuclear} + \boldsymbol{J}_{electron}$$

$$\Delta \boldsymbol{F} = 0, \pm 1$$

$$\Delta \nu^F = A\frac{C}{2} + B\frac{\frac{3}{4}C(C+1) - I(I+1)J(J+1)}{2(2I-1)(2J-1)IJ}$$

$$A = \frac{\mu_I B_e(0)}{IJ}$$

$$B = eQ_s \frac{\partial^2 V}{\partial^2 z}$$

The method allows to deduce magnetic (μ) and quadrupole (Q_s) momenta of the nucleus!

Our tools for in-source Laser Spectroscopy at ISOLDE

B. A. Marsh et al., 20013 EMIS conference, NIM B317, p.550 (2013)

WM: A.Andreyev et al, Phys. Rev. Lett 105, 252502 (2010)

MR-ToF MS: R. N. Wolf et al, NIM, A686, 82 (2012)

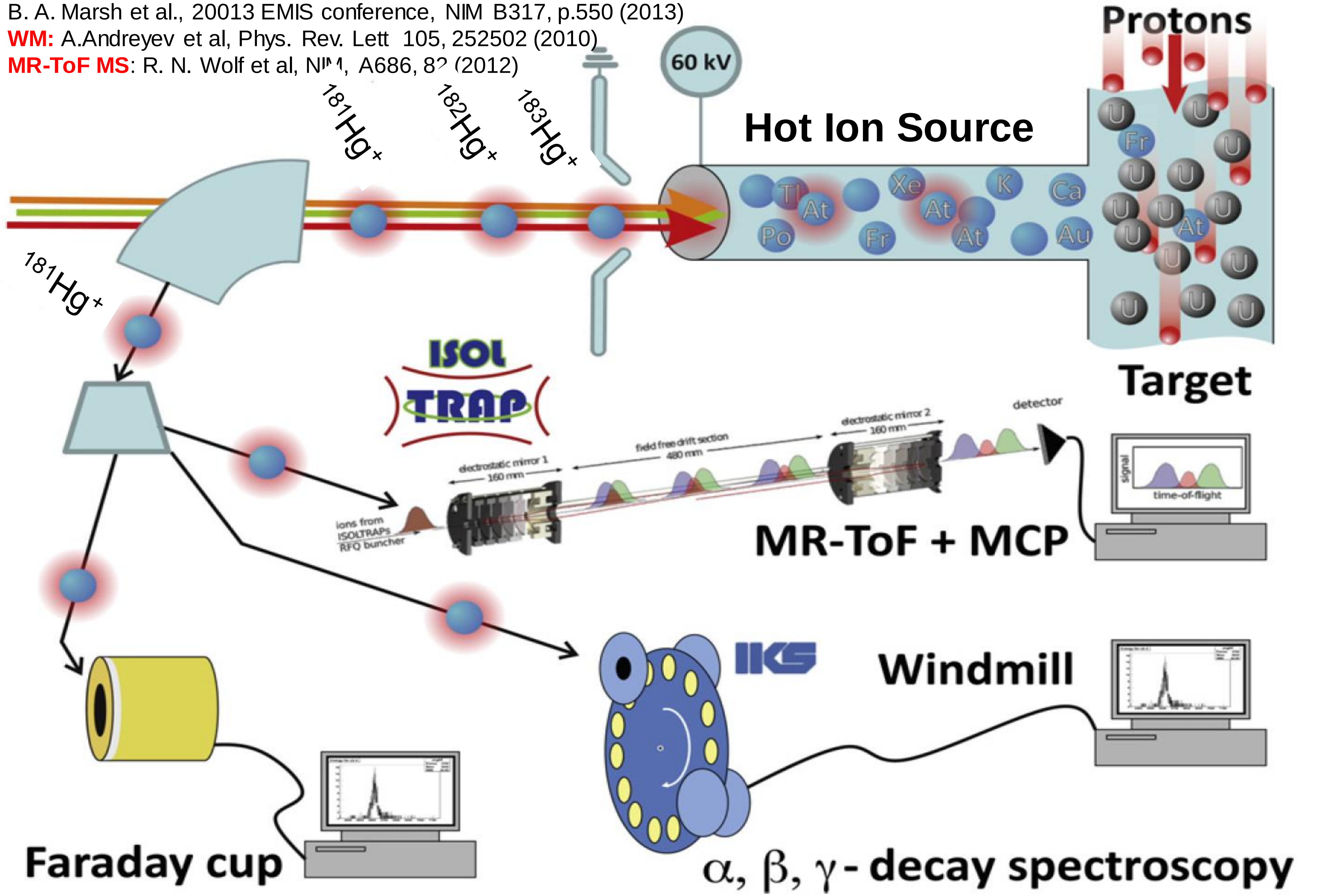

Windmill System at ISOLDE

(measurements of α, β, γ-decays)

A. Andreyev et al., PRL 105, 252502 (2010)

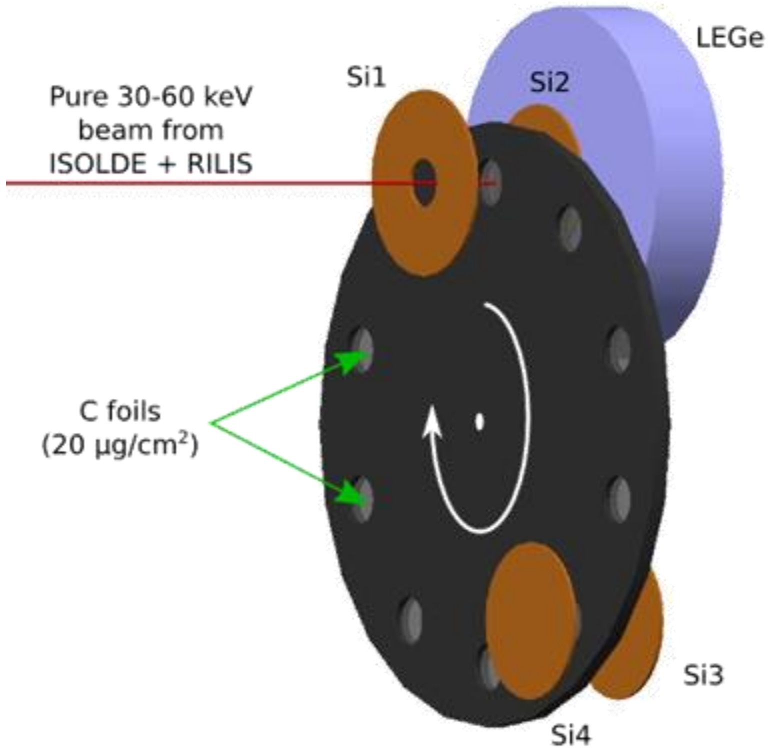

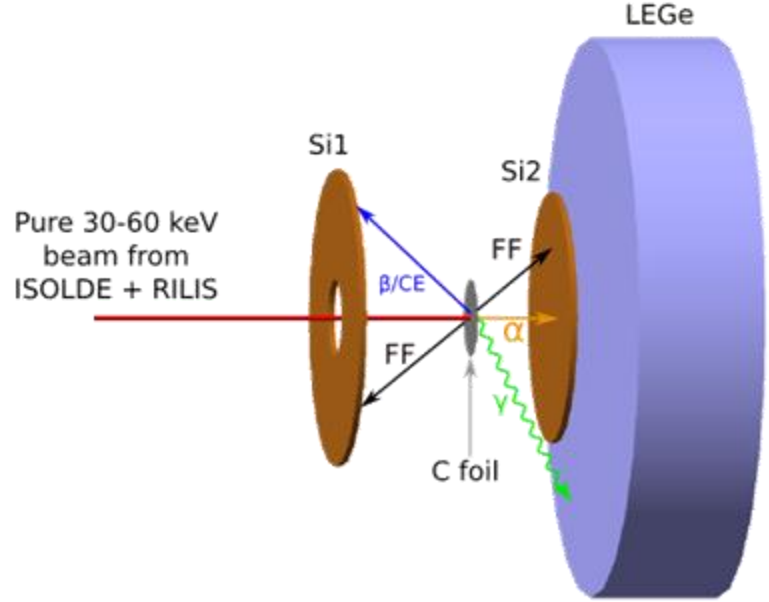

Setup: Si detectors both sides of the C-foil

- Simple setup & DAQ: 2 Surface barrier detectors (1 of them – annular) and 2 PIPS detectors.
- 34% geometrical efficiency at implantation site.
- Alpha-gamma coincidences
- Digital electronics

Multi-Reflection Time-of-Flight (MR-ToF) Spectrometer for **HFS studies and mass** measurements

- The WM technique requires **waiting for the decay** of the isotope. Not practical for long-lived or stable isotopes.
- Alternative – to **use 'counting' ions** (instead of waiting for decay)

MR-ToF MS: R. N. Wolf et al, NIM, A686, 82 (2012)

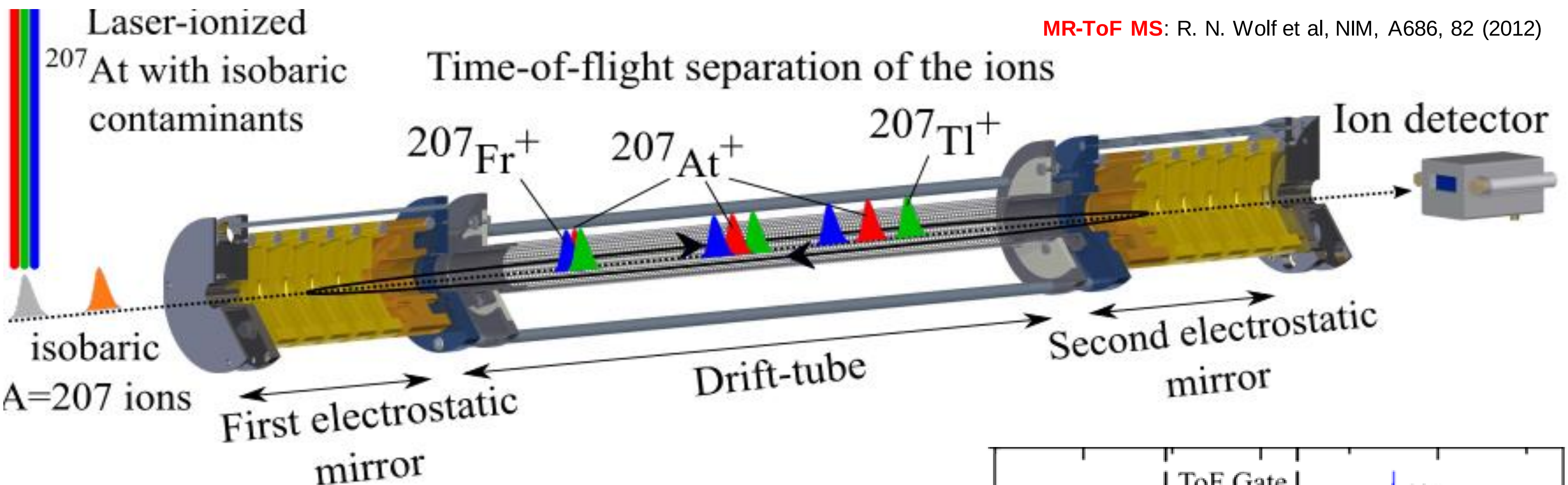

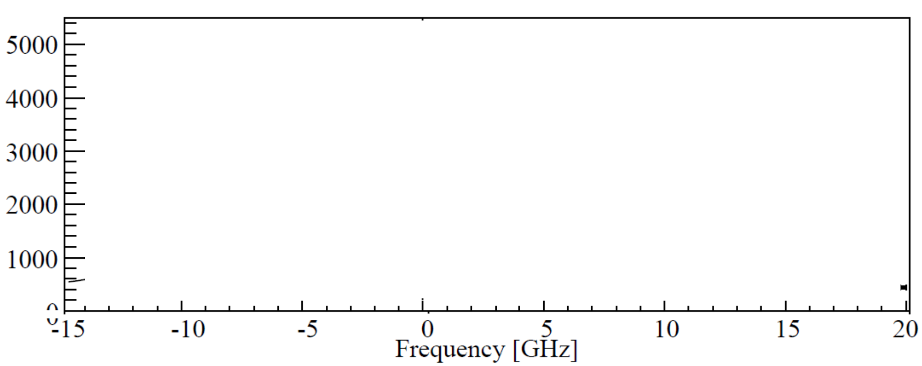

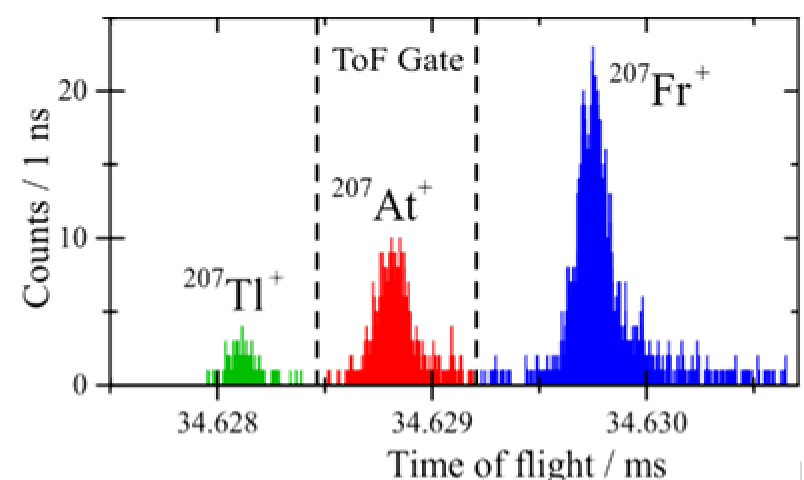

^{180}Hg@Windmill

Alpha-decay spectrum at A=180 (lasers on ^{180}Hg)
note the purity of the spectrum!

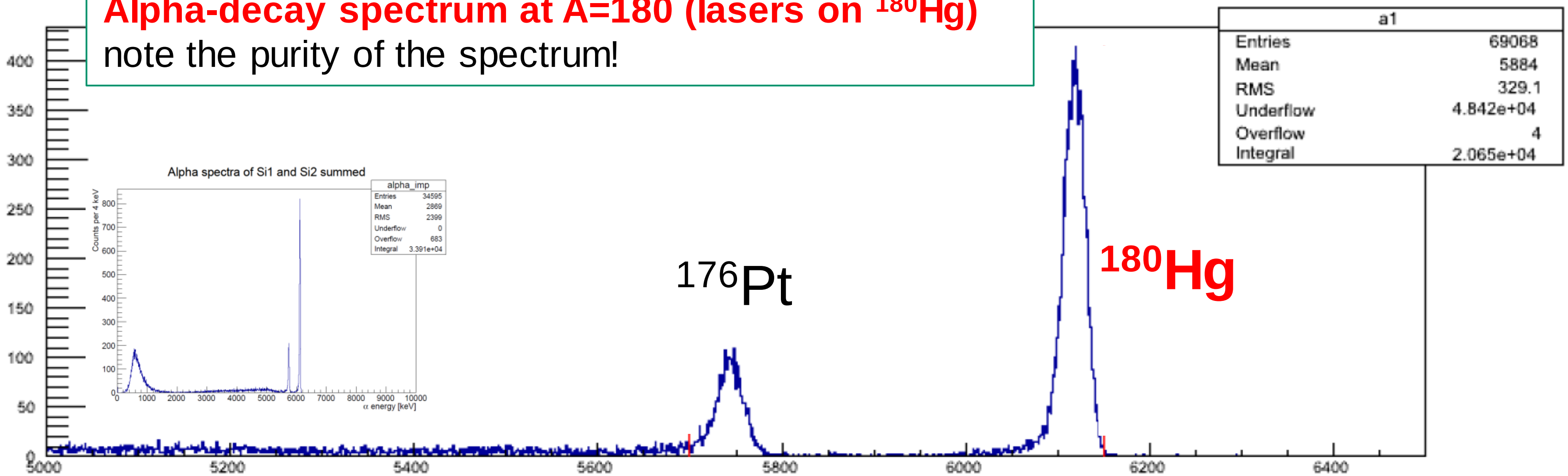

Optical spectrum (even-even case, I=0$^+$)
(number of α decays as a function of laser frequency)

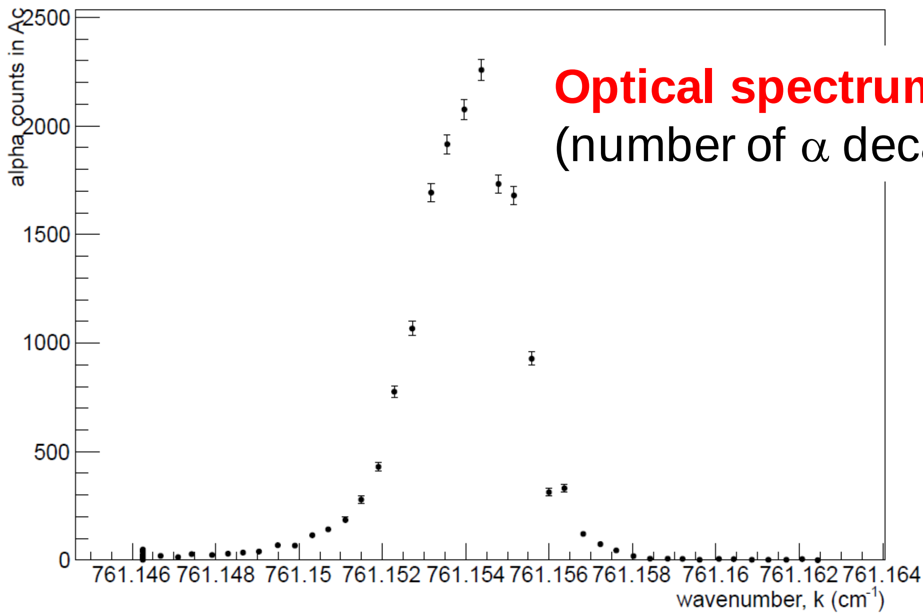

^{179,185,207,208}Hg

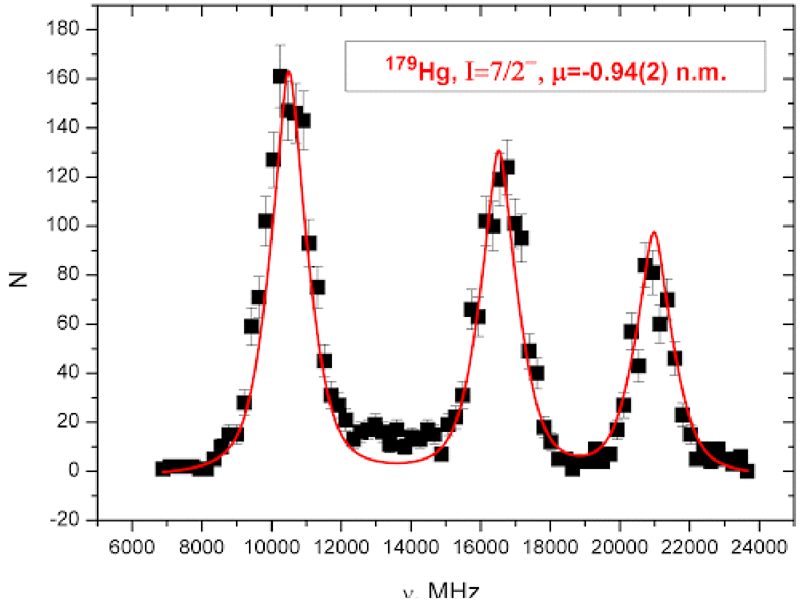

Isotopes with N>126

^{207}Hg HFS spectra@MR-ToF, I=9/2

also ^{208}Hg! I=0

^{185}Hg HFS spectrum@MR-ToF, gs+is

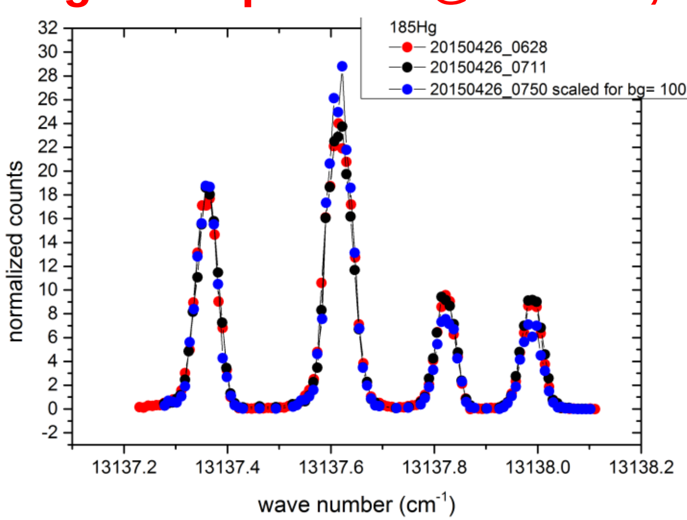

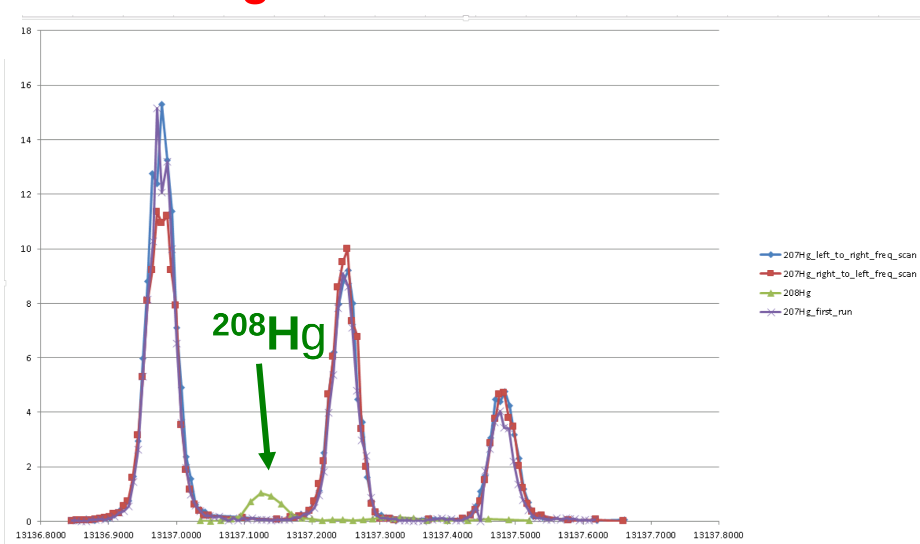

HFS spectra and Charge radii for Hg isotopes

B. Marsh, Nature Physics 14, 163 (2018)

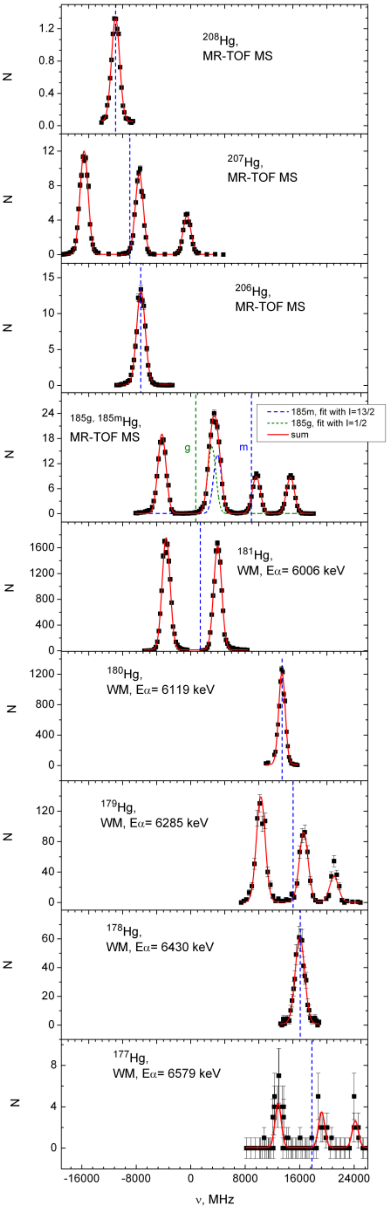

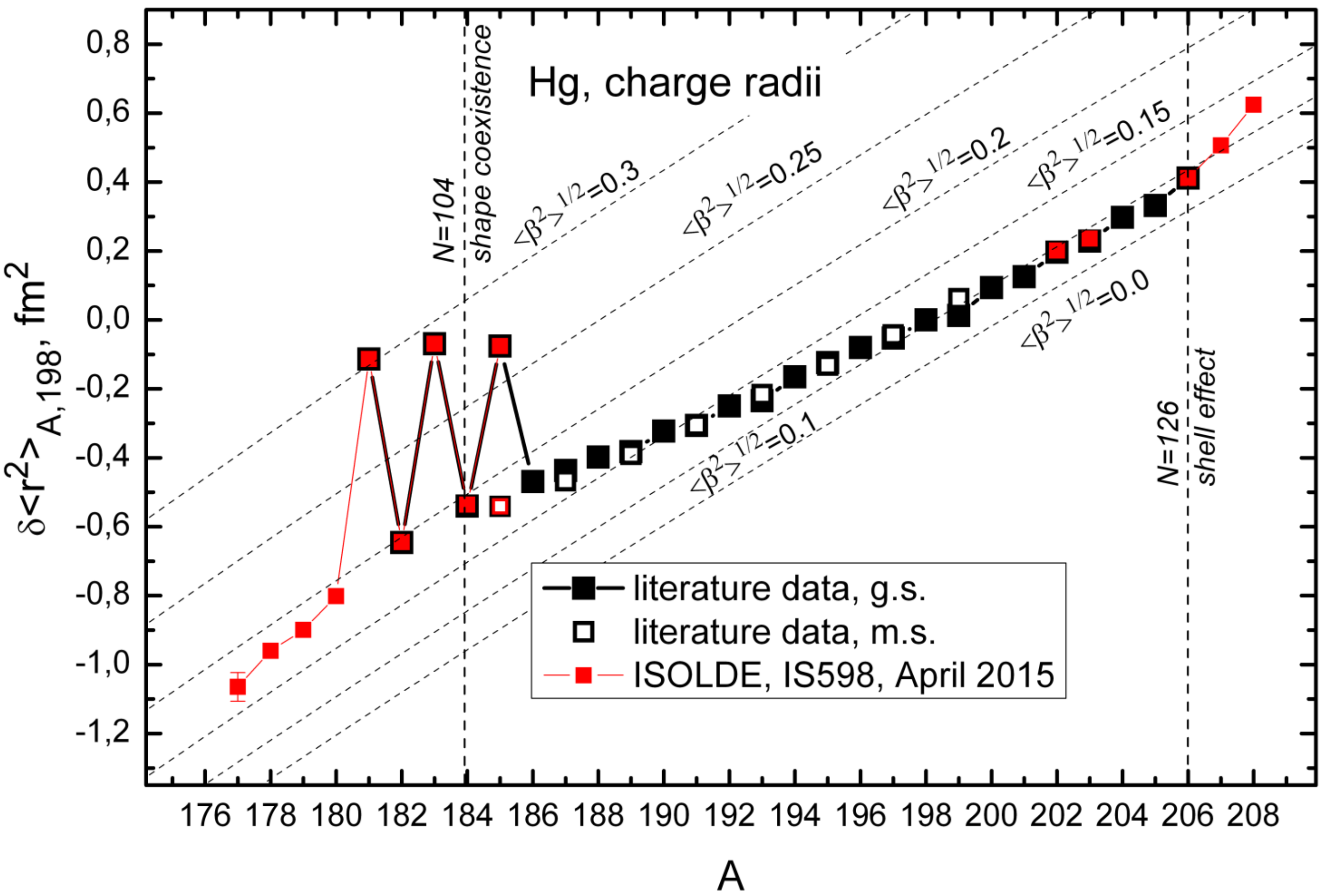

^{181,183,185}Hg- confirmation of earlier data on staggering for ½$^-$ gs

^{177,178,179,180}Hg (new) – trend towards sphericity

^{207,208}Hg (new): kink beyond N=126

DFT Potential Energy Surfaces (even-even Hg's)

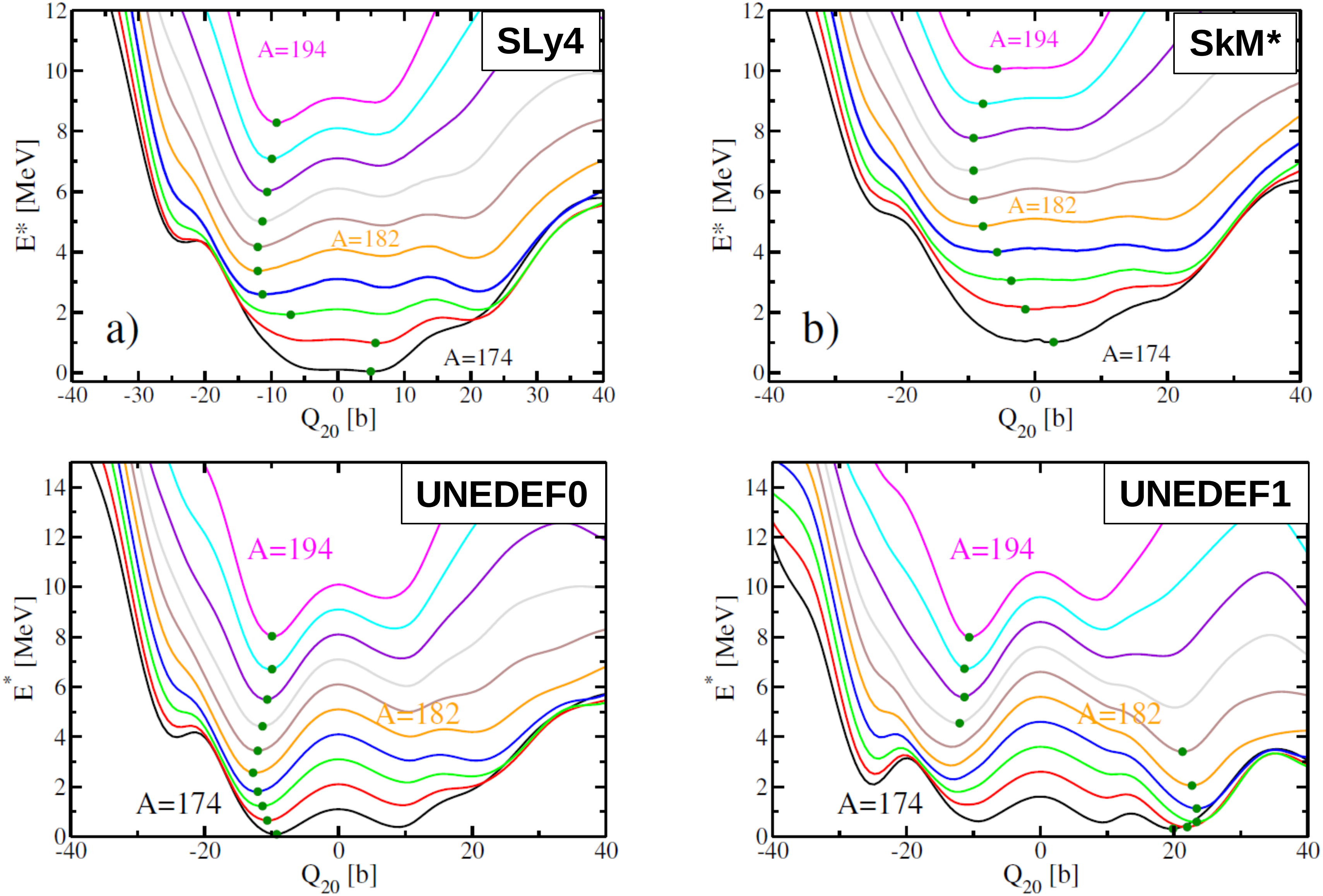

MCSM for Hg isotopes (Y.Tsunoda, T.Otsuka et al)
B. Marsh, Nature Physics 14, 163 (2018)

- Largest calculation of its kind, avoids diagonalization of >2x10^{42}-dimensional H matrix
- Radii are well reproduced.
- Results show an increase of >2 protons promoted into the h9/2 intruder state.

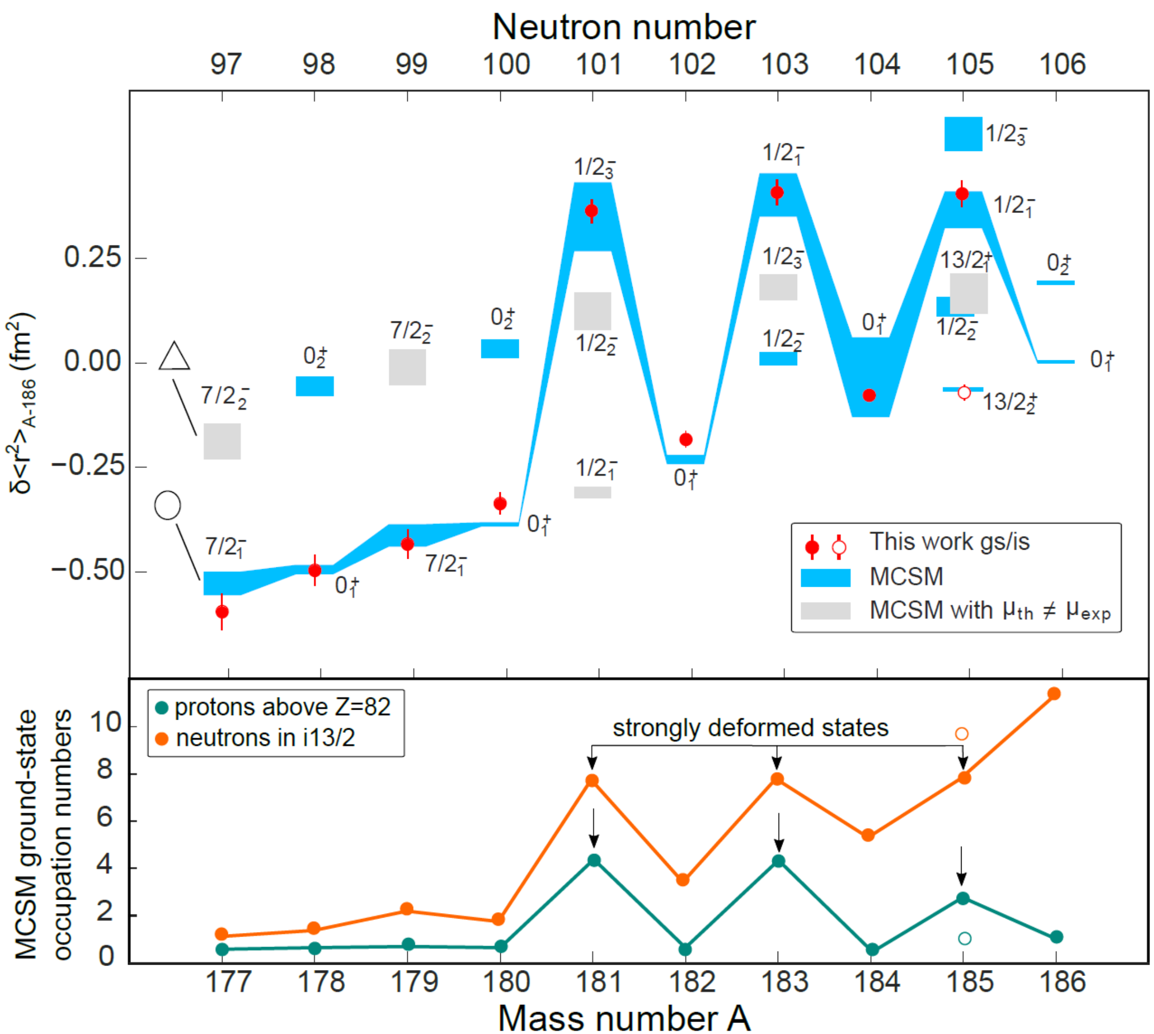

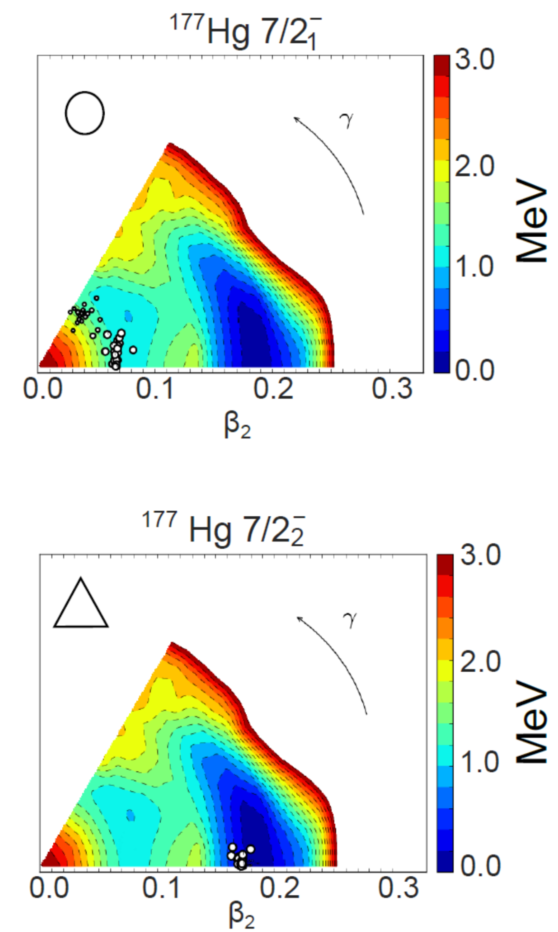

nature physics
LETTERS
https://doi.org/10.1038/s41567-018-0292-8

B.A. Marsh *et al.*, Nature Physics, 1745-2481 (2018)

One for the funding councils →

Characterization of the shape-staggering effect in mercury nuclei

B. A. Marsh[1*], T. Day Goodacre[1,2,18], S. Sels[3,18], Y. Tsunoda[4], B. Andel[5], A. N. Andreyev[6,7], N. A. Althubiti[2], D. Atanasov[8], A. E. Barzakh[9], J. Billowes[2], K. Blaum[8], T. E. Cocolios[2,3], J. G. Cubiss[6], J. Dobaczewski[6], G. J. Farooq-Smith[2,3], D. V. Fedorov[9], V. N. Fedosseev[1], K. T. Flanagan[2], L. P. Gaffney[3,10], L. Ghys[3], M. Huyse[3], S. Kreim[8], D. Lunney[11], K. M. Lynch[1], V. Manea[8], Y. Martinez Palenzuela[3], P. L. Molkanov[9], T. Otsuka[3,4,12,13,14], A. Pastore[6], M. Rosenbusch[13,15], R. E. Rossel[1], S. Rothe[1,2], L. Schweikhard[15], M. D. Seliverstov[9], P. Spagnoletti[10], C. Van Beveren[3], P. Van Duppen[3], M. Veinhard[1], E. Verstraelen[3], A. Welker[16], K. Wendt[17], F. Wienholtz[15], R. N. Wolf[8], A. Zadvornaya[3] and K. Zuber[16]

S. Sels *et al.*, Phys. Rev. C 99, 044306 (2019)

One with the interesting work in →

Shape staggering of mid-shell mercury isotopes from in-source laser spectroscopy compared with Density Functional Theory and Monte Carlo Shell Model calculations

S. Sels,[1,*] T. Day Goodacre,[2,3] B. A. Marsh,[3] A. Pastore,[4] W. Ryssens,[5] Y. Tsunoda,[6] N. Althubiti,[2] B. Andel,[7] A. N. Andreyev,[4,8] D. Atanasov,[9] A. E. Barzakh,[10] M. Bender,[5] J. Billowes,[2] K. Blaum,[9] T. E. Cocolios,[1] J. G. Cubiss,[4] J. Dobaczewski,[4,11] G. Farooq-Smith,[1] D. V. Fedorov,[10] V. N. Fedosseev,[3] K. T. Flanagan,[2] L. P. Gaffney,[12,1] L. Ghys,[13,1] P-H. Heenen,[14] M. Huyse,[1] S. Kreim,[9] D. Lunney,[15] K. M. Lynch,[3] V. Manea,[9] Y. Martinez Palenzuela,[1] T. M. Medonca,[3] P. L. Molkanov,[10] T. Otsuka,[6,16,1] J. P. Ramos,[3,17] R. E. Rossel,[3,18] S. Rothe,[3] L. Schweikhard,[19] M. D. Seliverstov,[10] P. Spagnoletti,[12] C. Van Beveren,[1] P. Van Duppen,[1] M. Veinhard,[3] E. Verstraelen,[1] A. Welker,[20] K. Wendt,[18] F. Wienholtz,[19] R.N. Wolf,[9] and A. Zadvornaya[1]

Example of Spin Determination from HFS measurements for ^{177,179}Au isotopes

Based on the number of HFS components and their intensity ratio, the gs spins of ^{177,179}Au are experimentally determined as 1/2

J.G.Cubiss et al, PLB, 786, 355, 2018

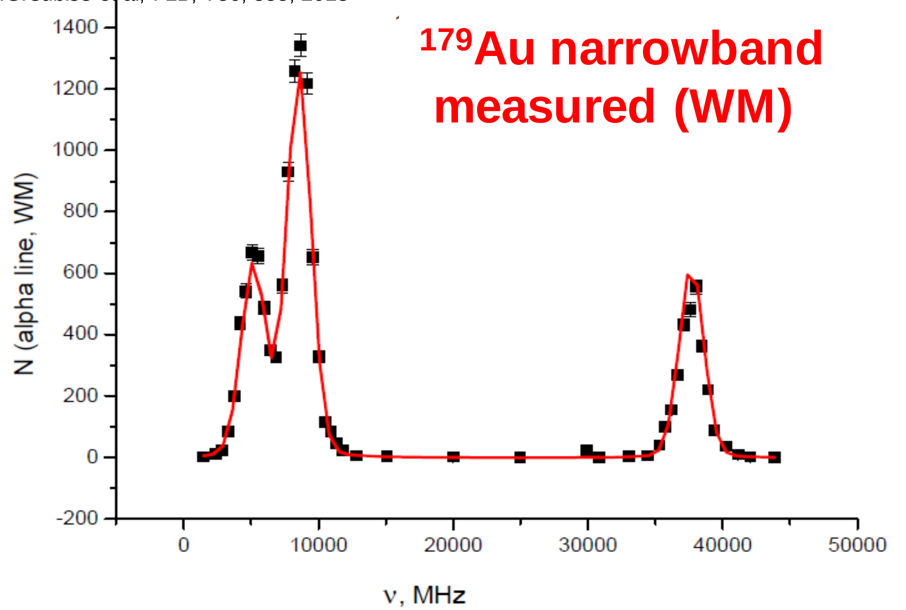

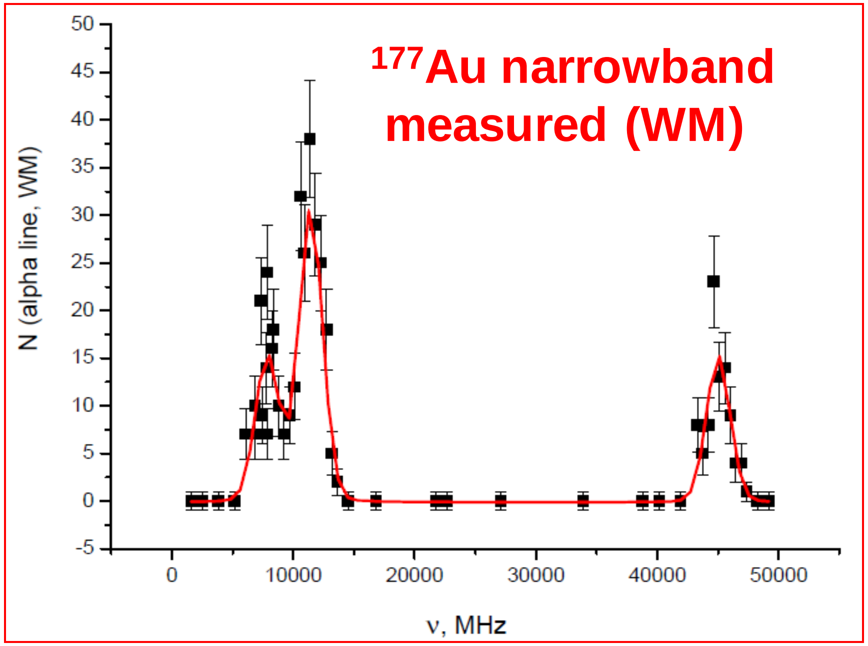

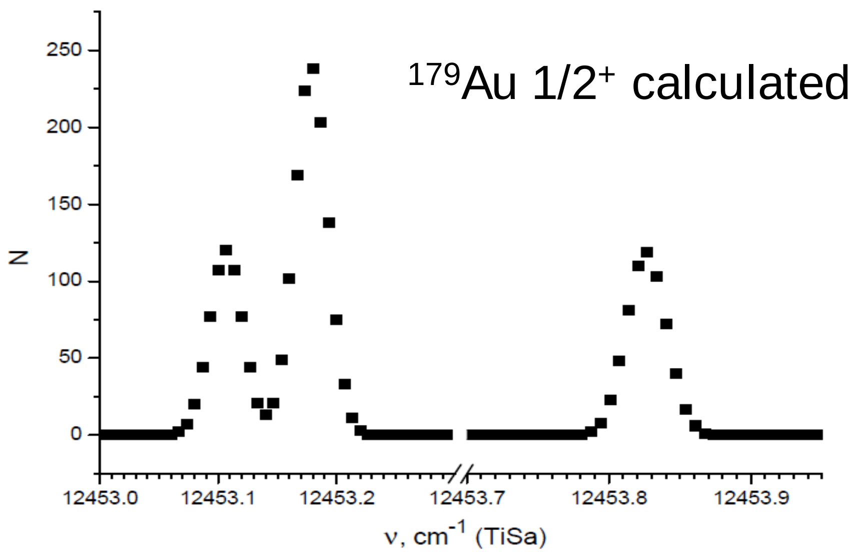

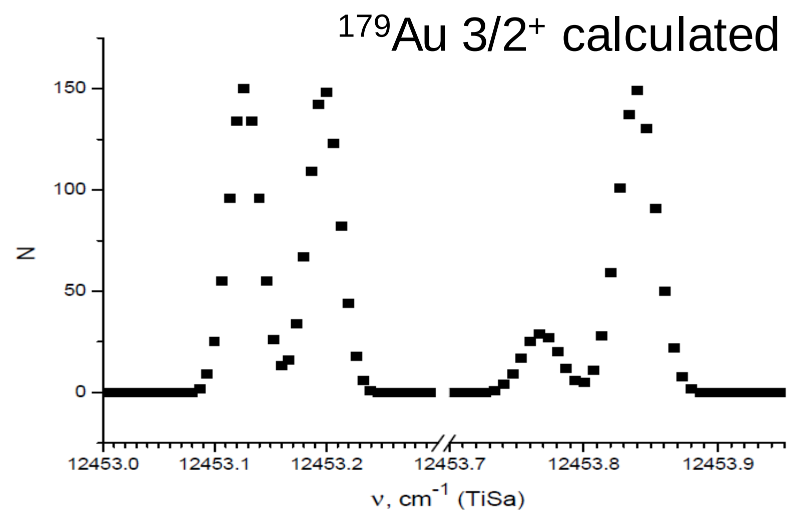

Example on Isomer Selectivity in $^{178gs,m}Au$

J.G. Cubiss (York) *et al.*, in preparation

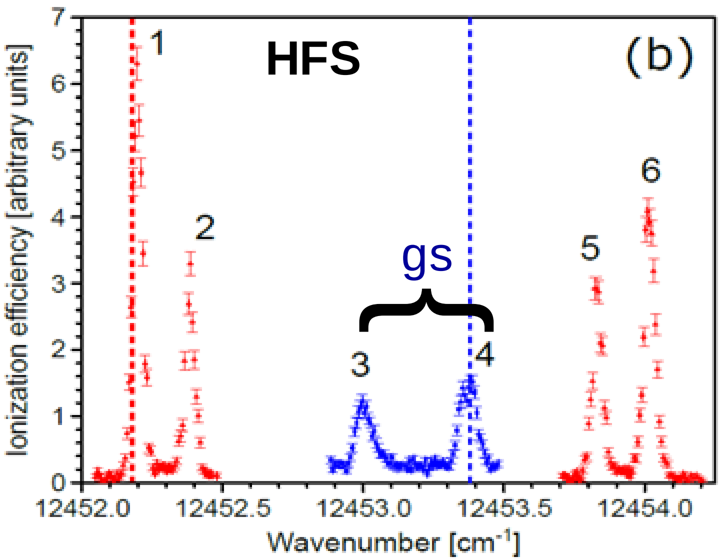

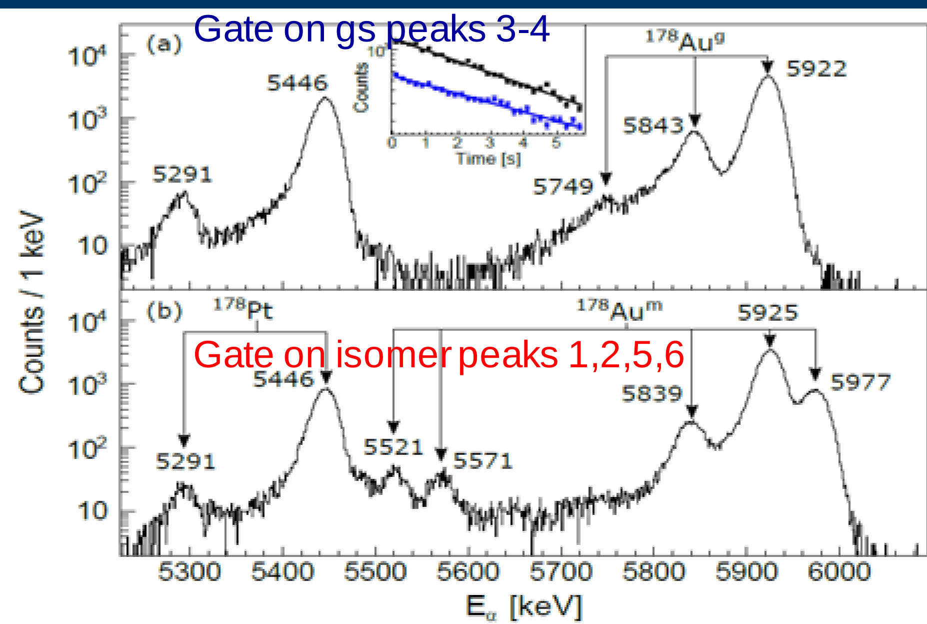

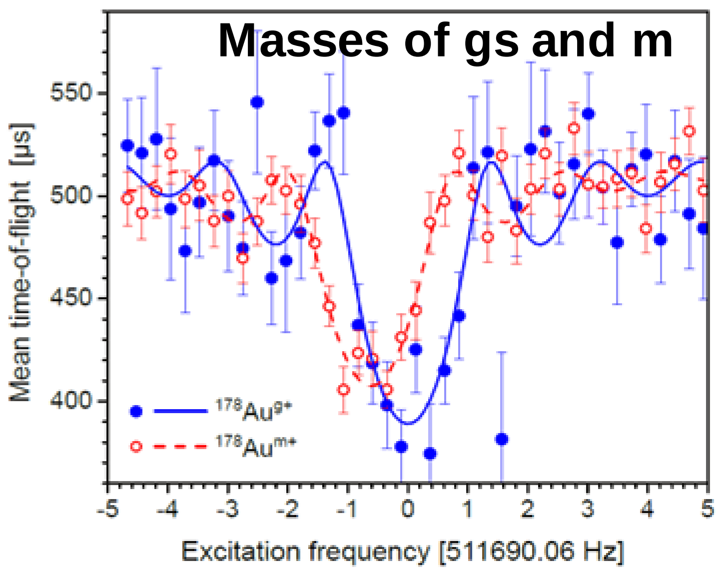

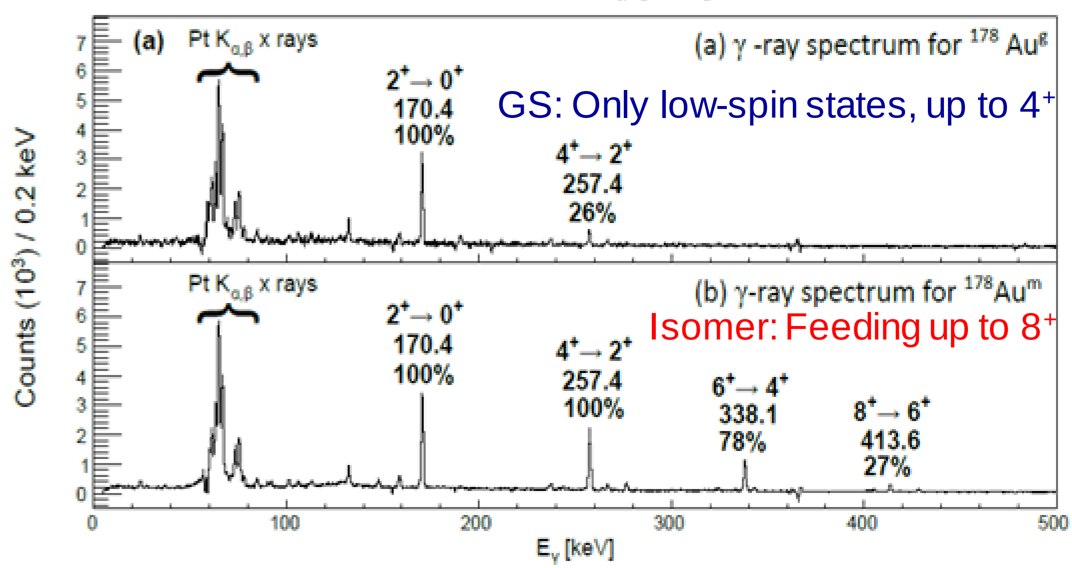

Opens up a totally new area of reactions studies with isomerically-clean beams! (e.g. spin-dependence of reactions, in this case with low spin ground state or with high-spin isomeric beam)

Lead Region: Summary/Status for 2019
WM-RILIS-MR-TOF MS+IRIS

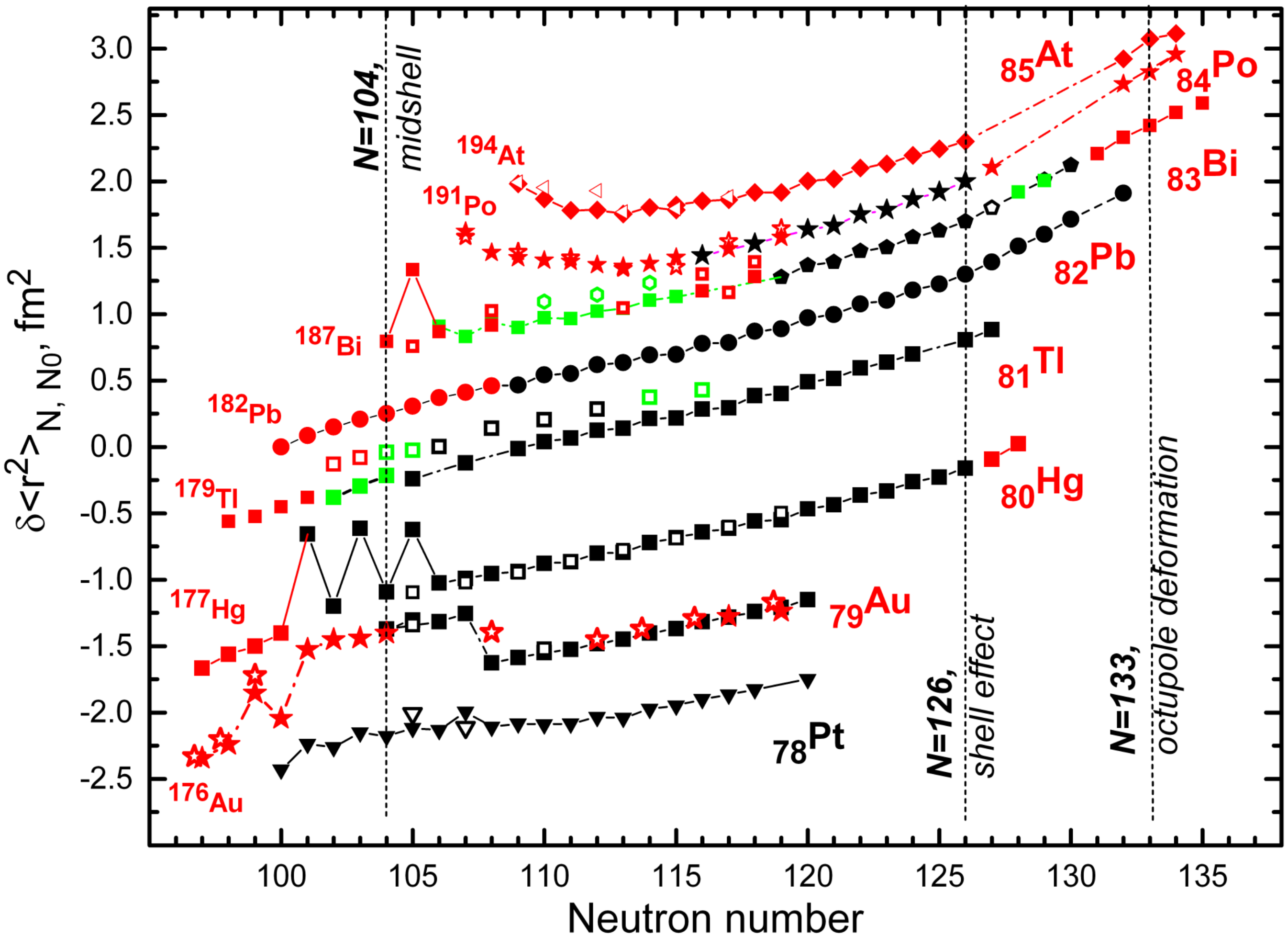

Red: our data from ISOLDE
Green points = Gatchina
Black points = literature

- IS/HFS/charge radii for >70 isotopes (and isomers) for Au,Hg,Pb,Bi,Po, At
- Back to sphericity" in the lightest Au and Hg isotopes
- Magnetic/quadrupole moments will be deduced
- Large amount of by-product spectroscopic information on for many isotopes

Case 2: Ca Puzzles probed by:

$E(2^+_1)$

Radii

Masses

(and further examples of modern experimental approaches!)

Isospin (N/Z-dependence) of Nuclear Properties
$^{34-60}Ca$ Isotopic Chain (as just one example)

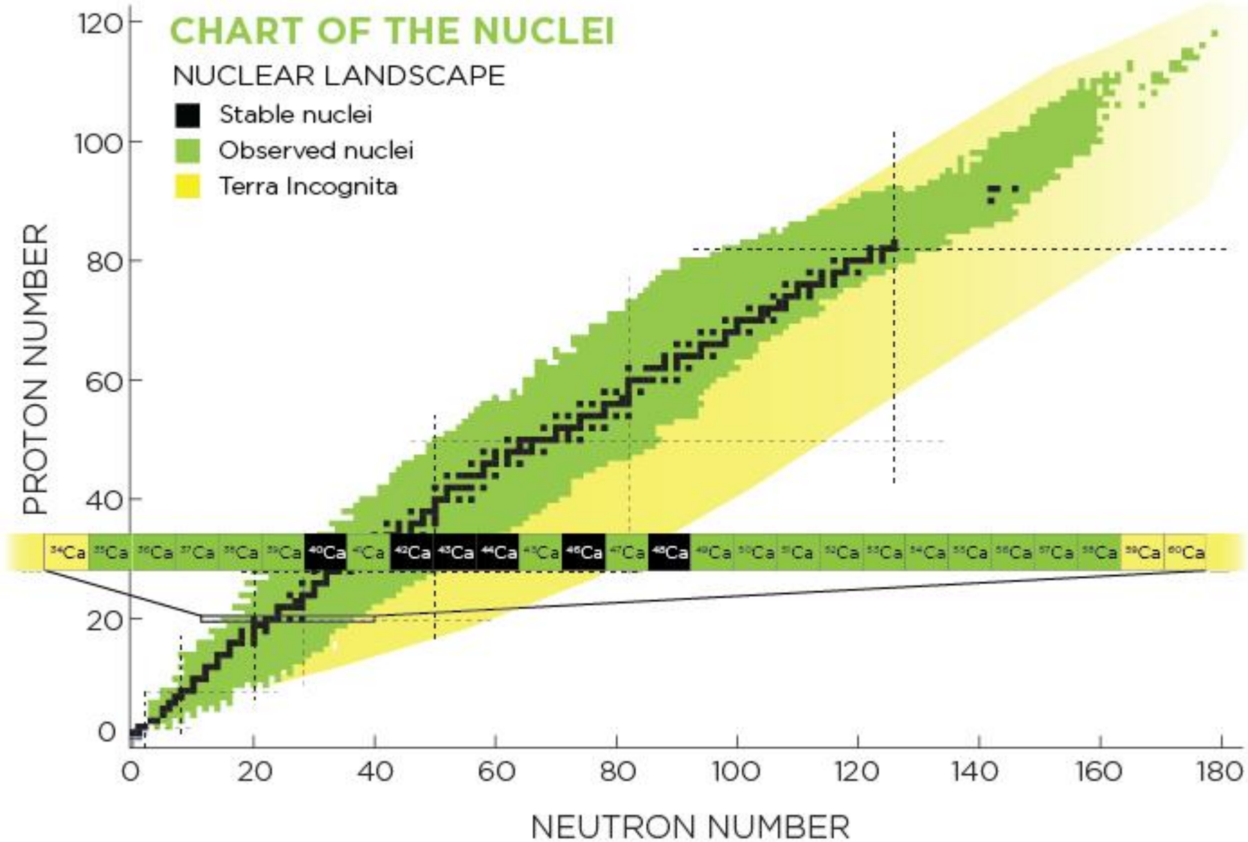

- Calcium isotopic chain: at present, spans 26 isotopes with N/Z=0.7-2
- 2 doubly-magic **spherical** isotopes: ^{40}Ca(Z=N=20), ^{48}Ca(Z=20, N=28)
- ^{60}Ca (Z=20,N=40), recently (2019) discovered at RIBF, only 2 events
- ^{70}Ca (Z=20, N=50) could exist (according to some theories), would it be doubly-magic/spherical?

Reminder on $E(2^+_1)$ energy systematics in Ca isotopes

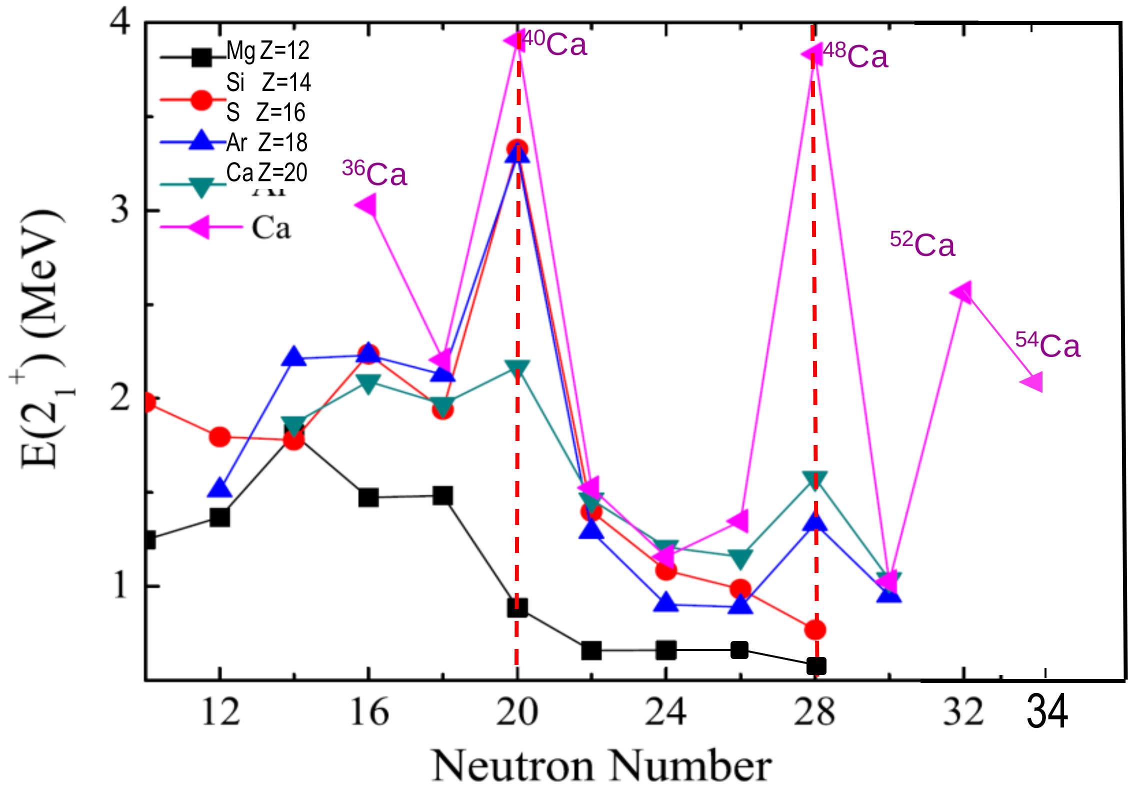

- High $E(2^+_1)$ values for ^{40,48}Ca – signatures for N=20,28 shell closures
- Low value at ^{50}Ca(N=30)
- ^{52,54}Ca(N=32,34): again high values. An evidence for a new magic number at N=32 and double-magicity of ^{52}Ca?

This should be seen/probed via other observables, e.g. radii and masses

R F Casten and R B Cakirli 2016 *Phys. Scr.* **91** 033004
^{54}Ca: D. Steppenbeck et al., Nature 502, 207 (2013)
^{40}Mg: H. Crawford et al., Phys. Rev. Letts, 122, 052501 (2019)

Charge Radii of $^{40-48}$Ca

The radius of a 'typical' calcium nucleus is ~ 3.5 fm, and the isotopic variations are much smaller! Still can measured by laser spectroscopy!

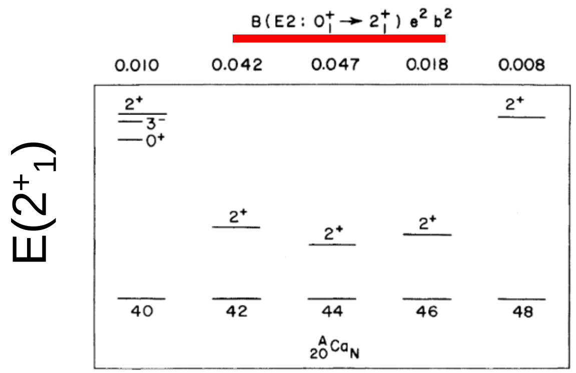

Fig. 2.3. Low-lying levels and B(E2) values for the even–even Ca nuclei. ^{40}Ca and ^{48}Ca are doubly magic.

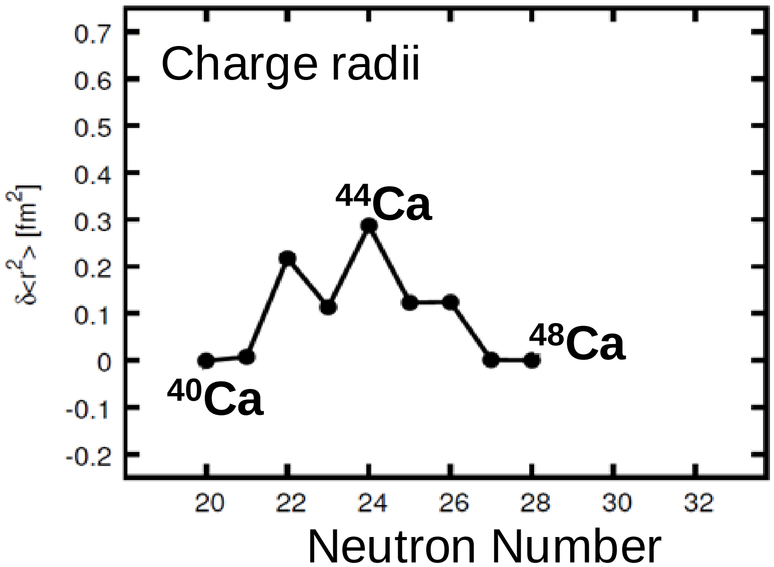

- Radii of ^{40,48}Ca are nearly equal, and smallest: **a signature for shell closures at N=20,28 (due to stronger binding, see discussion on masses)**
- Maximum of radii at mid-shell ^{44}Ca
- Odd-even staggering (as expected… homework!)
- Direct correlations between radii and $E(2^+_1)$/B(E2) values

So, what happens below N=20 and above N=28? Can radii confirm the inference from $E(2^+_1)$ on the double magicity of ^{52}Ca?

COLlinear LAser Spectroscopy (COLLAPS) at ISOLDE for charge radii of n-rich $^{49,51,52}Ca$ isotopes

R.F. Garcia Ruiz et al., Nature Physics 12, 594 (2016)

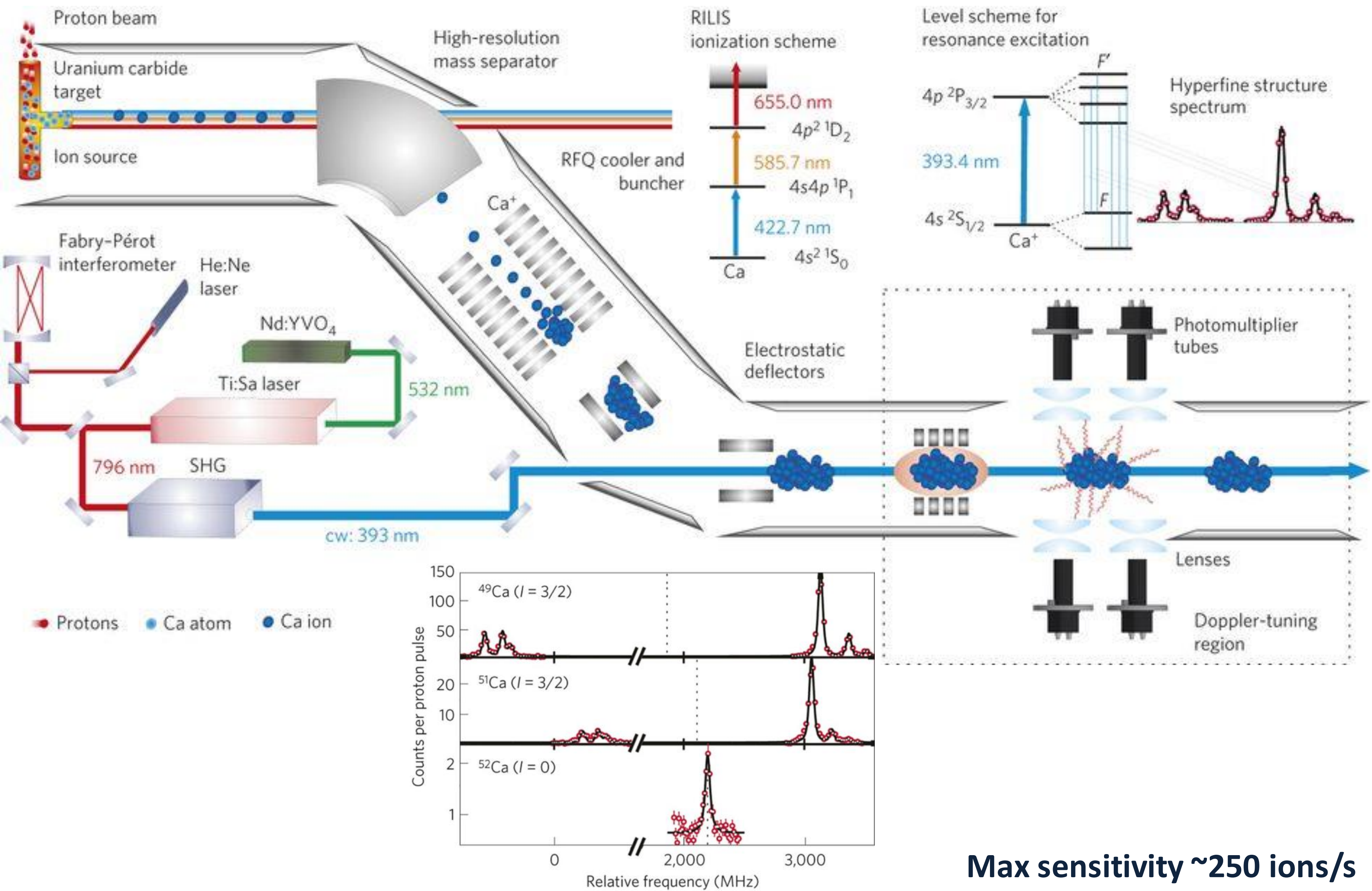

Max sensitivity ~250 ions/s

Resolution in Collinear Laser Spectroscopy vs in-source laser ionization

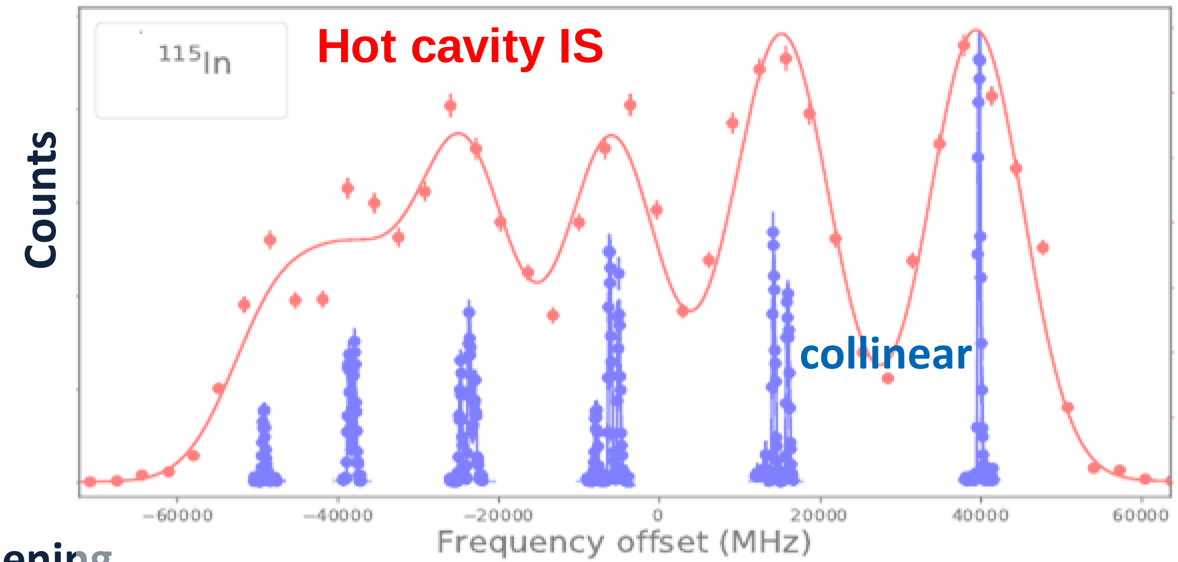

Doppler Broadening

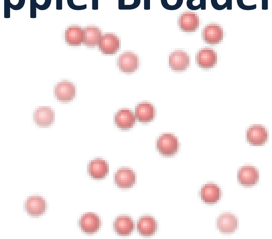

$$\Delta\nu_D = \frac{2\nu_0}{c}\sqrt{\frac{2\ln 2\, kT}{m}}$$

Ion mass

Room Temp. 300 K~ 25 meV

→ $\Delta\nu_D$ > GHz

Fast beams

Collinear laser spectroscopy

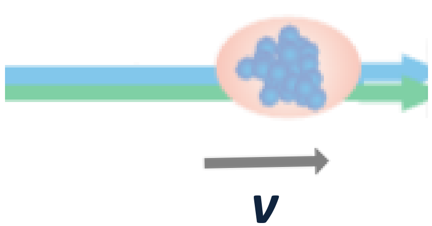

Energy spread

$$\delta\nu_D = \nu_0 \frac{\delta E}{\sqrt{2eUmc^2}}$$

Ion beam energy

- High precision/resolution (~MHz)
- High efficiency (<100 ions/s)
- High selectivity (>1/10^6)
- Short time scales (< 1 s)

→ at *eU*=40 keV

$\Delta\nu_D$ ~ MHz

Ca Charge Radii Beyond N=28?

R.F. Garcia Ruiz et al., Nature Physics 12, 594 (2016)

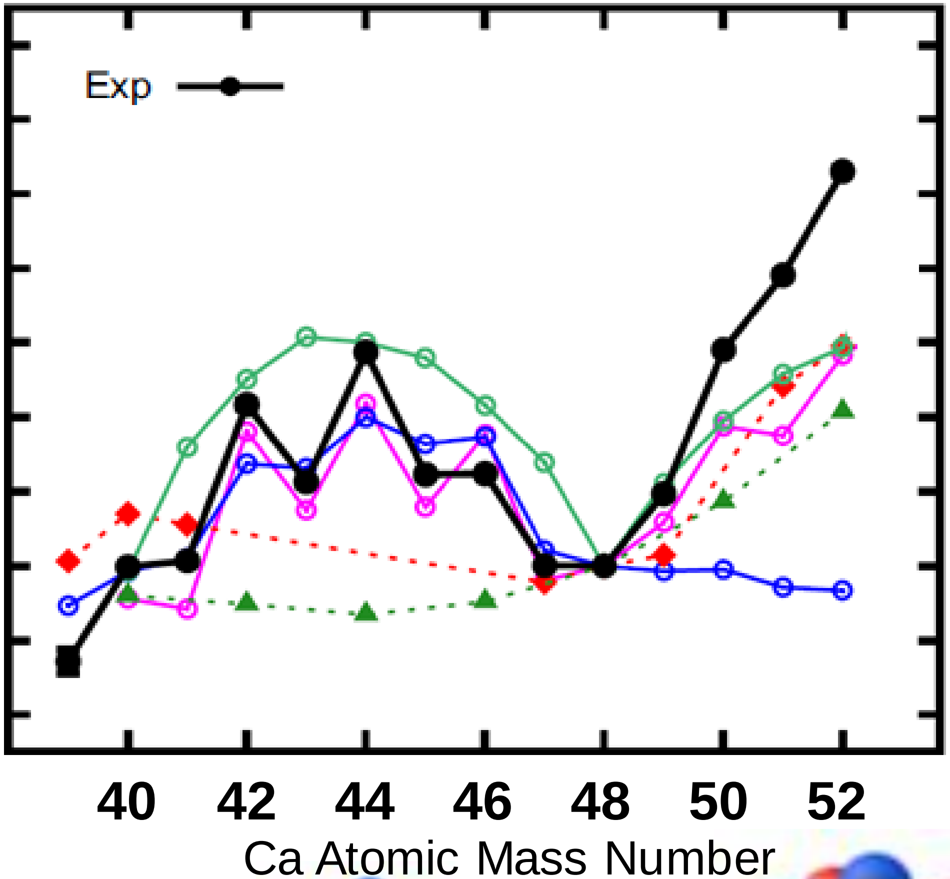

$NNLO_{sat}$ PRC 91, 051301 (2015)
Nature Physics 12, 180 (2016)

ZBM2 PLB 522, 240 (2001)
PRL 113, 052502 (2014)
PRC 92, 014305 (2015)

DF3-a NPA 676, 49 (2000)

UNEDF0 Nature 486, 509 (2012)

Wang et al. PRC 88, 011301(R) (2013)

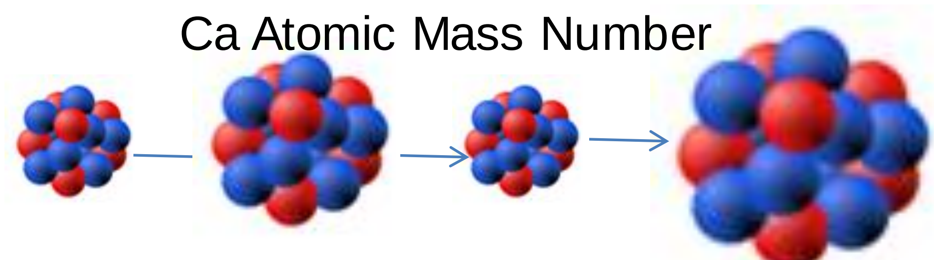

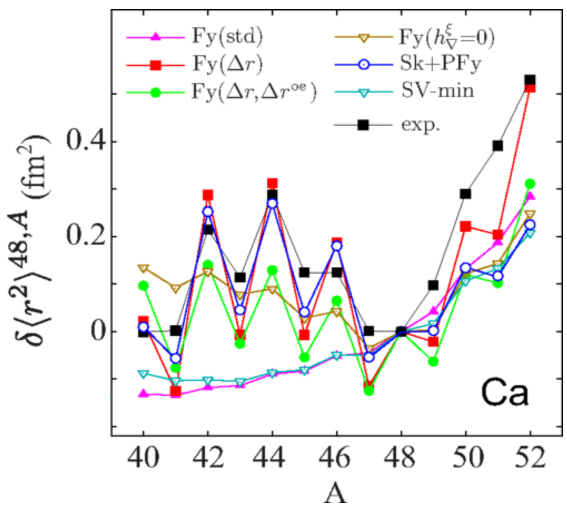

P.-G. Reinhard and W. Nazarewicz
Phys. Rev. C **95**, 064328

The large and unexpected increase of the size of the neutron-rich calcium isotopes beyond *N*=28 challenges the doubly-magic nature of ^{52}Ca!

Ca radii below N=20: BEam COoler and LAser spectroscopy (BECOLA@NSCL, MSU) for charge radii of n-deficient $^{36-38}Ca$ isotopes

A. J. Miller et al., *Nature Physics*, 2019

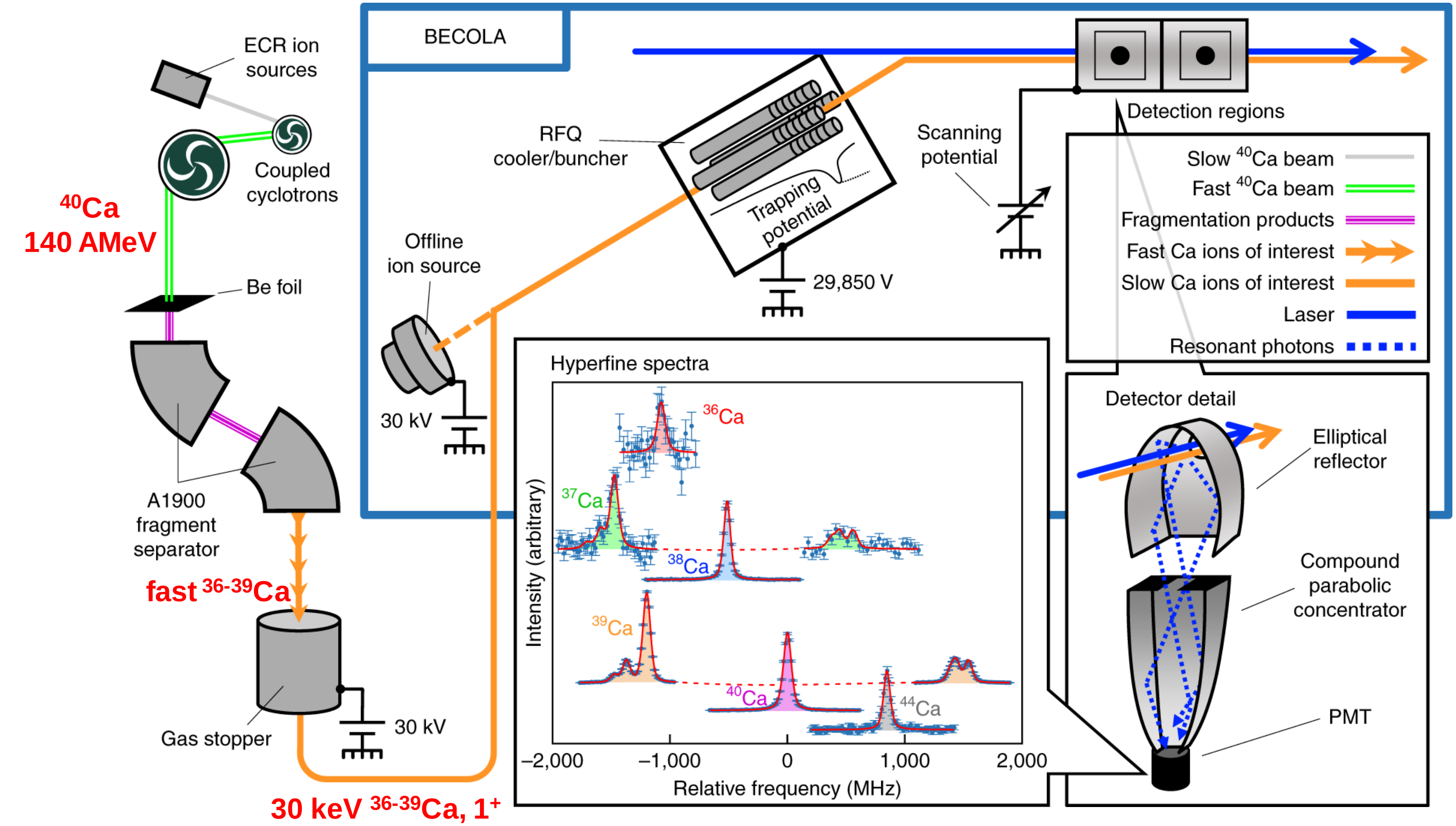

- Projectile-fragmentation method, breaking of ^{40}Ca (140 AMeV) beam in variety of lighter isotopes on a Be target (356 microns thickness)
- Separates the desired isotopes in-flight by A1900 fragment separator
- Stops them in a gas-cell stopper, thermalisation in the He gas results in 1+ charge state
- Extraction at 30 keV, the rest is ‘similar’ to ISOLDE’s experiment
- Scanning of the HFS by tuning the ‘scanning potential’ at the constant laser frequency

Charge Radii for $^{36-52}Ca$ isotopes

A. J. Miller et al., *Nature Physics*, 2019

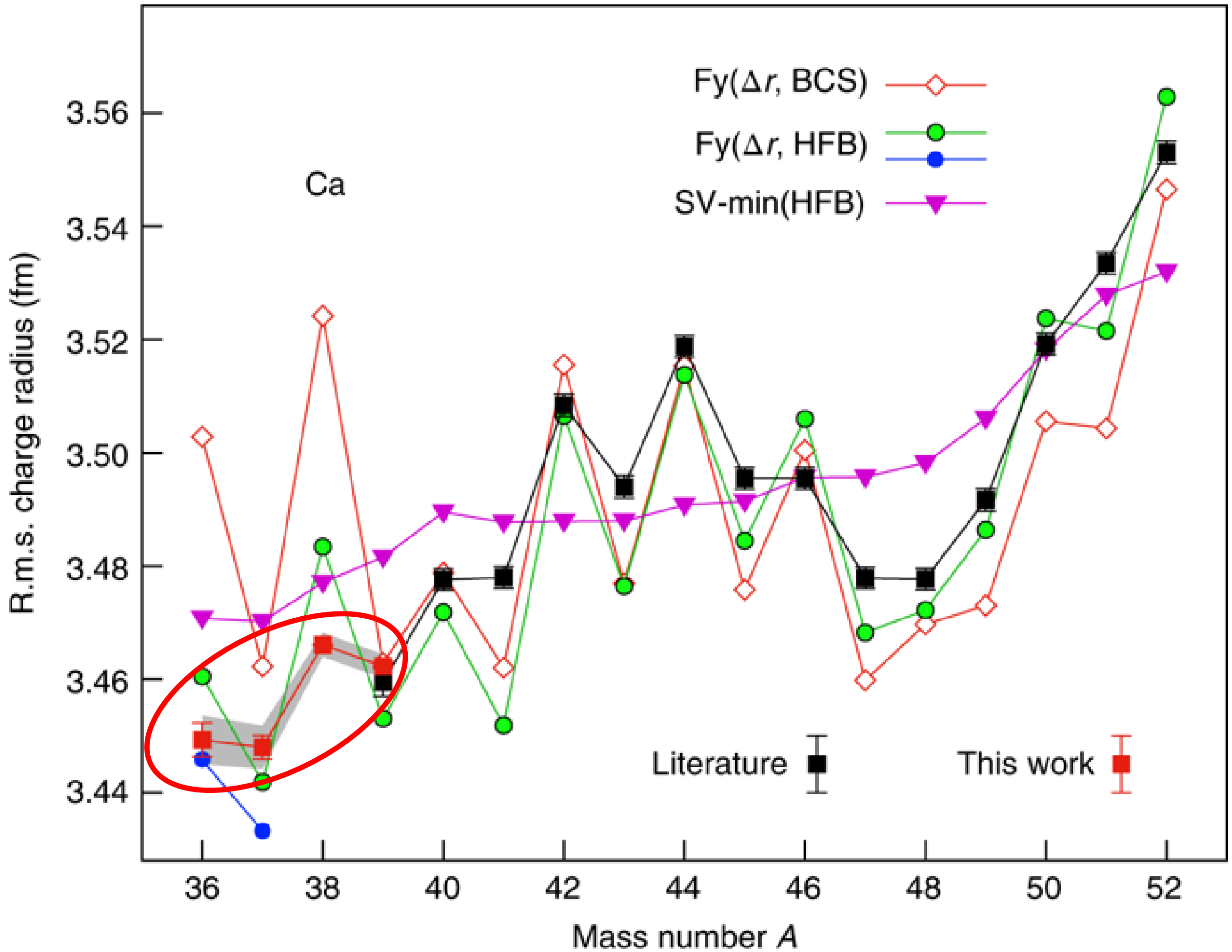

Continues decrease of Ca radii below $^{40}Ca(N=20)$ – follows ~$A^{1/3}$ dependence

Charge Radii Systematics around N=28-36

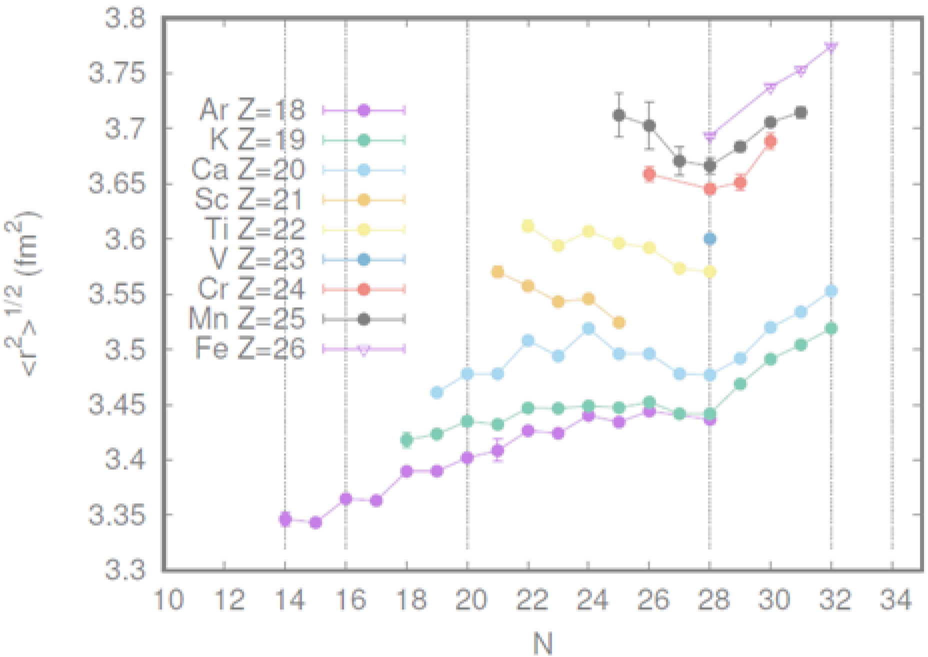

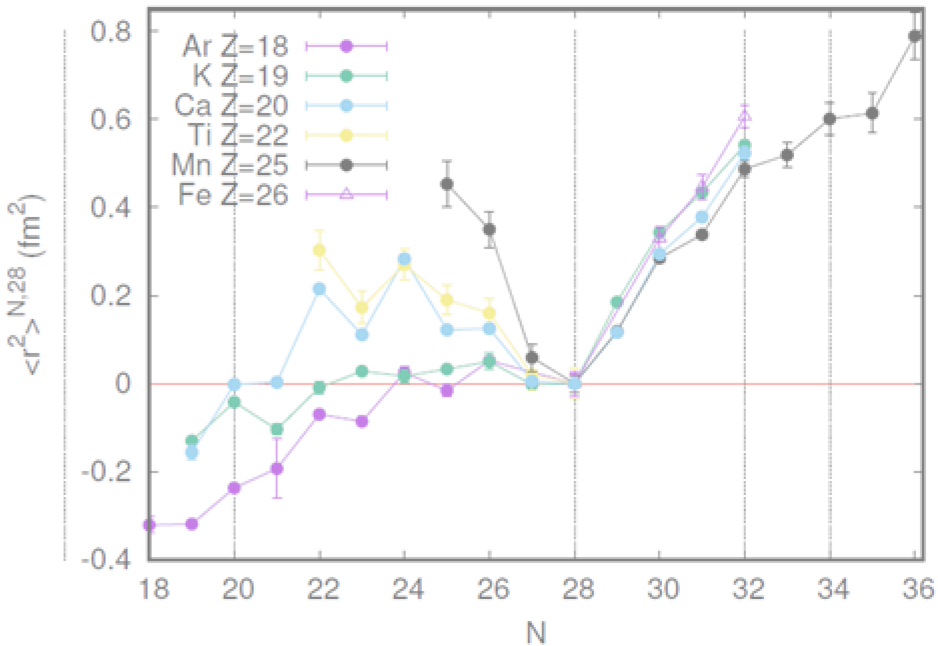

$^{50-61}$Mn (Z=25) → [H. Heylen et al, Phys. Rev. C 94, 054321(2016)]

$^{40-52}$Ca (Z=20) → [R.F. Garcia Ruiz et al., Nature Physics 12, 594 (2016)]

$^{38-51}$K (Z=19) → [K. Kreim et al, Phys. Lett. B 731, 97 (2014)]

$^{44-50}$Sc (Z=21) → [In preparation (2018)]

} COLLAPS/ISOLDE

$^{48-52}$K(Z=19) → [In preparation (2018)] } CRIS/ISOLDE

- Seems that all isotopic chains for Z=18-26 (where data are available) demonstrate a continues increase beyond N=28, with no apparent evidence for any magicity at N=32?
- Similarly, no kink at N=20 in Z=18,19,20 (Ar,K,Ca)

Summary from E(2^+_1) and Radii above ^{48}Ca

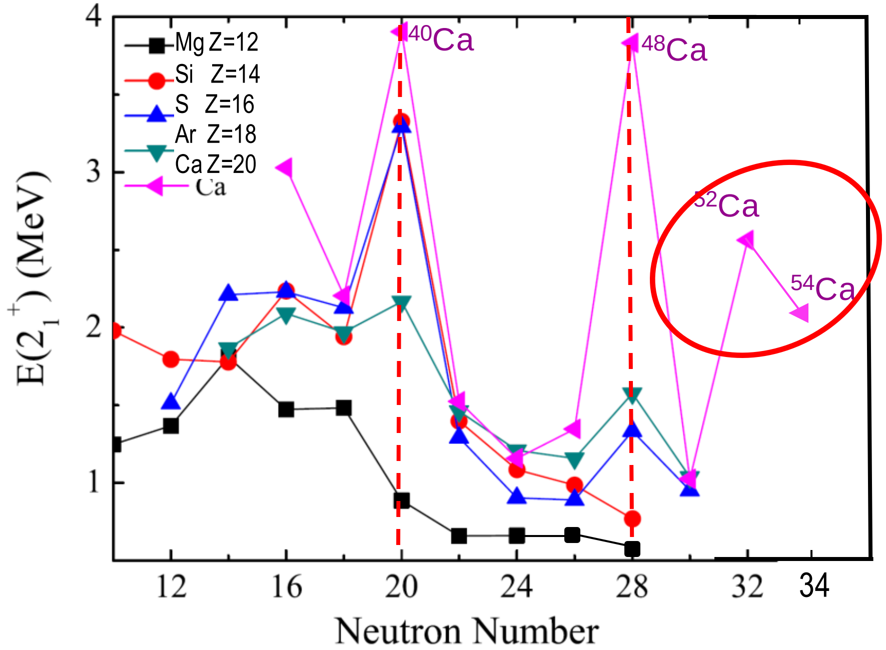

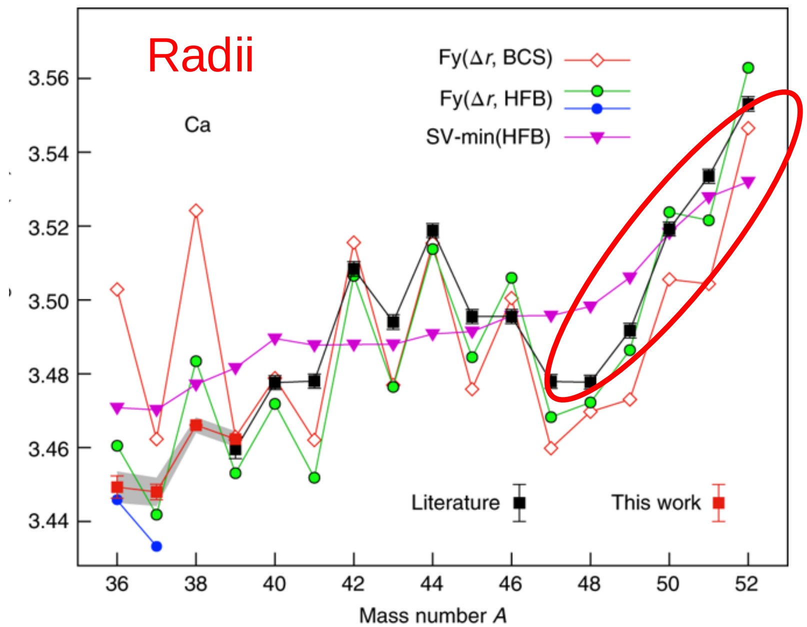

- The high values of E(2^+_1) for ^{52,54}Ca suggested the double-magicity of ^{52}Ca
- This is contradicted by the radii measurements, which demonstrate the large increase for ^{52}Ca!

So, let's try masses?

^{53,54}Ca Masses with MR-ToF Spectrometer at ISOLDE

F.Wienholtz et al, Nature, 498,346,2013

3.5 h measurement **after MR-ToF**

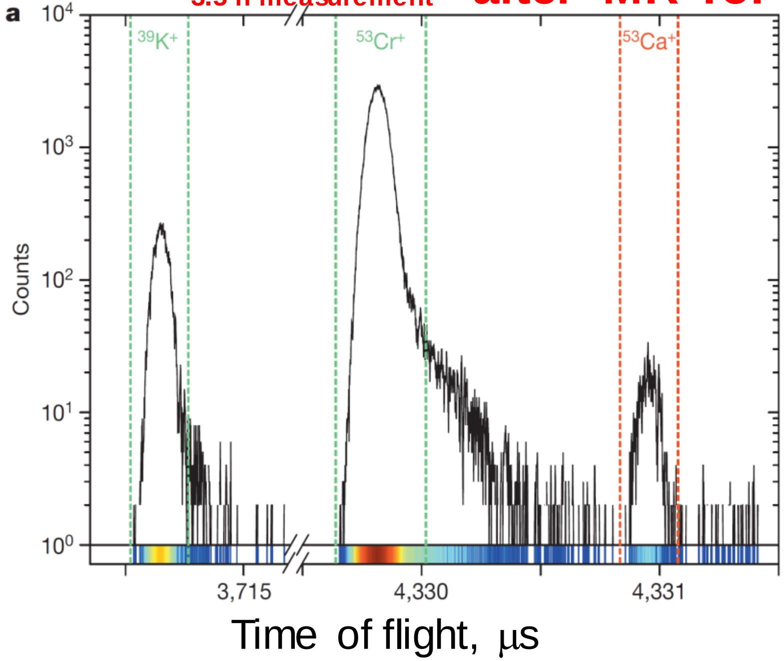

- MR-ToF provides clear separation from isobaric ^{53}Cr
- Allows to measure the masses by ToF
- ^{39}K and ^{53}Cr serve as reference masses
- (Typical) Resolving power: 10^5 (in ~tens ms)
- Rate limitation: ~1 pps (~tens ms half-life)

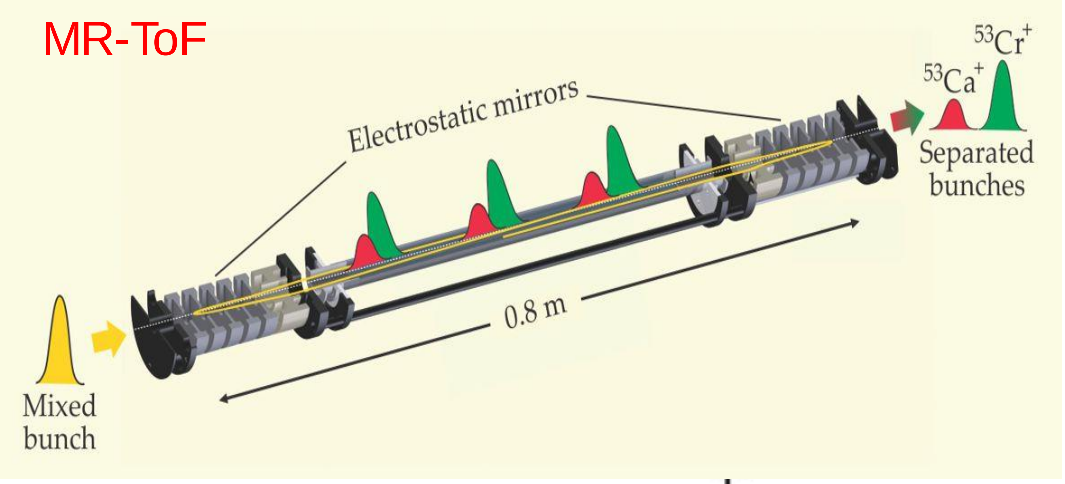

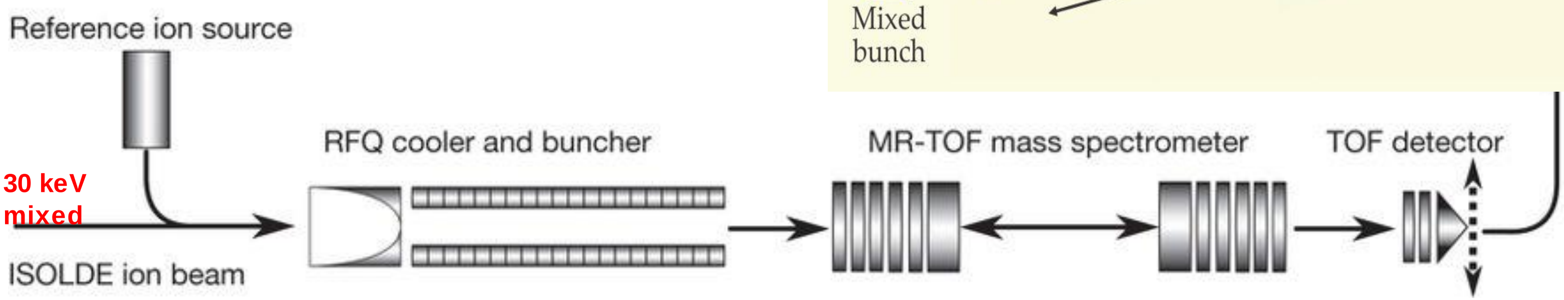

^{53,54}Ca Masses with MR-ToF Spectrometer at ISOLDE

F.Wienholtz et al, Nature, 498,346,2013

Table 1 | Results of the calcium mass measurements

Isotope	$T_{1/2}$	Meas. type	Ref. nuclide(s)	r_{ICR}	C_{TOF}	Mass excess (keV/c^2) ISOLTRAP	Mass excess (keV/c^2) TITAN TRIUMF
^{51}Ca	10.0(8) s	ICR	^{39}K	1.3079136760(144)	NA	−36332.07(0.58)	−36338.9(22.7)
^{52}Ca	4.6(3) s	ICR	^{39}K	1.3336358720(184)	NA	−34266.02(0.71)	−34244.6(61.0)
		MR-TOF	^{39}K, ^{52}Cr	NA	0.501632110(785)	−34271.7(10.2)	
^{53}Ca	461(90) ms	MR-TOF	^{39}K, ^{53}Cr	NA	0.50184761(309)	−29387.8(43.3)	—
^{54}Ca	90(6) ms	MR-TOF	^{39}K, ^{54}Cr	NA	0.50210648(323)	−25161.0(48.6)	—

$T_{1/2}$, half-life[30]; measurement (meas.) type (ICR, ion cyclotron resonance; MR-TOF, multi-reflection time-of-flight mass spectrometry); reference (ref.) nuclide(s) used for the calibration; r_{ICR}, experimental frequency ratio; C_{TOF}, TOF constant; mass excess, $M_{exc} = (M - Au)$, where M is the atomic mass, A is the atomic number and u is the unified atomic mass unit. For comparison, the TITAN[4] values are also listed. The mass values of the reference nuclides are $m(^{39}K) = 38963706.4864(49)$ µu, $m(^{52}Cr) = 51940506.26(63)$ µu, $m(^{53}Cr) = 52940648.17(62)$ µu, $m(^{54}Cr) = 53938879.18(61)$ µu (ref. 28). NA, not applicable.

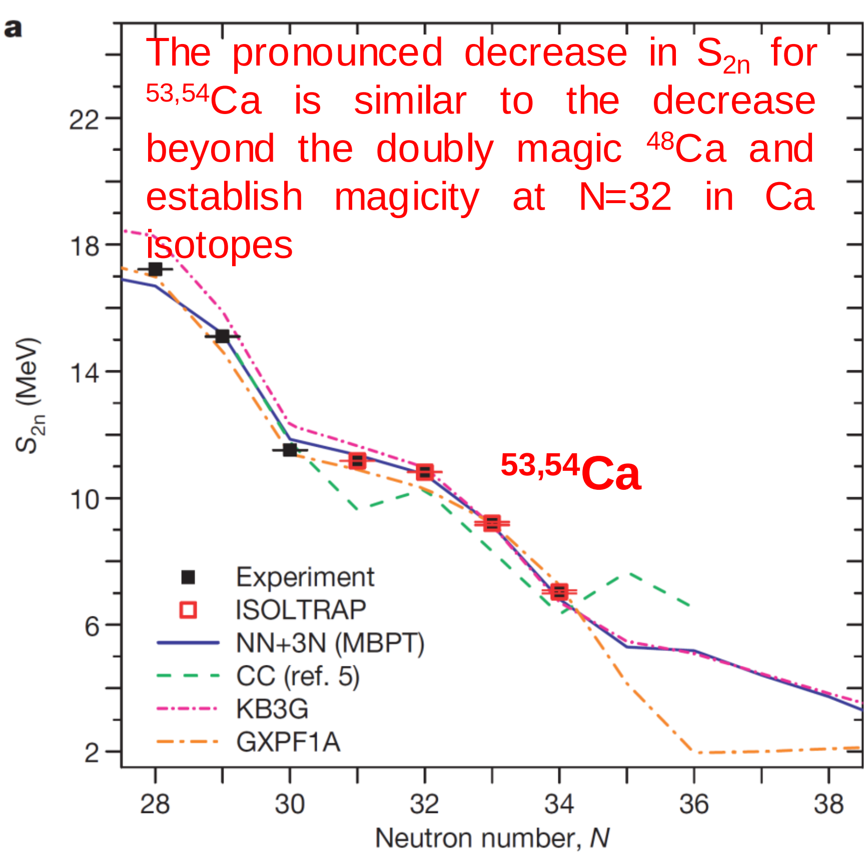

From the paper: We note **the advantages of the MR-TOF method as compared to Penning-trap mass spectrometry** will also be important for new experimental facilities, which will provide even more exotic ion beams.

The present and future developments of low-energy beams at facilities for the study of exotic nuclides such as ARIEL, CARIBU, FAIR, FRIB, HIE-ISOLDE, RIBF and SPIRAL 2 will considerably extend the available range of rare isotopes towards the nuclear driplines. The **minute production rates of isotopes with half-lives in the millisecond range and substantial isobaric contamination pose experimental challenges that are barely met by Penning traps now, but can be overcome with the MR-TOF method.**

$^{55-57}$Ca Masses with Time-of-Flight Magnetic Rigidity ToF-Bρ Method at BigRIPS@RIBF (RIKEN)

PHYSICAL REVIEW LETTERS **121,** 022506 (2018)

Magic Nature of Neutrons in ^{54}Ca: First Mass Measurements of $^{55-57}$Ca

S. Michimasa,[1,*] M. Kobayashi,[1] Y. Kiyokawa,[1] S. Ota,[1] D. S. Ahn,[2] H. Baba,[2] G. P. A. Berg,[3] M. Dozono,[1] N. Fukuda,[2] T. Furuno,[4] E. Ideguchi,[5] N. Inabe,[2] T. Kawabata,[4] S. Kawase,[6] K. Kisamori,[1] K. Kobayashi,[7] T. Kubo,[8,9] Y. Kubota,[2] C. S. Lee,[1,2] M. Matsushita,[1] H. Miya,[1] A. Mizukami,[10] H. Nagakura,[7] D. Nishimura,[11] H. Oikawa,[10] H. Sakai,[2] Y. Shimizu,[2] A. Stolz,[9] H. Suzuki,[2] M. Takaki,[1] H. Takeda,[2] S. Takeuchi,[12] H. Tokieda,[1] T. Uesaka,[2] K. Yako,[1] Y. Yamaguchi,[1] Y. Yanagisawa,[2] R. Yokoyama,[13] K. Yoshida,[2] and S. Shimoura[1]

^{70}Zr, 345 AMeV fragmentation on ^{9}Be target

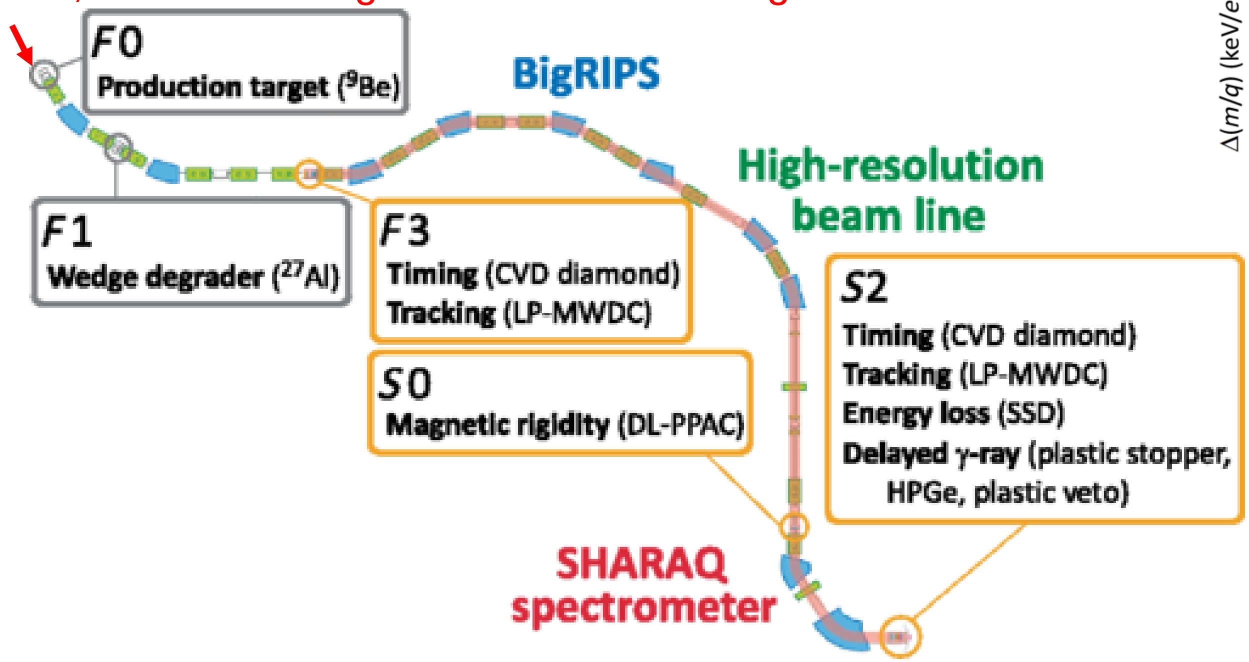

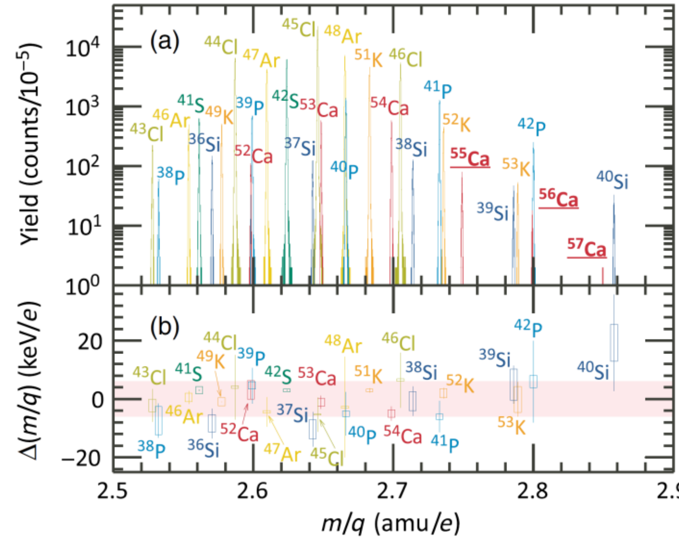

TABLE I. The atomic mass excesses determined in the present experiment and the AME2016 database [38].

Nucleus	Present (keV)	AME2016 (keV)
^{57}Ca	−7370(990)	...
^{56}Ca 11(2) ms	−13 510(250)	...
^{55}Ca	−18 650(160)	...
^{48}Ar	−22 330(120)	−22 280(310)
^{46}Cl	−13 700(110)	−13 860(210)
^{44}Cl	−20 540(110)	−20 380(140)
^{42}P	+1100(100)	+1010(310)
^{40}P	−8150(100)	−8110(150)
^{40}Si	+5700(130)	+5430(350)

3379 events ^{55}Ca
619 events – ^{56}Ca
29 events – ^{57}Ca

- **A “cocktail” of many isotopes! (but good for mass calibration)**
- Allows to access much shorter half-lives (>100 ns)
- ToF is measured between F3 and S2 (~105 m, ~540 ns flight time)
- Magnetic rigidity Bρ

$$\frac{m}{q} = \frac{B\rho}{\gamma L} t = \frac{B\rho}{c}\sqrt{\left(\frac{ct}{L}\right)^2 - 1},$$

$^{53-57}$Ca Masses from ISOLDE and RIKEN

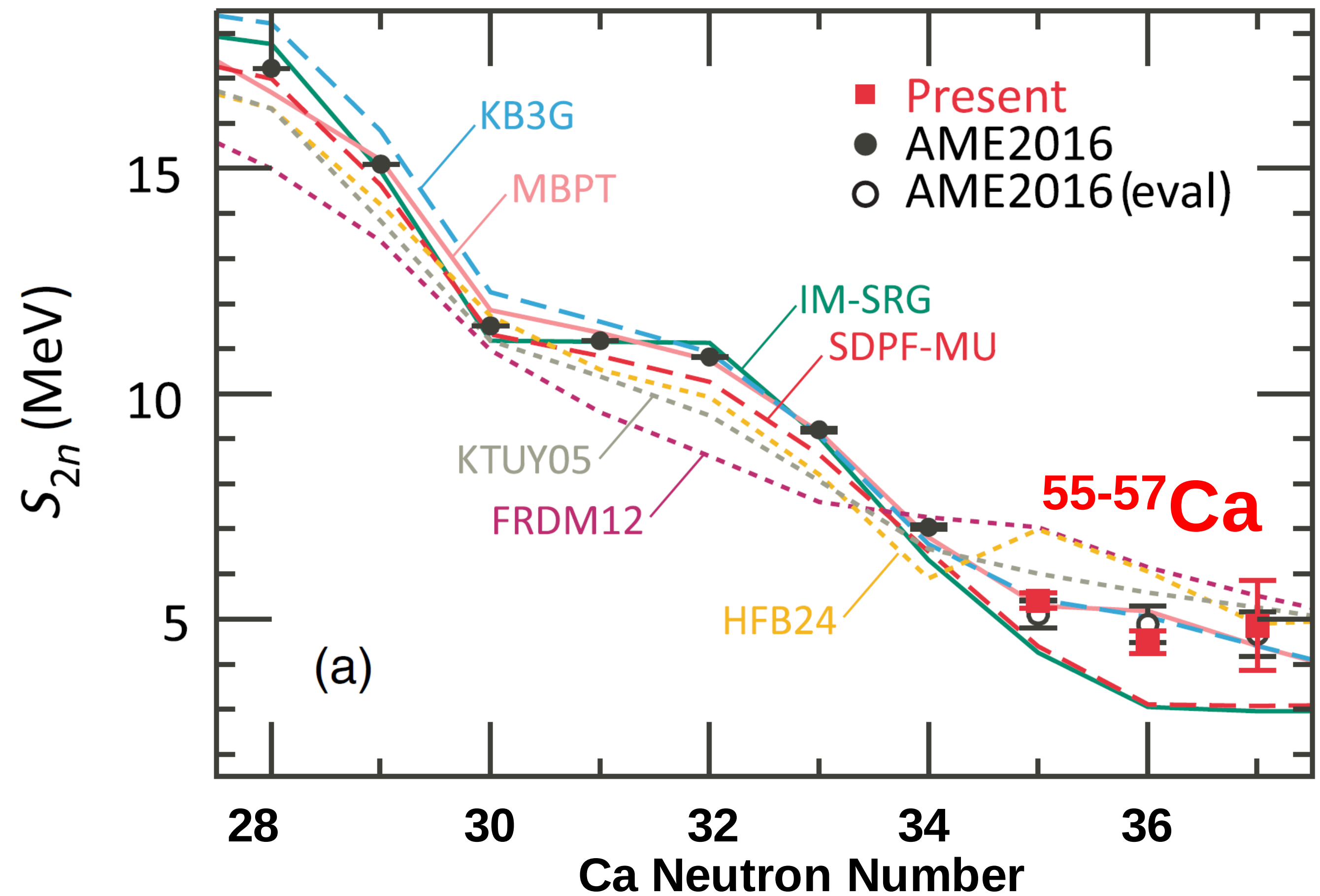

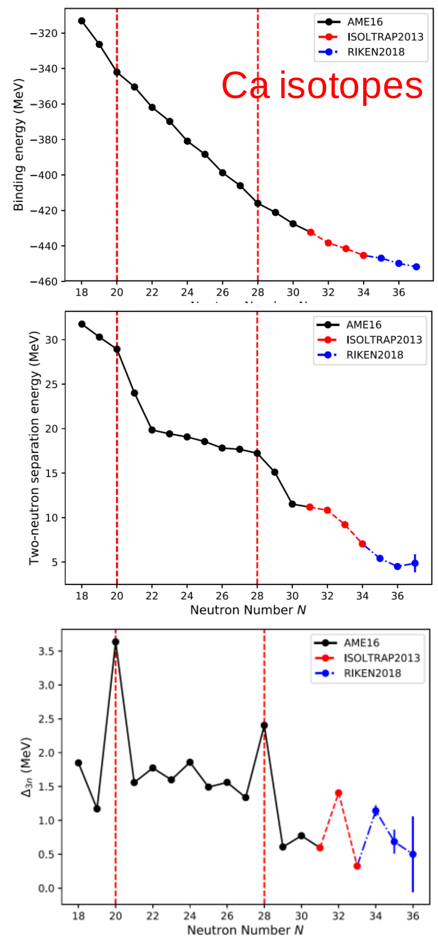

3-point binding-energy differences $\Delta_{3n}(N)=(-1)^N\times[B(N+1)+B(N-1)-2B(N)]/2$

By observation of the mass evolution in Ca isotopes beyond N=34, the magic nature at N=34 in the neutron-rich Ca region became evident

^{51,52}Ca, TITAN@TRIUMF, A. T. Gallant et al, PRL109, 2012
^{53,54}Ca, ISOLDE, F.Wienholtz et al, Nature, 498, 346, 2013
$^{55-57}$Ca, RIKEN, S. Michimasa et al, PRL121, 2018

^{60}Ca Experimental Setup and PID at BigRIPS

^{70}Zn beam @ 345 MeV/u
<I> = 200 pnA (1.25e12pps)

PID by TOF-Bρ-ΔE-TKE method: → Z, A/q, Q

- **New isotopes search**
- **Production cross section and momentum distribution measurement**
- **Secondary reactions yield measurement as target thickness**
- **New isomers search**

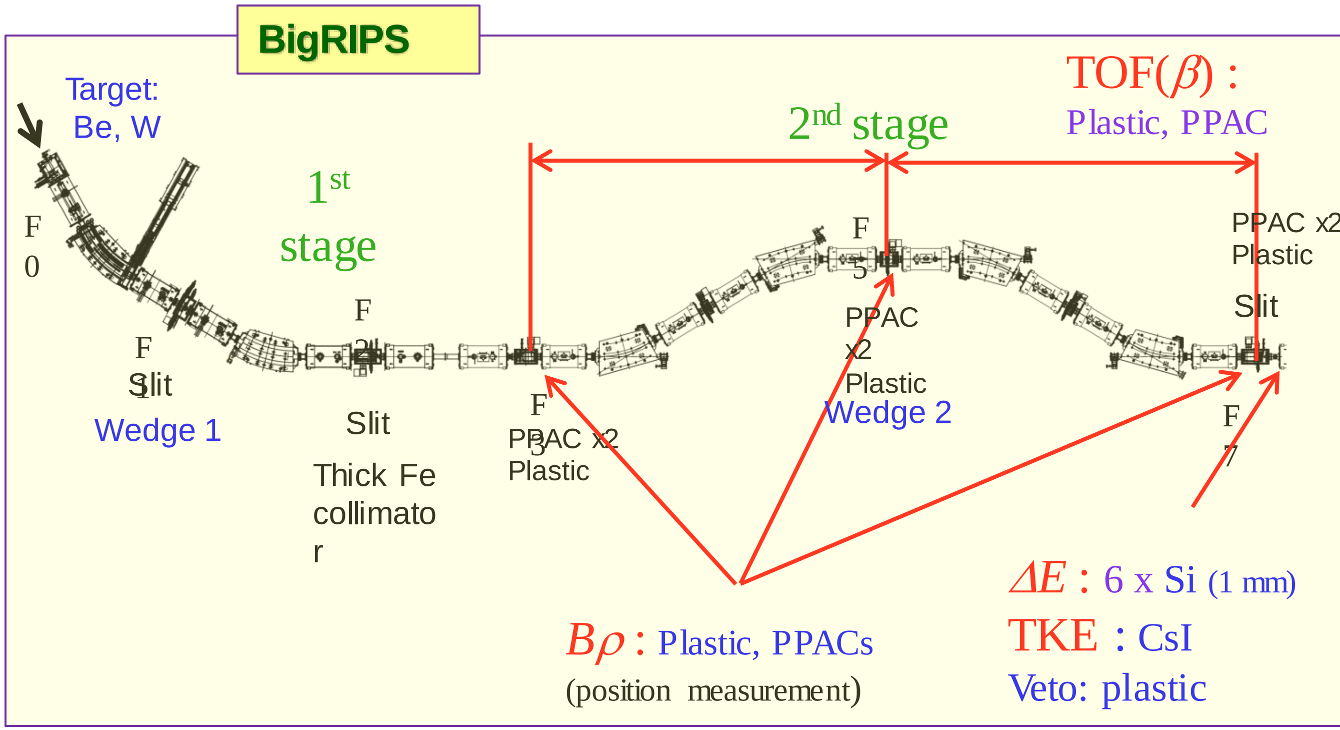

Total Experiment : 7 days

New isotopes search : 100.9 h (4.2 days)

^{60}Ca PID Plot and Identification of 8 new isotopes

PHYSICAL REVIEW LETTERS **121**, 022501 (2018)

Editors' Suggestion

Discovery of ^{60}Ca and Implications For the Stability of ^{70}Ca

O. B. Tarasov,[1,2,3] D. S. Ahn,[2] D. Bazin,[1] N. Fukuda,[2] A. Gade,[1,4] M. Hausmann,[5] N. Inabe,[2] S. Ishikawa,[6] N. Iwasa,[6] K. Kawata,[7] T. Komatsubara,[2] T. Kubo,[5] K. Kusaka,[2] D. J. Morrissey,[1,8] M. Ohtake,[2] H. Otsu,[2] M. Portillo,[5] T. Sakakibara,[6] H. Sakurai,[2] H. Sato,[2] B. M. Sherrill,[1,4] Y. Shimizu,[2] A. Stolz,[1] T. Sumikama,[2] H. Suzuki,[2] H. Takeda,[2] M. Thoennessen,[1,4] H. Ueno,[2] Y. Yanagisawa,[2] and K. Yoshida[2]

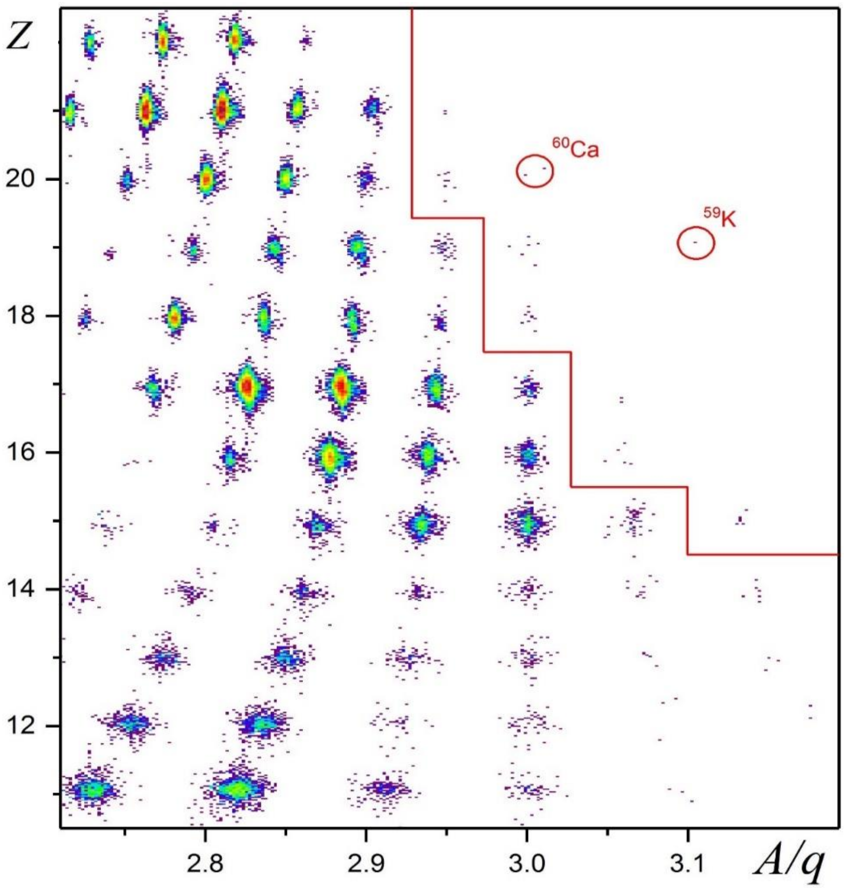

8 new isotopes including ^{60}Ca (+^{59}K)

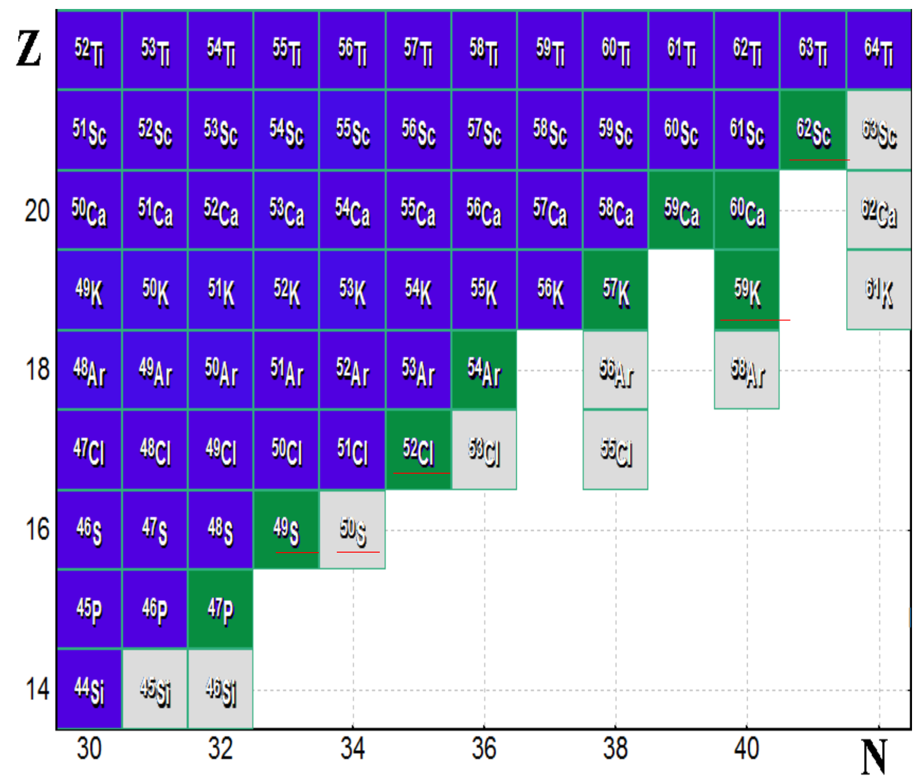

Green color : observed at the first time

Red color : particularly interesting isotopes

The region of the chart of nuclides studied in this work

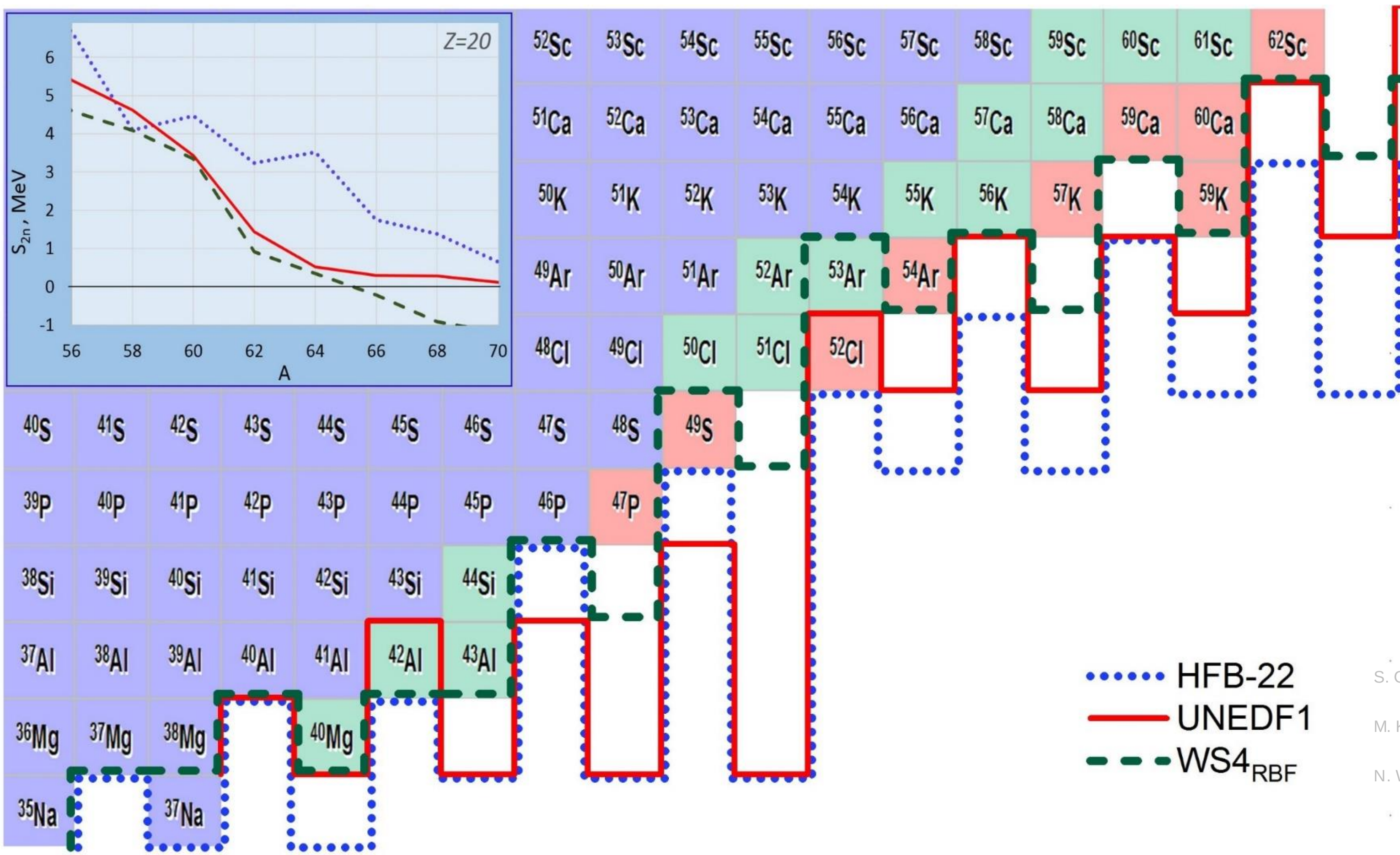

Red background : this experiment

Green background: at the NSCL since 2007

HFB-22 and the UNEDF0/1 functionals also predict the even-mass Ca isotopes are bound up to at least ^{70}**Ca**.

The inset shows the predicted S_{2n} values for even neutron-rich calcium Isotope.

S. Goriely et al., PRC 88, 024308 (2013)

M. Kortelainen et al., PRC 85, 024304 (2012)

N. Wang et al., PLB 734, 215 (2014)

Doubly-Magic ^{70}Ca (Z=20, N=50)?
(Neutron Drip Line in the Ca Region from Bayesian Model Averaging)

PHYSICAL REVIEW LETTERS **122**, 062502 (2019)

Neutron Drip Line in the Ca Region from Bayesian Model Averaging

Léo Neufcourt,[1,2] Yuchen Cao (曹宇晨),[3] Witold Nazarewicz,[4] Erik Olsen,[2] and Frederi Viens[1]
[1]*Department of Statistics and Probability, Michigan State University, East Lansing, Michigan 48824, USA*
[2]*FRIB Laboratory, Michigan State University, East Lansing, Michigan 48824, USA*
[3]*Department of Physics and Astronomy and NSCL Laboratory, Michigan State University, East Lansing, Michigan 48824, USA*
[4]*Department of Physics and Astronomy and FRIB Laboratory, Michigan State University, East Lansing, Michigan 48824, USA*

(Received 12 September 2018; revised manuscript received 15 November 2018; published 14 February 2019)

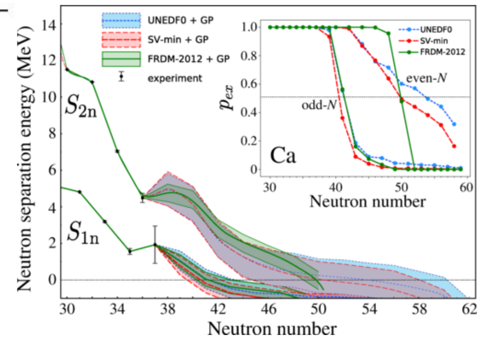

Using a Bayesian machine learning analysis of extrapolations via Gaussian processes*

L. Neufcourt, Y. Cao, W. Nazarewicz, and F. Viens, Phys. Rev. C 98, 034318 (2018).

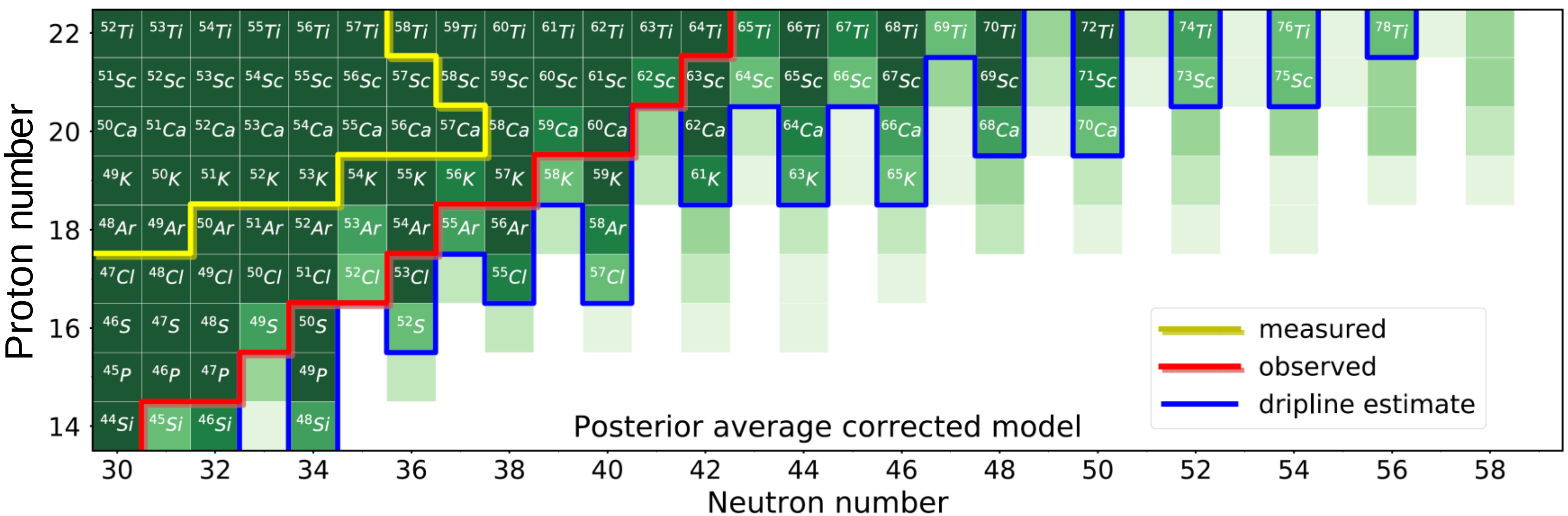

Using weights $w_k := p(\mathcal{M}_k | {}^{52}\mathrm{Cl}, {}^{53}\mathrm{Ar}, {}^{49}\mathrm{S}\ \mathrm{exist})$

Case 3 Back to basics: Superallowed Alpha decay

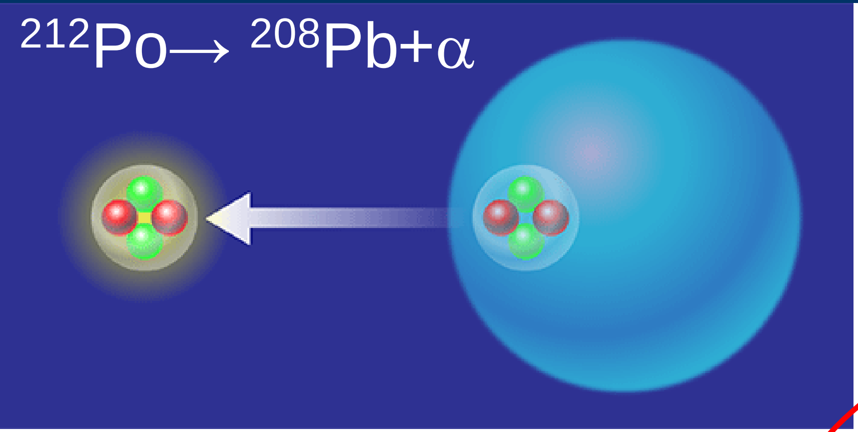

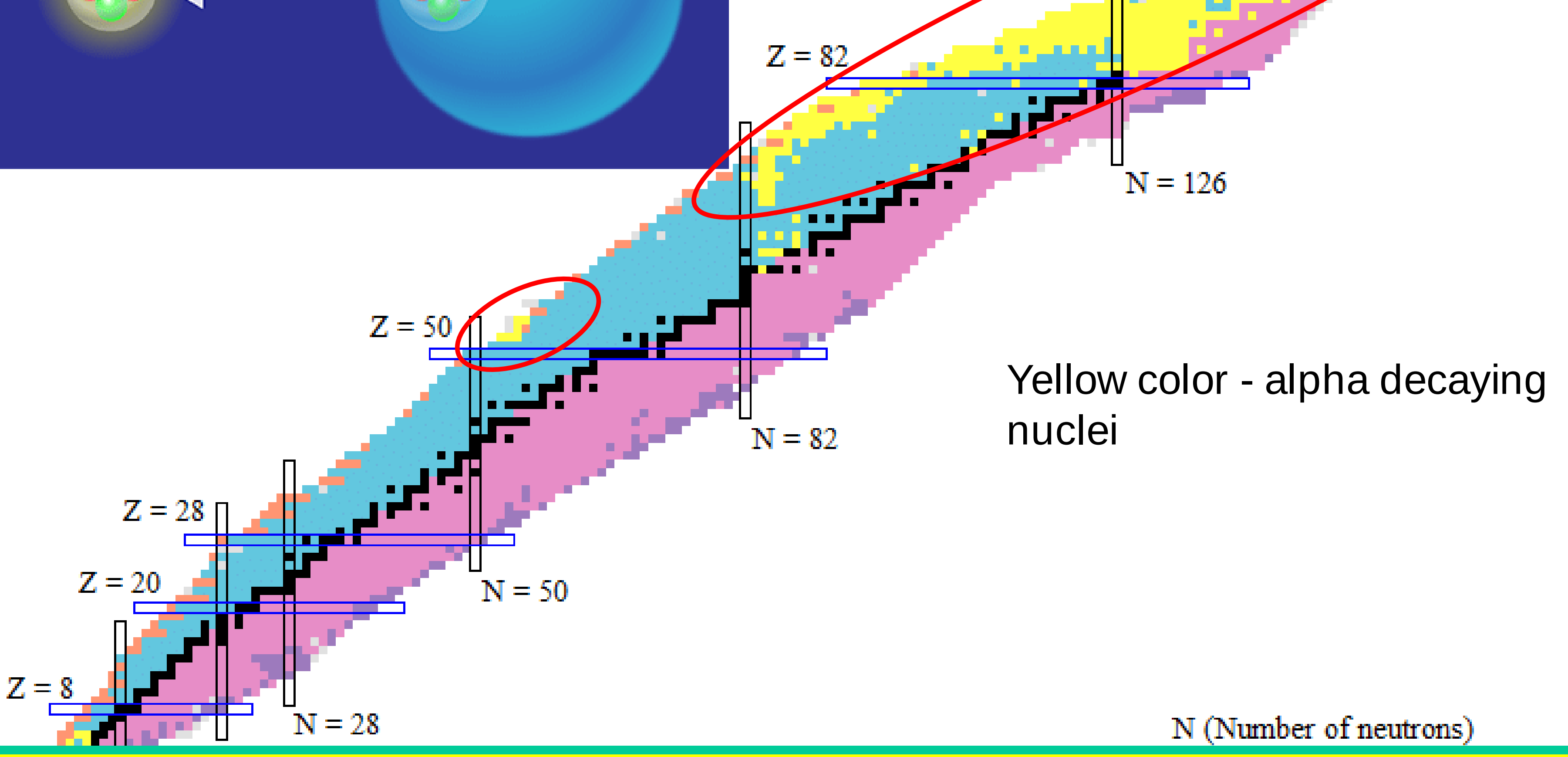

Yellow color - alpha decaying nuclei

Quiz: Several regions of alpha decay, some of them are always slightly above magic neutron numbers N=50, 82 and 126? Why?

Systematics of Q_α values in the Pb-Hs region

- Typical Q_α values are in the range of 2.5-12 MeV
- Not a smooth trend (as one would expect from SEMF)

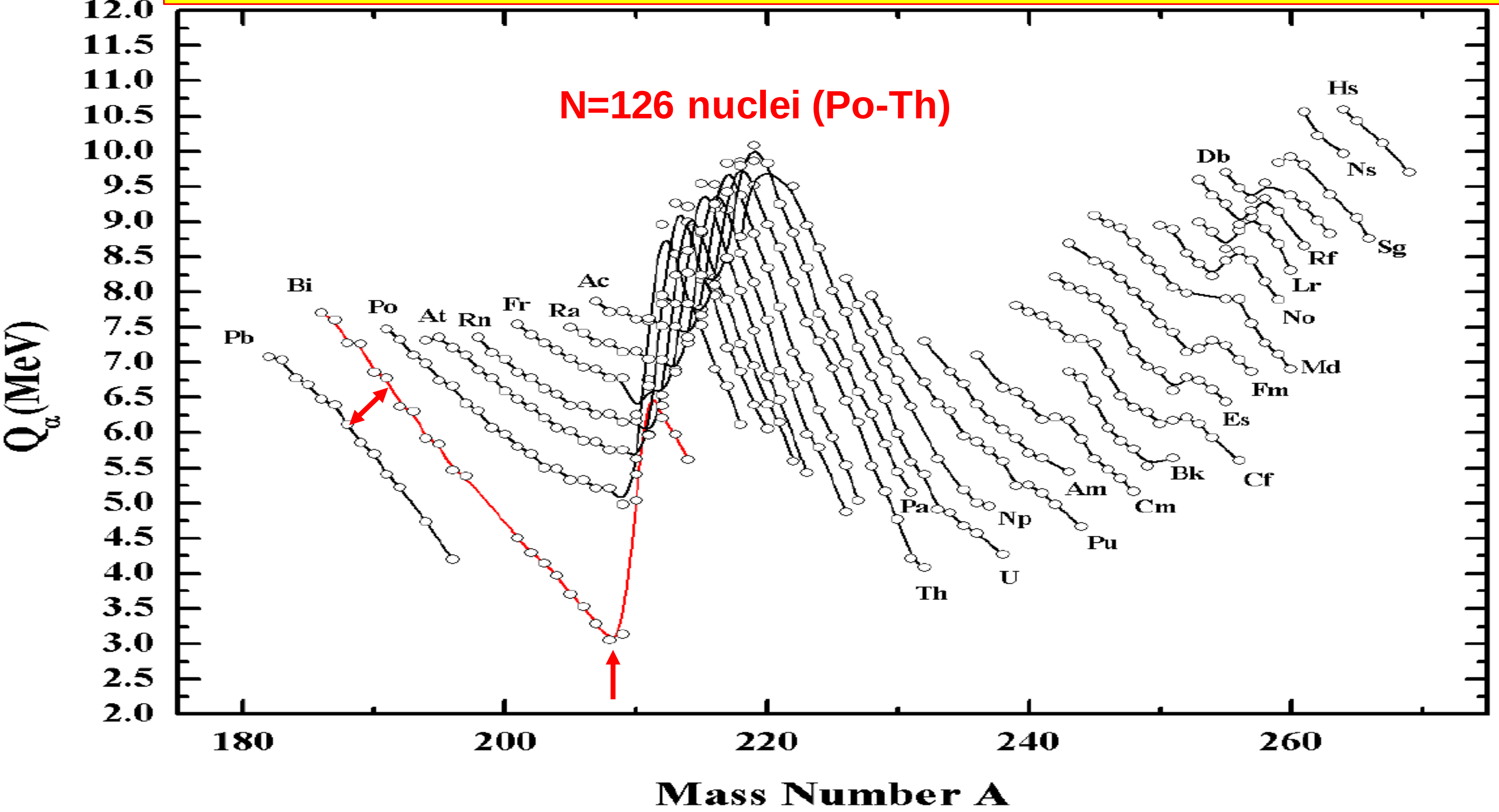

Larger separation between Pb(Z=82) and Bi(Z=83), due to **proton magic number Z=82**

Sharp drop an N=126 – due to the **neutron magic number N=126 (e.g. ^{209}Bi)**

A Reminder to (simplified) Alpha Decay Theory

Historically, the alpha decay rate (decay constant λ_α) was introduced as

$$\lambda_\alpha = FP \times F \times T$$

FP- **formation probability** of alpha particle inside the parent nucleus (a complex thing to derive theoretically, need to produce an alpha particle from 2 neutrons and 2 protons inside the nucleus, **in most cases they are in different shell model orbitals**)

F- **'assault' frequency** of this alpha particle on the barrier (easy to calculate)

T- **tunnelling** of alpha particle through the barrier ("easy" to calculate)

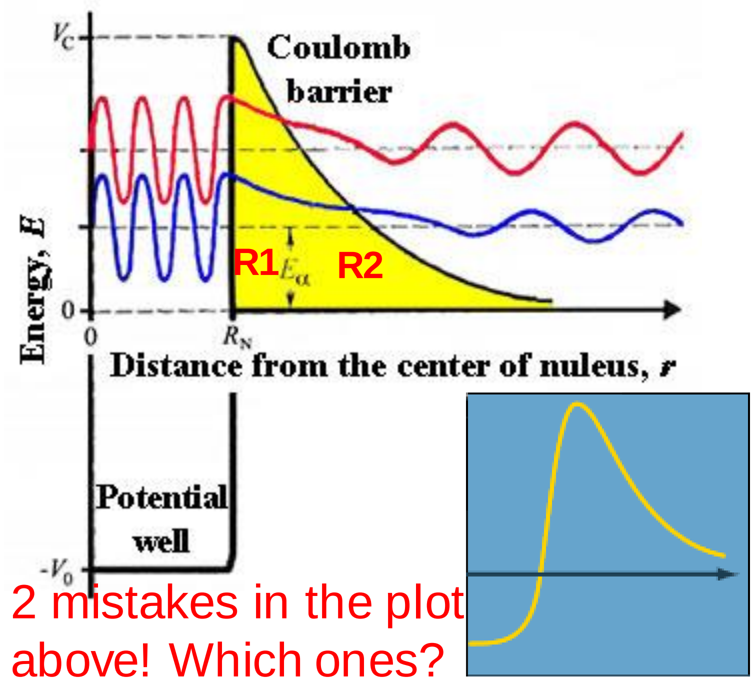

2 mistakes in the plot above! Which ones?

Penetrability through the barrier **depends exponentially on Q_α value**

$$T = e^{-\frac{2}{\hbar}\int_{R1}^{R2}\left[2\mu\left(\frac{Z_\alpha Z_D e^2}{r} - Q_\alpha\right)\right]^{1/2} dr}$$

Detailed Example for ^{212}Po (from Hyperphysics)

http://hyperphysics.phy-astr.gsu.edu/hbase/Nuclear/alpdet.html#c1

^{212}Po alpha decay, E_α=8.78 MeV, $T_{1/2,exp}$=0.3 μs

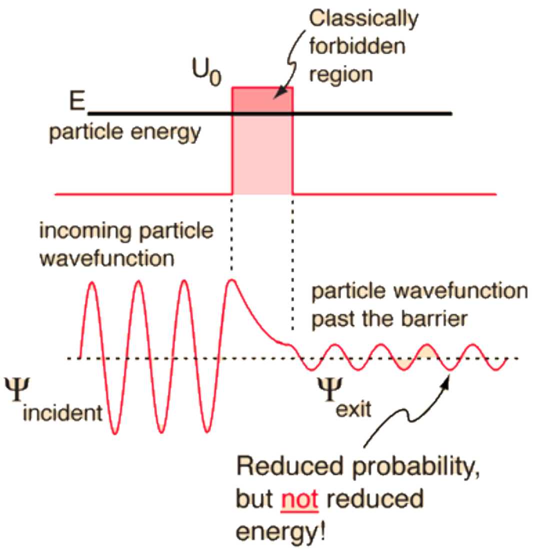

1. First, consider **a rectangular barrier** (as Gamow).

2. **Alpha-Daughter separation distance** $= 1.2\left[4^{1/3} + 208^{1/3}\right] = 9.01\,fm$

3. **Coulomb barrier:** $\dfrac{2(Z-2)ke^2}{r} = \dfrac{2(82)1.44\ \ MeV \cdot fm}{9.01\,fm} = 26.21\ \ MeV$

4. The **distance at which the Coulomb potential drops to the level of energy of the observed alpha**

$$8.78\,MeV = \frac{2(82)1.44\,MeV \cdot fm}{r}\ \ ;\ \ r = 26.9\,fm$$

5. Thus, the **width of the barrier**: $26.90\,fm - 9.01\,fm = 17.9\,fm$

6. The alpha emission rate depends upon how many times an alpha particle with this energy inside the nucleus will hit the walls. The **velocity of the alpha**:

$$8.78\,MeV = \frac{mv^2}{2} = \frac{3727\,MeV \cdot v^2}{2c^2} \qquad \frac{v}{c} = .00686;\ \ v = 2.06\ \ x\ \ 10^7\,m/s$$

7. The **frequency of hitting the walls** is then $f = \dfrac{v}{2R} = \dfrac{2.06\ \ x\ \ 10^7\,m/s}{2(9.01\,fm)(10^{-15}\,m/fm)} = 1.14\ \ x\ \ 10^{21}\ /s$

8. The tunneling probability for a rectangular barrier of height 26.2 MeV and width 17.9 fm is $Tunneling\ probability = 4\ \ x\ \ 10^{-29}$ (use: http://hyperphysics.phy-astr.gsu.edu/hbase/quantum/barr.html#c1)

9. The probability per second for alpha emission $(4\ \ x\ \ 10^{-29})(1.14\ \ x\ \ 10^{21}/s) = 4.57\ \ x\ \ 10^{-8}/s = \dfrac{-dN/dt}{N}$

10. **Finally, half-life** $N = N_0 e^{-\lambda t}\ ;\ T_{1/2} = \dfrac{.693}{\lambda} = \dfrac{.693}{4.57\ \ x\ \ 10^{-8}/s} = 1.5\ \ x\ \ 10^7 s$ **~10^{13} times too long? Why?**

What is the Formation Probability FP?

- Consider the 'text-book' case of ^{212}Po(Z=84,N=128)

- Wave-function for the α decay:

$\Psi(^{212}Po) \rightarrow \Psi(^{208}Pb) \times \Psi(\alpha) \rightarrow \Psi(^{208}Pb)\times$

So, one has a doubly-magic spherical to calculate theoretically) and 2 valenc neutrons coupled to it, **from which ar formed on the surface of the nucle**

- The problem is, however, that these **occupy different orbitals**: $h_{9/2}$ for pr

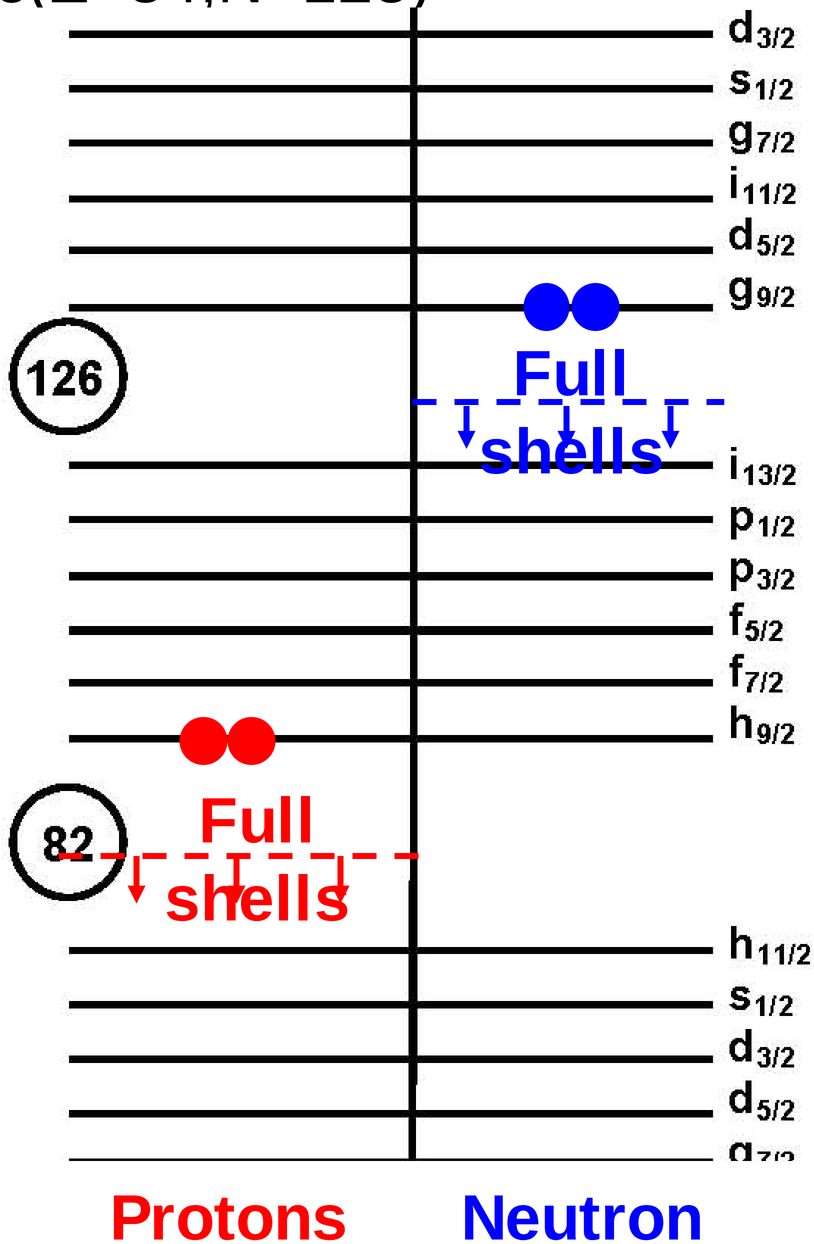

What is the Formation Probability FP?

- Consider the 'text-book' case of ^{212}Po(Z=84,N=128)

- Wave-function for the α decay:

$\Psi(^{212}\text{Po}) \rightarrow \Psi(^{208}\text{Pb}) \times \Psi(\alpha) \rightarrow \Psi(^{208}\text{Pb}) \times \Psi(\nu\nu\pi\pi)$.

So, one has a doubly-magic spherical ^{208}Pb core (probably, "easy" to calculate theoretically) and 2 valence protons and 2 valence neutrons coupled to it, **from which an alpha particle must be formed on the surface of the nucleus** ($\Psi(\alpha)$ value).

- The problem is, however, that these 2 protons and 2 neutrons **occupy different orbitals**: $h_{9/2}$ for protons and $g_{9/2}$ for neutrons.

  - Still, it works and due to very large Q_α value, the alpha decay of ^{212}Po **was the fastest known alpha decay**, if measured via the so-called **'reduced decay width δ_α^2**:

$$\delta_\alpha^2 = \lambda_\alpha / P$$

Superallowed Alpha Decay of ^{104}Te(Z=N=52) (or, does p-n pairing exist?)

- Now, what happens is we consider the decay of ^{104}Te (Z=N=52)

- Wave-function for the α decay:

$\Psi(^{104}\text{Te}) \rightarrow \Psi(^{100}\text{Sn}) \times \Psi(\alpha) \rightarrow \Psi(^{100}\text{Sn}) \times \Psi(\nu\nu\pi\pi)$.

So, one has a doubly-magic spherical ^{100}Sn core (probably, “easy” to calculate theoretically) and **2 valence protons and 2 valence neutrons in the same orbitals!**

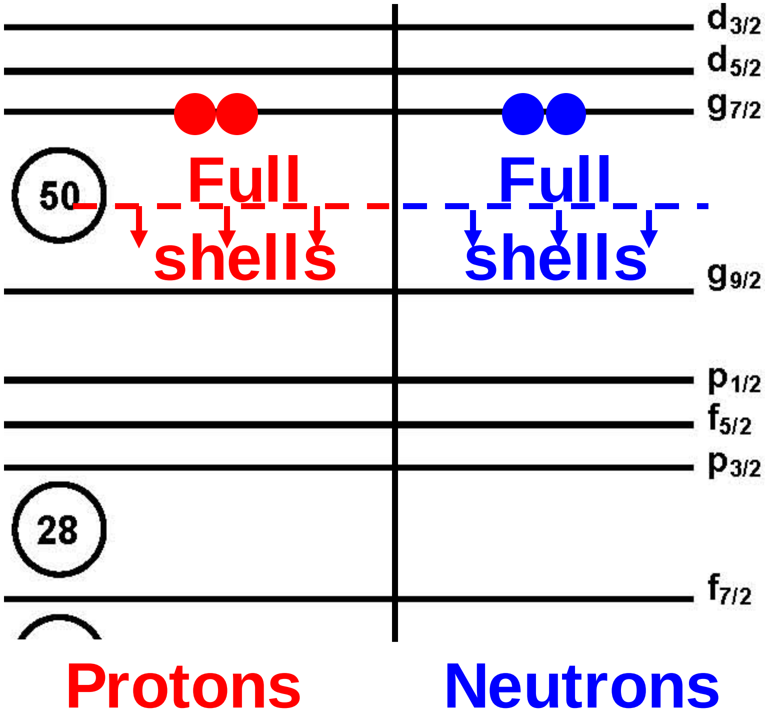

Superallowed Alpha Decay of ^{104}Te(Z=N=52) (or, does p-n pairing exist?)

- Now, what happens is we consider the decay of ^{104}Te (Z=N=52)

- Wave-function for the α decay:

$\Psi(^{104}\mathrm{Te}) \rightarrow \Psi(^{100}\mathrm{Sn}) \times \Psi(\alpha) \rightarrow \Psi(^{100}\mathrm{Sn}) \times \Psi(\nu\nu\pi\pi)$.

So, one has a doubly-magic spherical ^{100}Sn core (probably, "easy" to calculate theoretically) and **2 valence protons and 2 valence neutrons in the same orbitals!**

- Naively-speaking, one expects **that the α particle formation should be easier, also due to the possibility of p-n pairing!**

- This phenomenon was proposed in 1965 (R. D. Macfarlane and A. Siivola, Phys. Rev. Lett. 14, 114 (1965)) and is dubbed '**superallowed' alpha decay**.
- If confirmed, ^{104}Te **should be the fastest known alpha decay**, with a higher **'reduced decay width δ_α^2** than that of ^{212}Po.

Superallowed Alpha Decay of ^{104}Te(Z=N=52) (or, does p-n pairing exist?)

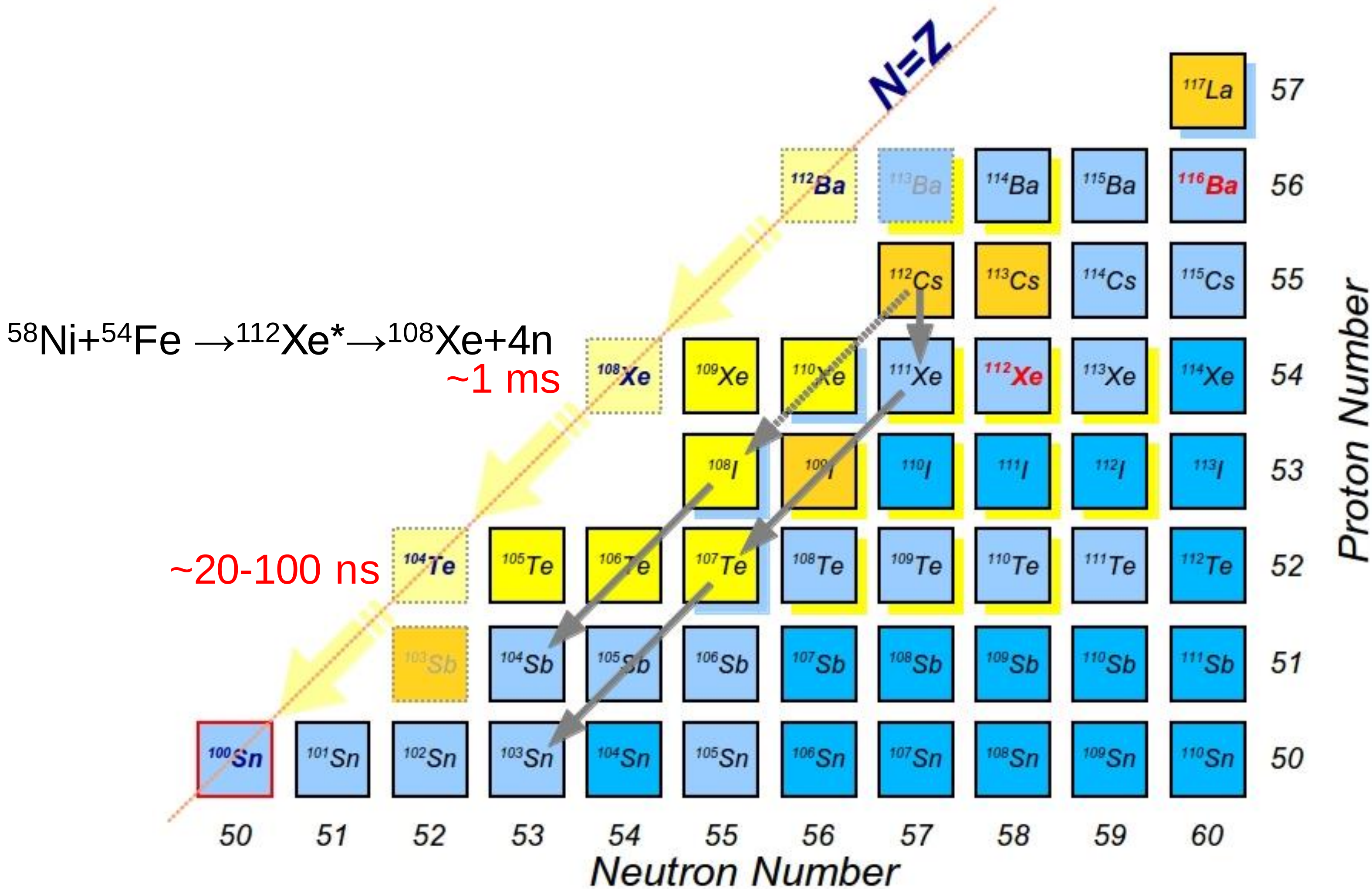

The problem: a very short half-life of ^{104}Te is expected, of the order of ~20-100 ns, thus the most plausible option to study its decay is to produce it via the decay of ^{108}Xe(Z=N=54), with expected half-life of ~a few ms

Superallowed Alpha Decay of ^{104}Te(Z=N=52) at Fragment Mass Analyzer (FMA) at ANL

PHYSICAL REVIEW LETTERS **121,** 182501 (2018)

Editors' Suggestion | Featured in Physics

Superallowed α Decay to Doubly Magic ^{100}Sn

K. Auranen,[1,*] D. Seweryniak,[1] M. Albers,[1] A. D. Ayangeakaa,[1,†] S. Bottoni,[1,‡] M. P. Carpenter,[1] C. J. Chiara,[1,2,§] P. Copp,[1,3] H. M. David,[1,‖] D. T. Doherty,[4,¶] J. Harker,[1,2] C. R. Hoffman,[1] R. V. F. Janssens,[5,6] T. L. Khoo,[1] S. A. Kuvin,[1,7] T. Lauritsen,[1] G. Lotay,[8] A. M. Rogers,[1,**] J. Sethi,[1,2] C. Scholey,[9] R. Talwar,[1] W. B. Walters,[2] P. J. Woods,[4] and S. Zhu[1]

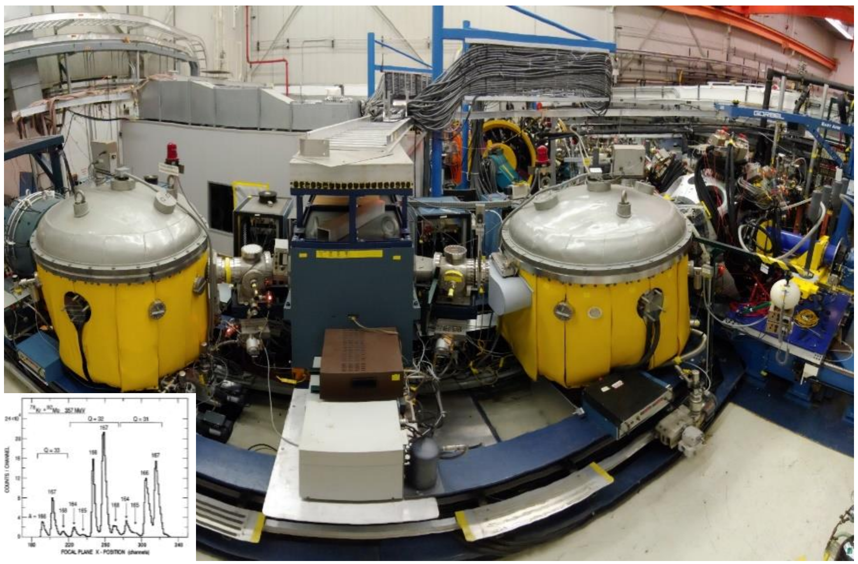

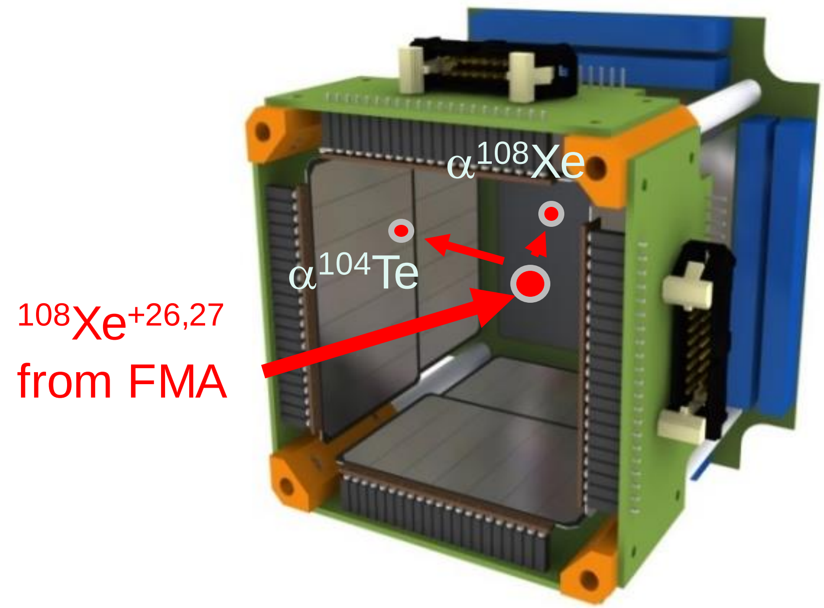

^{58}Ni(^{54}Fe,4n)^{108}Xe reaction, ~5 days , ~30 pnA

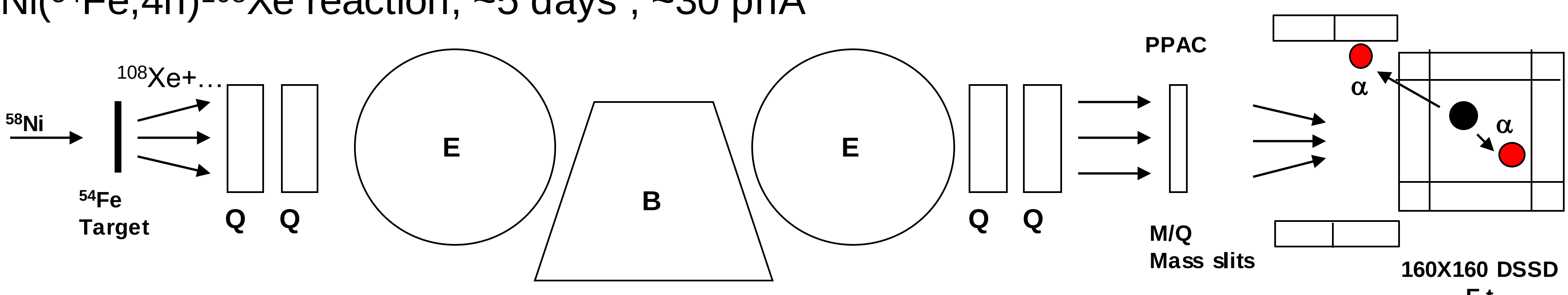

Recoil-alpha correlations in DSSD

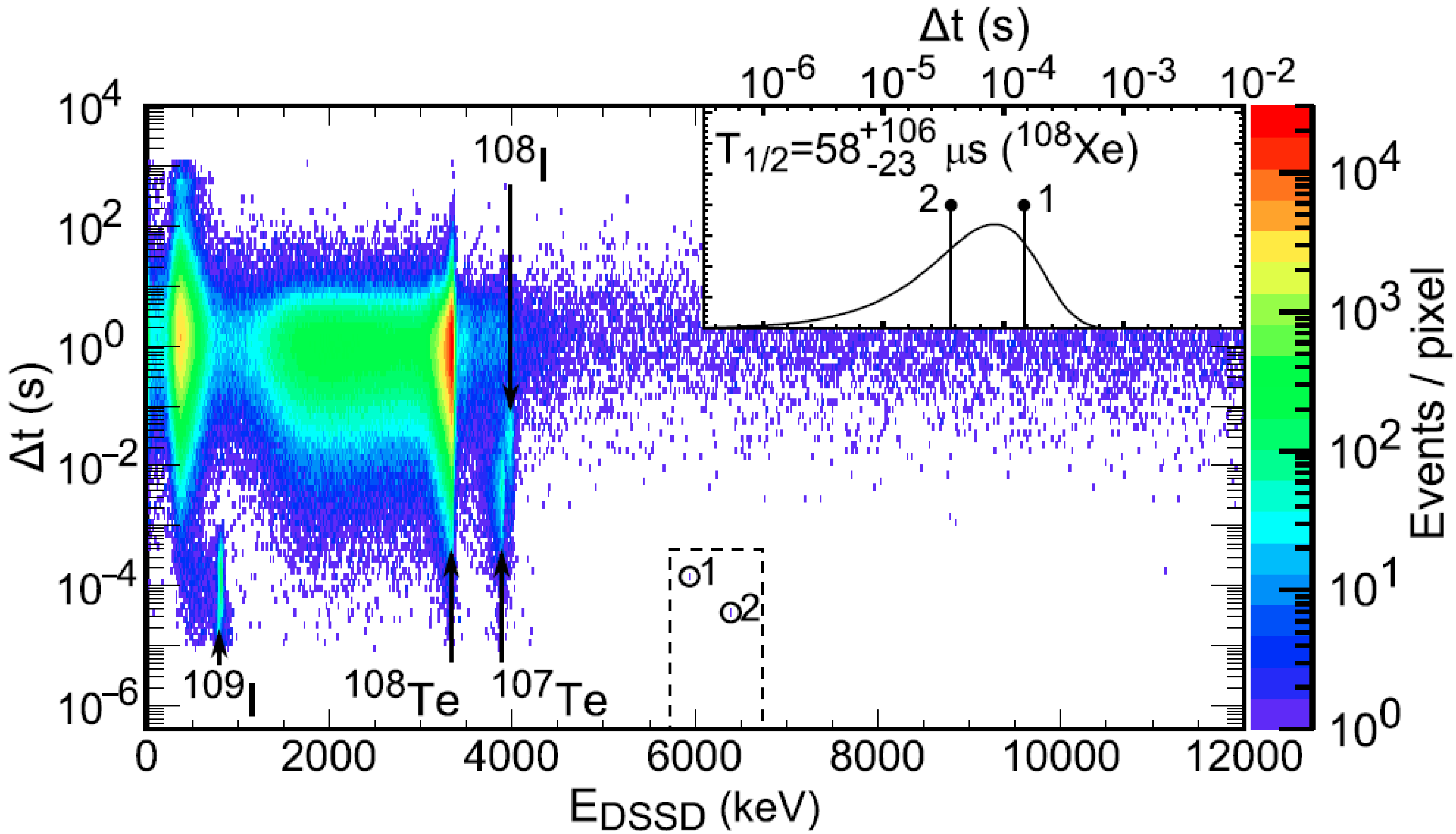

TWO fast high energy decay events (Expected **0.09** random events)

BOTH events where in coincidence with the Si box (1 out of 400)

- The same total energy for both events - **ΣE_{α}=9.3(1) MeV**
- Compared to α emitters different energy split

$E_{\alpha}(^{104}Te)$=4.9(2) MeV, $E_{\alpha}(^{108}Xe)$=4.4(2) MeV

DSSD traces for the ^{108}Xe-^{104}Te pile-up events

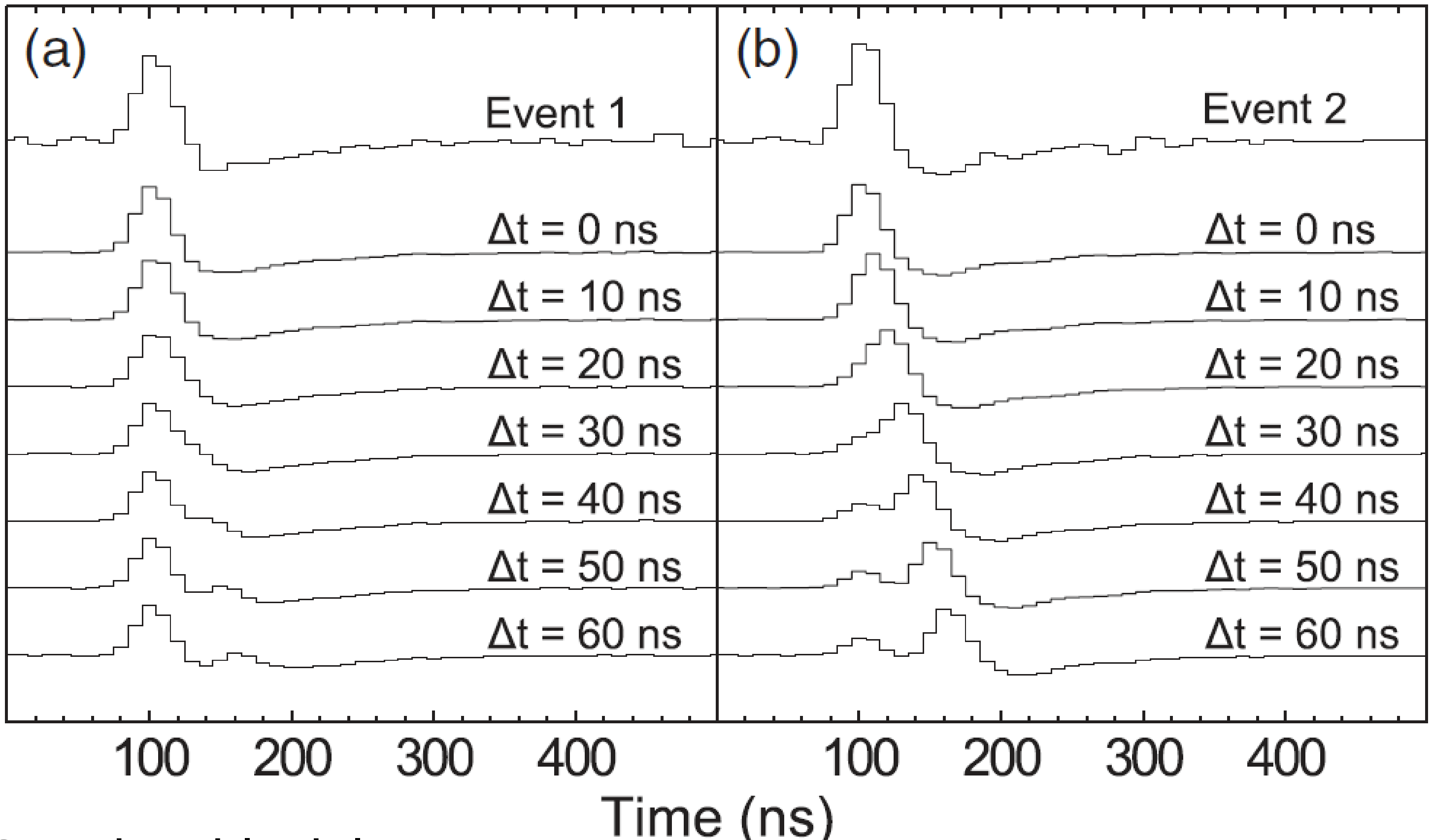

NO noticeable delay

TWO decays faster than 20 ns each imply **$T_{1/2}$<18 ns**

Nuclide	E_α (keV)	$T_{1/2}$	b_α (%)	**Ratio $\delta_\alpha^2/\delta_\alpha^2(^{212}Po)$**
^{108}Xe	4400(200)	58^{+106}_{-23} μs	100[a]	~3.7[b]
^{104}Te	4900(200)	<18 ns	100[a]	$\gtrsim$13.1[c]

Indeed, alpha decay of ^{104}Te is much faster than of ^{212}Po: superallowed!

DSSD traces for the ^{108}Xe-^{104}Te pile-up events

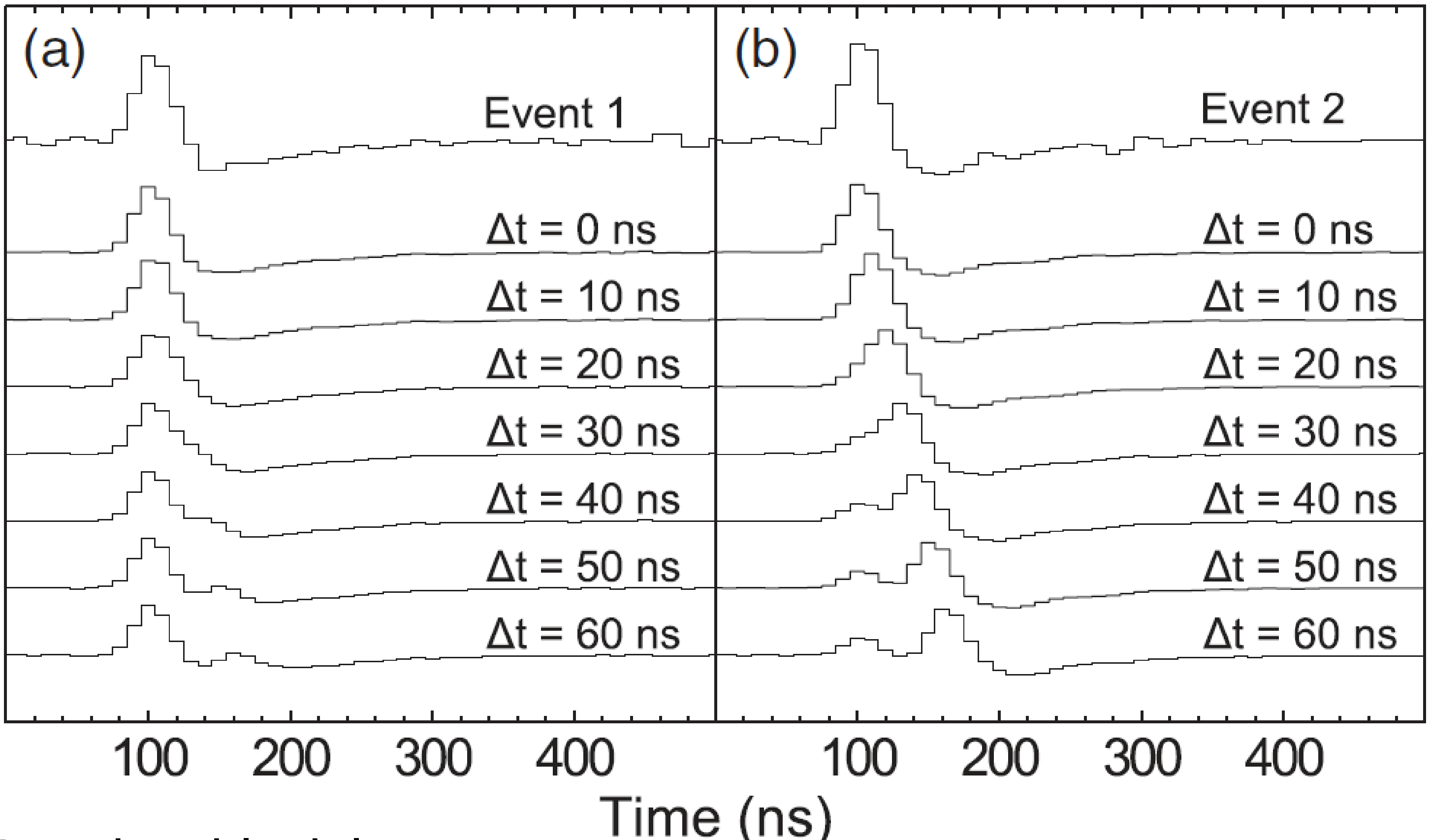

NO noticeable delay

TWO decays faster than 20 ns each imply **$T_{1/2}$<18 ns**

Nuclide	E_α (keV)	$T_{1/2}$	b_α (%)	Ratio $\delta_\alpha^2/\delta_\alpha^2(^{212}Po)$
^{108}Xe	4400(200)	58^{+106}_{-23} μs	100[a]	~3.7[b]
^{104}Te	4900(200)	<18 ns	100[a]	≳13.1[c]

Indeed, alpha decay of ^{104}Te is much faster than of ^{212}Po: superallowed!

Case Study 4: Pear-Shaped Nuclei?

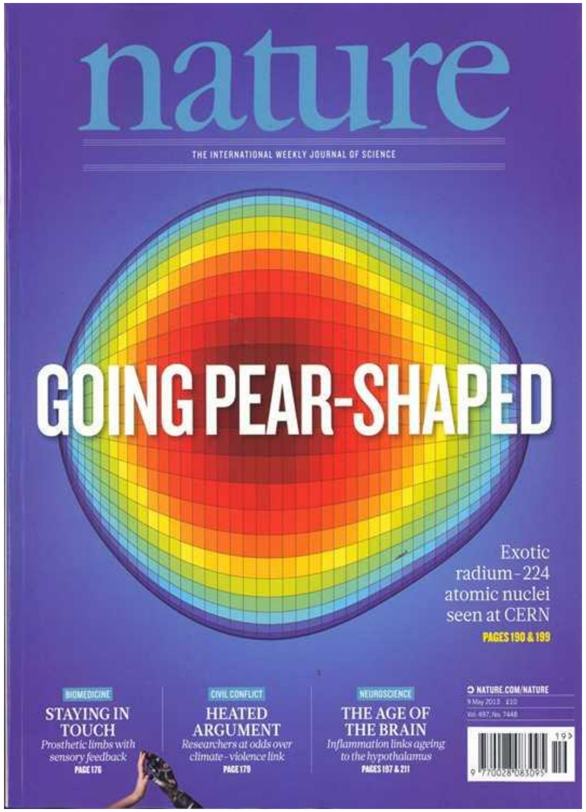

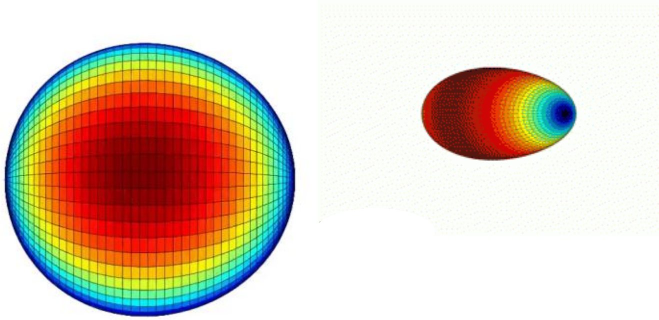

Studies of pear-shaped nuclei using accelerated radioactive beams
L. P. Gaffney et al. Nature 497, 199 (09 May 2013)

PRL 116, 112503 (2016) PHYSICAL REVIEW LETTERS week ending 18 MARCH 2016

Direct Evidence of Octupole Deformation in Neutron-Rich ^{144}Ba

B. Bucher,[1,*] S. Zhu,[2] C. Y. Wu,[1] R. V. F. Janssens,[2] D. Cline,[3] A. B. Hayes,[3] M. Albers,[2] A. D. Ayangeakaa,[2] P. A. Butler,[4] C. M. Campbell,[5] M. P. Carpenter,[2] C. J. Chiara,[2,6,†] J. A. Clark,[2] H. L. Crawford,[7,‡] M. Cromaz,[5] H. M. David,[2,§] C. Dickerson,[2] E. T. Gregor,[8,9] J. Harker,[2,6] C. R. Hoffman,[2] B. P. Kay,[2] F. G. Kondev,[2] A. Korichi,[2,10] T. Lauritsen,[2] A. O. Macchiavelli,[5] R. C. Pardo,[2] A. Richard,[7] M. A. Riley,[11] G. Savard,[2] M. Scheck,[8,9] D. Seweryniak,[2] M. K. Smith,[12] R. Vondrasek,[2] and A. Wiens[5]

nature COMMUNICATIONS 2019
https://doi.org/10.1038/s41467-019-10494-5 OPEN

The observation of vibrating pear-shapes in radon nuclei

P.A. Butler[1], L.P. Gaffney[1,2], P. Spagnoletti[3], J. Konki[2], M. Scheck[3], J.F. Smith[3], K. Abrahams[4], M. Bowry[5], J. Cederkäll[6], T. Chupp[7], G. de Angelis[8], H. De Witte[9], P.E. Garrett[10], A. Goldkuhle[11], C. Henrich[12], A. Illana[8], K. Johnston[2], D.T. Joss[1], J.M. Keatings[3], N.A. Kelly[3], M. Komorowska[13], T. Kröll[12], M. Lozano[2], B.S. Nara Singh[3], D. O'Donnell[3], J. Ojala[14,15], R.D. Page[1], L.G. Pedersen[16], C. Raison[17], P. Reiter[11], J.A. Rodriguez[2], D. Rosiak[11], S. Rothe[2], T.M. Shneidman[18], B. Siebeck[11], M. Seidlitz[11], J. Sinclair[3], M. Stryjczyk[9], P. Van Duppen[9], S. Vinals[19], V. Virtanen[14,15], N. Warr[11], K. Wrzosek-Lipska[13] & M. Zielinska[20]

Octupoles: Vibrations vs Deformation?

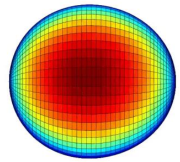

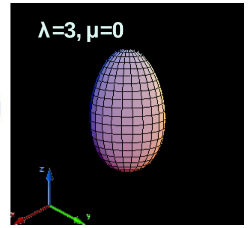

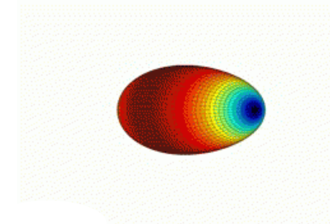

Macroscopically...

- Nuclei take on a “pear” shape
- Reflection asymmetric

Signatures...

- Feeding to low-lying 1^- states in α decay
- Odd-even staggering of states, -ive parity
- Parity doublets in odd-A nuclei
- Collective B(E3) transitions
- Inverse odd-even staggering in radii

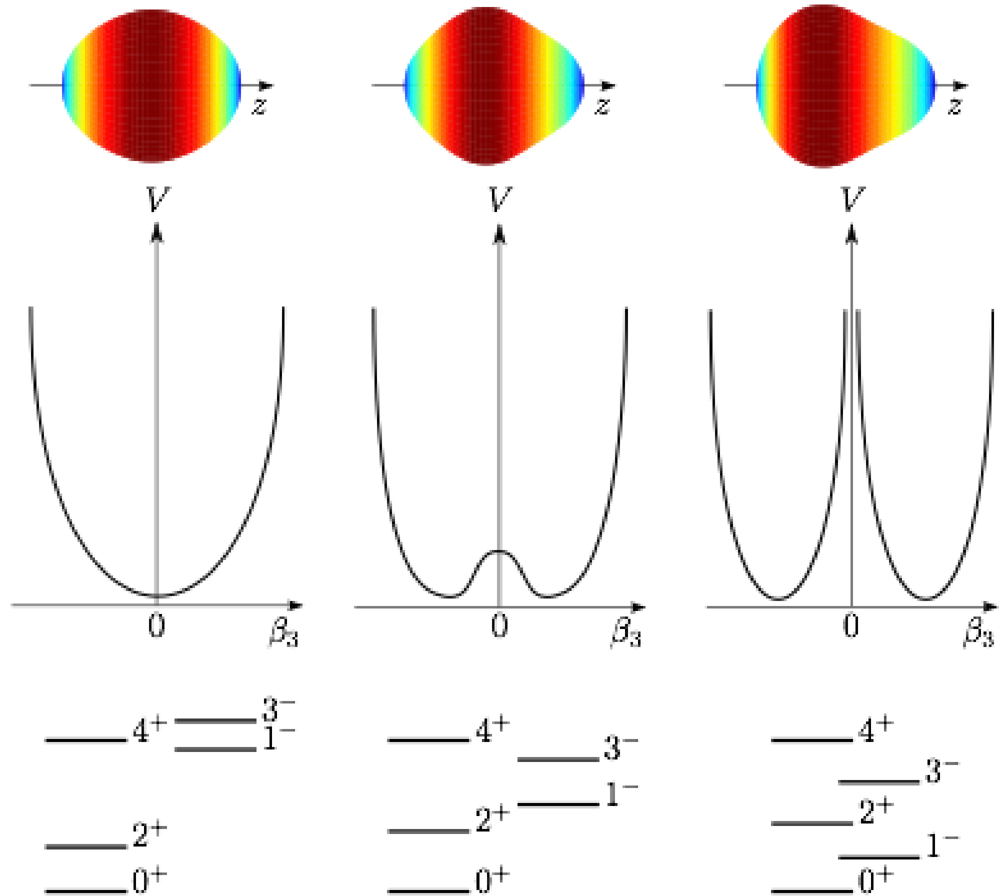

β_3-vibration Static β_3-deformation Rigid β_3-deformation (rotation)

Octupole Correlations

Microscopically driven: presence of proton and neutron orbitals near the Fermi surface which differ by $\Delta j, \Delta l = 3$ (*e.g. proton* $f_{7/2}$, $i_{13/2}$ and neutron $g_{9/2}$, $j_{15/2}$ in $Z>82$ region)

.

Enhanced at " octupole magic" numbers ***34, 56, 88, 134***

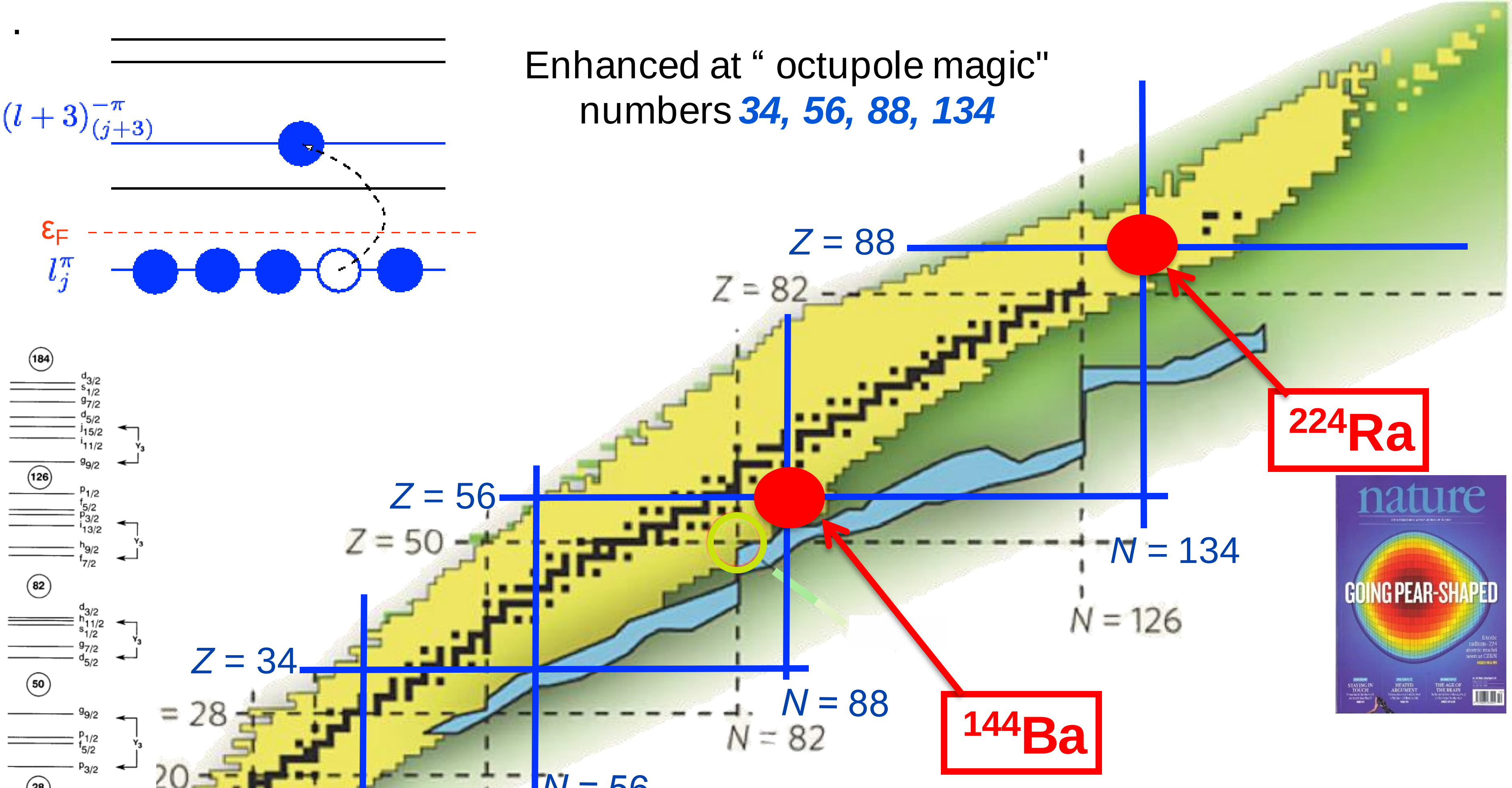

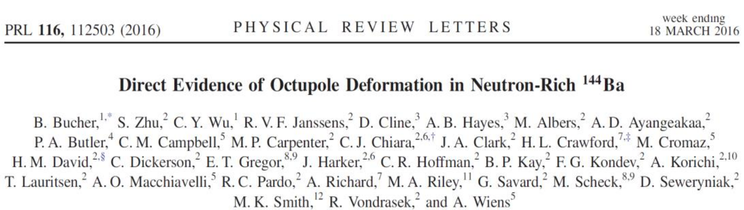
PRL **116,** 112503 (2016) PHYSICAL REVIEW LETTERS week ending 18 MARCH 2016

Direct Evidence of Octupole Deformation in Neutron-Rich ^{144}Ba

B. Bucher,[1,*] S. Zhu,[2] C. Y. Wu,[1] R. V. F. Janssens,[2] D. Cline,[3] A. B. Hayes,[3] M. Albers,[2] A. D. Ayangeakaa,[2] P. A. Butler,[4] C. M. Campbell,[5] M. P. Carpenter,[2] C. J. Chiara,[2,6,†] J. A. Clark,[2] H. L. Crawford,[7,‡] M. Cromaz,[5] H. M. David,[2,§] C. Dickerson,[2] E. T. Gregor,[8,9] J. Harker,[2,6] C. R. Hoffman,[2] B. P. Kay,[2] F. G. Kondev,[2] A. Korichi,[2,10] T. Lauritsen,[2] A. O. Macchiavelli,[5] R. C. Pardo,[2] A. Richard,[7] M. A. Riley,[11] G. Savard,[2] M. Scheck,[8,9] D. Seweryniak,[2] M. K. Smith,[12] R. Vondrasek,[2] and A. Wiens[5]

What is Coulomb Excitation (Coulex)?

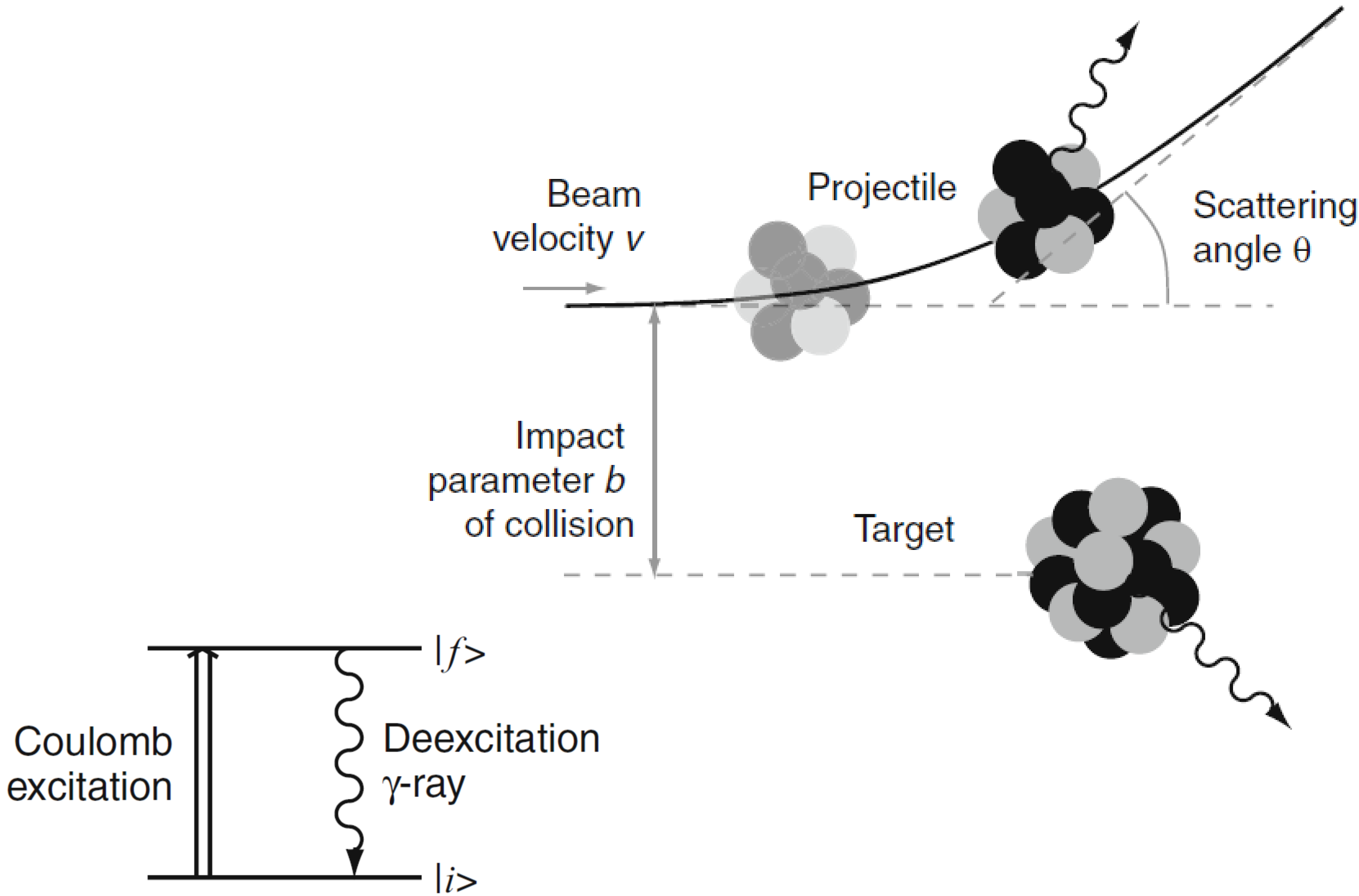

Coulex with Miniball and CD detector (ISOLDE)

HIE-ISOLDE **post-accelerated:**

6×10^5 pps ^{222}Rn (8 h)

1.1×10^5 pps ^{224}Rn (16 h)

2×10^3 pps ^{226}Rn (24 h)

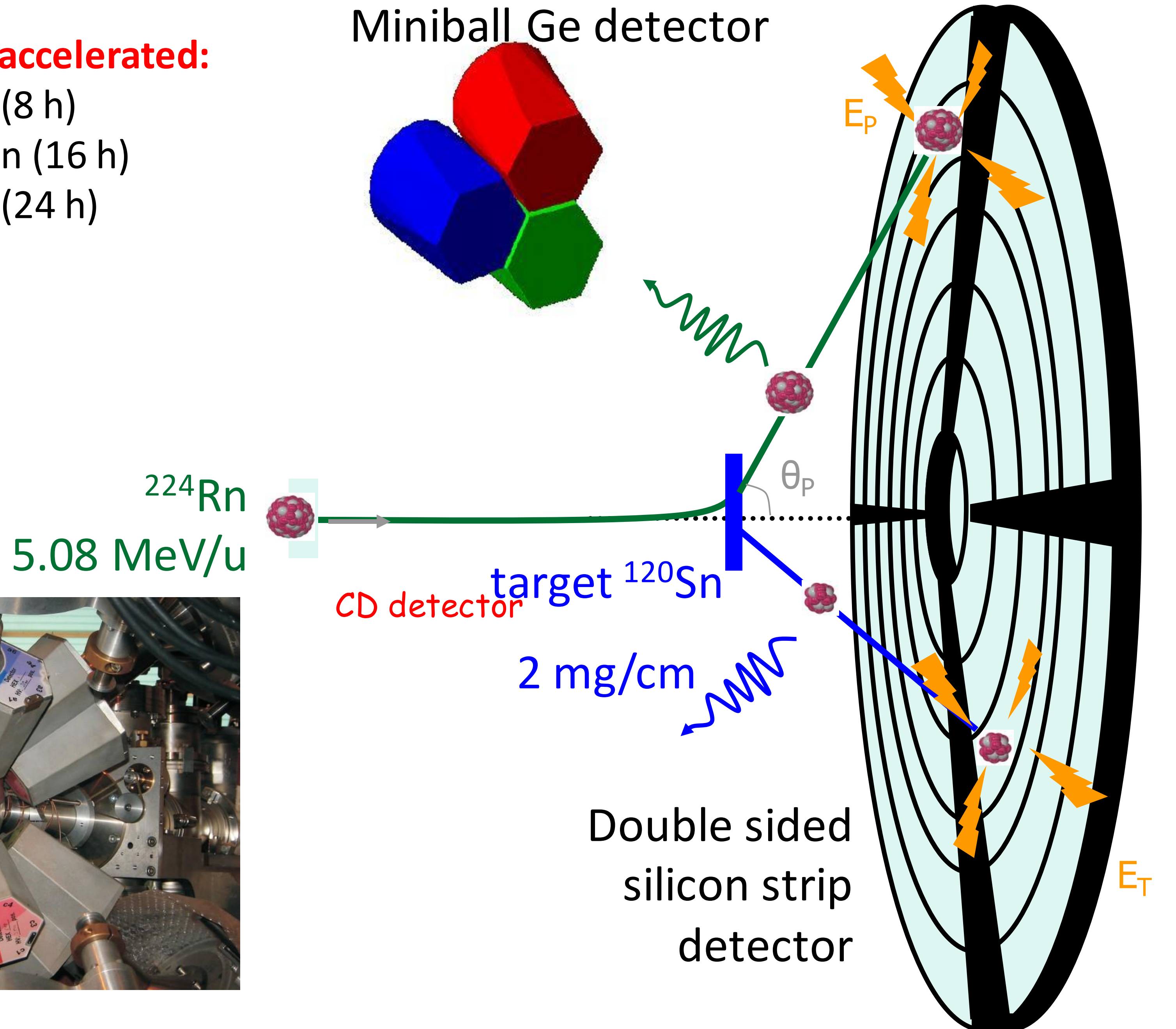

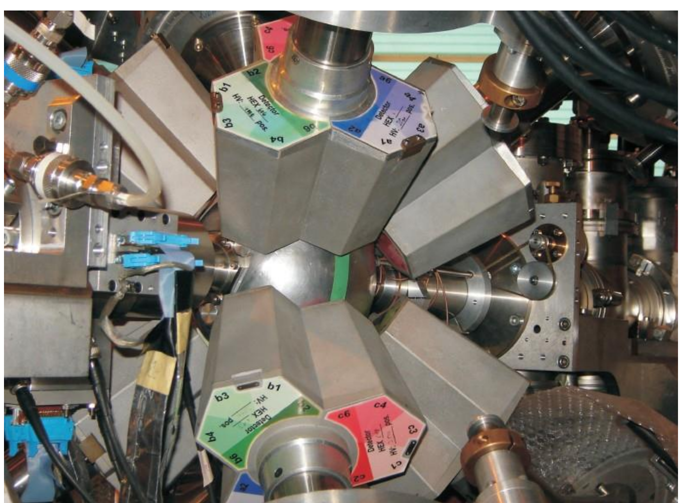

The Miniball Ge Detector Array (Europe)

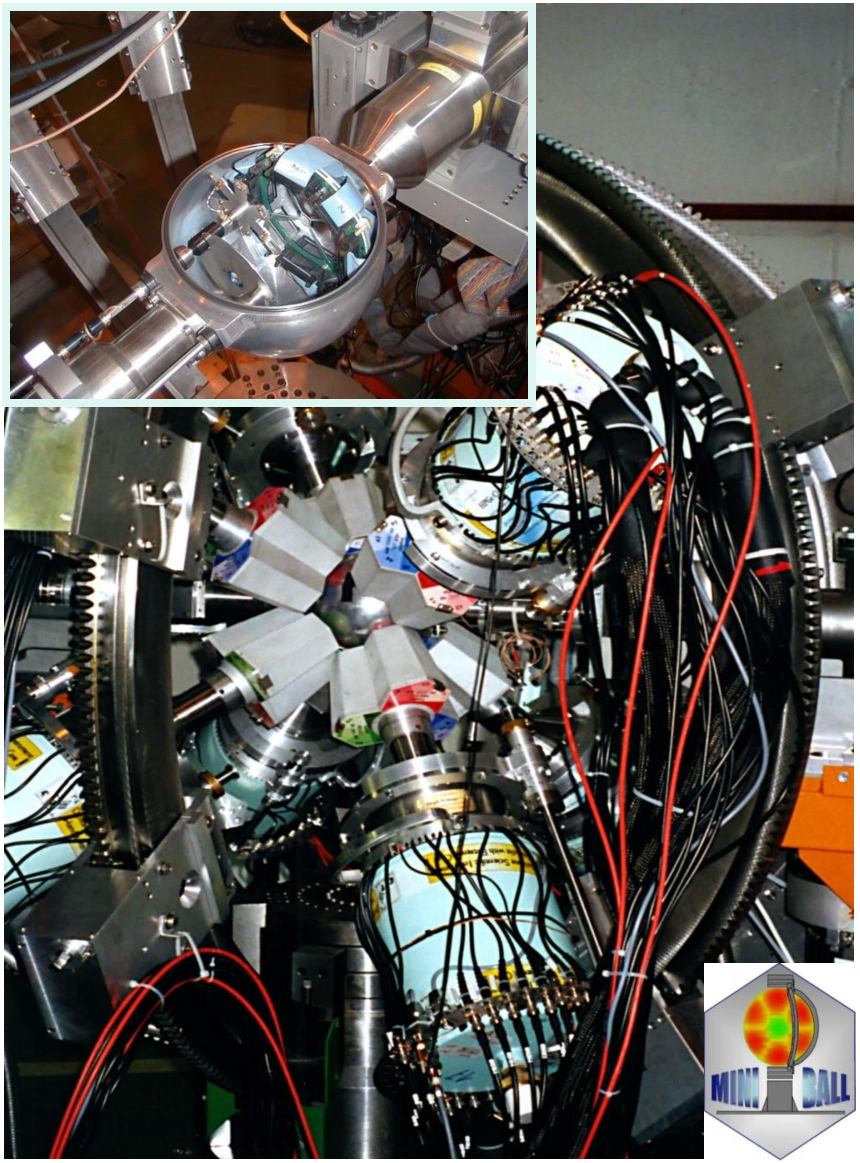

- 24 6-fold segmented Ge detectors (8 triple clusters)
- flexible geometry
- $\varepsilon_{full\ energy}$(@ 1.33 MeV) ≈ 7 %
- fully digital electronics + pulse shape analysis (PSA)
- electronic segmentation and PSA: 50-100 fold increase in granularity
- ρ from central core
- ϕ from induced charge in neighboring segments

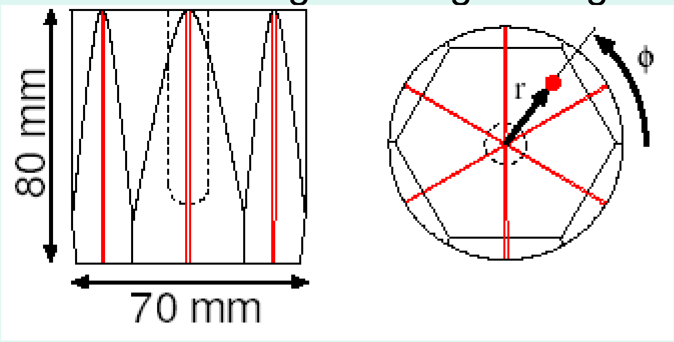

- low-multiplicity g-ray experiments with weak exotic beams

J. Eberth,- Prog. Part. Nucl. Phys. 46 (2001) 389

AGATA Ge Tracking Array (US)

Advance GAmma Tracking Array

- six-fold azimuthal segmentation
- six-fold longitudinalsegmentation

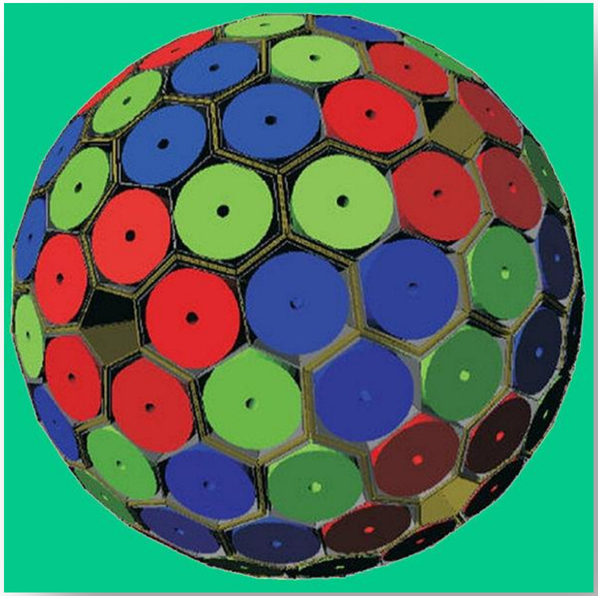

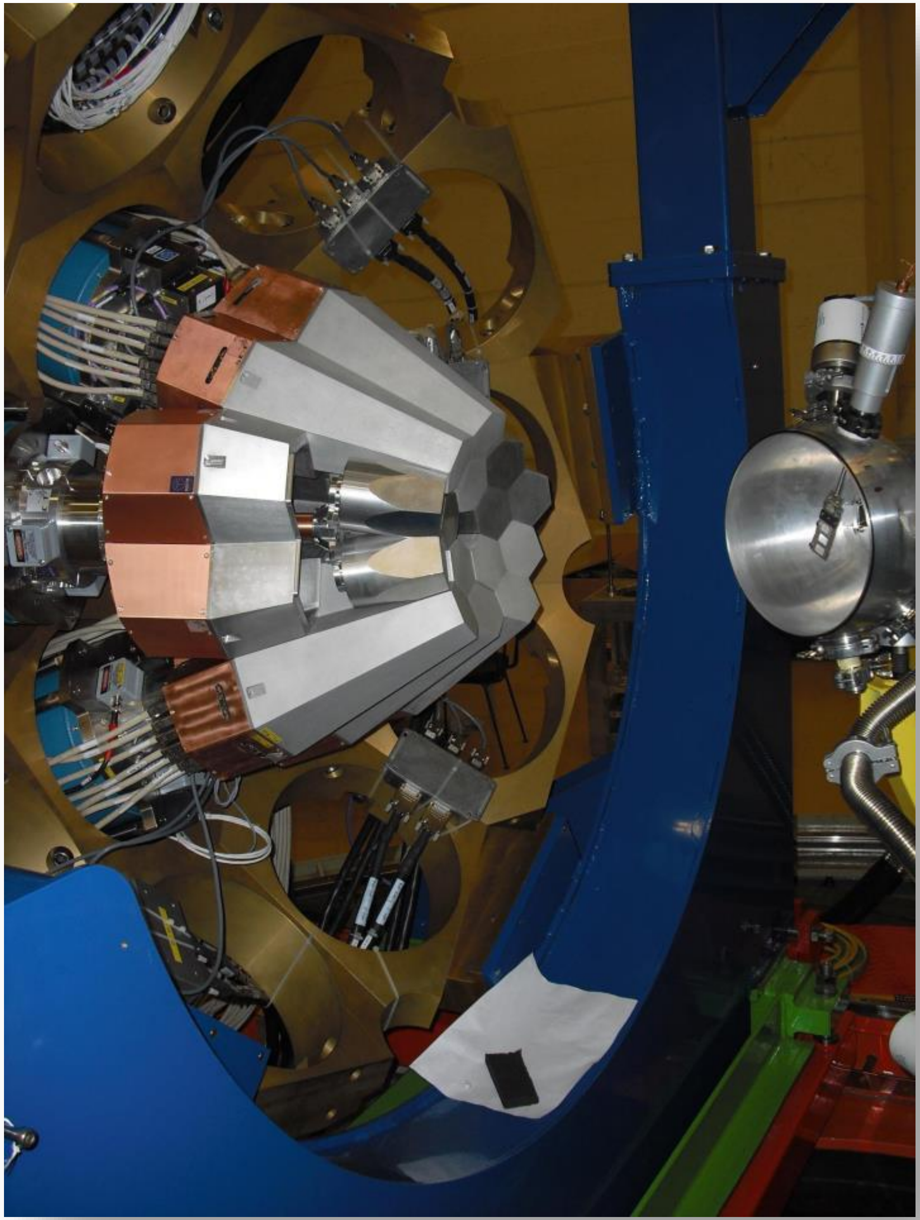

Octupoles at MINIBALL(ISOLDE) via Coulex Excitation

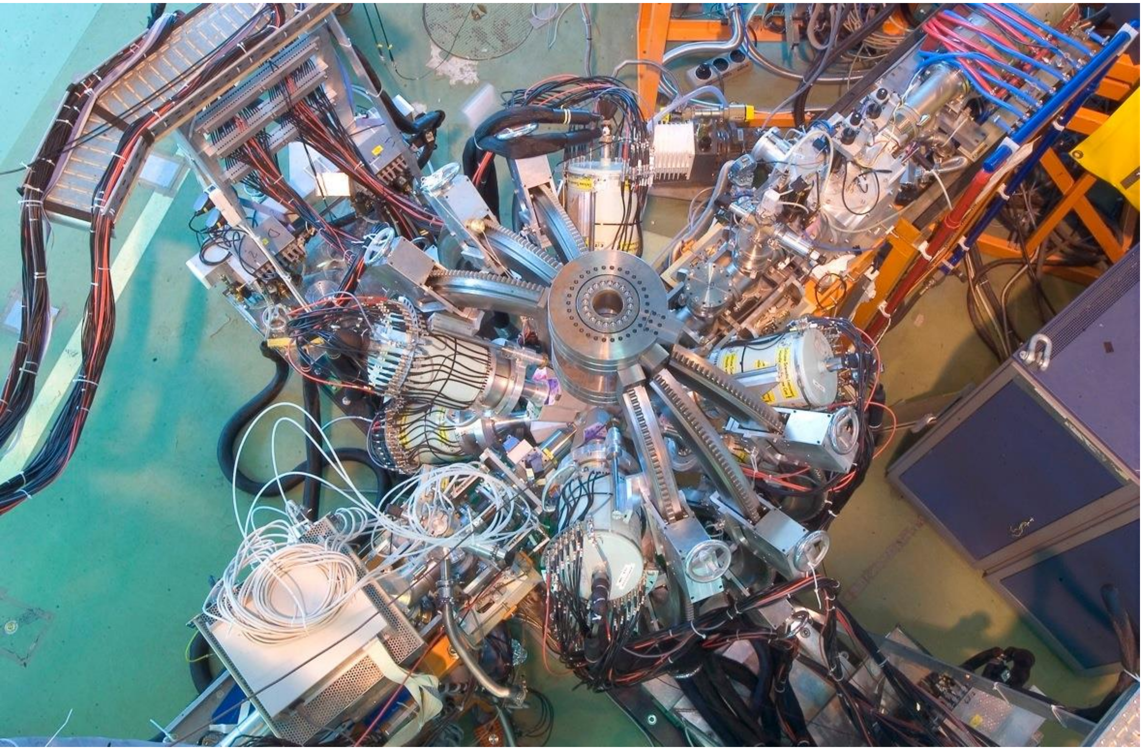

8 triple cluster Ge detectors

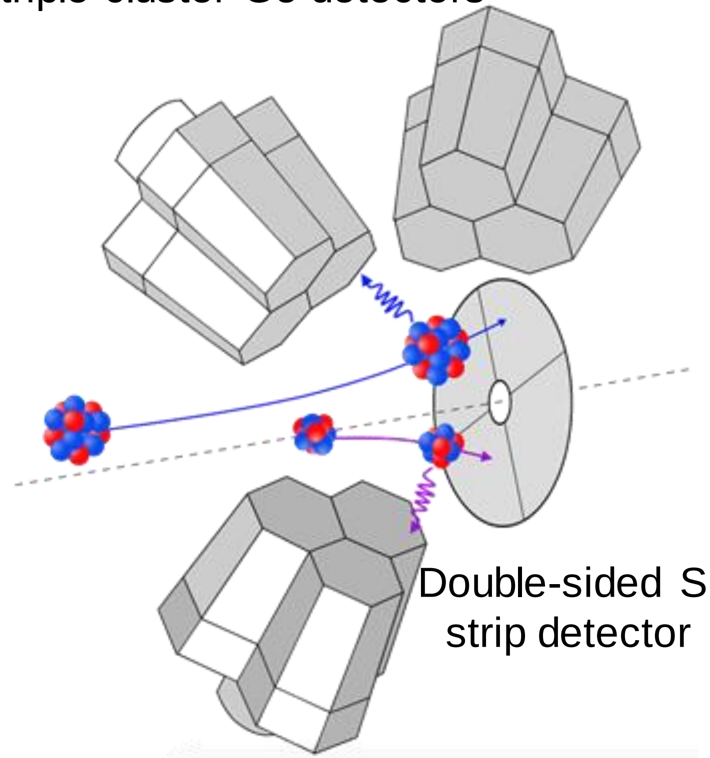

- Coincident detection of particles (Si) and γ-rays (HPGe)
  - ➢ Well-known electromagnetic interaction → $B(E3) \propto |Q_3|^2$
  - ➢ Large cross-section: suited to RIBs
  - ➢ Unparalleled energy resolution
  - ➢ **Currently only method for Q_3 in exotic nuclei**

N. Warr et al., EPJ **49** (2013)

Actinides: ^{220}Rn & ^{224}Ra

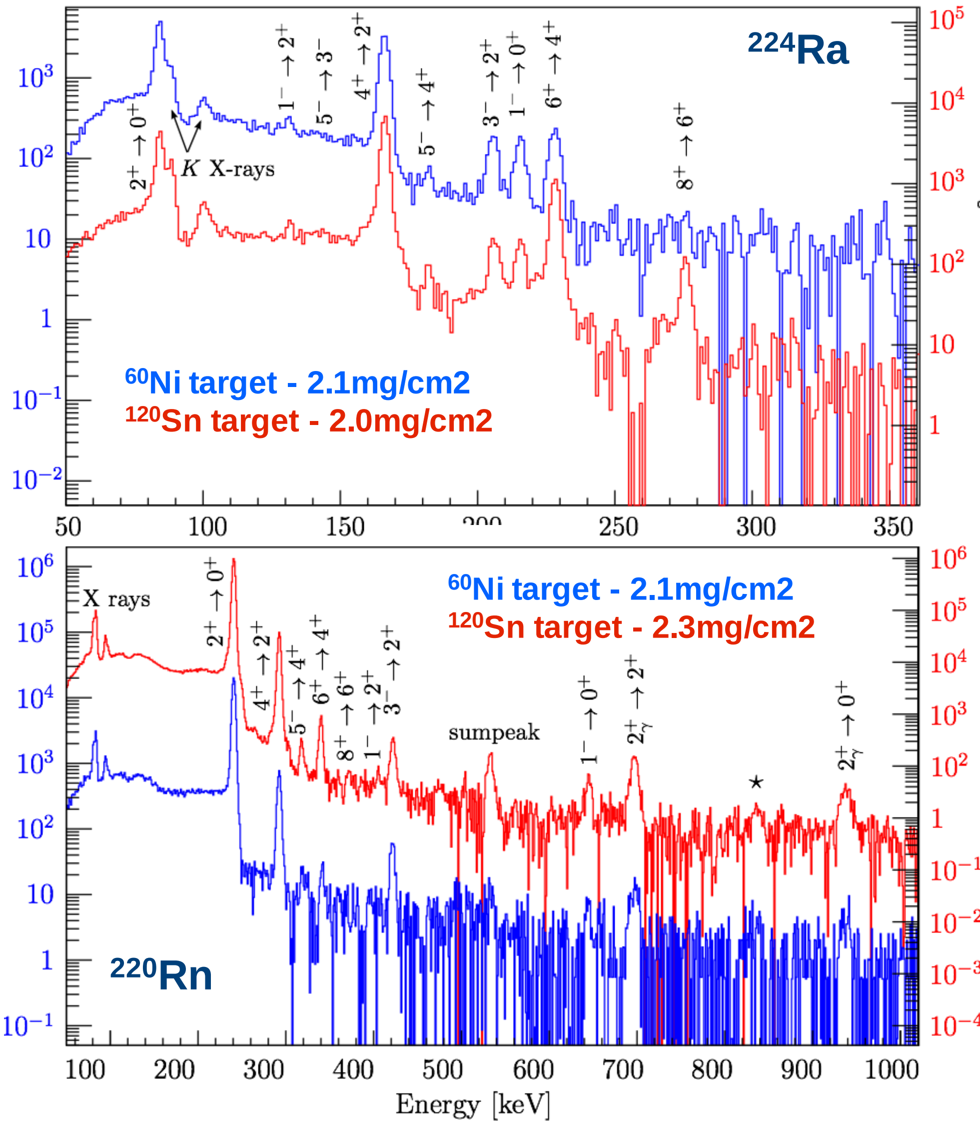

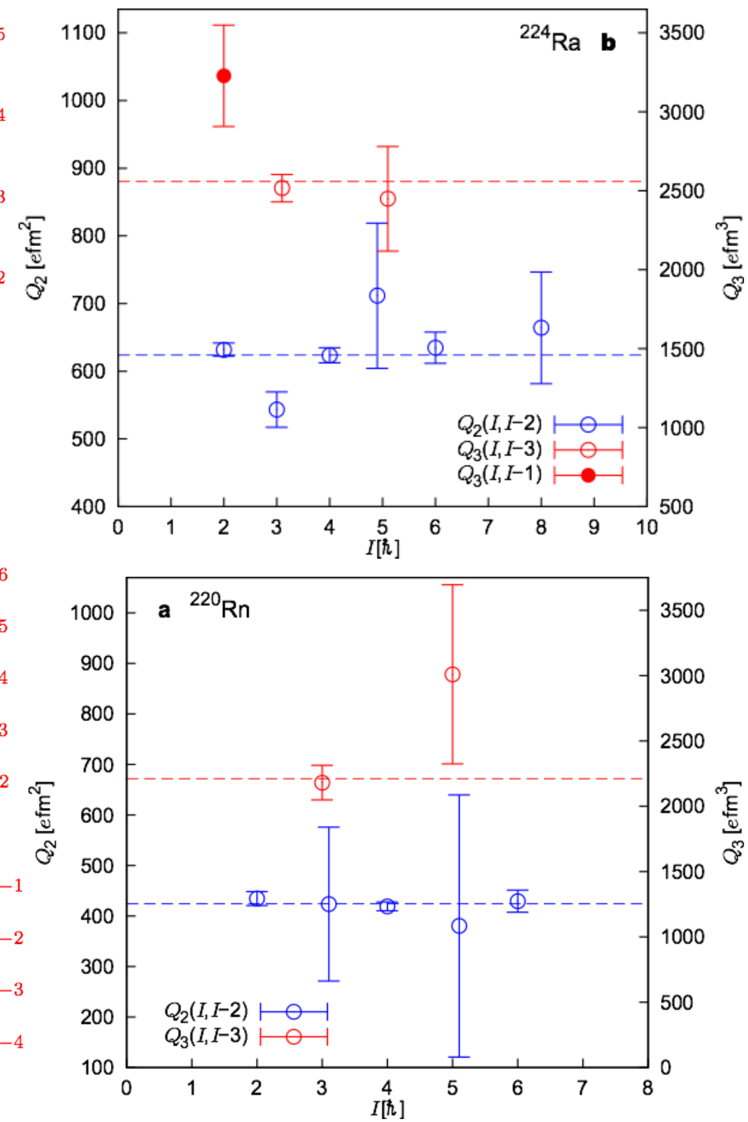

L. P. Gaffney et al., Nature **497**, 199 (2013).

E2 and E3 moments for Heavy Nuclei

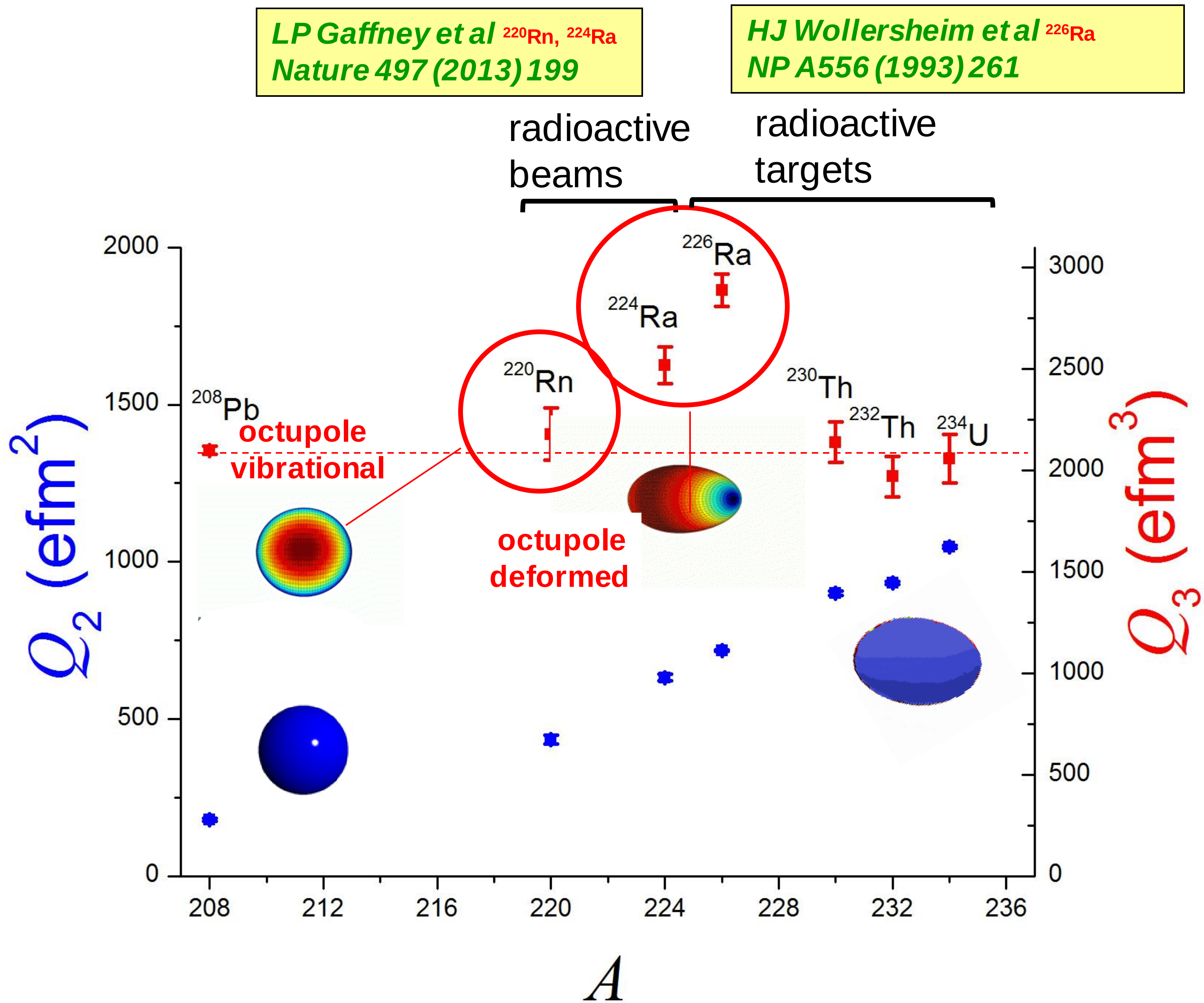

^{224,226}Rn – Virgin nuclei

- Previously unobserved positive- and negative-parity states in ^{224,226}Rn
- New data from HIE-ISOLDE at 5.1 MeV/*u*

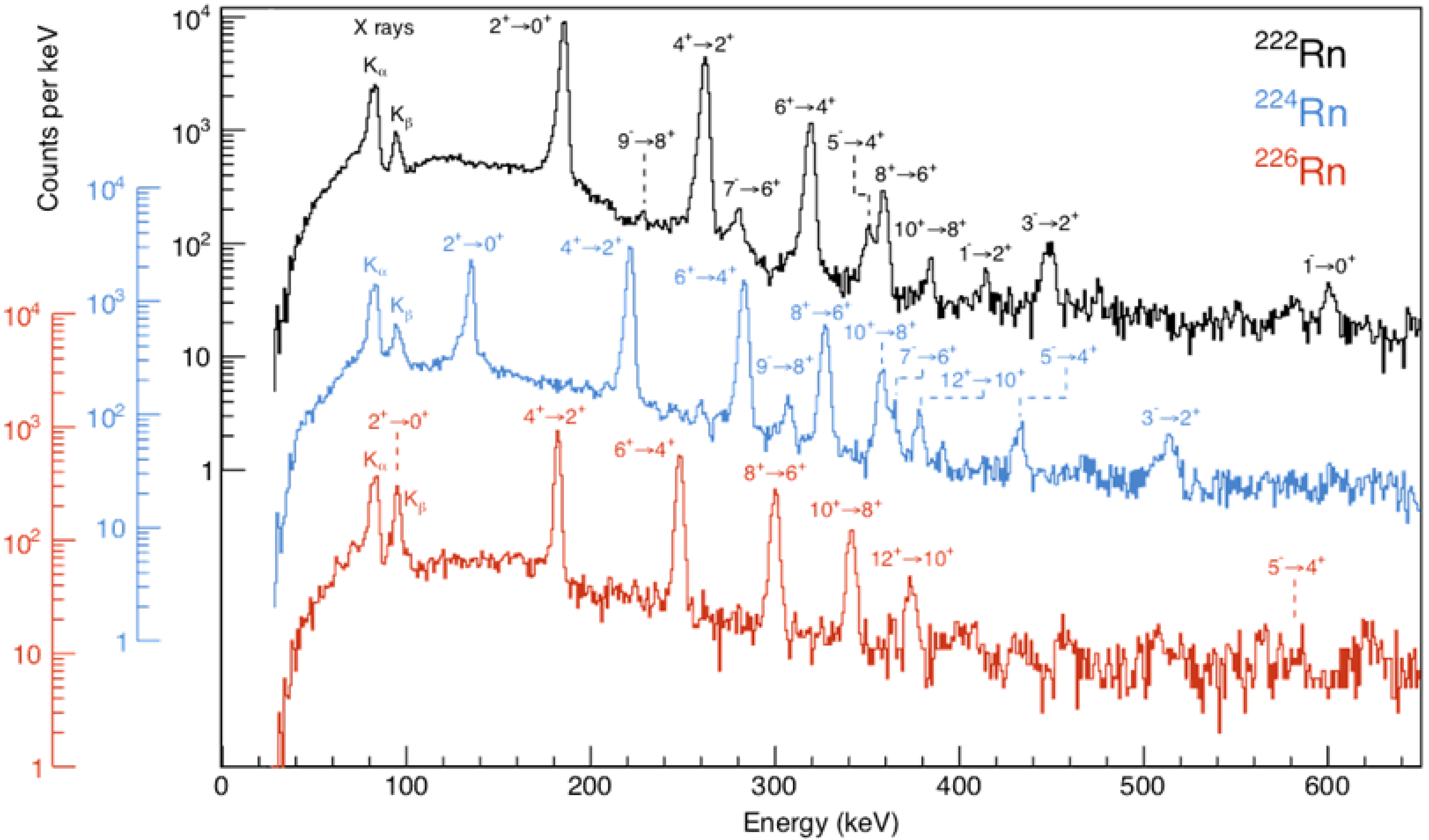

P. A. Butler et al, *Nature Communications* **10**, 2473 (2019).

Vibrational or deformed?

- Are ^{221,223,225}Rn good candidates for the EDM measurements?

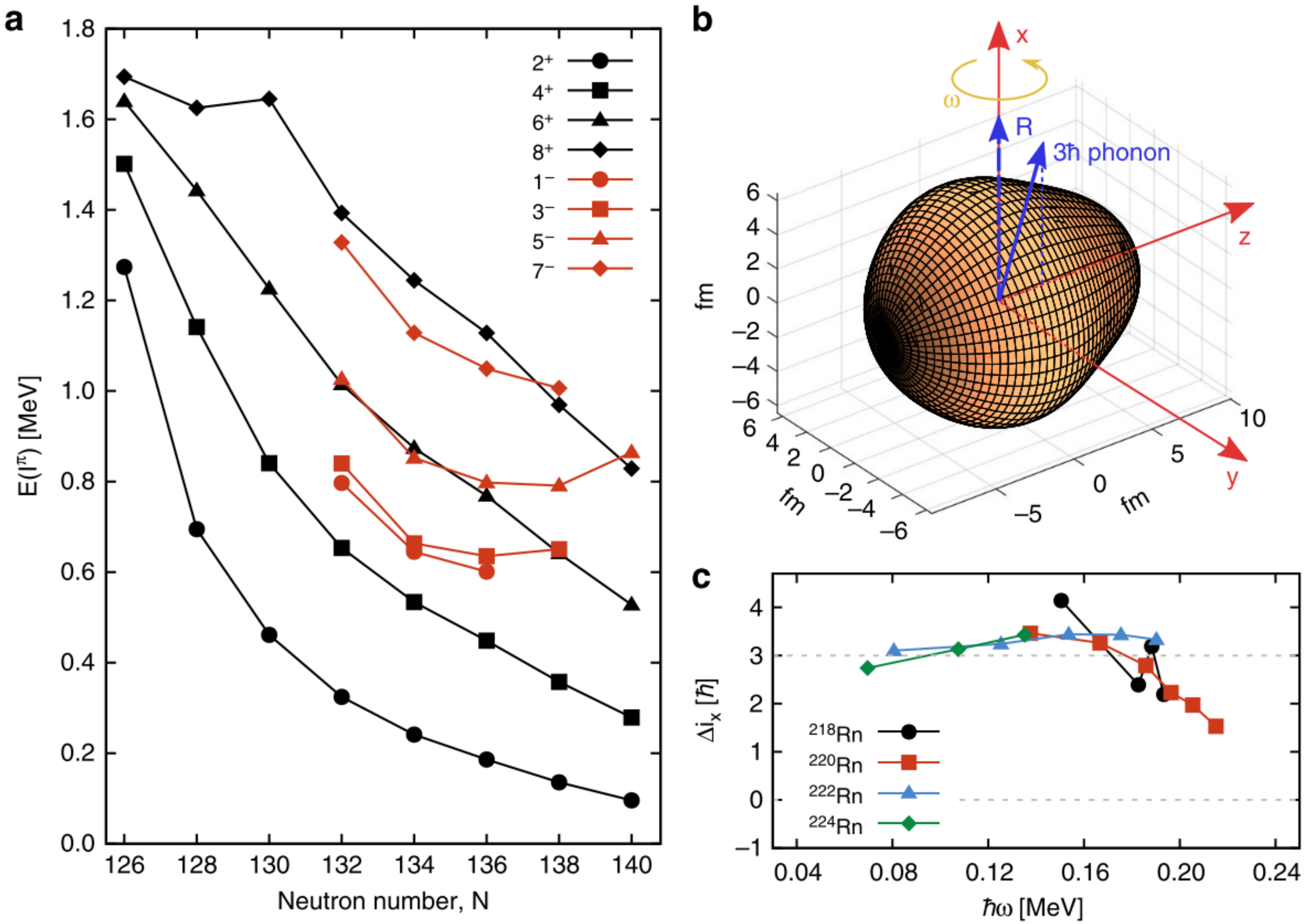

P. A. Butler et al, *Nature Communications* **10**, 2473 (2019).

Case Study 6: Quest for SuperHeavy Elements

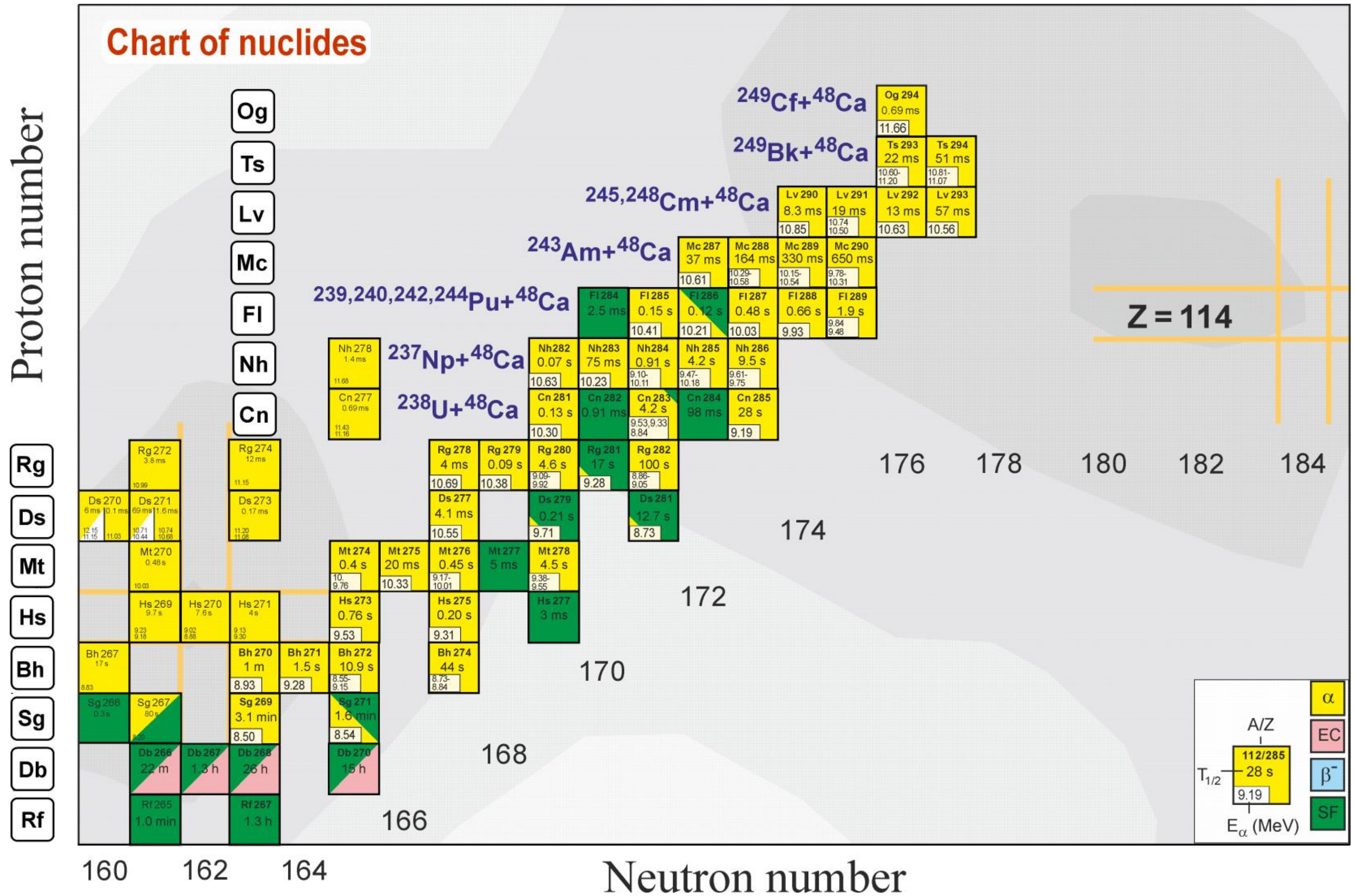

- Very active research field at JINR (Dubna), Berkeley, RIKEN, GSI and other places
- Large international collaborations

Dubna Gas-filled Separator (DGFS)

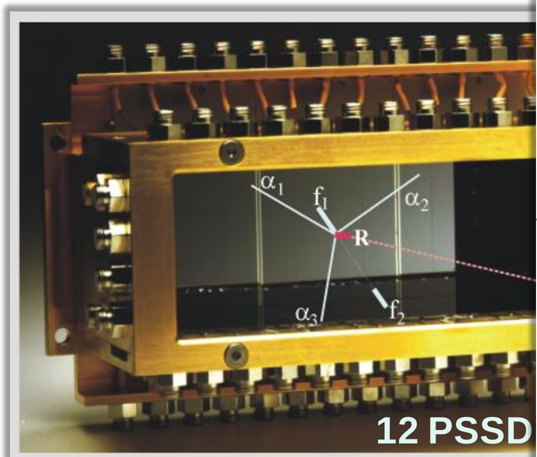

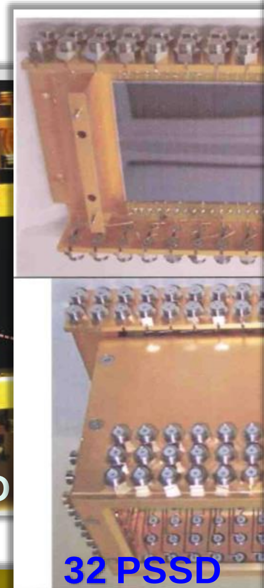

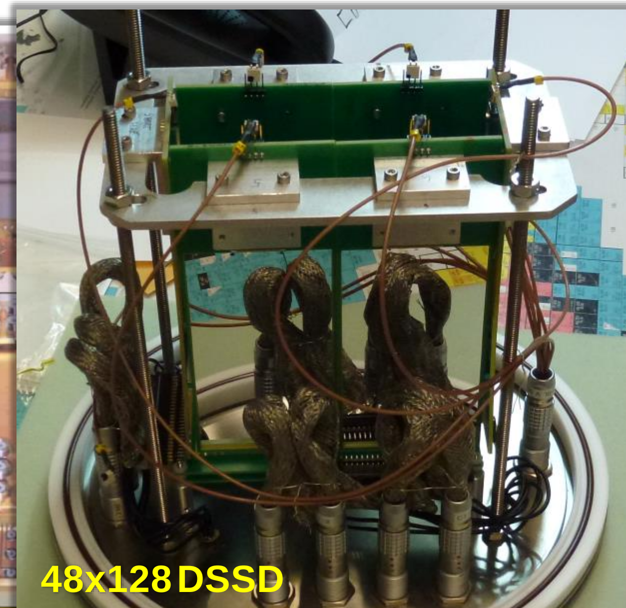

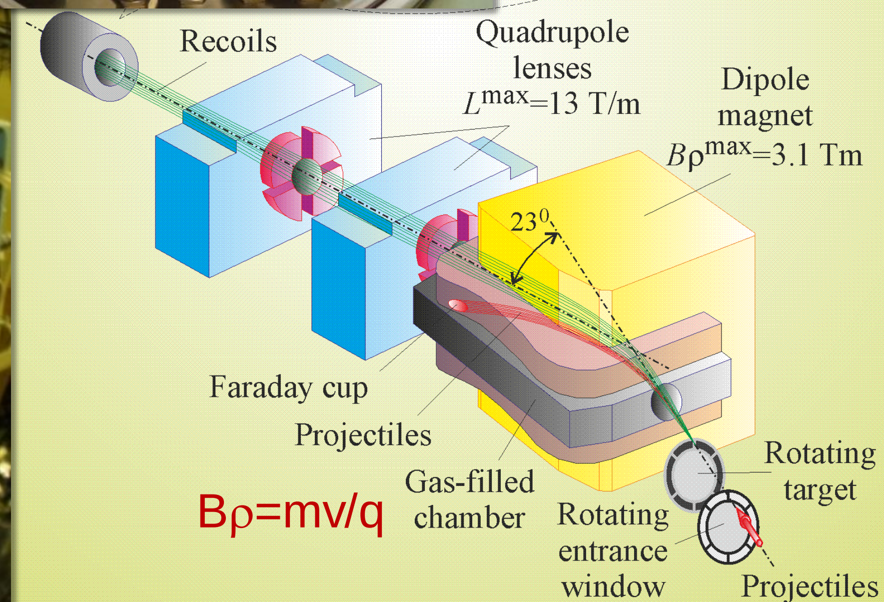

An example: Element Z=104 (Flerovium)

α–α correlation method

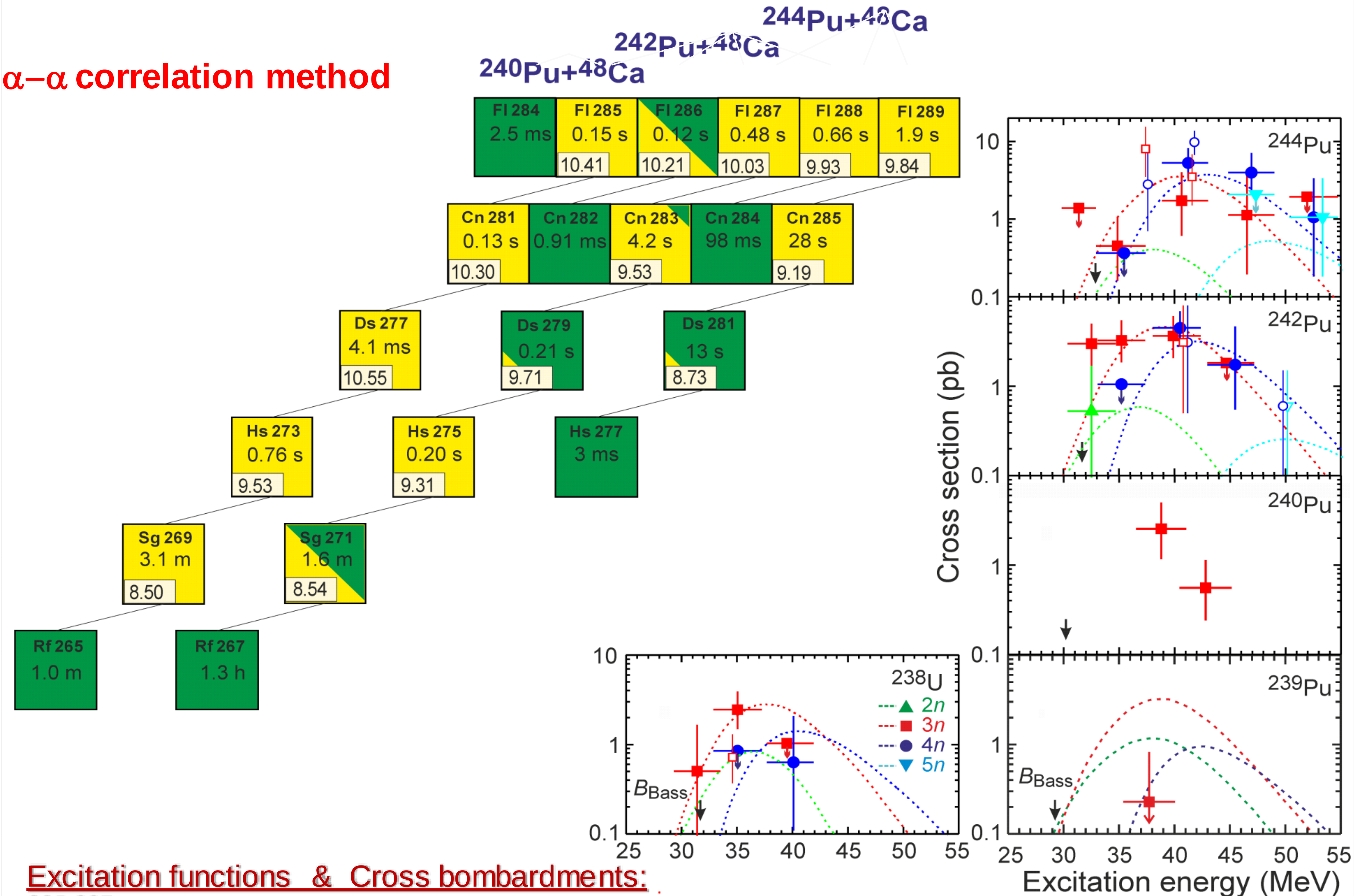

Excitation functions & Cross bombardments:

$^{285-287}$Fl, $^{281-283}$Cn – the same reaction channel

Thanks for your attention!

(An example) Modern 'state-of-the art' beyond mean-field calculations in the Pb region (SLy6+GCM)

J.M.Yao, M. Bender, P.-H. Heenen, PRC87,034322(2013)

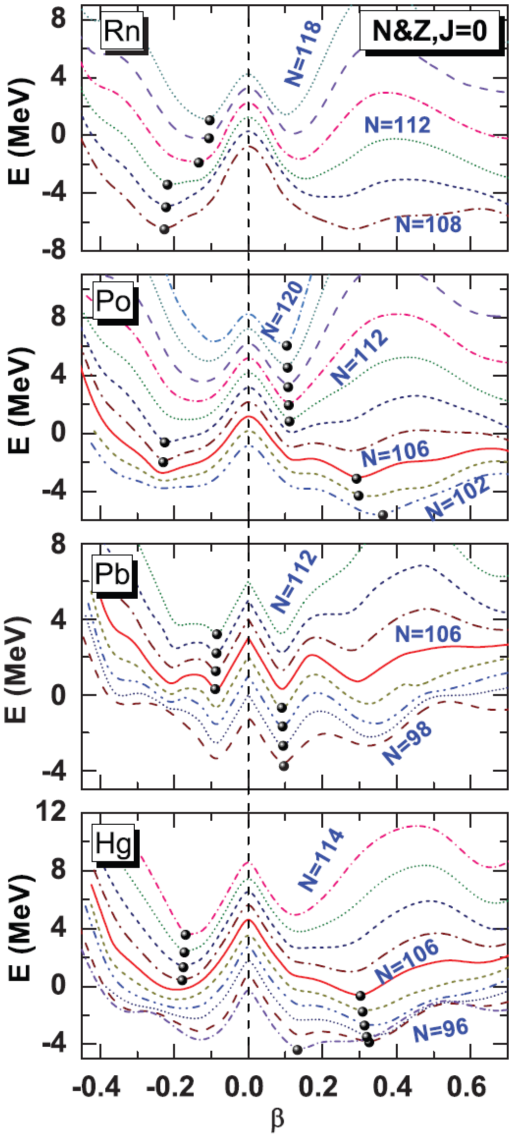

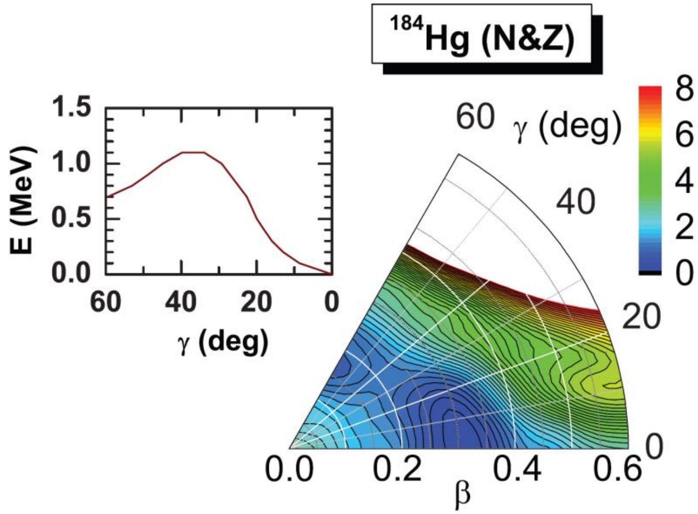

FIG. 4. (Color online) Quadrupole deformation energy surface for ^{184}Hg, normalized to the absolute minimum and projected on particle numbers. Each contour line is separated by 0.2 MeV. The inset shows the energy as a function of γ deformation along the path joining the two axial minima.

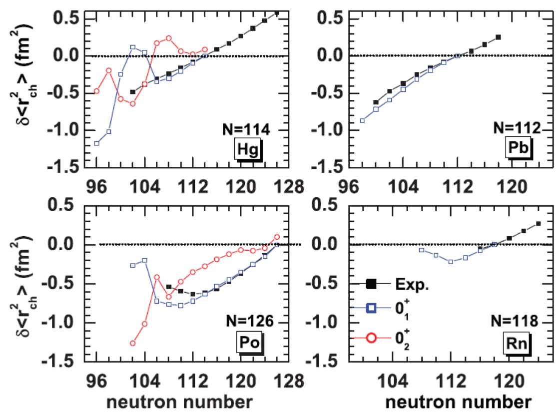

FIG. 13. (Color online) (Upper panel) Variation of the charge radii $\delta\langle r^2_{ch}\rangle$ for the lowest 0^+ states in Hg [normalized to the ground state (g.s.) of ^{194}Hg], Pb (normalized to the g.s. of ^{194}Pb), Po (normalized to the g.s. of ^{210}Po), and Rn (normalized to the g.s. of ^{204}Rn) isotopes, compared to the the experimental data for ground states taken from Refs. [18,49].

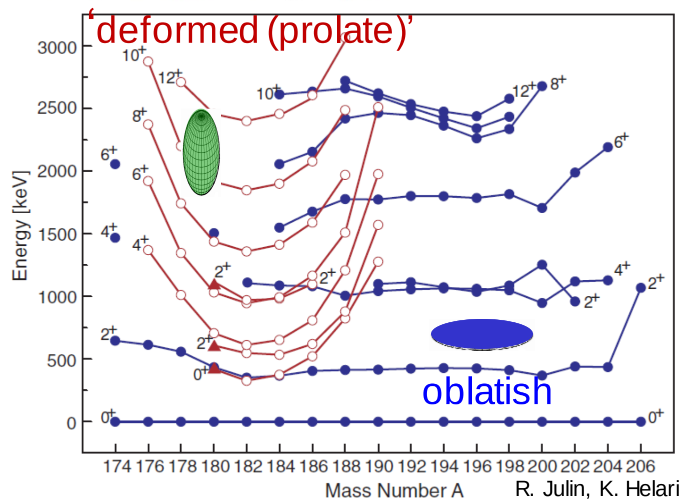

R. Julin, K. Helariutta, M. Muikku, J. Phys. G 27 (2001)

Nilsson Diagrams around Z~82 & 82<N<126 (WS)

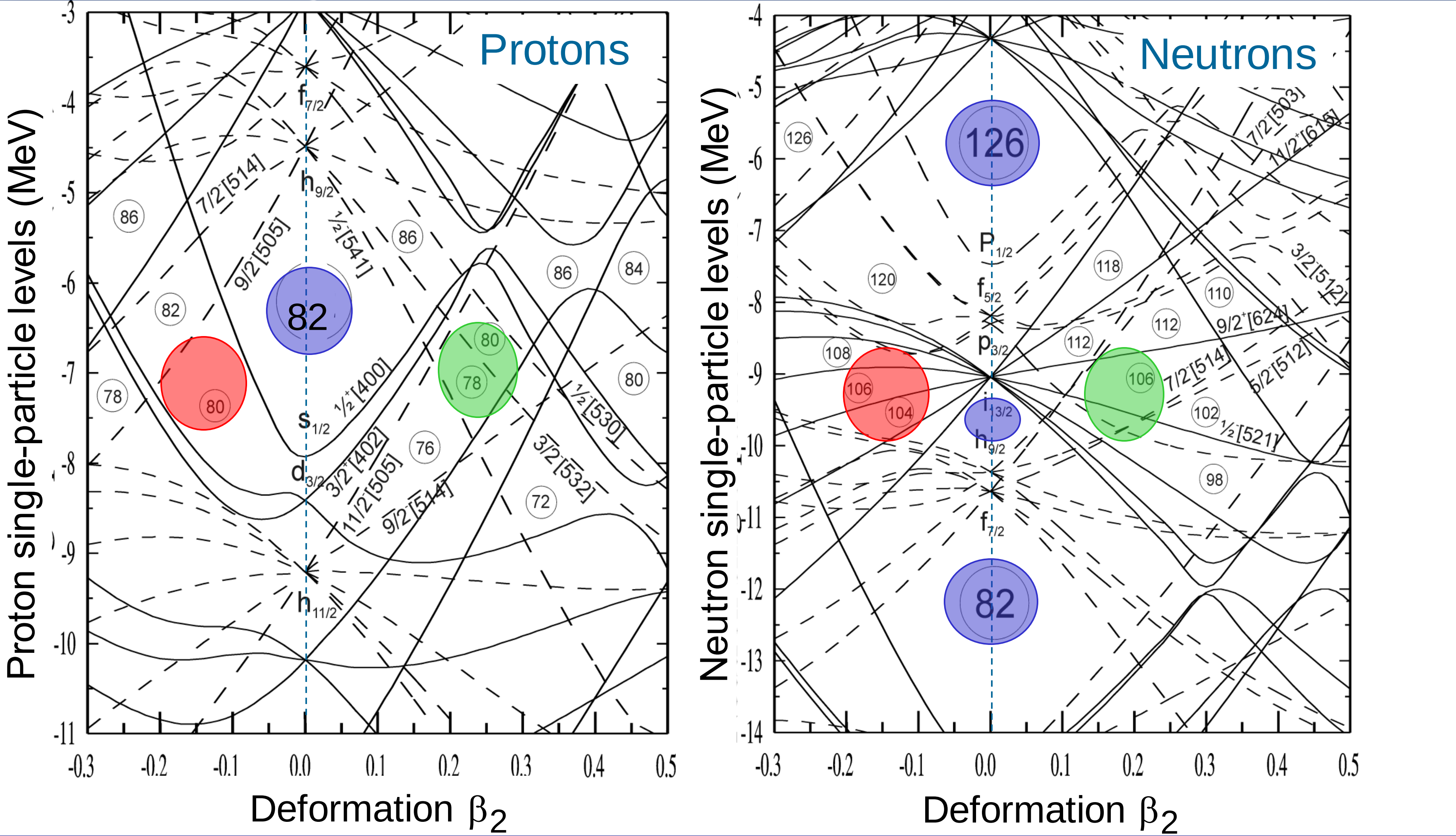

Around Z=82 and neutron mid-shell N=102-108, protons and neutrons coherently produce low-lying coexisting oblate and prolate shapes

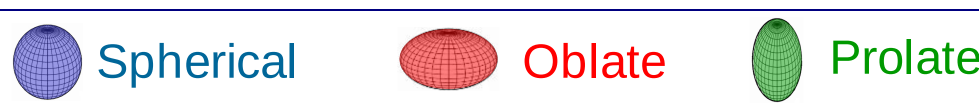

Density Functional Theory (DTF) Potential Energy Calculations (York-Lyon-Brussels Collaboration)

- Extensive Density Functional Theory blocked calculations performed by York-Lyon-Brussels Collaboration (14 parametrizations of Skyrme functional were probed)
- UNEDF0, UNDEF1, UNDED1^{SO}, SLy4, SkM*, SGII
  8 parametrizations of SLy5sX
- Variation of pairng strength and other parameters
- Full account in S.Sels et al, accepted to PRC, November 2018

DFT Potential Energy Surfaces (even-even Hg's)

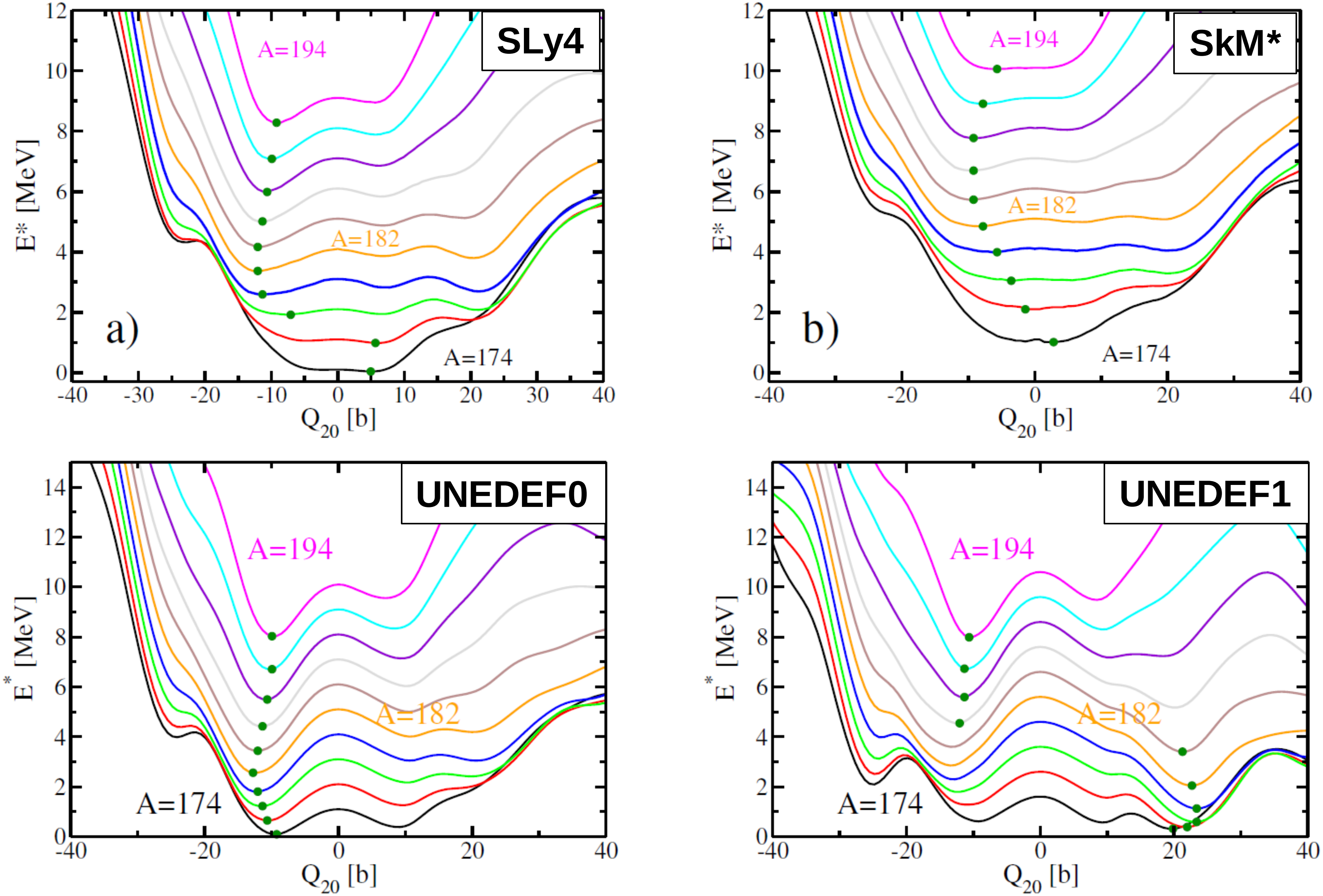

Charge radii for Hg isotopes (reduced pairing and blocking for odd-A)

Courtesy A. Pastore and J. Dobaczewski (York)

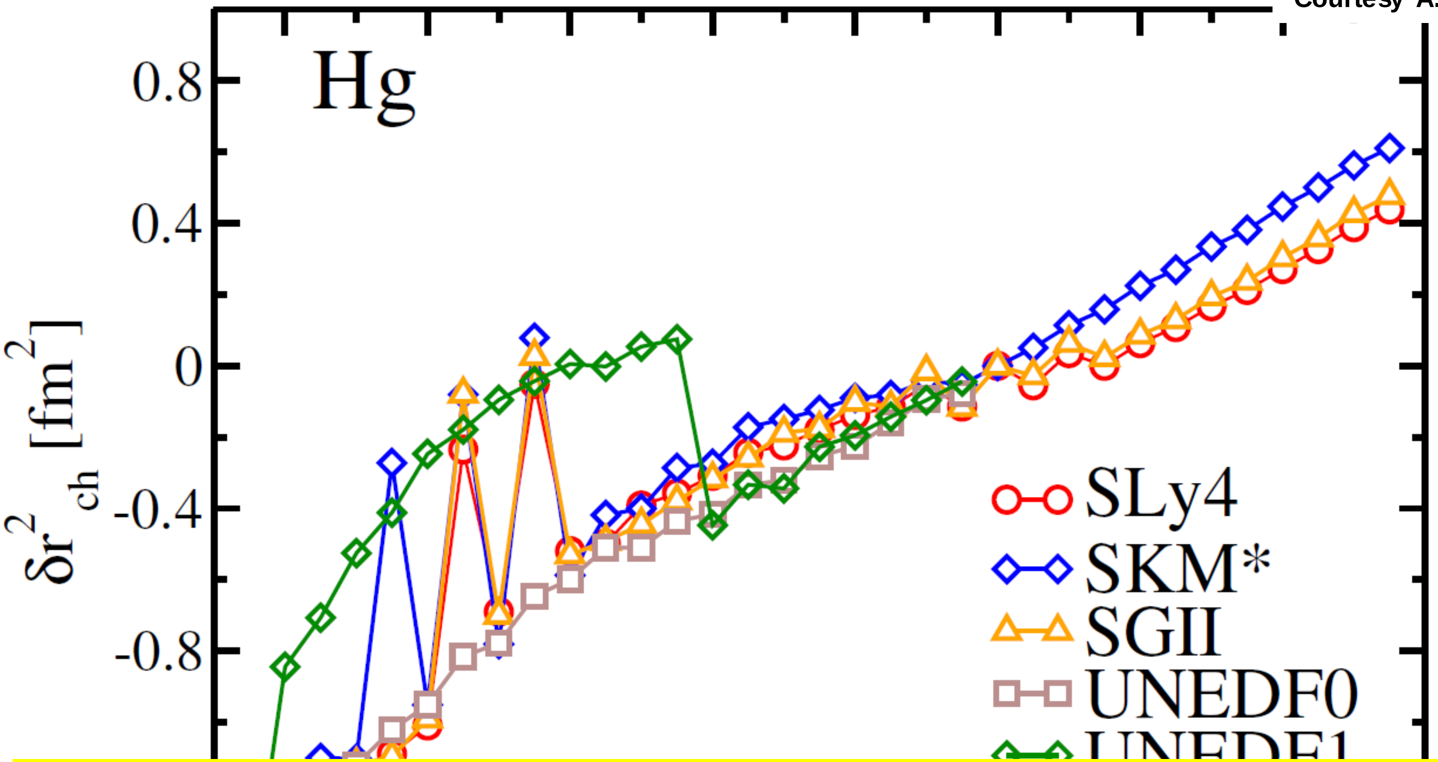

SLy4

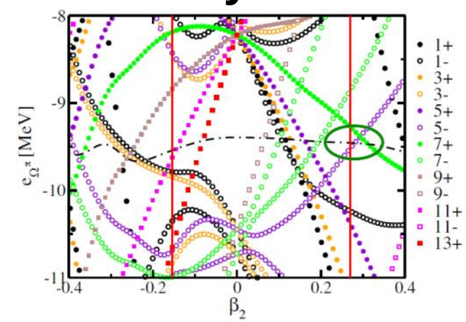

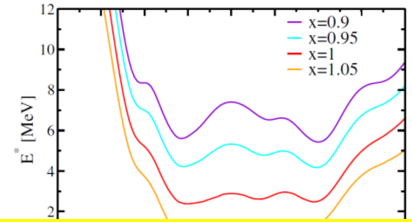

Mean-field theory summary (AP+JD):

- The phenomenon of the radii staggering in Hg is a subtle effect of an interplay between (i) shape coexistence, (ii) pairing strength, and (iii) deformed shell structure
- The presently available functionals **do not allow** for reuniting these three aspects in a consistent way (e.g. spins are not reproduced), although the essential features of the **effect can be reproduced**…"

Emerging!: Charge Radii via Electron scattering from RIBs

e.g. electron scattering from unstable nuclei (colliding accelerated electrons and low-energy radioactive ions!)
SCRIT at RIKEN (Japan) and ELISe at GSI (Darmstadt, Germany)

SCRIT@RIKEN

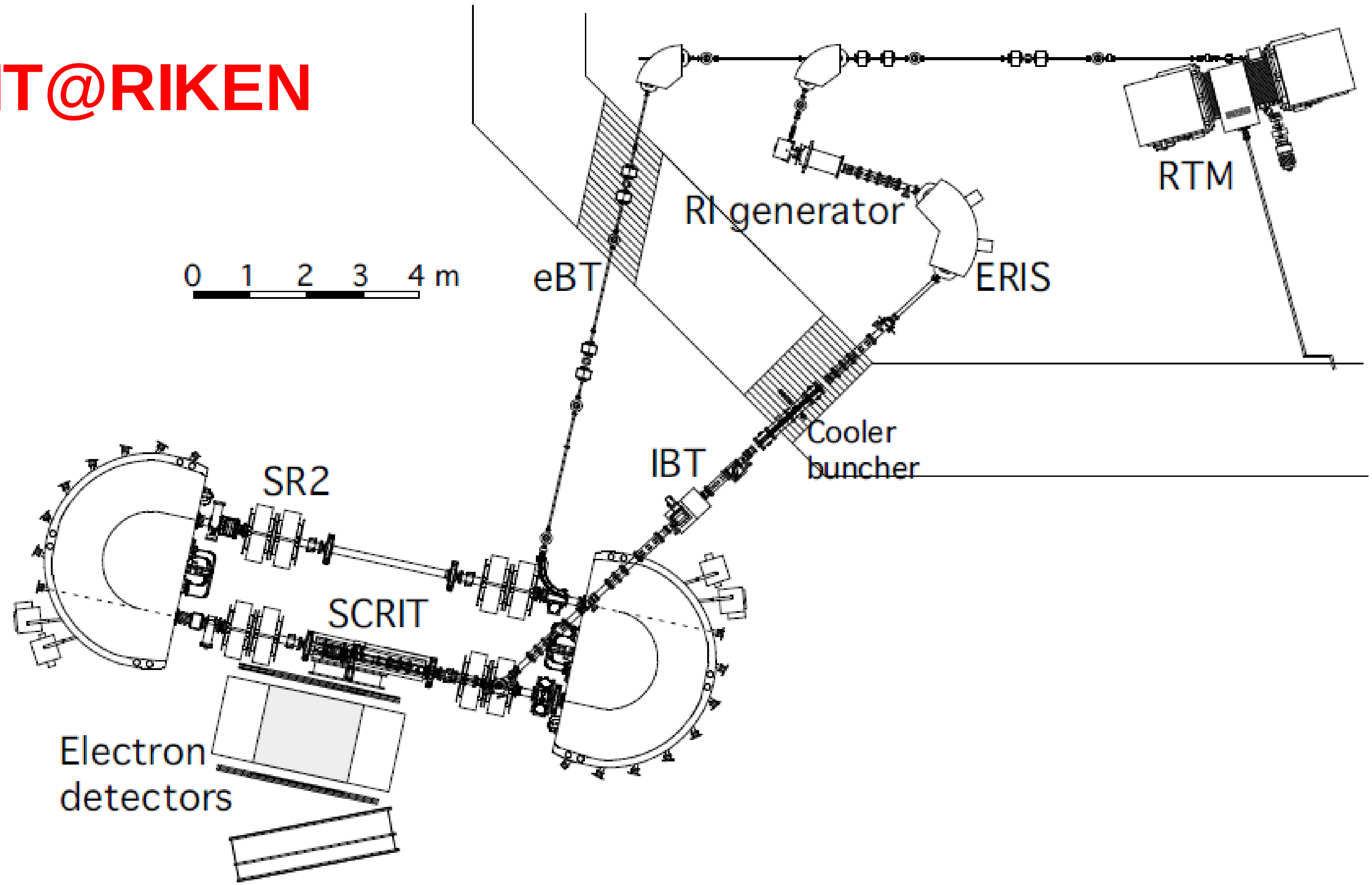

^{78}Ni(Z=28, N=50) revealed as a doubly magic stronghold against nuclear deformation

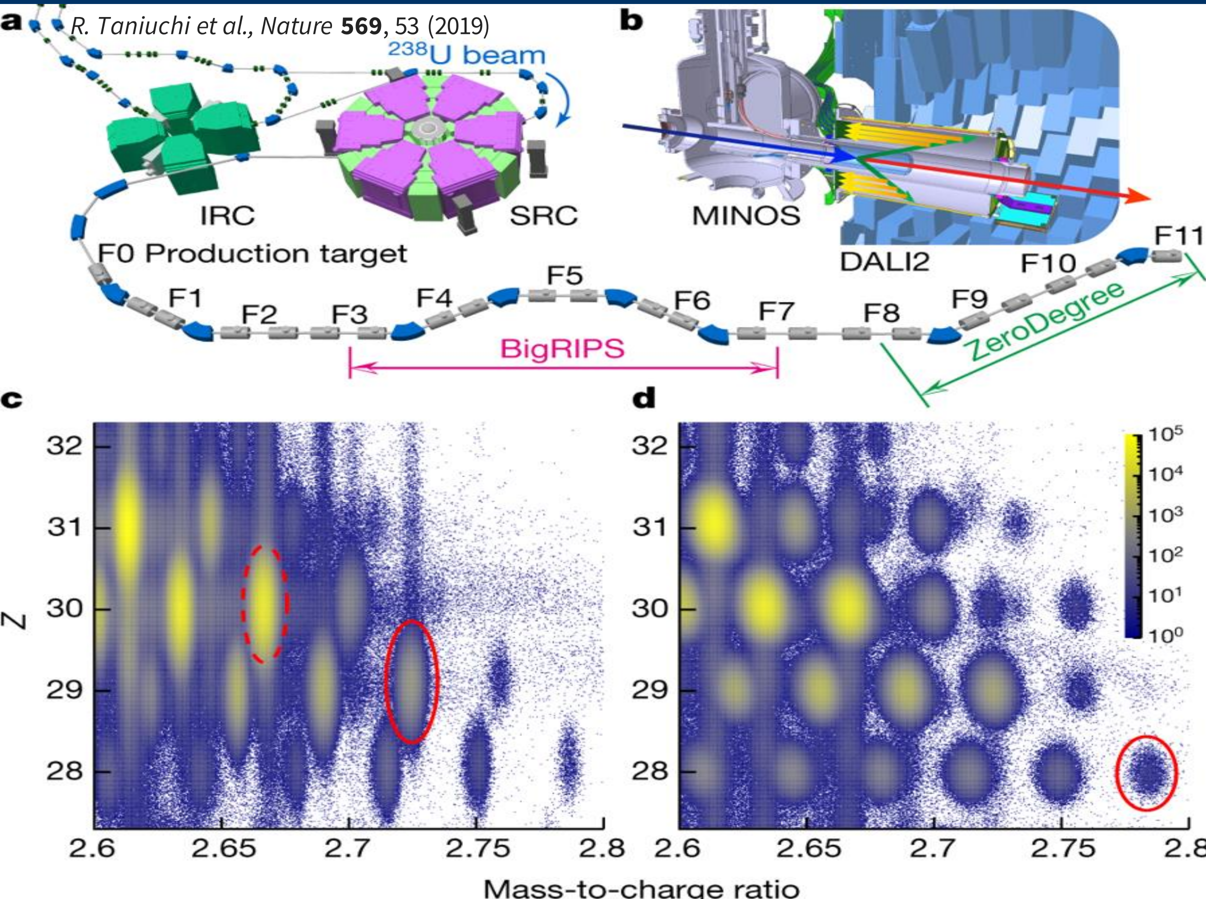

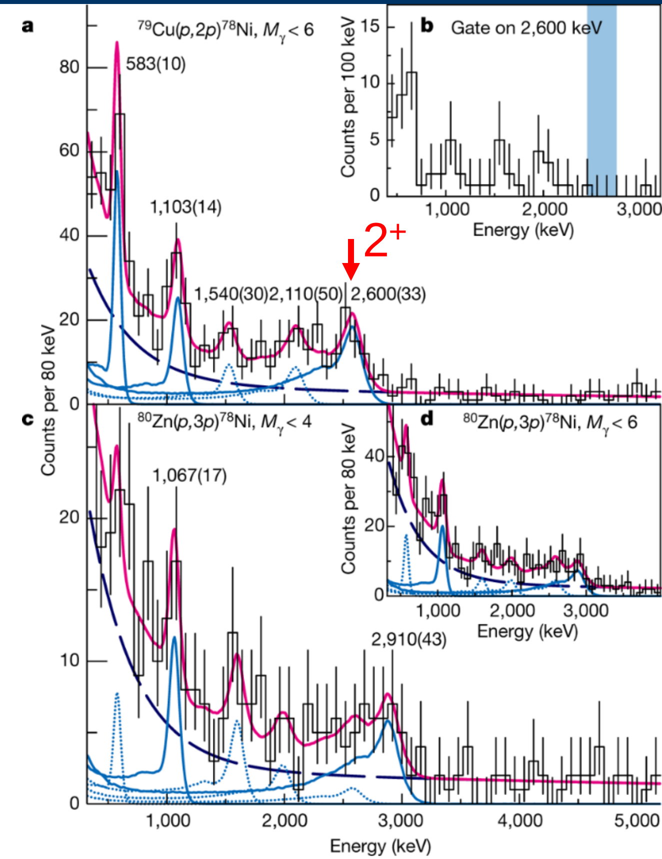

High E(2^+_1)=2600(33) keV confirms the doubly-magic nature of ^{78}Ni (initial hint came from S_{2n} values of n-rich Cu isotopes, A. Welker et al, PRL119, 192502, 2017)

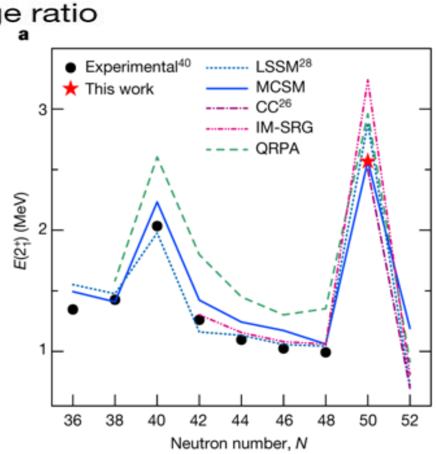

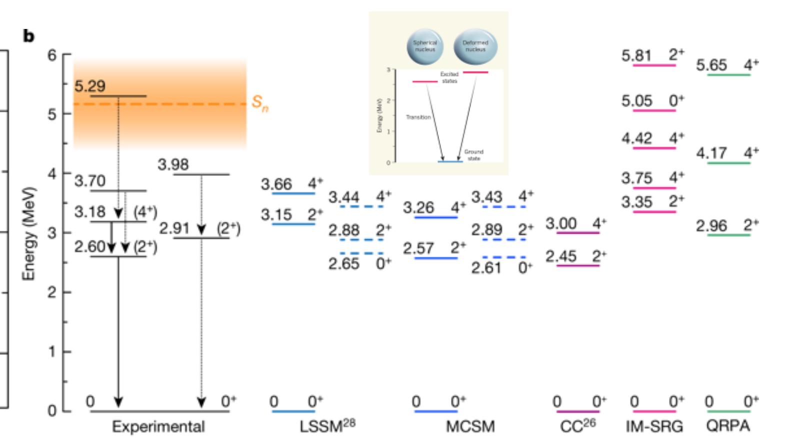

DSSD-Si box coincidences

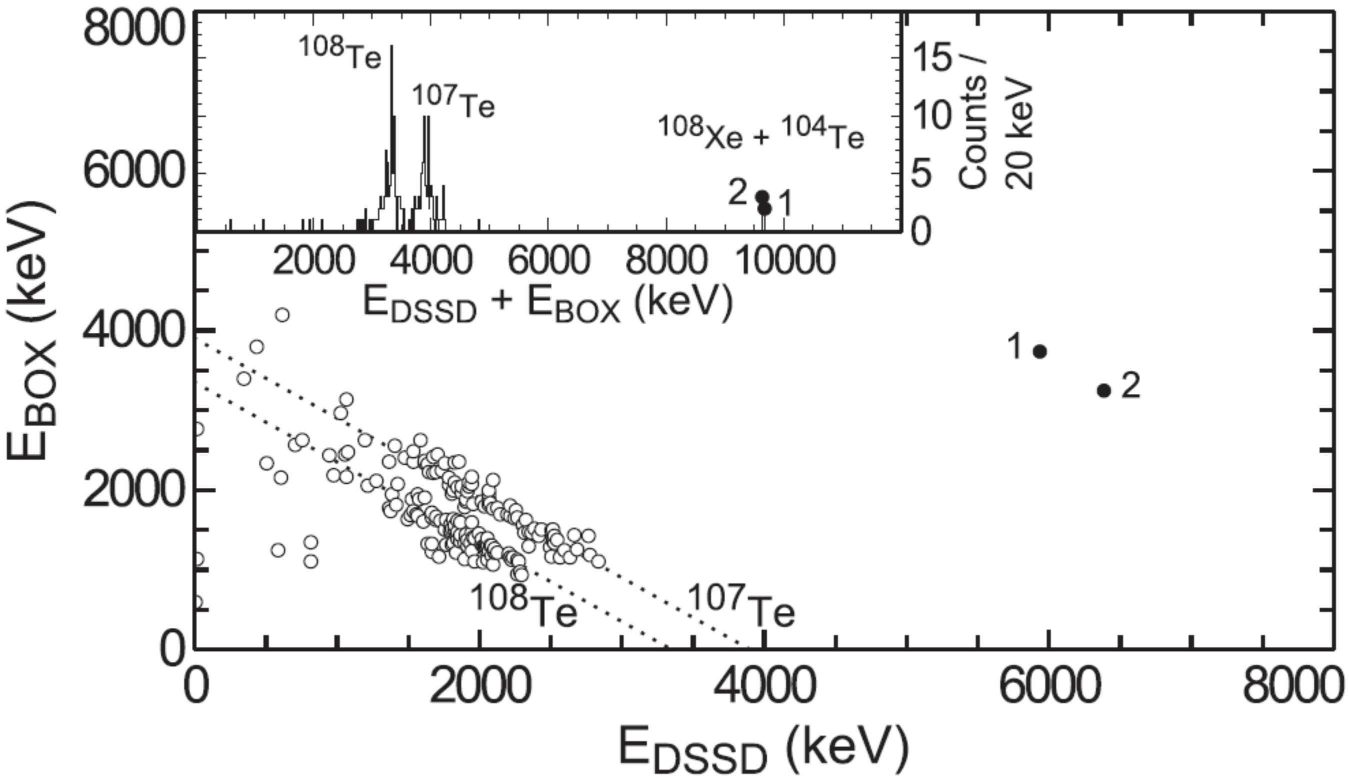

- The same total energy for both events - **ΣE_{α}=9.3(1) MeV**
- Compared to α emitters different energy split

E_{α}(^{104}Te)=4.9(2) MeV, E_{α}(^{108}Xe)=4.4(2) MeV

Selective Resonance Laser Spectroscopy of an Atom

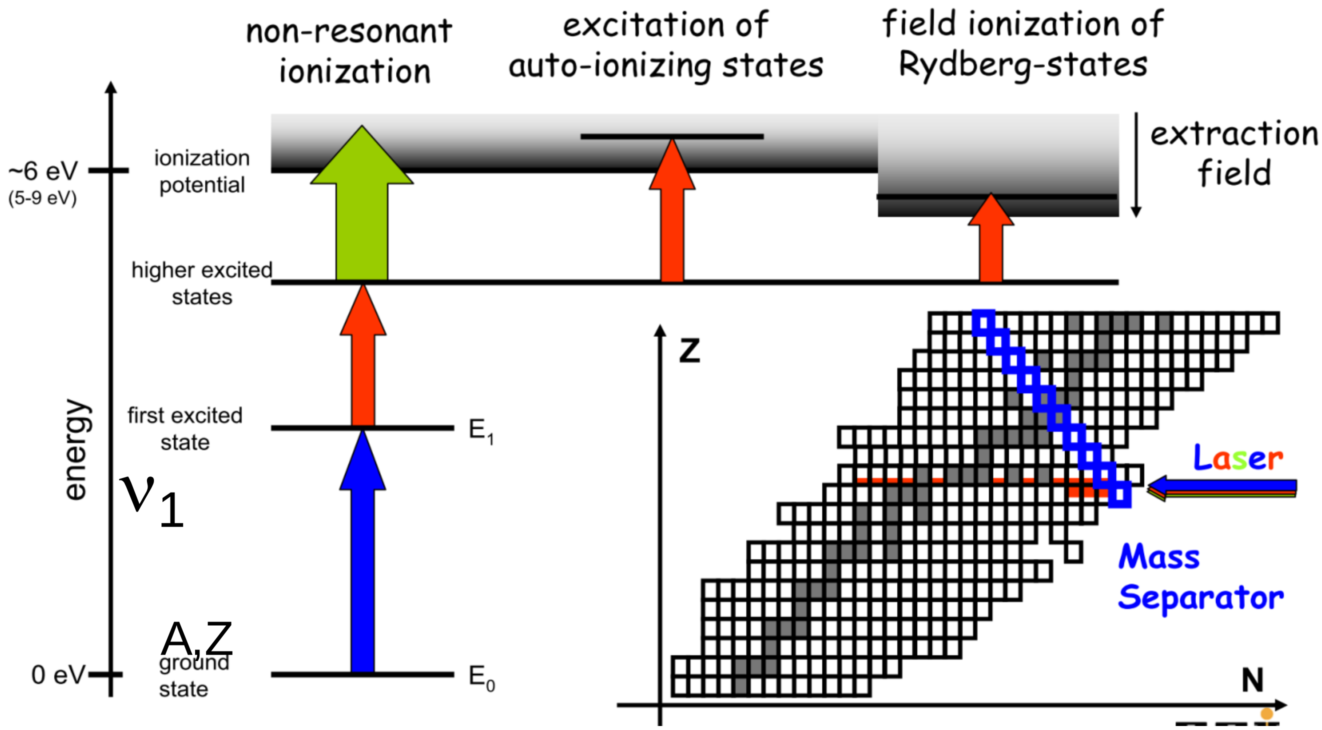

RILIS: Resonance Ionization Laser Ion Source

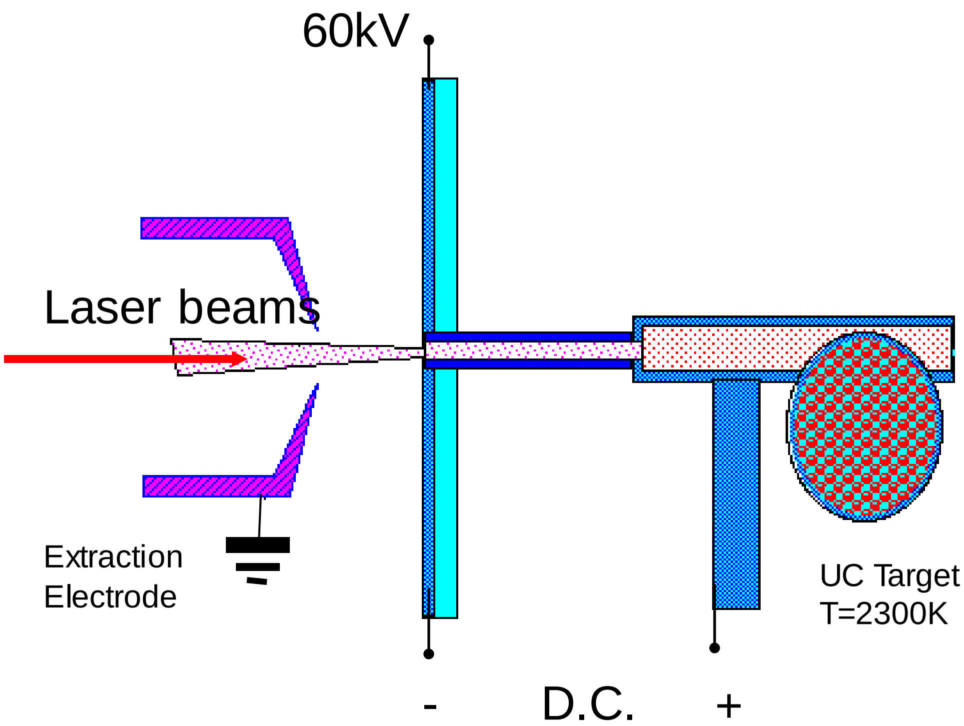

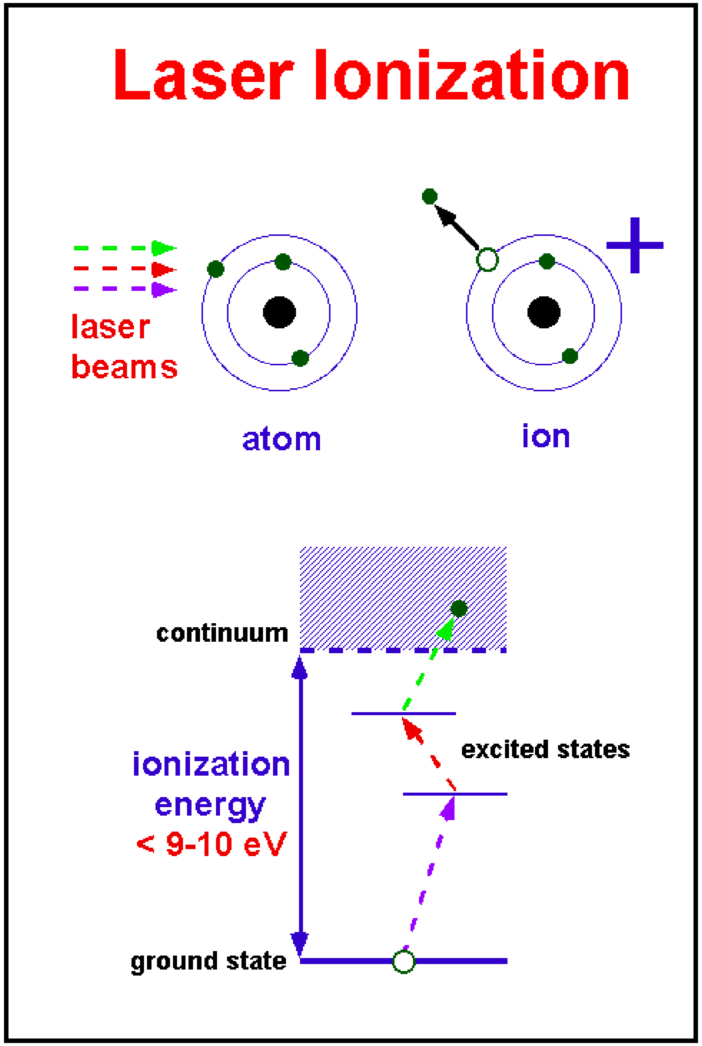

Element (Z) – selective!

ε_{laser} = 2% - 30%

	> 5%	- alkalies
$\varepsilon_{surface}$	= 0.1% -2%	- In, Ga, Ba, lanthanides
	< 0.1%	- others

An example: Charge radii from Charge Changing Cross Sections with RIBs

Sum of all reactions that decrease proton number of the projectile

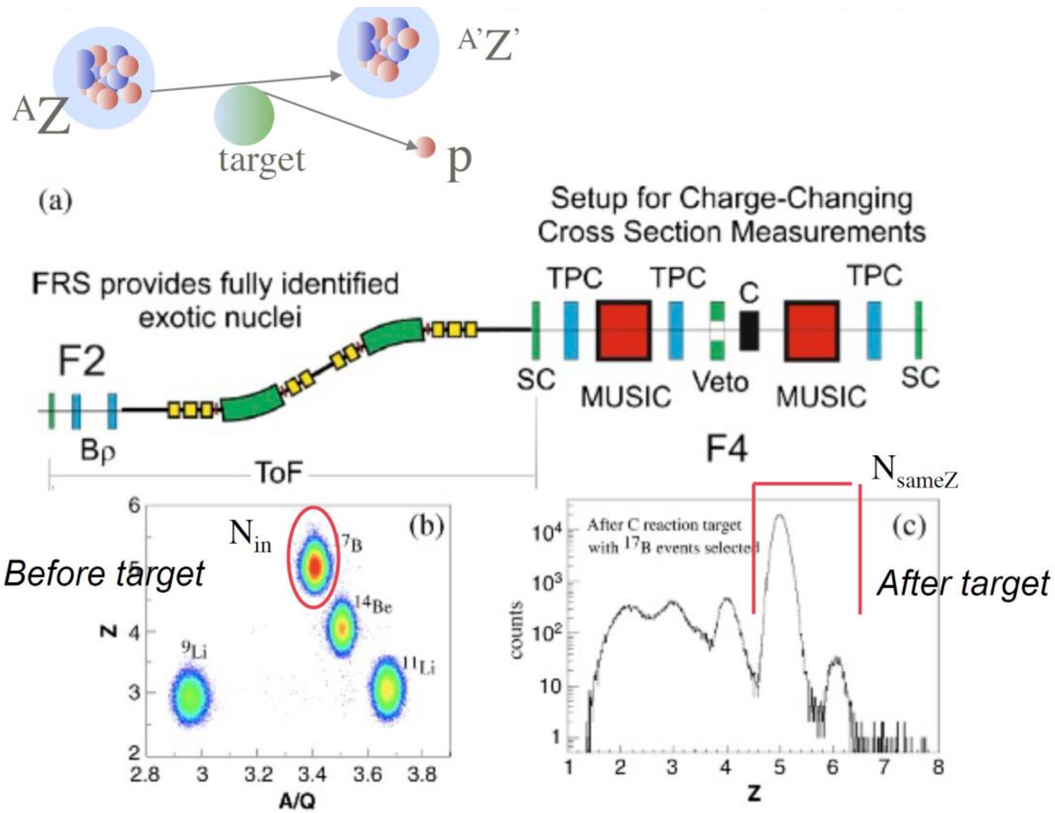

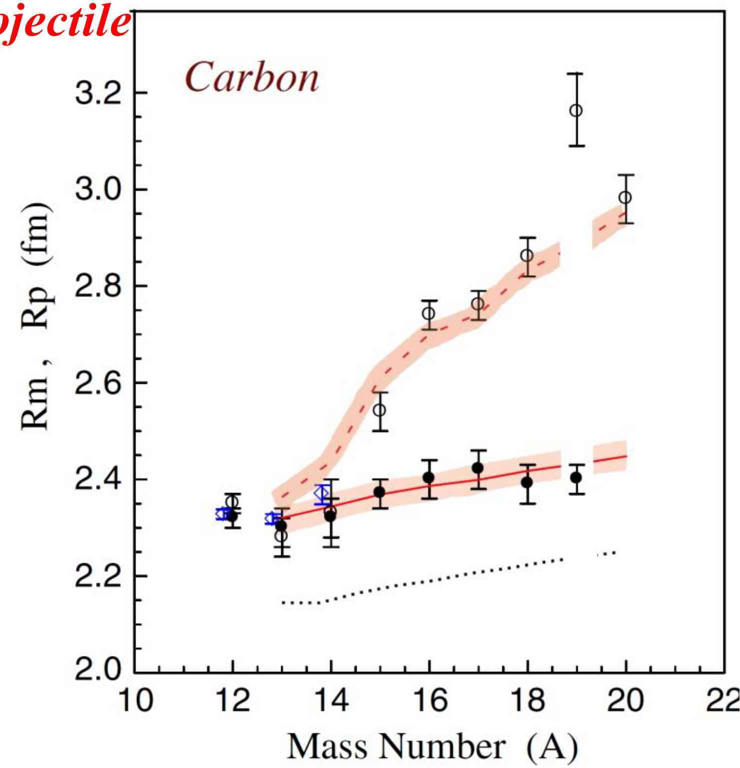

- Consistent with Rp from electron scattering

TABLE I. Secondary beam energies, measured σ_{CC} and the root-mean-square proton and matter radii derived from the data for the carbon isotopes.

Isotope	E/A (MeV)	σ_{CC}^{ex} (mb)	R_p^{ex} (fm)	$R_p^{(e^-,\mu)}$ (fm)	R_m^{ex} (fm)
^{12}C	937	733(7)	2.32(2)	2.33(1)	2.35(2)
^{13}C	828	726(7)	2.30(4)	2.32(1)	2.28(4)
^{14}C	900	731(7)	2.32(4)	2.37(2)	2.33(7)
^{15}C	907	743(7)	2.37(3)		2.54(4)
^{16}C	907	748(7)	2.40(4)		2.74(3)
^{17}C	979	754(7)	2.42(4)		2.76(3)
^{18}C	895	747(7)	2.39(4)		2.86(4)
^{19}C	895	749(9)	2.40(3)		3.16(7)

Carbon	R. Kanungo et al., Phys. Rev. Lett. 117 (2016) 102501
Boron	A. Estrade et al., Phys. Rev. Lett. 113 (2014) 132501
Beryllium	S. Terashima et al., Prog. Theor. Exp. Phys. (2014) 101D02

Courtesy R. Kanungo

Nilsson Diagrams around Z~82 & 82<N<126 (WS)

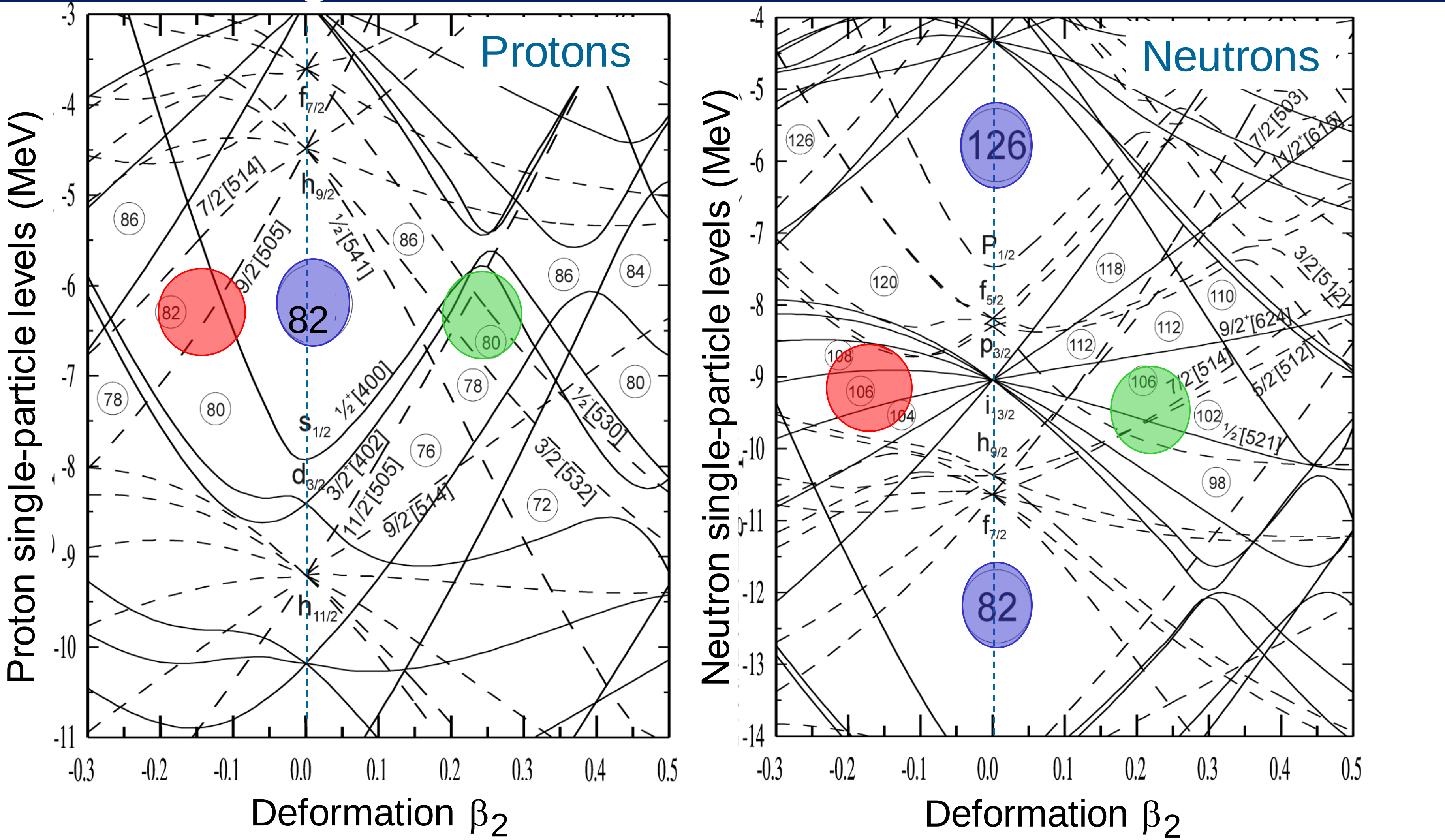

Around Z=82 and neutron mid-shell N=102-108, protons and neutrons coherently produce low-lying coexisting oblate and prolate shapes

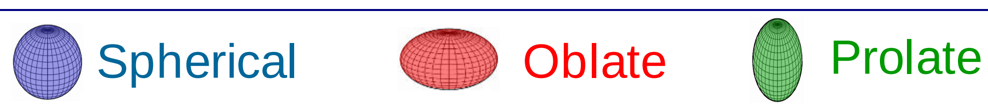

Resolution for In-source Laser Spectroscopy with RILIS

Main limitation for the resolution:

Doppler broadening due to hot ion source configuration

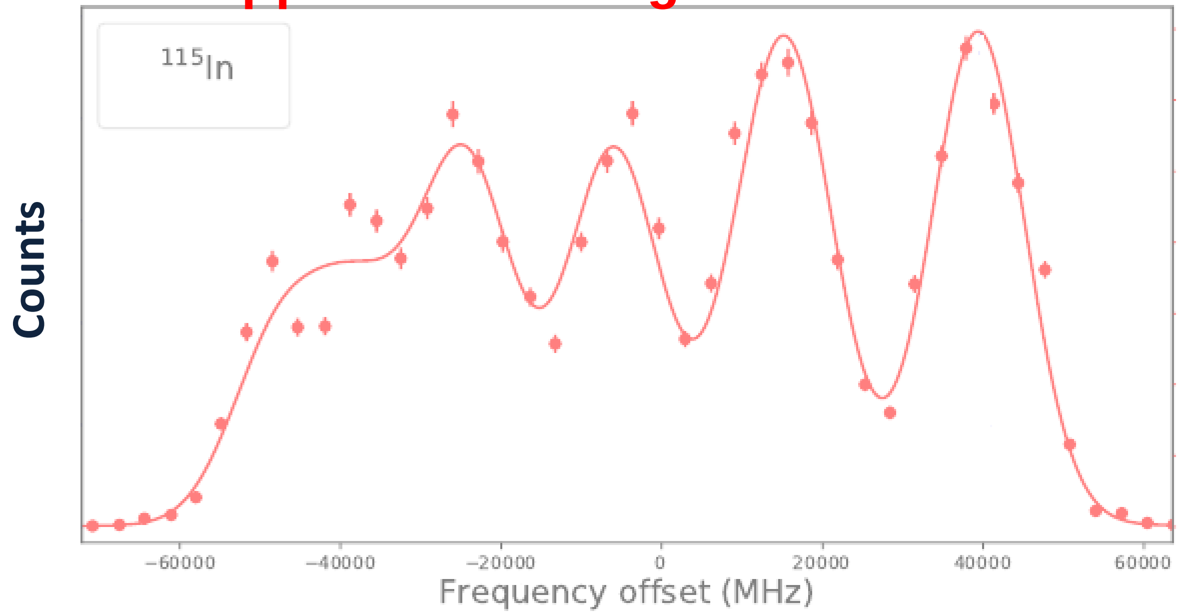

Doppler Broadening

$$\Delta\nu_D = \frac{2\nu_0}{c}\sqrt{\frac{2\ln 2\, k\, T}{m}}$$

Velocity — Source temperature — Ion mass

Room Temp. 300 K~ 25 meV

→ $\Delta\nu_D$ **> GHz**

FRIB

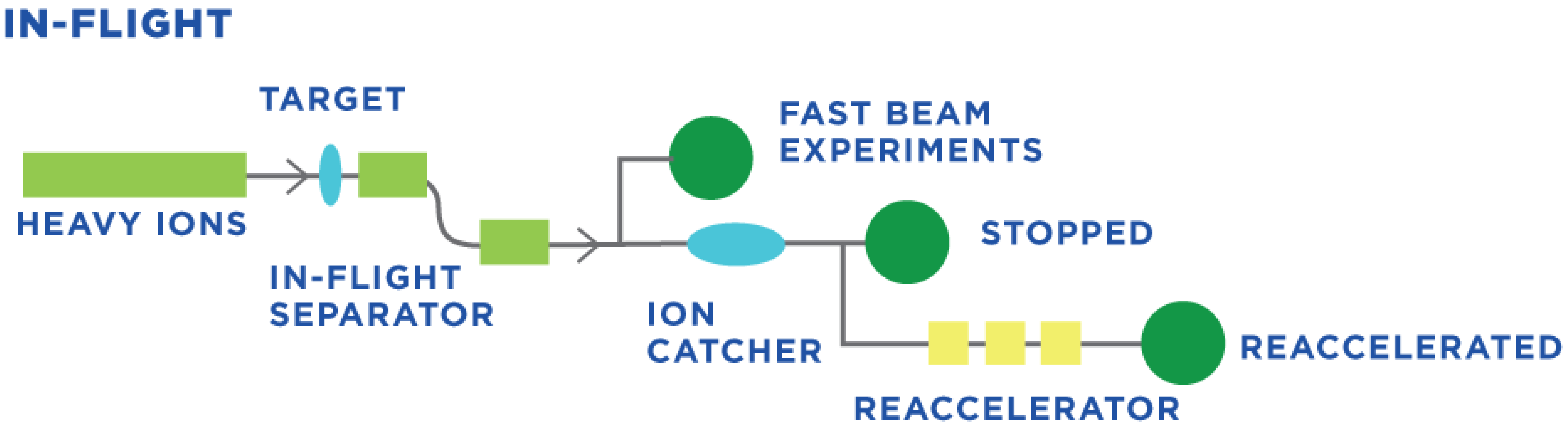
IN-FLIGHT
TARGET
HEAVY IONS
IN-FLIGHT SEPARATOR
FAST BEAM EXPERIMENTS
ION CATCHER
STOPPED
REACCELERATOR
REACCELERATED

DFT and Hg radii

Alessandro Pastore & Jacek Dobaczewski:

- The phenomenon of the radii staggering in Hg is a subtle effect of an interplay between:
  (i) shape coexistence
  (ii) pairing strength
  (iii) deformed shell structure

- The presently available functionals **do not allow** for reuniting these three aspects in a consistent way (e.g. spins are not reproduced), although the essential features of the **effect can be reproduced**…”

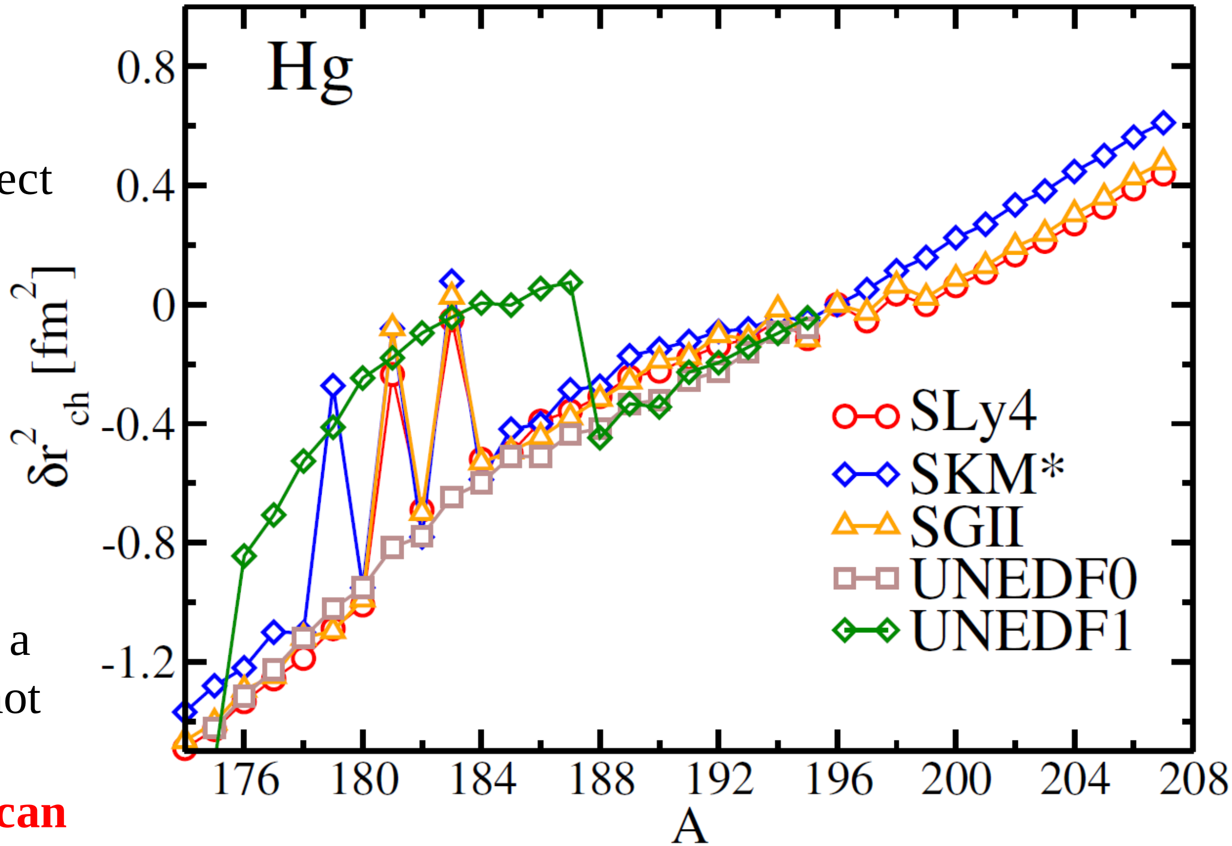

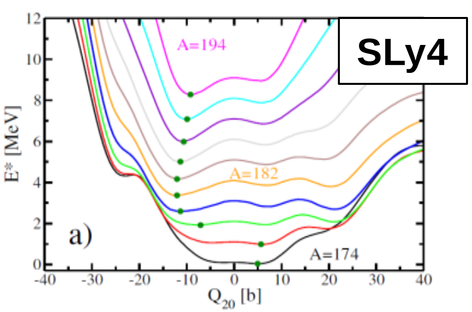

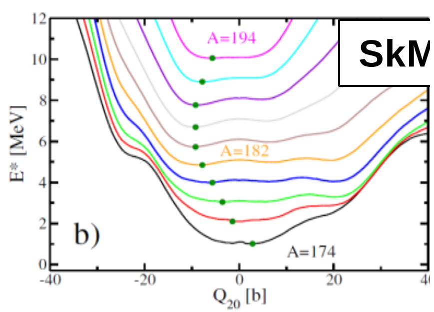

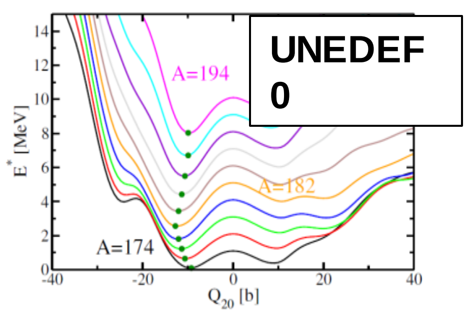

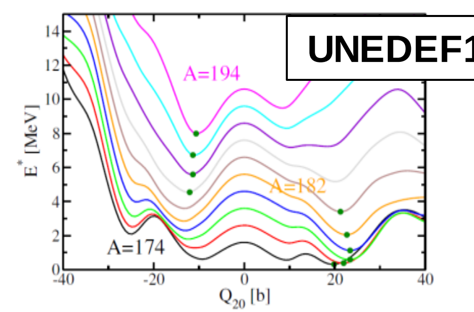

MCSM and Hg radii

Performed by Takaharu Otsuka

- Largest calculation of its kind, avoids diagonalization of $>2\times10^{42}$-dimensional H matrix.
- Radii are well reproduced.
- Results show an increase of >2 protons promoted into the h9/2 intruder state.

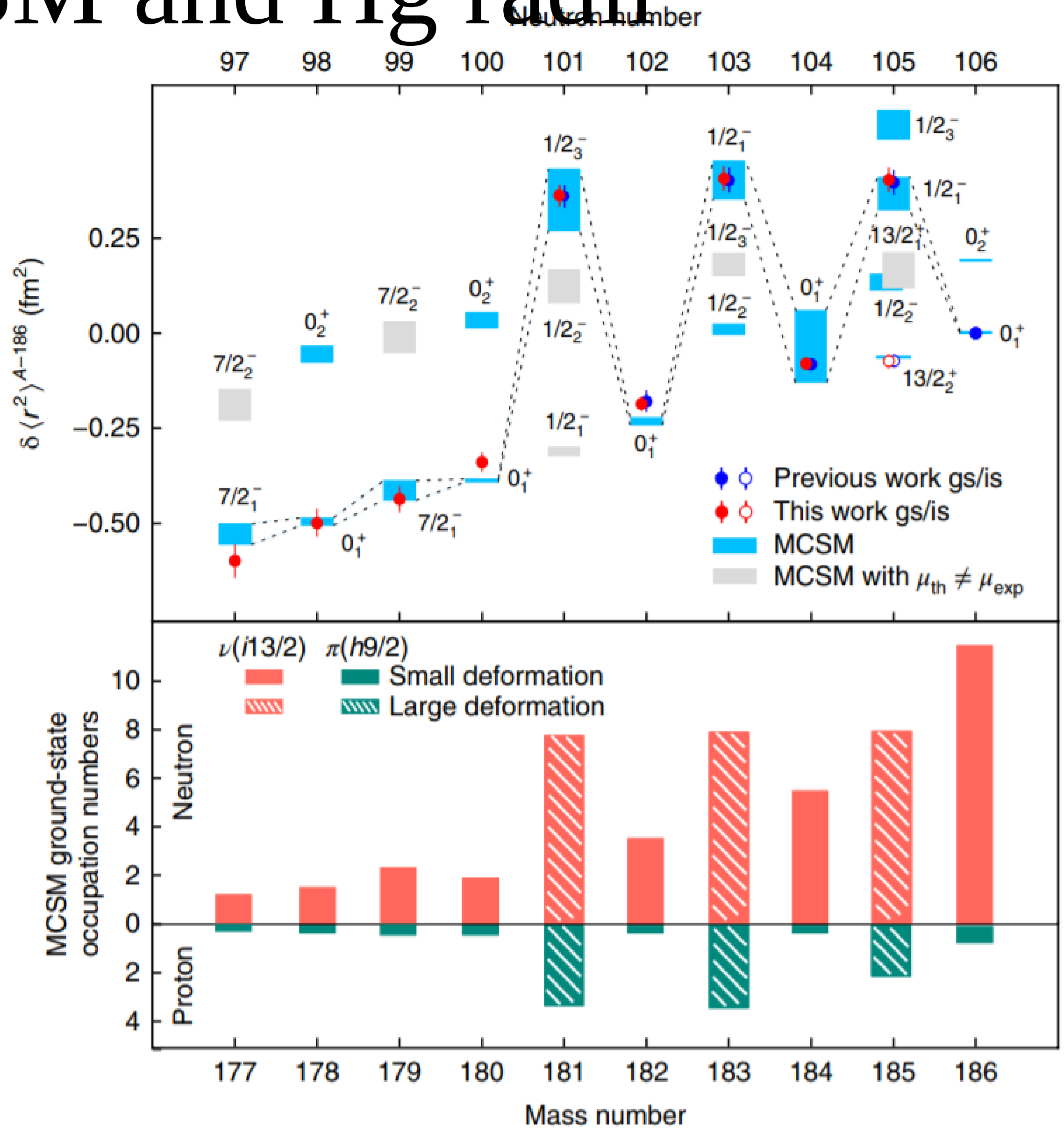

MCSM and Hg radii

Performed by Takaharu Otsuka

- Largest calculation of its kind, avoids diagonalization of $>2\text{x}10^{42}$-dimensional H matrix.
- Radii are well reproduced.
- Results show an increase of >2 protons promoted into the h9/2 intruder state.

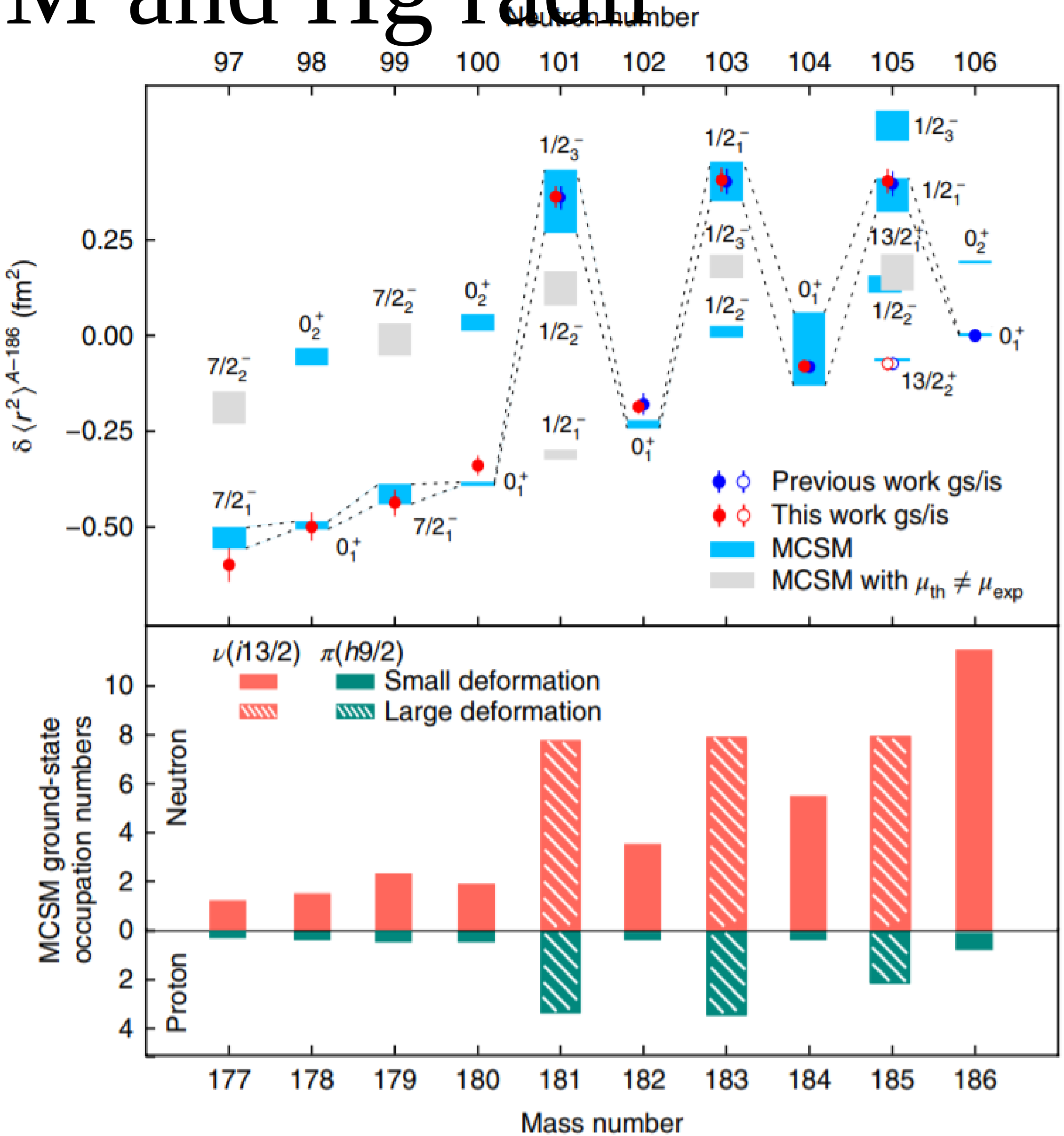

S_{2n}-values as the indicators of magic numbers

$S_{2n}(Z,N) = BE(Z,N-2) - BE(Z,N)$

- Systematic trend of mass difference is a direct indication of the ground state property.
- Two-neutron separation energy, S_{2n}, are shown. Sudden drops above $N = 50$ gap are evident.
- It's hard to reach exotic region.

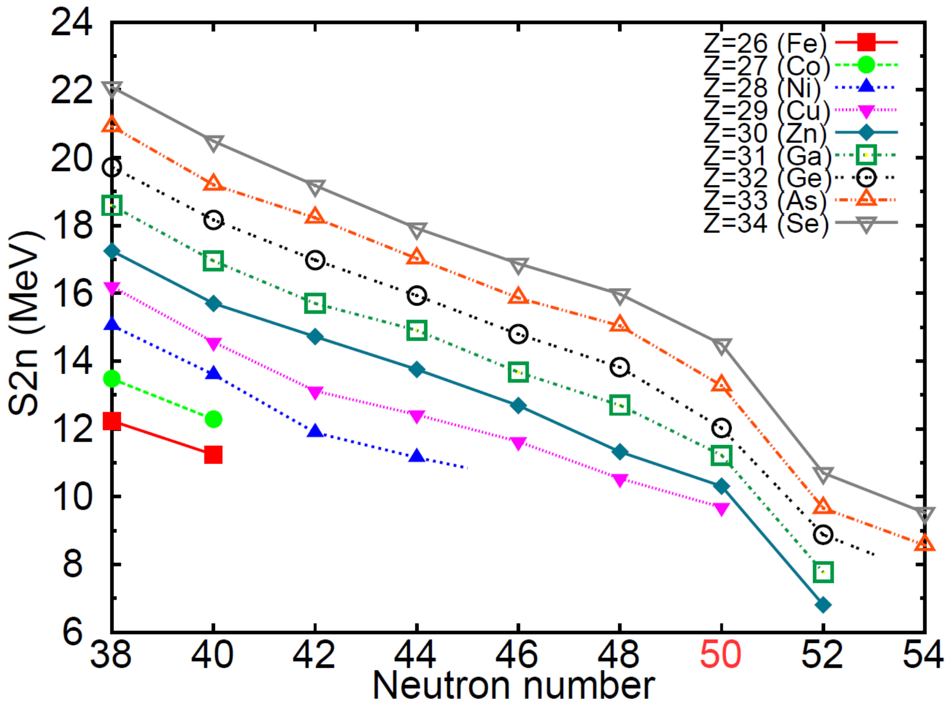

- Instead, the excitation energy works as a good indicator of shell closure and single particle energies.
- The energy of first 2^+ state of even-even nuclei is rather commonly used for a first clue of shell-closure.

$^{53,54}Ca$ Masses with Penning Trap at ISOLDE

F.Wienholtz et al, Nature, 498,346,2013

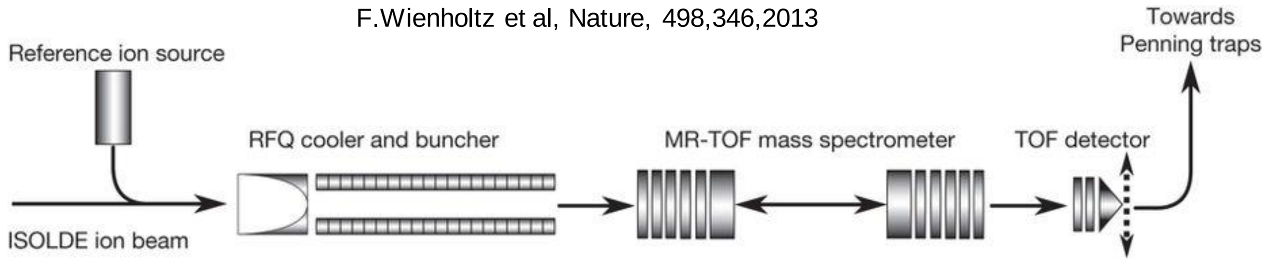

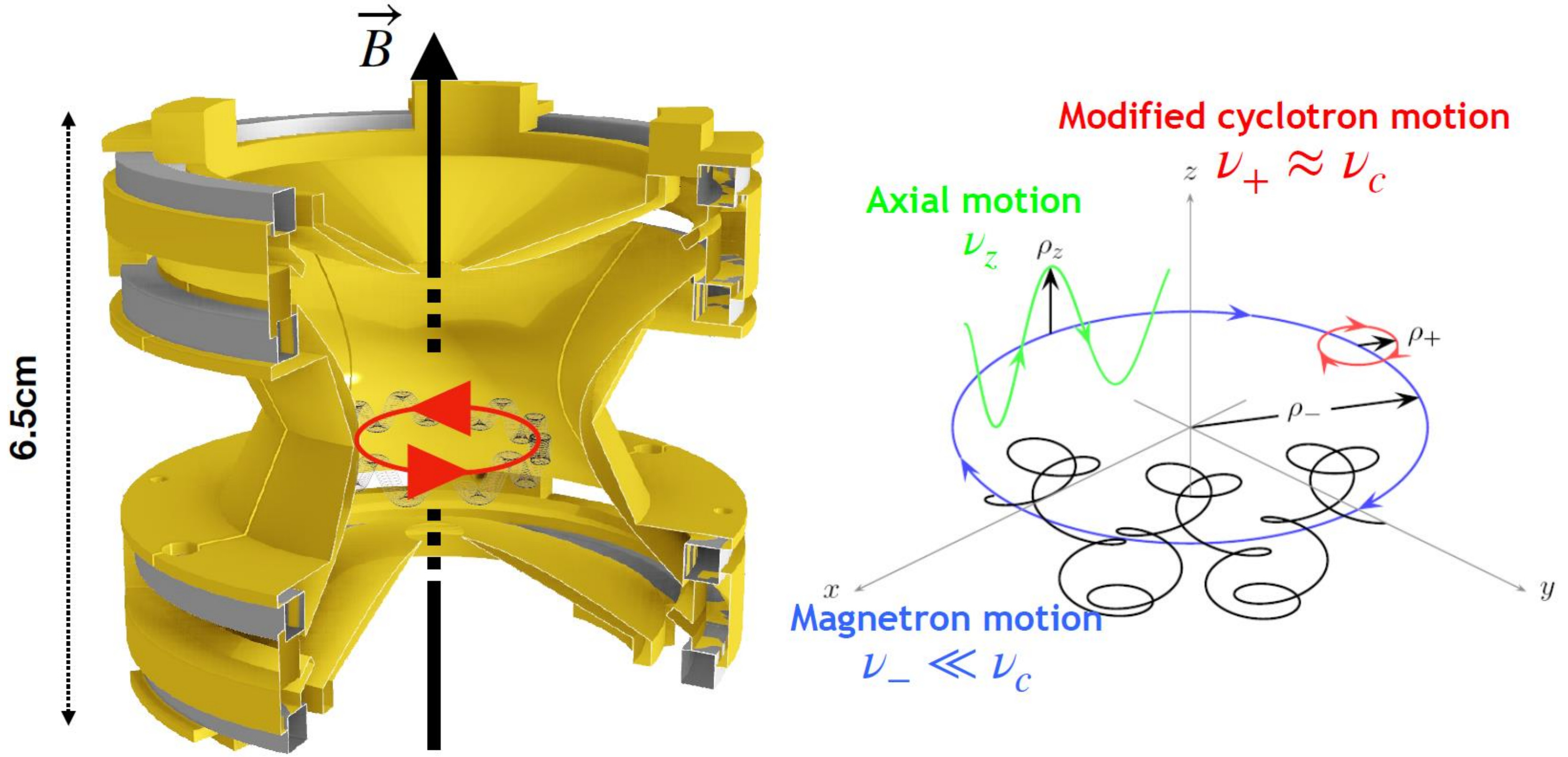

Important relation : $\nu_c = \nu_+ + \nu_- = \dfrac{qB}{2\pi m_{ion}}$

$^{53,54}Ca$ Masses with Penning Trap at ISOLDE

F.Wienholtz et al, Nature, 498,346,2013

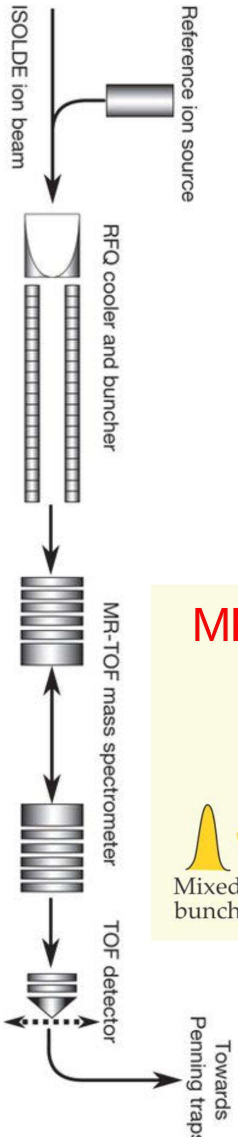

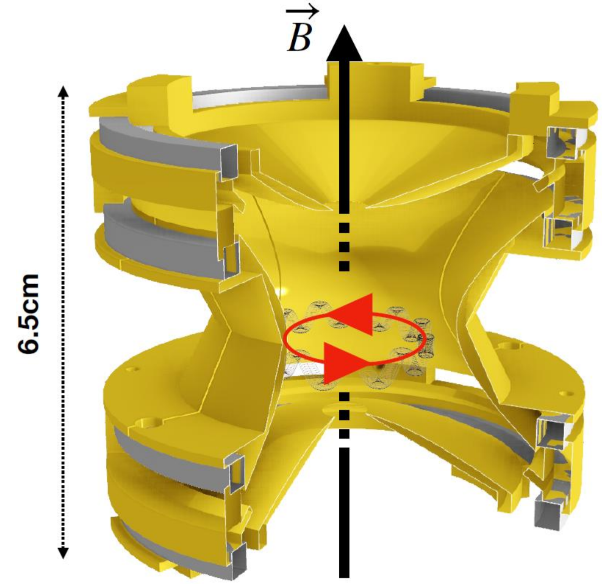

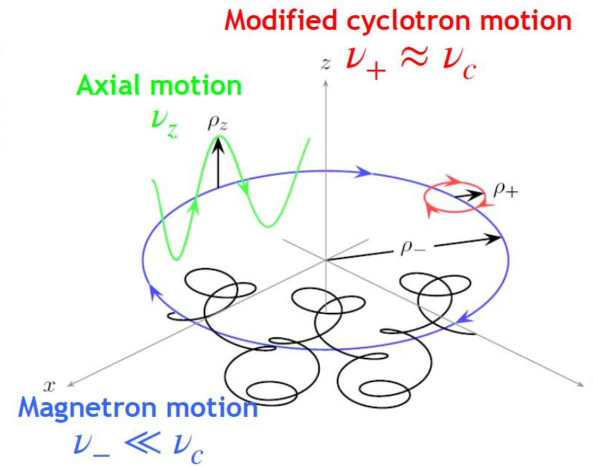

Important relation : $\nu_c = \nu_+ + \nu_- = \dfrac{qB}{2\pi m_{ion}}$

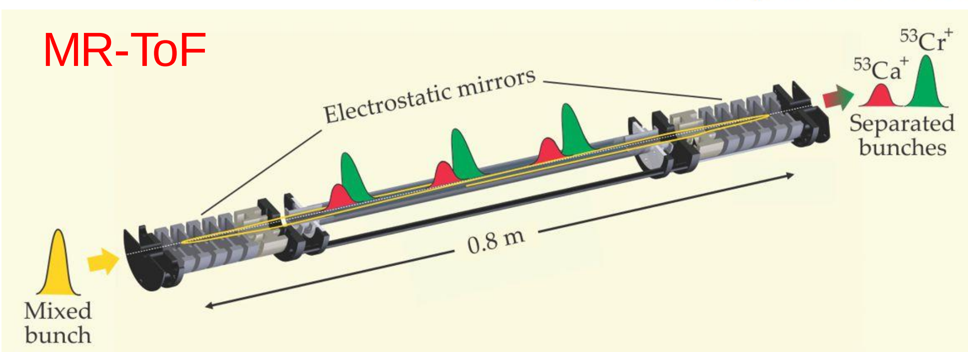

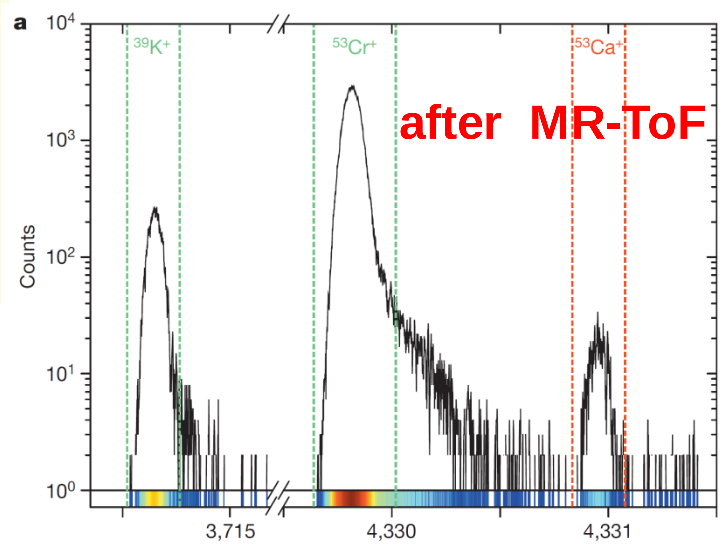

Useful Web-sites for Alpha decay theory/calculations (try them at home!)

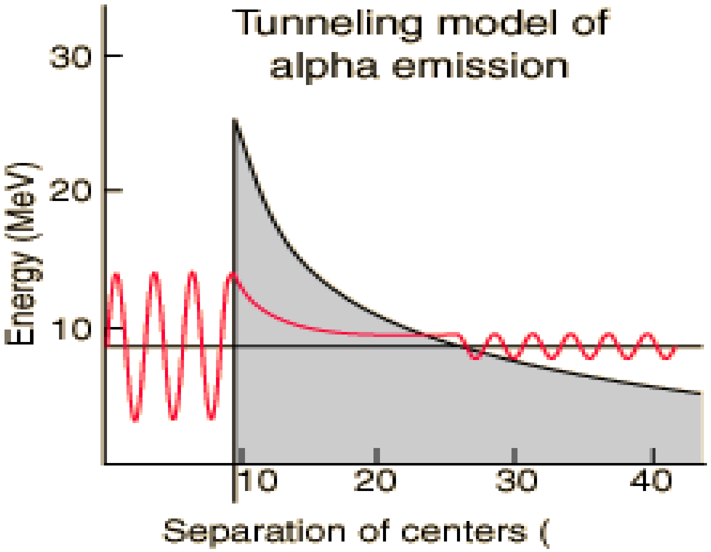

Penetrability through the barrier **depends exponentially on Q_α value**

$$T = e^{-\frac{2}{\hbar}\int_{R1}^{R2}\left[2\mu\left(\frac{Z_\alpha Z_D e^2}{r} - Q_\alpha\right)\right]^{1/2} dr}$$

NB: integration between R1 and R2

$$\log(t_{1/2}) = A + \frac{B}{\sqrt{Q_\alpha}}$$

Useful calculations:

http://hyperphysics.phy-astr.gsu.edu/hbase/nuclear/alptun.html

http://hyperphysics.phy-astr.gsu.edu/hbase/quantum/barr.html#c1

http://demonstrations.wolfram.com/GamowModelForAlphaDecayTheGeigerNuttallLaw/

Mass Separator ISOLDE (CERN, Geneva)

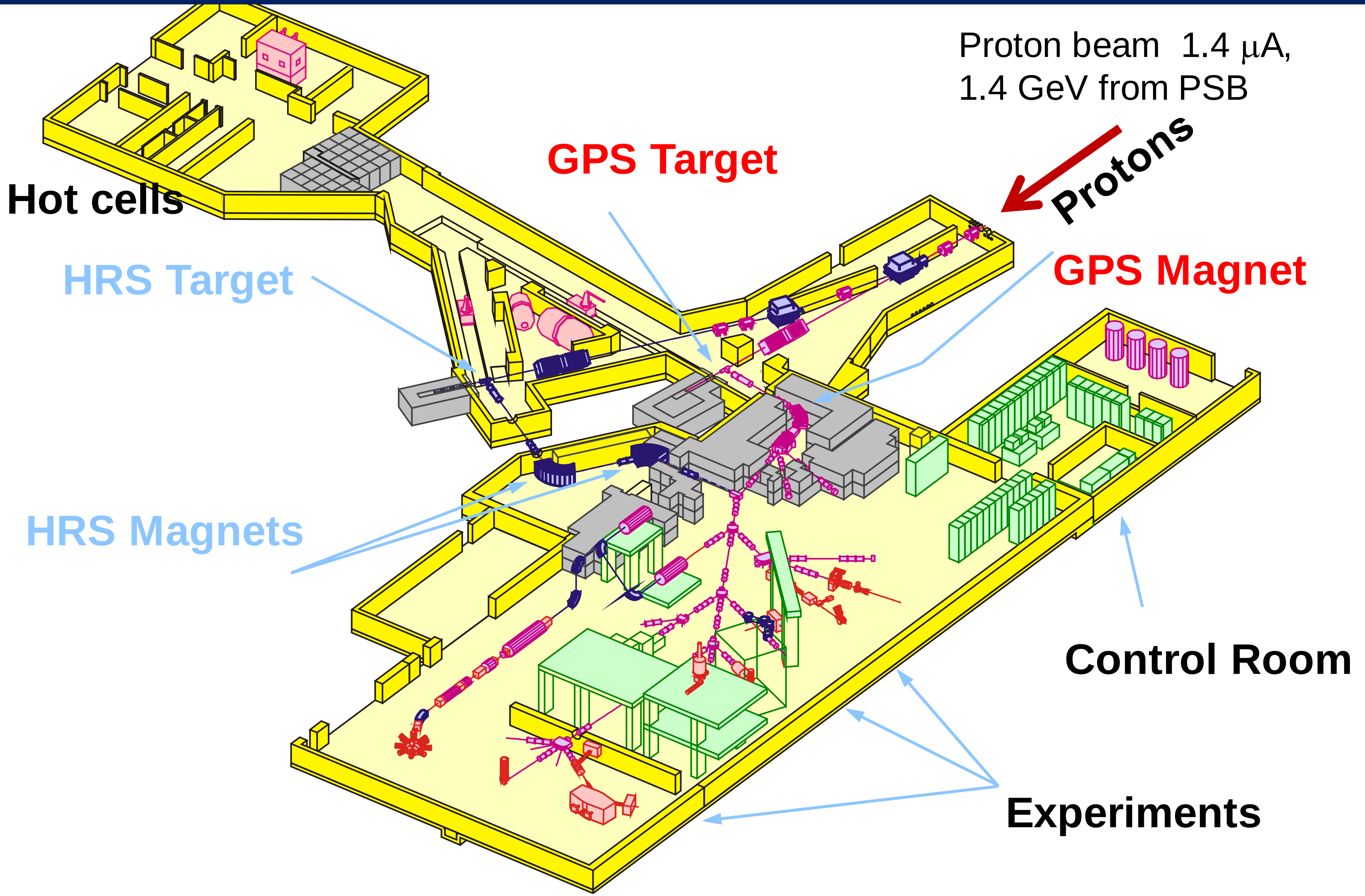

2 Target stations, 2 mass separators – GPS and HRS